

AD-A135 900

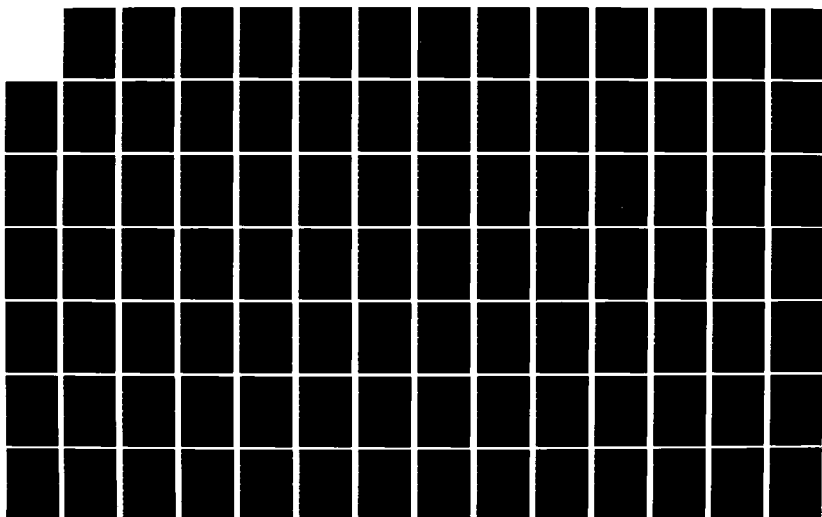
NUMERICAL FLUID DYNAMICS(U) HARVARD UNIV CAMBRIDGE MA
G BIRKHOFF 1983 N00014-75-C-0596

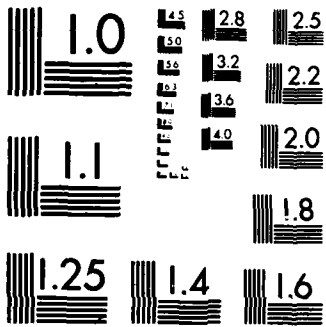
1/4

UNCLASSIFIED

F/G 20/4

NL





MICROCOPY RESOLUTION TEST CHART
NATIONAL BUREAU OF STANDARDS-1963-A

NUMERICAL FLUID DYNAMICS

By

Garrett Birkhoff
Harvard University

1983

Contract N00014-75-C-0596

AD-A755-900

DTIC FILE COPY

NOV 22 1983
DTIC

83 11 22 007

PREFACE

These lecture notes are intended to provide a helpful overview of progress in numerical fluid dynamics, since its conception in the mind of von Neumann 40 years ago.¹ Their main purpose, however, is not to serve as a historical record; still less are they intended to present a "state of the art" survey in a rapidly changing field. Instead, their purpose is to supply a thoughtful historical perspective which may help readers to assess future possibilities.

Qualitatively, everyone is aware of the enormous increase in the computing power that has become available, and specialists are familiar with the great variety of ingenious algorithms that have been proposed for solving mathematical problems originating in fluid mechanics. But reliable quantitative assessments of what can and what cannot be accomplished in a cost-effective manner are much harder to make. Indeed, experts agree that one can at best hope to make reliable order-of-magnitude estimates.

Only for a few very specific problems are cost estimates provided in these notes. Instead, a critical review is provided of the main achievement and limitations of various analytical and numerical models that have been proposed for predicting and/or simulating fluid motions.² For historical reasons and because they are more fundamental, analytical models are reviewed first, in Chapters 1 and 2.

Chapter 3 attempts to bring to life von Neumann's original brilliant insights, as seen in the light of later developments. Chapters 4 and 5 are concerned with simple mathematical models of fluid flow that have given useful quantitative insights into reality: those of potential flow and sound waves. These models are amenable to rigorous mathematical analysis, and they provide

¹Readers trying to decide whether to read these notes might look at my von Neumann lecture, published in SIAM Review 25 (1983), 1-34. This covers related material much more briefly, but in the same spirit.

²See the chart on p. 3, which is the key to the viewpoint stressed in this book.

a good testing ground for the dream of Euler, Poincare, and Hilbert: of making fluid mechanics into a mathematical science, like geometry.

Von Neumann, who seems to have considered the Laplace and wave equations dealt with in Chapters 4 and 5 as well understood, was fascinated by one-dimensional nonlinear waves in a compressible fluid. This may have been because they are not only relatively accessible mathematically, but were also accessible computationally even in his lifetime. Chapter 6 surveys some of the great theoretical and computational progress that has been made in treating them since that time, focussing on a few unsolved problems that should be solvable with moderate resources.

Chapter 7 deals with (mathematical) flows of an (idealized) incompressible viscous fluid. Experts are agreed that if we could integrate the Navier-Stokes equations which govern these, analytically or numerically, then a vast variety of important practical problems (pipe flow, airplane resistance at speeds $U < 200$ miles/hr) could be effectively treated without recourse to experiment. However, the phenomena of flow separation and turbulence have so far required extensive empirical data before becoming amenable to reliable computer simulation. A complex interplay of numerical and physical empiricism permeates the technical literature as a result of this situation; to compare the 'cost effectiveness' of different computational procedures in this area is therefore very difficult (and problem-dependent).

In their present form, these lecture notes were largely prepared while I was ONR Research Professor at the Naval Post-graduate School in Monterey, California. I wish to thank the Office of Naval Research for its continuing support of the effort required to understand an extraordinarily complex and many-sided subject, and to give a reasonably coherent survey of significant parts of it.

Garrett Birkhoff

TABLE OF CONTENTS ;

1. DYNAMICS OF IDEAL FLUIDS ;
Bibliography [A1] - [A12]
 1. Models of Fluids (pp. 1-5)
 2. Euler's Equations (pp. 5-7)
 3. Ideal Fluids (pp. 7-12)
 4. Potential Flows (pp. 12-16)
 5. Plane Potential Flows (pp. 16-18)
 6. Gravity Waves (pp. 19-22)
 7. Inertial Similarity (pp. 22-26)
 8. Fluid Resistance (pp. 26-29)
 9. Free Streamlines; Wakes (pp. 30-34)
 10. Plane Vortex Flows (pp. 34-39)
 11. Airfoil Theory (pp. 39-44)
 12. Convection of Vorticity (pp. 44-48)

2. COMPRESSIBILITY AND VISCOSITY ;
Bibliography [B1] - [B12]
 1. Introduction (pp. 1-3)
 2. Sound Waves (pp. 3-8)
 3. Helmholtz Equation (pp. 8-10)
 4. Equations of State (pp. 11-15)
 5. Thermodynamic Effects (pp. 16-19)
 6. Mach Numbers; Adiabatic Flow (pp. 20-22)
 7. Shock Formation (pp. 22-25)
 8. Viscosity (pp. 25-30)
 9. Reynolds Number (pp. 30-34)
 10. Boundary Layer Theory (pp. 35-37)
 11. Turbulence (pp. 37-39)
 12. Analytical Fluid Dynamics in 1940 (pp. 39-41)

3. VON NEUMANN'S INFLUENCE ;
Bibliography [C1] - [C15]
 1. Background (pp. 1-4)
 2. Progress Before 1930 (pp. 4-6)
 3. Stability Conditions (pp. 6-8)
 4. Southwell and 'Relaxation' Methods (pp. 6-11)
 5. Von Neumann's Vision (pp. 11-15)
 6. Von Neumann's Influence (pp. 15-18)
 7. Von Neumann's Legacy I (pp. 18-22)
 8. Von Neumann's Stability Test (pp. 23-25)
 9. The Wave Equation (pp. 25-27)
 10. Von Neumann's Legacy II (pp. 28-32)
 11. Molecular Models of Fluids (pp. 32-36)



A-1

- 4 -
4. POTENTIAL FLOWS
Bibliography [D1] - [D14]
 1. Introduction (pp. 1-3)
 2. Inverse Methods (pp. 4-5)
 3. A Potential Flow Problem (pp. 5-8)
 4. Corner Singularity (pp. 8-12)
 5. Added Mass (pp. 13-16)
 6. Container Effect (pp. 16-19)
 7. Two-Dimensional Airfoils (pp. 20-23)
 8. Free Surfaces (pp. 23-25)
 9. Ship Wave Resistance (pp. 25-28)
 10. Interfacial Instability (pp. 28-31)
 11. Free Streamlines (pp. 31-32)

 5. SOUND WAVES
Bibliography [E1] - [E16]
 1. Introduction (pp. 1-4)
 2. Boundary Conditions (pp. 4-6)
 3. Dispersion Analysis: Plane Waves (pp. 6-9)
 4. Second-order Accuracy: Plane Waves (pp. 10-14)
 5. Second-order Accuracy: Cylindrical Waves (pp. 14-20)

 6. NONLINEAR ONE-DIMENSIONAL WAVES
Bibliography [F1] - [F28]
 1. Introduction (pp. 1-3)
 2. Isentropic Flow (pp. 4-7)
 3. Shocks: Von Neumann-Richtmyer Scheme (pp. 7-10)
 4. Lax-Wendroff Scheme: Shock 'Capturing' (pp. 11-15)
 5. Artificial Viscosity; Recent Developments (pp. 16-18)
 6. Shock Fitting; Moretti's Program (pp. 18-22)
 7. Conservation Law Form (pp. 22-27)

 7. INCOMPRESSIBLE VISCOUS FLOWS
Bibliography [G1] - [G10]
 1. Introduction (pp. 1-3)
 2. Parallel Flows (pp. 4-9)
 3. Nearly Parallel Flows (pp. 10-13)
 4. Two Time-Dependent Examples (pp. 14-18)
 5. Vorticity Transport (pp. 19-22)
 6. Stokes Flows (pp. 23-25)
 7. Finite Element Methods (pp. 26-28)
 8. Boundary Layers (pp. 29-31)

 8. APPENDIX A
Lagrangian Dynamical Systems [A1] - [A5]

9. APPENDIX B

Conformal Maps and Potential Flows [B1] - [B9]

10. APPENDIX C

Fourier Analysis [C1] - [C3]

11. APPENDIX D

Navier-Stokes Equations [D1] - [D6]

12. APPENDIX E

Molecular Models of Matter [E1] - [E6]

13. APPENDIX F

'Courant' Stability Conditions and Application
Matrices [F1] - [F5]

14. APPENDIX G

Two Dimensional Airfoil Theory [G1] - [G4]

CHAP. 1. DYNAMICS of IDEAL FLUIDS

1. Models of fluids. Fluids (i.e., gases and liquids) differ from solids in their physical inability to withstand shear stress without deforming. As a result, fluid motions or "flows" are characterized by the large deformations which blobs of matter can undergo. Many models have been proposed for deriving their behavior from first principles, within the framework of Newtonian mechanics. This chapter will be concerned with the simplest model: that of a so-called ideal fluid. Such an "ideal" fluid is defined physically by two properties: (i) it is incompressible (volume is conserved), and (ii) it is subject to zero shear stress even when moving.

These assumptions (within the general framework of Newtonian continuum mechanics) will be formulated mathematically in §§2-3. But before discussing in detail the flows of such "ideal" fluids, we will list for contrast some other important mathematical models of fluids that have been studied in depth.

Eight of these are listed in tabular form in Table 1; we will consider all of them in this book. In this chapter, we will describe some successful uses of the first two of these models, both of which attempt to rationalize (i.e., predict quantitatively) the behavior of nearly ideal fluids that are very slightly compressed, and whose shear stresses are very much less than their pressure stresses.

In practice, mathematical treatments of fluid motions, whether analytical or numerical, ordinarily neglect most of the following: viscosity, compressibility, external gravity, and the effects of variations in temperature and entropy (e.g., natural convection). They often also neglect the effects of lateral or vertical velocity components, or their squares, as in the theories of sound waves and shallow water waves and in boundary layer theory. Indeed, many of the most successful mathematical models

of fluid flows are only asymptotic, in the sense that they depend on a parameter (e.g., the Reynolds number or its reciprocal), and are only accurate when this parameter is very small or very large.

Eight standard models. Among the many different initial-boundary value problems that have been proposed as realistic mathematical models for fluid flows, eight are especially significant. Each of these models is mathematically self-contained, in the sense that its basic equations can be regarded as an axiom system from which the behavior of various kinds of fluid motions can be deduced mathematically, in somewhat the same way that Euclid deduced geometrical theorems from his axioms, and that Newton and his successors (especially Laplace in his Mécanique Céleste) derived the orbits of the planets and their moons from three force laws and the law of universal gravitation.¹

Table 1 also lists (in the second column) the chapters in Lamb's classic treatise [A6] which summarize what was known about each model mathematically as of 1932, and the names of some key concepts which are associated with it. Table 1 can be viewed as a guide through Chaps. 1-3 below, which explain in more detail the significance and typical applications of these concepts.

Molecular effects. Diffusion, boiling, condensation, latent heat, and many other physical phenomena can only be understood, even qualitatively, in terms of the molecular structure of matter. Therefore, we have included kinetic theory in our list of analytical models, even though it is based on ordinary and not on partial DE's, and is very different for liquids than for gases. We will discuss this model in Chap. 3.

One may well ask: what is the purpose of studying mathematical models that are known to neglect physical variables such as compressibility and viscosity? There are three different answers to this question.

¹Actually, even celestial mechanics is not exact: it neglects relativistic effects and the asphericity of the sun and planets!

TABLE 1. EIGHT STANDARD ANALYTICAL MODELS FOR FLUID DYNAMICS

	<u>ORIGINATORS</u>	<u>LAMB Chaps.</u>	<u>KEY PHRASES</u>
1.	EULER-LAGRANGE POTENTIAL FLOW	III-VI VIII-IX	SOLID BOUNDARIES vs. FREE BOUNDARIES INTERFACES, SLIP- STREAMS GRAVITY WAVES
2.	HELMHOLTZ-KELVIN VORTICITY	VII	CYCLONES AND ANTICYCLONES
3.	NAVIER-STOKES STREAM FUNCTION INCOMPRESSIBLE	XI (pp. 563-663)	ASYMPTOTIC: BOUNDARY LAYER, LUBRICATION
4.	HELMHOLTZ-RAYLEIGH SOUND WAVES WAVE EQUATION	X	ACOUSTICS, WAVE FRONTS ANALOGY WITH GEOMET- RICAL OPTICS AND RAYS
<u>COMMENT:</u> THE REMAINING MODELS ARE LESS WELL DEVELOPED:			
5.	RIEMANN RANKINE-HUGONIOT	X (cont.)	SUPERSONIC FLOW SHOCK WAVES
6.	REYNOLDS PRANDTL-TAYLOR (RANDOM FUNCTIONS)	XI (cont.) (pp. 663-96)	EDDY VISCOSITY TURBULENCE $u(x,t;\omega)$
7.	MAXWELL DIFFUSION in GASES (MOLECULAR MEAN FREE PATH)	Secs. 325, 357	CAVITATION LATENT HEAT KINETIC THEORY
8.	TWO-PHASE FLOW		CAVITATION, BOILING FREE BOUNDARIES

In the first place, mathematical models (whether numerical or analytical) can contribute to our understanding of Nature, by showing at least qualitatively why various interesting phenomena occur. This was what scientists like Newton and Kelvin meant by the phrase Natural Philosophy. They were well aware that many of their formulas were not exact, but they hoped that their ingenious mathematical models would provide at least a first step toward eventual exact understanding. Models which do this well may be called philosophical models.

Second, models may predict very accurately what will happen over a wide range of controlled laboratory conditions. A good example is Poiseuille's formula,

$$(1.1) \quad \text{axial pressure gradient} = -8\mu Q/\pi a^4 .$$

This relates the pressure drop per unit length in a horizontal tube to the flow rate Q and the radius a , and is accurate as long as $Re = \rho Q/\pi\mu a < 1000$. We shall call such models scientific models.

Finally, partly as a consequence of their qualitative correctness, mathematical models may suggest rational methods for organizing, interpolating between, and extrapolating from experimental data. Even if this interpolation and extrapolation is accurate only to within $\pm 20\%$, and involves empirical constants or 'correlations', it can often greatly reduce the need for further costly experiments (e.g., parameter studies). We shall call models used for this purpose, engineering models.

This chapter will be concerned with the simplest model of an "ideal fluid", assumed to be incompressible and non-viscous (or 'inviscid'). This model, although easy to criticize from a physical standpoint, is so much more tractable mathematically than more realistic physical models that it is still the one most commonly used in engineering applications.

The next chapter will discuss compressibility and viscosity, thus completing a reasonably balanced (if necessarily sketchy) introduction to analytical fluid mechanics. With this background, we hope that our book will provide a stimulating and readable survey of numerical fluid dynamics, of interest to engineers as well as to mathematicians and applied physicists. To this end, we have included in Chapter 3 an account of von Neumann's ideas and influence on the subject (which was very great!), together with a discussion of some suggestive molecular models of fluids. We then take up a series of case studies of numerical methods in five different areas of fluid dynamics, to each of which a chapter is devoted. Chapter 4 is devoted to potential flows;

Chapter 5 to sound waves; Chapter 6 to nonlinear waves; Chapter 7 to the Navier-Stokes equations; and Chapter 8 to two-phase flows.

2. Euler's Equations. Fluid dynamics was first envisaged as a systematic science in Johann Bernoulli's Hydraulics (1737), in Daniel Bernoulli's Hydrodynamique (1738), and in d'Alembert's Traité ... des fluides (1744) and Théorie générale des vents (1745). Hunter Rouse² has retold the amazing story of how Johann withheld his son's manuscript from publication, while writing his own version of the subject, in the preface to the English translations of the two books, published by Dover in 1968.

The ideas expounded in these books were formulated mathematically as partial differential equations by Daniel Bernoulli's friend Leonhard Euler (1707-83), in two path-breaking papers (1752, 1755). In his second paper, Euler claimed optimistically that "all the theory of the motion of fluids has just been reduced to the solution of analytic formulas."

Euler was referring, first of all, to what are today called the equations of motion of a nonviscous fluid:

$$(2.1) \quad D u_i / D t = g_i - \nabla p / \rho \partial x_i, \quad i = 1, 2, 3 .$$

In (2.1), $\underline{u} = (u_1, u_2, u_3)$ is the vector velocity, $\underline{g} = (g_1, g_2, g_3)$ the gravitational force (per unit mass), p the pressure, and ρ the density; while D/Dt denotes the 'material' or 'substantial' derivative $\partial/\partial t + \sum u_k \partial/\partial x_k$. To quote Euler again:³ "If we add to these three equations [of motion - i.e., to (2.1)], first [the equation of continuity

$$(2.2) \quad \partial \rho / \partial t = -\nabla \cdot (\rho \underline{u}) = - \sum_{i=1}^3 \partial (\rho u_i) / \partial x_i ,$$

²See also Hunter Rouse and Simon Ince, History of Hydraulics, Iowa Inst. Hydraulic Research, 1957, Chaps. VII and VIII.

³See L. Euler, Opera Omnia (2), 12, p. LXXXV, translated and edited by C. Truesdell. We can interpret Euler's γ in gases as temperature (in nearly isothermal flow) or as $p/\rho\gamma$ (in nearly adiabatic flow).

then that [the equation of state

$$(2.3) \quad p = p(\rho) \text{ [or } \bar{p} = (p)]$$

which gives the relation between the elasticity p , the density ρ , and the other quality r which in addition to the density influences the elasticity, we shall have five equations which include all the theory of the motion of fluids."

Euler's conception of a purely rational fluid dynamics, based on what we have called Euler's equations, was magnificent. It is analogous to Newton's conception of a rational celestial mechanics, deducible from his universal law of gravitation and his three general "laws of force".

However, fluid mechanics is many orders of magnitude more complicated than celestial mechanics. Whereas the latter is primarily concerned with predicting the regular and periodic advance of the moon and planets past a background of stationary stars, with due attention to eclipses, the phenomena of fluid mechanics are infinitely varied and involved (e.g., wind patterns on a stormy day).

Moreover even in celestial mechanics, the elaboration and verification of Newton's mathematical 'model' of the solar system took nearly two centuries. Therefore, it is hardly surprising that progress in correlating Euler's mathematical model of a 'fluid' with experimental observations was even slower. Indeed, its early successes concerned the one-dimensional motions of homogeneous incompressible fluids of constant density $\rho = \rho_0$. We will call such a fluid an ideal fluid.

Lagrange's Mécanique Analytique. A milestone in the progress of fluid dynamics was the Mécanique Analytique of J. L. Lagrange (1736-1813). Published in 1788, it remained the standard treatise on mechanics for at least 50 years. Its last three chapters, dealing with "hydrodynamique", included several fundamental results based on Euler's equations. Euler's equations fit beautifully into Lagrange's general concept of a (conservative) dynamical system having infinitely many degrees of freedom, like

a 'vibrating string'. Lagrange's general theory of 'small oscillations', having a basis of 'normal modes of oscillation' (eigenfunctions, in modern terminology), applies to wave motions of fluids, whether gravity waves (see §6) or ocean waves (see Chap. 2).

In the resulting Euler-Lagrange model, incompressible fluids (often imagined as 'liquids') were soon seen to have a quite different theory from (idealized) compressible fluids (or 'gases'). This chapter will be devoted to the former, and indeed to (idealized) homogeneous incompressible fluids, of constant density $\rho = \rho_0$.

3. Ideal fluids. We may call a fluid that satisfies Euler's equations (2.1)-(2.3) with $\rho = \rho_0$ an 'ideal fluid'. For a century after Euler first proposed his equations, fluid dynamics was concerned almost exclusively with ideal fluids.

Steady flows. Euler's first major triumph was his mathematical derivation of Daniel Bernoulli's formula, relating the pressure to the velocity in a conservative gravitational field $\underline{g}(\underline{x}) = -\nabla G$ with gravitational 'potential' $G(\underline{x})$. This formula is

$$(3.1) \quad p + \rho_0 \left(\frac{1}{2} |\underline{u}|^2 + G \right) = \text{const.};$$

it is valid along any streamline in any 'steady flow' of a fluid of constant density ρ_0 with time-independent velocity $\underline{u}(\underline{x})$.

A streamline is defined physically as the path of a particle in steady flow. Mathematically, it is the orbit of a solution of the autonomous system $dx_k/dt = u_k(\underline{x})$. Noting that in steady flow, the material derivative D/Dt in (2.1) reduces to $\sum u_k \partial/\partial x_k$, and introducing the convenient symbol q for the flow speed $[\sum u_i^2]^{1/2}$, it is very easy to derive Bernoulli's formula today. Indeed, we have (in steady flow)

$$(3.1') \quad \frac{D}{Dt} \left(\frac{1}{2} q^2 \right) = \sum u_k \left(\sum u_i \frac{\partial u_i}{\partial x_k} \right) = \sum u_i \left(\sum u_k \frac{\partial u_i}{\partial x_k} \right) = \sum u_i \frac{Du_i}{Dt},$$

by the commutativity of multiplication.

Substituting into the last expression from Euler's equation of motion,

$$Du_i/Dt = - \frac{1}{\rho} \partial p / \partial x_i + g_i ,$$

we get ($\rho = \rho_0$ being constant)

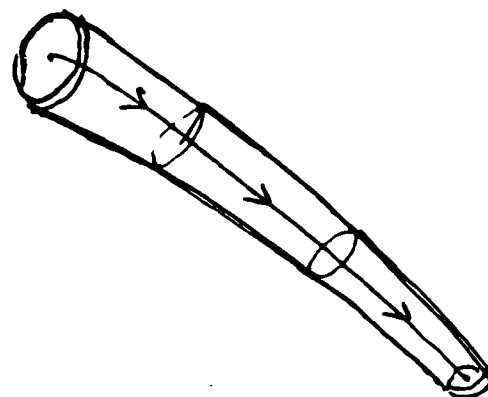
$$\sum u_i \left(- \frac{\partial}{\partial x_i} \left(\frac{p}{\rho_0} \right) - \frac{\partial G}{\partial x_i} \right) = - \frac{D}{Dt} \left(\frac{p}{\rho_0} + G \right)$$

Substituting back into (3.1'), this gives

$$(3.2) \quad \frac{D}{Dt} \left(\frac{1}{2} q^2 \right) + \frac{p}{\rho_0} + G = 0 ,$$

whence (3.1) follows, as claimed.

Bernoulli's formula. We will discuss several generalizations of Bernoulli's formula (3.1) below, and it is suggestive to derive it also from the physical principles of conservation of mass and energy. To this end, consider a thin stream tube composed of a bundle of streamlines around a given streamline. Let s denote arc-length along the central streamline, and let $dA(s)$ denote the cross-section of the tube. Since the pressure is everywhere normal to the boundary, no work is done by the pressure on a segment of the (moving) fluid in the stream tube, except through the motion of its ends. There the rate of work (per unit time) is $\dot{W} = p_0 u_0 dA_0 - p_1 u_1 dA_1$; moreover by the conservation of mass and density (hence volume dR), $u_0 dA_0 = u_1 dA_1 = Q$, the rate at which volume enters and leaves the segment (per unit time); the corresponding mass is $\dot{m} = \rho_0 Q = Q$.



The rates of convection of kinetic energy into and out of the ends of the stream tube are $\frac{1}{2} \dot{m} q_0^2$ and $\frac{1}{2} \dot{m} q_1^2$, respectively.

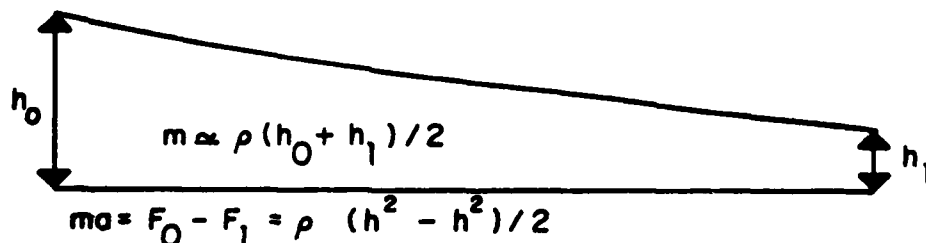
This gives a simple physical meaning to ρ_0 times (3.2), in terms of conservation of energy. Rewritten as

$$(3.4) \quad \left(\rho_0 + \frac{1}{2} \rho q_0^2 + G_0\right) = \left(\rho_1 + \frac{1}{2} \rho q_1^2 + G_1\right),$$

it states that the rate of work done on any fluid segment of a stream tube by the difference in pressure at its ends, $(p_0 - p_1)$, is the sum of the rates of increase of its kinetic energy, $\frac{1}{2} \dot{m} (q_1^2 - q_0^2)$, and its potential energy, $\frac{1}{2} \dot{m} (G_1 - G_0)$.

'Long' waves. A second early triumph of the 'ideal fluid' model, was its successful prediction (by Lagrange in 1781) of the velocity of propagation of 'long' waves of length λ and 'infinitesimal amplitude' in 'shallow water' of depth $h \ll \lambda$.

We emphasize that Lagrange's formula,⁴ $c = \sqrt{gh}$, is not exact. It is asymptotic, and valid for gravity waves of 'infinitesimal amplitude', in a 'canal' of otherwise constant depth. It assumes that such waves are, to a first approximation, horizontal surges, in which the vertical velocity and momentum are negligible in comparison with the horizontal velocity and momentum. It then considers the horizontal component of Euler's equations of motion (see the Figure).



⁴Note that our derivation avoids the assumption of potential flow made by Stoker in [A10, §2.2]. What we call 'long waves' are called 'tidal waves' by Lamb [A6, Chap. VIII], because the basic assumption of nearly horizontal motion applies to tides, whose wave length is thousands of miles.

More precisely, it assumes that the vertical acceleration is negligible, so that the pressure satisfies

$$(3.3) \quad p = p_a + g\rho_0(\eta - y) ,$$

where $y = \eta(x)$ is the elevation of the surface. Hence, at all points of the wave $p_x = g\rho_0\eta_x$. This is independent of y , and so all particles in the same plane $x = x_1$ perpendicular to x have the same horizontal velocity and acceleration. It follows that, for a fluid initially at rest, all particles in a given vertical plane parallel to the direction of motion stay in that plane $x = \xi(t)$, in Lagrange's model.

For 'small oscillations', moreover, terms like uu_x that are quadratic in u , like uu_x , can be neglected. Hence the equation of horizontal motion,

$$\rho_0(u_t + uu_x) = -p_x = -g\rho_0\eta_x ,$$

can be simplified to

$$(3.4) \quad \rho_0 u_t = -g\rho_0 \eta_x .$$

On the other hand, $v_y = -u_x$ by the equation of continuity, which is a function of x alone, whence

$$(3.5) \quad \eta_t = -u_x h .$$

Combining with (3.4) (divided through by ρ_0), we get

$$(3.6) \quad u_{tt} = -g\eta_{xt} = -g\eta_{tx} = gh u_{xx} .$$

Similarly, $\eta_{tt} = -hu_{xt} = hu_{tx} = +gh\eta_{xx}$. In conclusion, the one-dimensional wave equation

$$(3.7) \quad u_{tt} = gh u_{xx}$$

characterizes 'long waves' of 'small amplitude' in a canal of constant depth h . Likewise, we can derive

$$\eta_{tt} = (-hu_x)_t = -h(u_t)_x = -c^2 \eta_{xx} .$$

As d'Alembert had shown (and is easily verified), the general solution of (3.7) is $u = F(x-ct) + G(x+ct)$, $c^2 = gh$. Thus such 'long waves' are superpositions of two waves, each traveling with constant speed c without change of form, but in opposite directions. Such waves are called progressive waves.

Tsunamis. Analogous to tides are 'tidal waves' or tsunamis, typically caused by earthquakes. In an ocean N^2 miles deep, these travel with a speed ($c = \sqrt{gh}$ of about $412N$ f/s).

Simply harmonic waves. In the theory of waves, a central role is played by 'simply harmonic' progressive waves, of the special form

$$(3.8) \quad u = A_k \cos(kx-ckt) + B_k \sin(kx-ckt) \\ = C_k \cos k(x-ct-\gamma_k) .$$

In (3.8), $C_k = (A_k^2 + B_k^2)^{1/2}$ is the amplitude, while $\gamma_k = \arctan(B_k/A_k)$ is the phase constant. The waves (3.8) are 'progressing' with wave velocity c in the direction of increasing x without change of form; by changing the $-$ signs to $+$ signs, we get waves moving in the opposite direction.

Standing waves. By superposing two simply harmonic waves of equal amplitude moving in opposite directions, we get standing waves. A typical example is the 'long wave'

$$(3.9) \quad u = B \sin k(x-ct) + B \sin k(x+ct) \\ = 2B \cos ckt \sin kx .$$

Since $u_x = v_y = 0$ and $v = 0$ on the horizontal bottom $y = 0$, the vertical velocity is:

$$(3.10) \quad v = 2kBy \cos ckt \cos kx .$$

It is greatest at the crests and troughs of the wave, where $kx = n\pi$ and the horizontal velocity is zero. The horizontal velocity is greatest at the nodes of the waves, where

$x = \pm\pi/2k, \pm3\pi/2k, \dots$. The variations in elevation are easily computed from (3.10) to be

$$(3.10') \quad \eta = (2Bh/c) \sin ckt \cos kx ,$$

since $y = h$ at the surface; they are 90° out-of-phase in space and time with the horizontal velocity field.

Seiches. In a shallow tank of constant depth h and length ℓ , such sinusoidal 'long' periodic standing waves of the special form

$$(3.11) \quad u_m = \begin{cases} \cos \\ \sin \end{cases} ck_m t \sin k_m x, \quad k_m = m\pi/\ell$$

form a basis for the 'long' horizontal surges or 'seiches'. Mathematically, these can be expressed as superpositions

$$(3.12) \quad u = \sum_{m=1}^{\infty} B_m \sin k_m x \cos [ck_m (t-t_m)]$$

of such sinusoidal waves.

The approximations made in deriving the preceding formulas are valid when $\lambda = 2\pi/k = 2\ell/m \gg h$, and the maximum surface slope

$$(3.13) \quad (\eta_x)_{\max} = khB/c \ll 1 .$$

The dominant mode of oscillation is commonly that of 'sloshing', with $k = 1$. In this case, the condition (3.13) is simply that the vertical amplitude $(hB/c) \ll 1$, or $B \ll \sqrt{g/h}$.

4. Potential flows. In a fluid of constant density ρ_0 , conservation of mass is equivalent to incompressibility, i.e., to conservation of volume. Moreover, the net flux of mass out of any bounded region Ω with boundary $\Gamma = \partial\Omega$ is evidently

$$\iint_{\Gamma} \rho_0 u_n dS = \rho_0 \iint_{\Gamma} \underline{u} \cdot d\underline{S} .$$

By the Divergence Theorem, the last integral equals $\iiint_{\Omega} \nabla \cdot \underline{u} dR$.

Hence mass conservation (zero net flux of mass) is equivalent to

$$(4.1) \quad \nabla \cdot \underline{u} = \sum \partial u_k / \partial x_k = \text{div } \underline{u} = 0 .$$

This is a special case of Euler's Eq. (2.2), and is obtainable from it by setting $\rho = \rho_0$, whence $\rho_t = 0$ and $\nabla \cdot (\rho \underline{u}) = \rho_0 \nabla \cdot \underline{u}$.

Definition. By a potential flow is meant a volume-conserving flow whose velocity-field $\underline{u}(\underline{x};t)$ has at all times t a single-valued velocity potential $\phi(\underline{x};t)$ such that $\underline{u} = \nabla \phi$, i.e., whose velocity-field is a gradient field. Substituting from $\underline{u} = \nabla \phi$ into (4.1), we get Laplace's equation

$$(4.2) \quad \nabla^2 \phi = 0 \quad \text{in any potential flow.}$$

In a simply connected region, the existence of a velocity potential is equivalent to the condition that the vector vorticity vanishes:

$$(4.3) \quad \underline{\omega} = (\xi, \eta, \zeta) = (w_y - v_z, w_x - u_z, v_x - u_y) = \underline{0} .$$

Thus, in tensor notation, $\underline{u} = \nabla \phi$ implies

$$\partial u_i / \partial x_j - \partial u_j / \partial x_i = \partial^2 \phi / \partial x_i \partial x_j - \partial^2 \phi / \partial x_j \partial x_i = 0 .$$

Stated loosely, a flow in a simply connected domain is a 'potential flow' if and only if its velocity-field is incompressible and irrotational. However, in the multiply connected exterior of the unit circle $r = 1$, the velocity-field

$$(-y/r^2, x/r^2) = \text{grad } \theta, \quad \theta = \arctan y/x ,$$

is not strictly a potential flow, because θ is multiple-valued.

Example 1. In three dimensions, the velocity-field of a simple source, with velocity potential $\phi = -1/r$, is a potential field. So is that of an axial dipole, with $\phi = \partial(-1/r) / \partial x_i$.

In the velocity-field of a simple source, $u_i = \partial \phi / \partial x_i = x_i / r^3$, whence

$$\nabla^2 \phi = \sum_{i=1}^3 \partial u_i / \partial x_i = 3/r^3 - 3[x_i^2/r^5] = 0 .$$

For a dipole parallel to the x-axis, the potential is $\phi = \partial(1/r)/\partial x = -x/r^3$, whence the velocity-field is

$$(4.4) \quad \underline{u} = \nabla\left(\frac{-x}{r^3}\right) = \frac{1}{r^5}(-r^2 + 3x^2, 3xy, 3xz) \\ = r^{-5}(2x^2 - y^2 - z^2, 3xy, 3xz) .$$

The outward radial velocity component of this field is clearly

$$(*) \quad u_r = (xu + yv + zw)/r \\ = r^{-6}[2x^3 - xy^2 - xz^2 + 3xy^2 + 3xz^2] = 2x/r^4 .$$

Bernoulli equation. We now derive another form of the Bernoulli equation.

THEOREM 1. In a fluid of constant density ρ_0 , Euler's equation of motion (2.1) holds if and only if the pressure satisfies

$$(4.5) \quad p + \rho_0 G + \rho_0 \left[\frac{u_k^2}{2} + \rho_0 A(\underline{x}; t) \right] = P(t) ,$$

where $P(t)$ is a constant depending only on the time, and $A(\underline{x}; t)$ is an acceleration potential, so that $\nabla A = \underline{u}_t(\underline{x}; t)$.

Proof. Setting $\rho = \rho_0$ in (2.1), we get

$$\partial u_i / \partial t + \sum u_k \partial u_i / \partial x_k = g_i - \partial p / \rho_0 \partial x_i .$$

But since $u_i = \partial \phi / \partial x_i$, $\partial u_i / \partial x_k = \partial u_k / \partial x_i$. Hence if $g_i = \partial G / \partial x_i$, (2.1) is equivalent to

$$\frac{\partial u_i}{\partial t} + \sum u_k \frac{\partial u_k}{\partial x_i} = \frac{\partial G}{\partial x_i} - \frac{1}{\rho_0} \frac{\partial p}{\partial x_i} .$$

Multiplying through by dx_i and summing over i , we get

$$\sum \frac{\partial u_i}{\partial t} dx_i + d(\sum u_k^2/2) = dG - \frac{dp}{\rho_0} .$$

Hence at any time t , $\sum (\partial u_i / \partial t) dx_i = d[G - \sum u_k^2/2 - \frac{P}{\rho_0}]$, is an exact differential dA . It follows that $\underline{u}_t = \nabla A$ is a gradient field. If we call the A for which $\underline{u}_t = \nabla A$ the acceleration potential, and multiply by $\rho_0 m$ then we have

$$d[\rho_0 (A - G - \sum u_k^2/2) - p] = 0 ,$$

whence the quantity in square brackets depends only on t , and may be denoted $P(t)$.

COROLLARY. In steady (time-independent potential flow, we have $A(t) = 0$, and so

$$(4.5') \quad p + \rho_0 G + \rho_0 q^2/2 = P(t), \quad q^2 = \sum u_k^2 .$$

This form of the Bernoulli equation is one of the most useful equations of hydraulics and aeronautics.

Flow around a sphere. As an example, we consider the axially symmetric flow with harmonic velocity potential

$$(4.6) \quad \phi(\underline{x}) = [r + (a^3/r^2)]U \cos \phi ,$$

and velocity field

$$(4.6') \quad \underline{u}(\underline{x}) = U\mathbf{x} + \frac{Ua^3}{2r^3}(2x^2 - y^2 - z^2, 3xy, 3xz) ,$$

obtained by superposing a uniform flow with constant velocity U parallel to the x -axis on an opposing dipole velocity-field. (Note that since the Laplace equation $\nabla^2 \phi = 0$ is linear, any linear combination of harmonic velocity potentials is itself harmonic.) On the x -axis $y = z = 0$, $\phi = Ux + Ua^3/x$ and so $u = \phi_x = U - a^3U/x^2$. The velocity is thus zero at $(\pm a, 0, 0)$: these are stagnation points of the flow.

More generally, everywhere on the sphere $r = a$ (i.e., $x^2 + y^2 + z^2 = a^2$), the radial velocity is $u_r = U_x/r - (Ua^3/2)(2x/a^4)$, by (*), and this vanishes when $r = a$. The flow is thus tangential to the sphere $r = a$.

It is a good exercise to work out the pressure distribution for the potential flow around a sphere obtained in this way.

5. Plane potential flows. In general, a planar (or "two-dimensional") flow is one whose velocity-field can be written as

$$(5.1) \quad \underline{u}(x;t) = (u(x,y,t)v(x,y,t), t)$$

in a suitable rectangular coordinate system. It is then said to be parallel to the (x,y) -plane $z = 0$. Hence a plane potential flow is one having a velocity potential $\phi = \phi(x,y)$ that satisfies $\phi_{xx} + \phi_{yy} = 0$.

Complex potential. If $\phi = \phi(x,y)$ is any harmonic function of two variables, with gradient $(u(x,y), v(x,y)) = \nabla\phi$, then $d\psi = (u dy - v dx)$ is an exact differential since $u_x + v_y = 0$. Moreover the complex potential $W(x,y) = \phi + i\psi$ ($i = \sqrt{-1}$) is an analytic function of the complex position variable $z = x + iy$.

Indeed, this is immediate since the Cauchy-Riemann equations⁵ are

$$(5.2) \quad \phi_x = \psi_y = u(x,y), \quad \phi_y = -\psi_x = v(x,y).$$

The complex derivative $dW/dz = u - iv$ is moreover the complex conjugate $\bar{\zeta}$ of the vector velocity $u + iv$. The verification of these remarkable formulas will be left to the reader; in the next section, we will see how useful they are.

Examples. For example $\ln z = \ln r + i\theta$ is the complex potential of a simple source, with velocity potential $\phi = \ln r$. In space, this corresponds to flow with radial velocity $\phi_r = 1/r$

⁵For the notions of exact differential, Cauchy-Riemann equations, etc., see Thomas or Finney-Thomas.

from a line source.

Differentiating, we get $d(\ln z)/dz = 1/z$, whence

$$u + iv = \zeta^* = 1/z^* = z/zz^* = z/r^2 .$$

Alternatively, we can consider $1/z = (x-iy)/r^2$ as the complex potential of a dipole flow. Its velocity is the complex conjugate of

$$\begin{aligned} d(1/z)/dz &= -1/z^2 = -(x-iy)^2/r^4 \\ &= -[x^2 - y^2, -2xy]/r^4 . \end{aligned}$$

This complex conjugate is easily shown to be $-[\cos 2\theta, \sin 2\theta]/r^2$. Hence the radial velocity is

$$\begin{aligned} u_r &= (xu_x + yu_y)/r = (-x^3 + xy^2 - 2xy^2)/r^5 \\ &= -xr^2/r^5 = -x/r^3 . \end{aligned}$$

It is easy to show that the superposition

$$(5.3) \quad W = z + 1/z ,$$

of the complex potential of a uniform flow parallel to the x-axis with a dipole flow, gives a plane potential flow around the cylinder $r = 1$. We could prove this by computing $u_r = 0$ when $r = 1$, but it is more instructive to prove it in a different way.

Stream function. Namely, let us call the complex conjugate $\psi(x,y)$ of the velocity potential $\phi(x,y)$ the stream function of that flow. Since $\nabla\phi = (u,v)$ implies $\nabla\psi = (-v,u)$, we see that the lines $\psi = \text{const}$ (whence $d\psi = \psi_x dx + \psi_y dy = -vdx + udy = 0$) are everywhere tangent to the flow direction: they are streamlines. In the special case of (5.3), clearly

$$(5.3') \quad \psi = y - y/r^2 = (r - 1/r) \sin \theta ,$$

whence $\psi = 0$ is the streamline $r = 1$ (the flow is around the unit cylinder).

Similarly, the complex potentials $W = z + a^2/z$ and

$$\begin{aligned} W &= iz + a^2/iz \\ &= -(r+a^2/r) \sin \theta + i(r-a^2/r) \cos \theta , \end{aligned}$$

with stream functions $(r-a^2/r) \sin \theta$ and $(r-a^2/r) \cos \theta$ describe potential flows around the cylinder $r = a$, with 'free stream' vector velocities

$$U = \lim_{r \rightarrow \infty} (\psi_Y, -\psi_X) = (1,0) \quad \text{and} \quad (0,1) ,$$

respectively.

Elliptic cylinders. We now consider the effect of the transformation $z \mapsto (z + z^{-1}) = t$ on the circles $|z| = r = a > 1$ in the z -plane. Note that since $dt = (1 - z^{-2})dz$, the transformation is conformal (i.e., angle-preserving) except where $1 - z^{-2} = 0$, i.e., except at $z = \pm 1$. Writing $z = ae^{i\theta} = a(\cos \theta + i \sin \theta)$, we get

$$(5.4) \quad t = (a + a^{-1}) \cos \theta + i(a - a^{-1}) \sin \theta .$$

This is an ellipse with major semi-axis $\alpha = a + a^{-1}$ and minor semi-axis $\beta = a - a^{-1}$. Moreover the flow speed $q = |dW/dz|$ goes into

$$q' = |dW/dt| = q|dz/dt| = q/|1 - z^{-2}| .$$

Finally, $|1 - z^{-2}| = |z - z^{-1}|/|z| = |z - z^{-1}|/a$, where

$$\begin{aligned} |z - z^{-1}| &= [(a - a^{-1})^2 \cos^2 \theta + (a + a^{-1})^2 \sin^2 \theta]^{1/2} \\ &= [(a^2 + a^{-2}) - 2 \cos 2\theta]^{1/2} . \end{aligned}$$

We conclude that

$$(5.5) \quad q' = aq/[(a^2 + a^{-2}) - 2 \cos 2\theta]^{1/2} .$$

We will show in §7 how to extract useful numerical information from these formulas.

6. Gravity waves. We next take up the beautiful mathematical theory of periodic (sinusoidal) "surface waves" in an ocean of infinite depth, and more generally of analogous waves in a "lake" (or "canal") of constant finite depth h . This theory, due to Green (1839) and Airy (1845),⁶ assumes the potential flow model of §4, in an 'ideal' (incompressible, inviscid) fluid of constant density. In other words, it assumes that a velocity potential $\phi(\underline{x};t)$ exists and satisfies the Laplace equation

$$(6.1) \quad \nabla^2 \phi = 0 \quad \text{inside the liquid .}$$

To determine the flow mathematically, one must also impose suitable boundary conditions. One boundary condition is obvious. On the horizontal bottom, the condition of no penetration by the water (or other liquid) implies that the fluid velocity u_n normal to the boundary must be zero. Hence we have

$$(6.2) \quad \partial \phi / \partial n = 0 \quad \text{on the fixed bottom .}$$

To utilize the physically plausible⁷ 'free surface' condition of constant atmospheric pressure,

$$(6.3) \quad p = p_{\text{atm}} = \text{const.} \quad \text{on the liquid surface,}$$

is more difficult. Indeed, to make the resulting boundary value problem mathematically tractable, this condition is usually linearized to give the second boundary condition:

$$(6.4) \quad \phi_{tt} = g\phi_y \quad \text{on the 'mean water level' } y = 0 .$$

We will next derive Eq. (6.4), assuming a vertical gravity field with $G = gy$, y being the depth below the water level, to prove

⁶See Lamb [A6, pp. 367, 368] footnotes.

⁷This is plausible because the ratio ρ'/ρ of the density of air to that of water is so small (about .0013), so that its inertia is negligible in a light breeze. Clearly (6.4) is most accurate for waves of 'small amplitude'.

THEOREM 5. Equations (6.1), (6.2), and (6.4) are valid for waves of infinitesimal amplitude, in an incompressible, non-viscous fluid in a uniform vertical gravity field.

Proof. By the Bernoulli equation for potential flow,

$$(6.5) \quad p/\rho_0 + [q^2/2 - G + \partial\phi/\partial t] = F(t) ,$$

the free surface condition (6.3) is equivalent to

$$(6.6) \quad G - \partial\phi/\partial t - \frac{1}{2} \nabla\phi \cdot \nabla\phi = F(t) .$$

If the free surface is nowhere vertical, so that it can be expressed by an "elevation function" $\eta(x,z;t)$, with

$$(6.7) \quad -y = \eta(x,z;t) \quad \text{on the free surface,}$$

then equation (6.6) is exact on $-y = \eta$. Moreover, since any $\phi + F(t)$ is just as valid a velocity potential as ϕ (they have the same gradient everywhere at all times), we can assume $F(t) = 0$ without losing generality.

Finally, we linearize. In the case of waves of small amplitude: it is reasonable to neglect terms quadratic in the velocity, like $q^2 = \nabla\phi \cdot \nabla\phi$. This reduces (6.6) to

$$(6.8) \quad gy + \partial\phi/\partial t = 0 \quad \text{on } y = -\eta .$$

Moreover, to a higher order of infinitesimal, $-\partial\eta/\partial t = \partial\phi/\partial y = v$, the vertical component of velocity. Hence, using (6.8), we get

$$(6.9) \quad g \partial\phi/\partial y = -g \partial\eta/\partial t = \partial^2\phi/\partial t^2 \quad \text{on } y = -\eta .$$

For waves whose amplitude is small in comparison with the wave length λ , this implies the same equation on $y = \alpha$, which is (6.4) above. Q.E.D.

Periodic standing waves. Since Airy's model for gravity waves is linear, we can apply harmonic analysis to express a wide class of solutions as superpositions (Fourier integrals) in time

of simply harmonic, periodic standing waves having velocity potentials of the form

$$(6.10) \quad \phi(x, y, z; t) = \begin{cases} \sin \\ \cos \end{cases} \omega t \phi(x, y, z) .$$

The product (6.10) satisfies Eqs. (6.1) and (6.2) if and only if

$$(6.11) \quad \nabla^2 \phi = 0, \quad \text{and} \quad \partial \phi / \partial n = 0 \quad \text{on fixed boundaries.}$$

Equation (6.4) holds if and only if

$$(6.12) \quad g \frac{\partial \phi}{\partial n} = \omega^2 \phi \quad \text{on} \quad y = 0 .$$

Hence Eqs. (6.11)-(6.12) are characteristic for (simply) periodic standing waves.

Ocean waves. A limiting case of especial interest concerns waves in an 'ocean' of infinite depth. In this case, there is no fixed boundary; hence we replace the equation $\partial \phi / \partial n = 0$ of (6.11) by the condition that it must hold asymptotically at great depths.

Actually, the velocity dies off exponentially with depth: it is easy to verify that, for any $k > 0$, the 'reduced velocity potential' $\phi = \begin{cases} \sin \\ \cos \end{cases} kx e^{-ky}$ dies off exponentially with depth and satisfies $\nabla^2 \phi = 0$ (hence (6.11)). In the 'small amplitude' approximation of the linearized free surface condition (6.12), therefore,

$$(6.13) \quad \phi(x, y, z; t) = \begin{cases} \sin \\ \cos \end{cases} kx e^{-ky} \begin{cases} \sin \\ \cos \end{cases} \omega t$$

is the velocity potential of a possible (standing) ocean wave if and only if (6.12) holds. The condition for this is easily verified to be $\omega^2 = gk$.

By superposing standing waves of the form (6.13), we can construct progressive ocean waves with velocity potentials

$$(6.13') \quad \cos(kx+\omega t) = \cos kx \cos \omega t \pm \sin kx \sin \omega t .$$

Moreover, since $\omega = \sqrt{gk}$, the wave velocity $c = \omega/k$ (or 'celerity') of such waves is $\sqrt{g/k}$; since the wave length $\lambda = 2\pi/k$, we have

$$(6.14) \quad c = (g\lambda/2\pi)^{1/2} \quad \text{for ocean waves .}$$

Waves in a canal. The case of waves in a canal of constant depth h can be treated similarly. Here it is convenient to make $y = 0$ the bottom of the canal, and to direct y vertically upward. The reduced velocity potential

$$(6.15) \quad \phi(x,y) = \begin{cases} \sin \\ \cos \end{cases} kx \cosh ky$$

satisfies (6.11), for any $k > 0$. Moreover (6.12) holds if and only if $\omega^2 \cosh kh = gk \sinh kh$, whence the wave velocity is

$$(6.16) \quad c = \omega/k = [gk \tanh kh]^{1/2}/k \\ = \sqrt{\frac{g\lambda}{2\pi} \tanh (2\pi h/\lambda)} .$$

The predicted wave velocities (6.14) and (6.16) have been very well confirmed experimentally.

Particle orbits. In standing waves, the motion of any particle is sinusoidal and in one direction. It is vertical at the crests and troughs, and horizontal at the 'nodes' midway between these. In progressive waves, the orbits are circular in deep water, and elliptical in shallow water.

7. Inertial similarity. The idea of similarity, which underlies dimensional analysis and the use of scale models, is one of the most important ideas of physics. Prandtl-Tietjens devote Chapter II of [A8] to it; for a thorough discussion of it, see [A2, Chapters IV and V].

To explain 'similarity', one should first define a group of transformations as a set of transformations of 'space' or 'space-time' which contains with any two transformations their product (the result of performing them in succession), and with any one transformation its inverse.

Evidently, all the laws of Newtonian physics are invariant under translations $\underline{x} \rightarrow \underline{x} + \underline{a}$ of space. They are also invariant under all rotations $\underline{x} \rightarrow A\underline{x}$, A an arbitrary orthogonal matrix with $AA^T = I$. In particular, they are invariant under reflections like $(x_1, x_2, x_3) \rightarrow (-x_1, x_2, x_3)$ and $(x_1, x_2, x_3) \rightarrow (-x_1, -x_2, -x_3)$.

Some geometric facts. For convenient reference, we recall a few important geometric facts. By definition, reflections are orthogonal transformations T such that $T^2 = I$; if $T\underline{x} = A\underline{x} + \underline{b}$, this implies that $A = A^t$ (that A is a symmetric matrix). Any rigid motion of the plane is a translation $\underline{x} \rightarrow \underline{x} + \underline{c}$ or a rotation $(\underline{x} - \underline{c}) \rightarrow A(\underline{x} - \underline{c})$ about a fixed center \underline{c} if $|A| = 1$, and a reflection if $|A| = -1$. In space, Euler proved that a rigid motion $\underline{x} \rightarrow A\underline{x}$ with determinant $|A| = 1$ is necessarily a rotation through some angle about some 'axis of rotation' (its unique real eigenvector). Any reflection has at least three orthogonal eigenvectors ($\underline{x} \rightarrow -\underline{x}$ obviously has many more).

Together, translations and rotations generate the Euclidean group of all rigid motions of space. If we neglect the earth's (vertical) gravitational field, the laws of fluid mechanics are also invariant under this group. Consequently, we can locate the origin and axes of any rectangular ('Cartesian') coordinate system wherever we like, without altering the differential equations used, provided gravity can be neglected.

Hydrostatic buoyancy. In an ideal fluid of constant density ρ_0 the net effect of gravity is to add a resultant buoyancy force $\rho_0 V$ acting through the center of gravity of any immersed solid (generalized Law of Archimedes). To prove this, we note that the effect of a conservative gravitational field $\underline{g} = -\nabla G$, with gravitational potential $G(\underline{x}; t)$, is simply to superimpose a hydrostatic pressure field $-\rho_0 G(\underline{x}; t)$ on the dynamic pressure

field needed to accelerate the fluid. This is, of course, only true if space is filled with the ideal fluid; if it has a free surface, waves are propagated by gravity as described in §§3, 6.

THEOREM. In a space-filling ideal fluid, the pressure field is the algebraic sum of the hydrostatic pressure field due to gravity, the dynamic pressure due to the fluid motion, and an arbitrary constant (the 'pressure at infinity').

Hence in studying flows around submarines, and around airplanes at speeds up to 200 mi/hr, we can eliminate gravity from the equations of motion, and use the Euclidean group. We shall discuss buoyancy forces further in Chaps. 2, 4, and 7 below.

The inertial group. Actually, the Euler-Lagrange DE's for an ideal fluid of constant density ρ_0 are invariant under a much larger 'inertial group', which includes all changes of scale of length ($\underline{x} \mapsto \alpha \underline{x}$), time ($t \mapsto \beta t$), and mass ($\rho_0 \mapsto \gamma \rho_0$). This is easily verified mathematically by direct substitution. In this verification, it helps to remember that all velocities are multiplied by α/β under such a transformation, so that

$$(7.1) \quad \underline{u}(\underline{x};t) \mapsto \underline{v}(\alpha \underline{x};\beta t) = (\alpha/\beta) \underline{u}(\underline{x};t) .$$

Likewise, dynamic pressures p are multiplied by $\alpha^2 \gamma / \beta^2$, since pressure = force/area = (density \times volume \times acceleration)/area.

Similarity. The preceding result, though easily verified mathematically, is so important physically that we will discuss it in some detail here, and elaborate on its significance later in many places. First of all, note that changes of length scale $\underline{x} \mapsto \alpha \underline{x}$ characterize geometric similarity (as contrasted with congruence under the Euclidean group). The similarity group of geometry consists of all products of translations, rotations, and changes of scale. It is this 'similarity group' that is exploited in map-making, and similarity plays a key role in Euclidean geometry.

When a change of length scale is combined with a change of time scale, $t \mapsto \beta t$, we get what is called kinematic similarity.

This is what is exploited in 'slow motion' pictures. These transformations, together with transformations to 'moving axes', moving with constant velocity, generate the so-called Galilei-Newton group, described by Felix Klein as the group leaving Newtonian mechanics invariant.⁸

Now consider ideal fluids specifically. Any such fluid is characterized physically by its density ρ_0 ; two kinematically similar fluid motions (velocity-fields $\underline{u}(\underline{x};t)$) which differ only in the (constant) densities $\rho_0, \rho_1 = \gamma \rho_0$ involved are said to be dynamically similar.⁹ In two such dynamically similar flows, corresponding masses obviously differ by the constant factor $\gamma \alpha^3$.

Pressure coefficient. The addition of a constant pressure to any ideal fluid motion, by the transformation $p \rightarrow p + p_0$, also preserves the Euler-Lagrange equations. To compensate for this in analytical fluid dynamics, one usually considers the overpressure $p - p_\infty$, where p_∞ is an assumed limiting "pressure at infinity". Note that the addition of a constant pressure does not affect the hydrostatic buoyancy discussed earlier in this section, since its resultant $p_0 \iint dS = 0$.

To avoid the ambiguity inherent in the ambient pressure level (called the 'pressure at infinity' in aerodynamics), one usually considers the overpressure coefficient defined by

$$(7.2) \quad C_p = (p - p_\infty) / \frac{1}{2} \rho U^2 ,$$

where p_∞ is the 'ambient pressure' (pressure at infinity), and U is a 'characteristic velocity' (usually, the relative velocity of a solid object moving through a fluid).

⁸After the advent of Einstein's special relativity, Klein contrasted the Galilei-Newton group with the Lorentz group of Lorentz and Poincaré, which governs Maxwell's electromagnetic theory and relativistic mechanics.

⁹The descriptive name "dynamically similar" was coined by Rayleigh; the group of transformations leaving the theory of ideal fluids invariant includes the Galilei-Newton group and Rayleigh's group (which was used earlier by Fourier implicitly).

THEOREM. Any two similar flows of an ideal fluid of constant density have the same pressure coefficient at corresponding points.

One can easily verify the truth of this statement in the special cases of the potential flows around a sphere and a cylinder, derived in §§4-5 above; we omit the general proof.

Reversibility paradox. The preceding theorem has a surprising and disconcerting corollary, whose devastating significance seems to have been first appreciated by d'Alembert. Namely, if one reverses any steady flow satisfying the Euler-Lagrange equations by the transformation $\underline{u} \rightarrow -\underline{u}$, and leaves the pressure distribution and \underline{x} unchanged, then the Euler-Lagrange equations will still be satisfied for the same $\rho = \rho(p)$. Hence flow reversal should leave the net thrust on an obstacle unchanged; moreover this theoretical prediction applies to compressible as well as to incompressible non-viscous fluids. Since in fact the net thrust is usually reversed, we may call the preceding theoretical result the reversibility paradox associated with the Euler-Lagrange equations.¹⁰

As a corollary of this reversibility paradox, if an obstacle having fore-and aft symmetry is moving steadily through a fluid, the drag (if determinable theoretically from the Euler-Lagrange equations) must be zero. For, the predicted pressure distribution (if well-determined by theory) will be invariant under $\underline{x} \rightarrow -\underline{x}$, $\underline{u} \rightarrow \underline{u}$.

Again, one can easily verify the truth of this statement (usually referred to as the d'Alembert paradox) in the special cases of the potential flows around a sphere or cylinder.

8. Fluid resistance. In general, the problem of explaining quantitatively the thrust exerted by a fluid on a solid moving steadily through it must be regarded as unsolved. As Lamb

¹⁰ For more detailed discussions of the reversibility paradox, see [A2, §§6, 18], and Am. J. Math. 68 (1946), 247-56.

observed, "our knowledge of it is still largely empirical" [A6, §370].

However, the ideal fluid model does predict correctly the dimensional variation of the pressure and the pressure thrust, over wide ranges. Indeed, in ranges of ρ , d , and U over which the total drag D varies by a factor of 10^4 , the dimensionless drag coefficient $C_D = 8D/\pi d^2 U^2$ normally varies by a factor of less than five. Moreover, several useful ideal fluid models have been constructed which simulate qualitatively (up to a factor of two or so) the most important phenomena associated with fluid resistance. The rest of this chapter will describe several such models, all based on the theory of ideal ('frictionless') fluids of constant density. The effects of compressibility and viscosity will be discussed in Chapter 2.

In general, as might be expected from ideal fluid models, "the agreement between theoretical and experimental results becomes better as the viscosity becomes smaller".¹¹ This is especially true of streamlined bodies, to which a thin "boundary layer" clings as the fluid flows by, without "separating" until the extreme rear is reached. The art of "streamlining" airfoils and struts, so as to minimize the resistance ("form drag") associated with flow separation, will be discussed again (from a mathematical standpoint) in Chapters 4 and 7 below.

Flows past properly streamlined bodies can have very small drag indeed, less than 2% of that of a broadside flat plate of the same cross-section. This is in some sense a vindication of the d'Alembert paradox!

On the other hand, when "the boundary layer leaves the body", it is not easy to obtain even qualitative agreement between theory and experiment. For "bluff bodies" such as a broadsiding flat plate, cylinder, or sphere, the best 'ideal fluid' model of resistance is provided by the 'wake' theory to be introduced in

¹¹We are quoting freely from the Introduction to [A8], here and below.

the next section, and discussed more carefully in Chapter 4. If suitable allowance is made for 'wake underpressure', this predicts quite well not only the net resistance, but also the entire pressure distribution around the body. We will give some specific comparisons in Chapters 4 and 7.

By superposing a suitable plane vortex flow on potential flow, a quite realistic model of airfoil lift can also be constructed. We will discuss this model in §§11-13; its predictions are naturally most reliable for highly streamlined airfoils at small angles of attack, from which flow separation occurs (on the upper side) for back, quite near the 'trailing edge'. The 'drag' under such circumstances (still zero for the model of §11) is largely due to boundary layer 'skin friction', to be discussed in Chapters 2 and 7, and an 'induced drag' due to a three-dimensional 'vortex sheet' behind the airfoil.

Angle of stall. At higher angles of attack, the point of flow separation can jump rapidly from (near) the trailing to the leading edge; making the drag increase and the lift decrease dramatically. The angle at which this occurs is called the "angle of stall", and the occurrence of 'stall' is justly dreaded by airplane pilots. Kirchhoff's wake model (§9) provides the most realistic simple mathematical model for the pressure distribution above the angle of stall.

Added mass. Although potential flow theory gives in general a totally unrealistic prediction of the real fluid resistance to steady flow, it predicts very well the fluid resistance to acceleration, especially from rest (with $\underline{u}(x;0) = 0$). We will derive next the fluid resistance encountered by a cylinder and of a sphere, accelerated from rest in an ideal fluid.

In this case formula (4.5) simplifies to

$$(8.1) \quad p + \rho_0 G + \rho_0 A(x;t) = p_\infty(t) .$$

Hence the theoretical pressure differs from the hydrostatic pressure $p_\infty(0) - \rho_0 G$ by $-\rho_0 A(x;0)$, where $A(x;0)$ is the

acceleration potential. If $a = \ddot{x}(t)$ is the acceleration of the C.G. the additional acceleration potentials are, for a circular cylinder of radius r moving with acceleration a

$$(8.2) \quad ax/r^2 = (a \cos \theta)/r$$

Hence, the additional 'acceleration pressure' on the surface of the cylinder is $(\rho_0 a \cos \theta)/r$. Note that, conforming to our hypothesis of 'acceleration from rest', we have assumed the fluid velocity at infinity to be zero. Integrating the axial pressure component over in $\theta \in [0, 2\pi]$, we get

$$(8.2') \quad F = \rho_0 a \oint \cos^2 \theta \, d\theta = \pi \rho_0 a$$

for the net force. We thus have $F = ma$, where $m = \pi \rho_0$ is the mass of the water displaced by the cylinder. This is called the added mass of the cylinder.

Inertial similarity. Note also, by the principle of inertial similarity (§7) for the motion of an ideal fluid, the preceding result must hold for a cylinder of arbitrary radius.

Similarly, for the axially symmetric potential flow around a unit sphere in an ideal fluid, at rest at infinity, the acceleration potential is

$$(8.3) \quad A = x/2r^3 = (\cos \theta)/2r^2 .$$

Hence the net force is

$$\frac{\rho_0 a}{2r^2} \int_0^\pi \cos^2 \theta \, dS(\theta), \quad dS(\theta) = 2\pi a^2 \sin \theta \, d\theta .$$

Since $\int_0^\pi \cos^2 \theta \sin \theta \, d\theta = [-(\cos^3 \theta)/3]_0^\pi = 2/3$, the net thrust on the sphere is easily computed from this formula; it is ma , where $m = 2\pi \rho_0/3$ is half of the mass of displaced fluid (e.g., water). We conclude

THEOREM. The added mass of a circular cylinder equals the mass of the water that it displaces; that of a sphere is half of the mass of the water displaced.

*9. Free streamlines; wakes.¹² We next describe some steady plane potential flows bounded by 'free' streamlines at constant pressure. Most notable is an ingenious wake model proposed by Kirchhoff in 1869. He treated in detail the flow past a flat plate moving broadside. He assumed that it was a two-dimensional potential flow that 'separated' at the plate edges and enclosed a stagnant wake at constant pressure, as in Fig. 3a. By adroit use of the conformal mapping technique introduced in §5, he was able to deduce a theoretical drag coefficient $C_D = 0.88$.

Jet from nozzle. The simplest model of a 'free streamline' is provided by a horizontal straight jet, issuing at constant speed from a nozzle, as in Fig. 1a, and surrounded by fluid at rest. In an ideal fluid, the bounding free 'streamlines of discontinuity' would be in equilibrium with the surrounding fluid on both sides.

Irreversibility of real jets. Physically, jets from nozzles, pipes and channels behave much as Fig. 1a suggests, though a vortex may form around the mouth if the jet discharges into a container, as we shall explain in §7. But if the direction of flow is reversed, and fluid is sucked into a pipe or channel instead, the streamline pattern looks entirely different. As is indicated in Fig. 1b, the streamlines come in radially toward the mouth (which acts as a 'sink') from all directions. This shows that real flows in and out of tubes are not reversible!

We now derive the exact plane potential flow having the streamlines indicated in Fig. 1b. To derive it, we will examine more carefully the complex variable interpretation introduced in §5, with special reference to conformal mapping techniques.

THEOREM. Let $\zeta(W)$ be a complex analytic function of the (complex) variable $W = \phi + i\psi$, and let

$$(9.1) \quad z = \int \zeta^{-1} dW .$$

¹²This section can be skipped in a first reading of this chapter, and returned to when potential flows are treated systematically in Chapter 3.

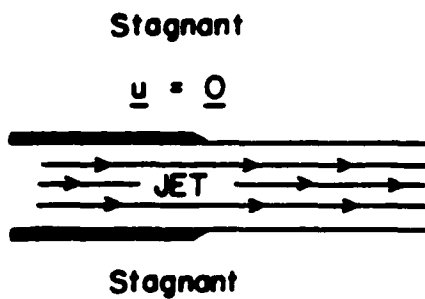


Figure 1a
Jet from tube

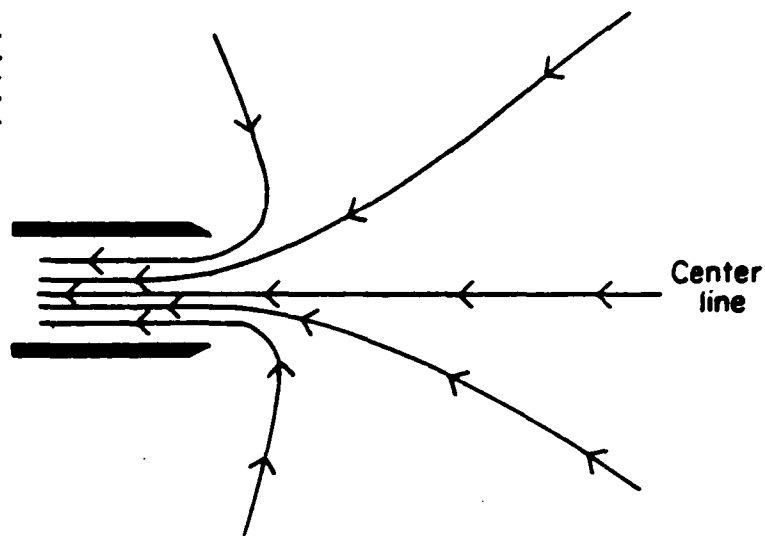


Figure 1b
Flow sucked into tube

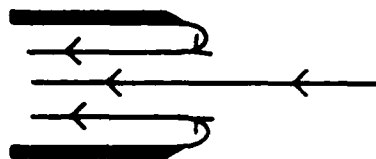


Figure 2
Borda tube

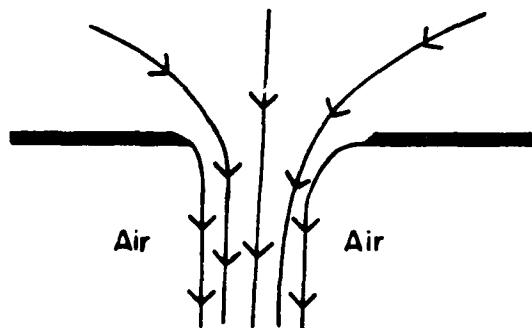


Figure 2b
Jet from slot

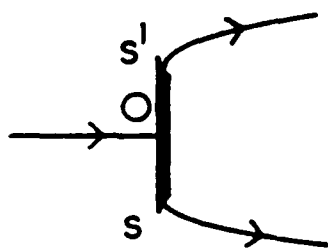


Fig. 3a

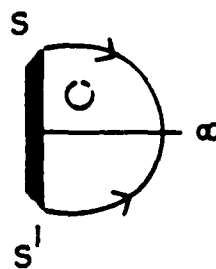


Fig. 3b



Fig. 3c

Then $W = \phi + i\psi$, where ϕ is the velocity potential of a potential flow, ψ its stream function at the point $z = x + iy$ in the physical plane. The complex conjugate $\zeta = u - iv$, is the vector velocity at the point $z = x + iy$.

Sketch of local proof. As in (5.2), the conditions of local incompressibility and irrotationality on the velocity-field $(u(x,y), v(x,y))$ for real x, y, u, v :

$$\frac{\partial u}{\partial x} = -\frac{\partial v}{\partial y}, \quad \frac{\partial u}{\partial y} = \frac{\partial v}{\partial x},$$

are equivalent to the Cauchy-Riemann equations on the complex variable $\zeta = u - iv$ as a function of $z = x + iy$. Hence, except where $\zeta = 0$ (i.e., except near stagnation points), they imply that $\zeta^{-1} = (u + iv)/(u^2 + v^2)$ is a complex analytic function of z . By the elementary theory of functions of a complex variable, it follows that (9.1), which in real form is

$$(9.2) \quad x = \int \frac{u d\phi - v d\psi}{u^2 + v^2}, \quad y = \int \frac{v d\phi + u d\psi}{u^2 + v^2},$$

defines $z = \int \zeta^{-1} dW$ locally as a complex analytic function of W --hence W as a complex analytic function of z .

We will now discuss complex potentials $W(z)$ associated with three different plane potential flows. In Chapter 4, we will describe conformal mapping techniques that make it possible to describe a wide variety of plane potential flows systematically.

Example 8.¹³ The function $z = e^{-W}$ -- W is associated with the potential flow into a channel. As was stated above, this gives a fair approximation to reality. It is the reverse of the potential flow out of a channel, whose complex potential is

$$(9.3) \quad z = e^W + W, \quad -\pi \leq \psi \leq \pi,$$

in the physical plane. Each is real on the real axis, where $\psi = 0$. Hence, it defines a flow having the (real) x-axis $y = 0$

¹³See Lamb [A6, p. 743].

as an axis of symmetry. Specifically, consider (9.3) as a conformal transformation mapping the infinite strip $-\pi \leq \psi \leq \pi$ in the W -plane onto the z -plane with channel walls $y = \pm 1$, $x \leq 0$ covered on both sides. On the boundary of the strip,

$$dz/dW = e^W + 1 = e^\phi (\cos \psi + i \sin \psi) + 1 = 1 - e^\phi,$$

since $\psi = \pm\pi$. Hence the (real) velocity $\zeta = u = dW/dz = 1/(1 - e^\phi)$ increases inside the channel from 1 at the upstream point at ∞ to infinity at the edges $z = \pm i\pi$ of the channel, reversing sign and tending to zero as $\phi \uparrow \infty$.

As Helmholtz noted, since $|u| = \infty$ at the edges of the plates $1 \pm i\pi$, there would be by Bernoulli's Theorem (3.1) infinite negative pressure at the edges of the plates, if the potential flow model was taken literally, and this would cause cavitation to occur.

Borda tube. Using his "free streamline" concept, Helmholtz constructed in 1868 a third mathematical model for flow into a channel. In this model, sketched in Fig. 2a, the flow "separates" from the edges of the channel ("Borda tube") to form a jet which fills only half of the tube. This avoids the paradox of infinite negative pressure mentioned above; we will postpone its mathematical derivation to Chapter 4.

In the Helmholtz model, the pressure is assumed to be constant in the (static) air on both sides of the jet. Hence by Bernoulli's Theorem (neglecting gravity), the flow velocity $q = (u^2 + v^2)^{1/2}$ is a constant on the free streamlines bounding the jet. The boundary of half the flow (above its axis of symmetry) thus bounds a semicircle in the ζ -plane, whose center corresponds to the 'stagnation point at infinity' outside the channel, where $\zeta = 0$. The function $\frac{1}{2}(\zeta + \zeta^{-1}) = T$ maps this semicircular hodograph (which we can take to be the unit semicircle by proper scaling) onto the lower half of the T -plane. In turn, $\ln T$ maps this onto an infinite strip in the W -plane (see Chapter 4 for more details).

Example 9. Helmholtz also constructed an analogous potential flow model for the jet from a slot. We have sketched this flow defined by Helmholtz in Fig. 2b. In this case ([A3, p. 33 and Chapter 4]), we have

$$(9.4) \quad W = \ln \zeta - \ln(\zeta^2 + 1)$$

whence $dW = d\zeta/\zeta - 2\zeta d\zeta/(\zeta^2 + 1)$ and

$$(9.5) \quad z = \int dW/\zeta = \ln \zeta + \arctan \zeta .$$

The predicted coefficient of contraction is $C_C = 0.611$, which is very near to that observed experimentally.

Kirchhoff's 'wake' model. In 1869, Kirchhoff applied Helmholtz's "free streamline" concept to define a plausible model for fluid resistance or drag D in a fluid of small viscosity, thus resolving the d'Alembert paradox within the framework of the Euler-Lagrange equations.

For a flat plate held broadside to an infinite stream, as sketched in Fig. 3, Kirchhoff assumed that the fluid approaching the plate underwent a plane potential flow that 'separated' at the plate edges S, S' , enclosing a stagnant wake at constant pressure. For this mathematical model, the predicted drag coefficient is $C_D = 0.88$.

10. Plane vortex flows. The following two examples show that not all steady plane flows of an ideal fluid are potential flows.

Example 10. For any velocity 'profile' $f(y)$, the flow $\underline{u}(x) = (f(y), 0, 0)$ of a fluid of constant density ρ_0 satisfies the Euler-Lagrange equations.

More generally, this is true of the flow through a straight pipe parallel to the x -axis, for any velocity profile $\underline{u} = (f(y, z), 0, 0)$.

Example 11. In cylindrical coordinates, any cylindrical swirl around the z -axis, with velocity components

$$(10.1) \quad u_r = u_z = 0 \quad \text{and} \quad u_\theta = f(r), \quad f \text{ arbitrary},$$

and $p = p_0 + \rho_0 \int_0^r u_\theta^2 dr/r$, satisfies the Euler-Lagrange equations.

In cylindrical swirls, the pressure obviously has to counteract the 'centrifugal force', which is $\rho u_\theta^2/r$ per unit volume. A very important special cylindrical swirl is the locally irrotational swirl around a point-vortex. This has the multiple-valued velocity-potential $\phi = \theta = \arctan(y/x)$, and hence the velocity $u_\theta = 1/r$ counter-clockwise, around the origin. Its complex potential is given by

$$(10.2) \quad W = \phi + i\psi = \theta - i \ln r = i \ln z.$$

Loosely speaking, we may say that the flow around a point-vortex is a potential flow except at the origin, which is a singular point.

Vortex lines. The three-dimensional flow corresponding to a point-vortex at the origin $(0,0,c)$ in each plane $z = c$ is said to be the flow around the vortex line $x = y = 0$ (the z -axis). This is again a locally irrotational potential flow with multiple-valued velocity potential $\phi = \arctan y/x$, and velocity field

$$(10.3) \quad u(x,y,z) = -y/(x^2+y^2), \quad v(x,y,z) = x/(x^2+y^2), \quad w = 0.$$

A very different vortex flow is provided by rigid rotation around the z -axis with angular velocity ω and velocity field $u = -y$, $v = x$, $w = 0$.

Vortex pairs. The motion of two or more point-vortices in the plane, each under the influence of the others, provides a very intriguing and suggestive model for vortex motion. The following simple examples are typical.

Example 12. Two point-vortices of equal strength α and the same sign, initially at $(\pm c, 0)$, gyrate around the origin in a circle; their coordinates at time t are

$$(10.4) \quad \pm c(\cos \omega t, \sin \omega t), \quad \text{where } \omega = \alpha/c .$$

Example 13. Two point-vortices of equal strength α and opposite signs, at $(\pm c, 0)$ when $t = 0$, translate with constant vertical velocity $(0, \alpha/c)$ perpendicular to the chord joining them, so that their paths are $(\pm c, \alpha t/c)$ for $t > 0$.

Wall effect. Note that the y -axis $x = 0$ is a streamline in Example 13. Hence we can replace one of the two point-vortices by a rigid wall, without affecting the flow. This suggests that a vortex will move parallel to a nearby straight rigid wall, with the same speed as would be induced by an equal and opposite vortex at the 'image point' under reflection in that wall. This is indeed the case. The analogous effect of a 'free surface' is equal and opposite.¹⁴

Trochoidal waves. An interesting family of unsteady plane vortex flows is provided by Gerstner's (1809) progressive "trochoidal" gravity waves in deep water. In Lagrangian coordinates, these are defined by

$$(10.5) \quad \begin{aligned} x(a, b; t) &= a + e^{-kb} \sin k(a + ct) \\ y(a, b; t) &= b + e^{-kb} \cos k(a + ct) . \end{aligned}$$

The pressure distribution associated by the Euler-Lagrange equations with the periodic plane vortex flow (10.5), in a uniform vertical gravity field of strength g , has a very remarkable property. Namely, when $c^2 = g\lambda/2\pi$, each particle surface $b = \text{const.}$ can be taken as a free surface at constant pressure. For details, see Lamb [A6, p. 421]; Lamb's normalization differs from (10.5) by a factor $1/k = \lambda/2\pi$. Note that the wave velocity c coincides with that predicted by Airy's linearized potential flow model for 'ocean waves'.

¹⁴The fascinating book on "Hydrodynamische Fernkräfte (Leipzig, 1900), based on 19th century researches of C. A. Bjerknes, treats analogous image effects for pulsating sources. The models treated in it are fundamental in the theory of underwater explosion bubbles. (See R. H. Cole, "Underwater Explosions", Princeton Univ. Press, 1950.)

Stream function. In an incompressible fluid, the line integral at any time t ,

$$(10.6) \quad \int_a^x [u(x,y)dy - v(x,y)dx] = \psi(x,y;t)$$

is independent of the path, because $u_x + v_y = 0$ (area is conserved). Hence it always defines a stream function $\psi(\underline{x},t)$ in (possibly time-dependent) plane flows of an ideal fluid, even though only locally irrotational flows have a velocity potential. Evidently, the velocity components of a plane vortex flow are the partial derivatives of its stream function: by the converse of (10.6), we have at any time t ,

$$(10.6') \quad u(x,y) = \psi_y, \quad v(x,y) = -\psi_x .$$

Vorticity. The vorticity $\underline{\omega}(\underline{x})$ of a velocity-field $\underline{u}(\underline{x}) = (u(\underline{x}), v(\underline{x}), w(\underline{x}))$ is defined as its curl:

$$(10.7) \quad \underline{\omega} = \nabla \times \underline{u} = (w_y - v_z, u_z - w_x, v_x - u_y) .$$

Substituting into (10.7) from (10.6'), we see that in plane vortex flow, we have generally at any time t ,

$$(10.7') \quad \zeta(x,y) = -\nabla^2 \psi ;$$

the vorticity is the Laplacian of the stream function.

Vorticity convection. We conclude this section by a classic characterization of those plane vortex flows of an ideal fluid which satisfy Euler's equations of motion.

THEOREM. In an ideal fluid, a plane flow satisfies Euler's equations of motion if and only if its vorticity satisfies the convection equation

$$(10.8) \quad D\zeta/Dt = \zeta_t + u\zeta_x + v\zeta_y = 0 .$$

Proof. To prove this result, we first define the circulation $\Gamma = \Gamma(t)$ of an instantaneous velocity field $\underline{u}(\underline{x};t)$ around a

closed curve γ is defined as the contour integral¹⁵

$$(10.8') \quad \Gamma(t) = \oint_{\gamma} \underline{u}(\underline{x};t) \cdot d\underline{x} = \oint_{\gamma} u_k dx_k = \oint_{\gamma} u_k(\underline{x};t) dx_k .$$

Since the vorticity ζ is the limit of the ratio (circulation)/(area enclosed) = Γ/A , as the area shrinks to zero, it suffices to prove that Γ is a constant. And this result, proved in its final form by Kelvin, is one of the most basic results of theoretical fluid dynamics. It can be suggestively restated as follows.

Principle of Invariance of Circulation. In an ideal fluid, the total circulation around any closed curve γ moving with the fluid is constant in time: Γ depends only on γ .

Sketch of proof.¹⁶ Since γ is assumed to move with the fluid, it suffices to prove that $D\Gamma/Dt = 0$. But by definition and the Euler's equations of motion, we have

$$(10.9) \quad D\Gamma/Dt = \oint_{\gamma} (D\underline{u}/Dt) \cdot d\underline{x} + \oint_{\gamma} \underline{u} \cdot D(d\underline{x}/dt) dt ,$$

where since $D\underline{u}/Dt = \underline{g} - \nabla p/\rho_0$,

$$(10.9') \quad \oint_{\gamma} (D\underline{u}/Dt) \cdot d\underline{x} = \oint_{\gamma} \underline{g} \cdot d\underline{x} - \frac{1}{\rho_0} \oint_{\gamma} \nabla p \cdot d\underline{x} .$$

The two path integrals on the right side of (10.9') are $\oint_{\gamma} dG = 0$ and $\rho_0^{-1} \oint_{\gamma} dp = 0$, respectively; hence it remains to evaluate the last term of (10.9). In Lagrangian coordinates $\underline{a} = (a_1, a_2, a_3)$, this is

$$\oint_{\gamma} u_k [D(\partial x_k / \partial a_i) / Dt] da_i = \oint_{\gamma} u_k [\partial u_k / \partial a_i] da_i .$$

Since this is $\oint_{\gamma} d(\frac{1}{2}u^2) = 0$, (10.9) simplifies to $D\Gamma/Dt = 0$, completing the proof.

¹⁵The analogies with the work integral $\int \sum X_k dx_k$ and the potential energy integral $\int \sum g_k dx_k$ are obvious.

¹⁶Many readers may wish to omit studying this proof; to make it rigorous requires much painstaking thought. Cf. Lamb [A6, Arts. 15-17].

Conversely, the condition that $D\zeta/Dt = 0$ is equivalent to the equation of plane motion (for some single-valued pressure function) in an inviscid, incompressible fluid. In Lagrangian coordinates, therefore, $\zeta = \zeta(a,b)$ must be independent of t , so that in steady flow $\zeta = F(\psi)$ must be constant on any streamline. Since $\zeta = \nabla^2\psi$, there follows a classic characterization of steady flows of an incompressible fluid whose motion is governed by inertia alone:

COROLLARY. The steady plane flows of an ideal fluid are the flows whose stream function satisfies the DE

$$(10.10) \quad \nabla^2\psi = F(\psi) .$$

11. Airfoil theory.¹⁷ When the powered flight of heavier-than-air vehicles began to seem like a real possibility, it became urgent to understand the lift L that would be experienced by an airfoil moving through the air with speed U at an 'angle of attack' α . According to the simplest and most natural interpretation of the (reversible) Euler-Lagrange equations, as we have seen, it would not experience any lift or drag at all!

When Rayleigh applied Kirchhoff's stagnant 'wake' model to this problem, he found that the predicted lift coefficient per unit area¹⁸

$$(11.1) \quad C_L = \frac{2L}{\rho U^2 \ell} = \frac{\pi \sin 2\alpha}{4 + \pi \sin \alpha}$$

was probably too small to sustain flight, and (fortunately) less than half of the real lift. It was not until around 1900 that the German Kutta and the Russian scientist Joukowsky invented a

¹⁷For a first-hand account of the 'heroic age of aeronautics', see Th. von Kármán, Aerodynamics, Cornell Univ. Press, 1954, especially Chapters 2 and 3.

¹⁸Formula (11.1), in which ℓ is the chord length, assumes the principle of inertial modeling. For low-speed aircraft ($U < 200$ knots) this holds very well.

fairly realistic, if ad hoc model that approximates quite well the aerodynamic flow producing lift at small angles of attack α , for well-designed (i.e., "streamlined") wings.

Magnus effect. The Kutta-Joukowski model assumes potential flow with nonzero circulation. A similar model had been previously used by Rayleigh, to explain "the irregular flight of a tennis ball", whose trajectory bends down under the influence of topspin, but which goes above its gravity trajectory when undercut. This so-called Magnus effect is also familiar in baseball, golf, and other sports, where it is observed that a spinning ball is acted on by an aerodynamic force that curves its trajectory in the direction of reverse spin. The following 'potential flow' model is often said to explain this phenomenon.

Example 14. For any 'circulation' Γ , the superposition of a dipole and a vortex of strength γ on a uniform stream has the potential

$$(11.2) \quad \phi = U(x + a^2x/r^2) - \gamma\theta .$$

It defines a flow having the cylinder $r = a$ as a streamline, with the stream function

$$(11.2') \quad \psi = U(y - a^2y/r^2) + \gamma \ln r ;$$

clearly $\psi = \text{const.}$ on the circle $r = a$.

It is interesting to compute the pressure distribution and the dividing streamlines for this flow, whose complex potential is, by (11.2) and (11.2')

$$(11.3) \quad W = \phi + i\psi = U(z + a^2/z) + i\gamma \ln z .$$

Clearly, $\phi = U(a + a^2/a) \cos \theta - \gamma\theta$ on the surface $|z| = a$ of the cylinder, whence

$$q = \partial\phi/\partial\theta = -2U \sin \theta - \gamma/a .$$

By Bernoulli's theorem, $p = p_\infty - \rho q^2/2$, giving

$$(11.4) \quad p = p_{\infty} - \rho [2U^2 \sin^2 \theta - (2\gamma U \sin \theta)/a + \gamma^2/2a^2] .$$

The resultant lift, $L = - \oint p a \sin \theta \, d\theta$, is by (11.4) the sum of integrals of constant multiples of $\sin^3 \theta$, $\sin^2 \theta$, and $\sin \theta$. Since by symmetry, $\oint \sin^3 \theta \, d\theta = \oint \sin \theta \, d\theta = 0$, and since $\oint \sin^2 \theta \, d\theta = \pi$, we thus conclude

$$(11.5) \quad L = 2\gamma U \rho \oint \sin^2 \theta \, d\theta = \rho \Gamma U, \quad \Gamma = 2\pi\gamma .$$

This is a special case of the following result.

THEOREM. The lift L associated with a plane potential flow of an ideal fluid with horizontal free stream velocity U and clockwise circulation Γ is $\rho U \Gamma$.

Method of proof. A quite short general proof can be constructed, using the conservation laws for mass and momentum [A7, Chapter XIV], and asymptotic formulas (valid for large z) of complex variable theory.

Proof. The Euler-Lagrange equations are equivalent to the law of conservation of momentum. Hence L must balance the net rate of efflux of vertical momentum per unit time, plus the integrated net downward external pressure, integrated over any large circle. We now compute these two terms by an asymptotic calculation, based on the (convergent) Laurent series expansion for horizontal flow with circulation:

$$(11.6) \quad W = Uz + \frac{i\Gamma}{2\pi} \ln z + \frac{c_1}{z} + \dots$$

Differentiating termwise, we see that the conjugate complex velocity is

$$(11.7) \quad \zeta = u - iv = U + \frac{i\Gamma}{2\pi z} + o(1/r^2) .$$

The underpressure $p = p_{\infty} - \frac{1}{2} \rho q^2$ is $\rho(\Gamma U/2\pi r) \sin \theta + o(1/r^2)$, and its vertical component is $\rho(\Gamma U/2\pi r) \sin^2 \theta$. Integrating over the circumference $2\pi r$, we get a net vertical pressure thrust of $\rho \Gamma U/2 + o(1)$.

Likewise the rate of efflux of mass per unit time and θ , ignoring $O(r^{-2})$ terms, is $\rho U \cos \theta$. The rate of loss in the vertical upward component of momentum is, by (11.7), $(\Gamma/2\pi r) \cos \theta$ per unit mass-efflux. Taking the product, and integrating with respect to θ from 0 to 2π , we get $\rho U \Gamma/2$, all plus $o(1)$. Since $\rho U \Gamma/2 + \rho U \Gamma/2 = \rho U \Gamma$, the proof is complete.

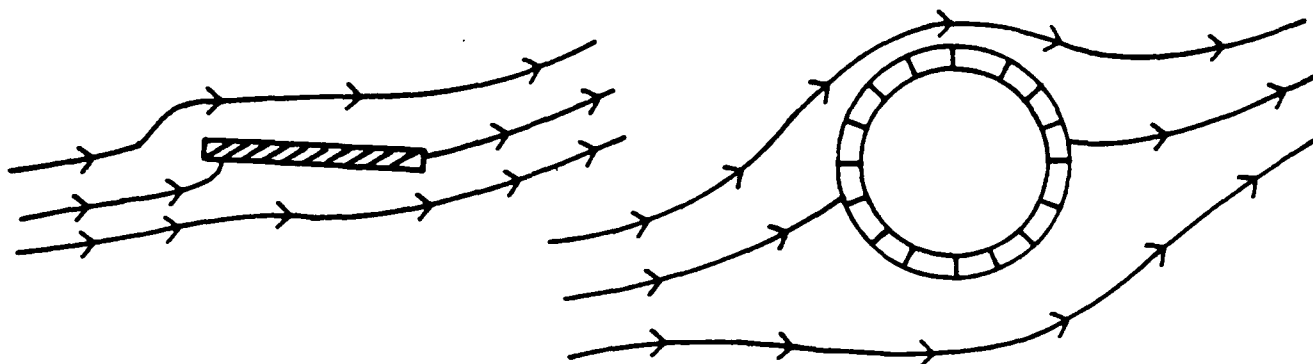
Two-dimensional lift theory. We now define the mathematical model used by Kutta and Joukowski to calculate the pressure distribution around airfoil sections having a given profile. Like the model used to rationalize the Magnus effect, their model assumes a multiple-valued, locally harmonic velocity potential of the form

$$\phi(x,y) = F(x,y) + \gamma \theta, \quad \theta = \arctan(y/x) = \text{Im}(\ln z),$$

where F is a globally harmonic function, whence $\nabla^2 \phi = 0$ since $\nabla^2 \theta = 0$. This model predicts a lift of $L = \rho U \Gamma$, where $\Gamma = \oint (u dx + v dy) = 2\pi \gamma$ is the circulation around the airfoil. The constant γ is chosen to assure "finite velocity at the trailing edge", where the flow is assumed to come together smoothly from both sides.

By the Fundamental Theorem of Conformal Mapping (not proved rigorously until around 1905), the exterior of the unit disk $|t| = 1$ can be mapped conformally onto the exterior of any closed curve by an analytic transformation of the form $z = kt + \sum_{k=0}^{\infty} c_k t^{-k}$, $k > 0$. For some unique γ , the inverse image of the 'trailing edge' can be made the rear stagnation point of the potential flow (11.2). Hence the potential flow of two-dimensional airfoil theory is mathematically well-defined in all cases.

For airfoils whose profile is a flat plate, this gives a complex potential $W = \phi + i\psi$ which can be obtained by the conformal transformation $z = \frac{1}{2}(t + t^{-1})$ from the flow (11.2) with circulation around a disk in an auxiliary t -plane and having just enough circulation to make the rear stagnation point at $t = 1$. For this flow, $U = 2$ and $\Gamma = 2\pi \sin \alpha$, since



$$(11.6) \quad W = e^{-i\alpha}t + e^{i\alpha}/t + (2i \sin\alpha)\ln t .$$

By the Kutta-Joukowski Theorem, the lift (strictly, cross-force)¹⁹ is therefore $L = 4\pi\rho \sin\alpha$, and $C_L = 2\pi \sin\alpha$, about four times the amount predicted by (11.1). In the case of streamlined airfoils at small angles of attack,²⁰ real flows are approximated fairly well by ideal Joukowski flows like (11.6).

Joukowski profiles. An especially simple class of examples, whose consequences were worked out by Joukowski in his pioneer paper, are provided by the images in the z -plane of the circles $|t + \epsilon| = 1 + \epsilon$ ($\epsilon > 0$). However, these are not very practical profile shapes, either structurally or aerodynamically. The mathematical treatment of practical airfoil profiles is fairly sophisticated, and will be taken up in Chapter 4.

Final remarks. The preceding ideal fluid model does not avoid the d'Alembert paradox of zero predicted drag, as can be shown by an easy calculation based on (11.2)-(11.2') in the case of a broadside cylinder, or a harder asymptotic calculation in the general case. Though the prediction of zero drag is obviously overoptimistic, the real lift is 75%-90% of that predicted, and real lift/drag ratios can be as much as 50.

¹⁹ This discrepancy is the Cisotti paradox of [A2, p. 15].

²⁰ At larger angles of attack $\alpha > 15^\circ$ (say), the flow separates ("stall") and Kirchhoff's 'wake' theory gives a better approximation!

The preceding 'two-dimensional theory of airfoil lift' was completely worked out by Richard von Mises during World War I, when airplanes had been flying for less than 15 years.²¹ One of its elegant formulas, based on an asymptotic calculation similar to that given above, and due to Lagally (ZaMM 2(1922), 409-22) gives also the moment of the pressure distribution of any potential flow around an airfoil. A Moebius transformation allows one to compute a potential flow with circulation around a circular arc airfoil. But unfortunately, predictions based on such more refined models are not very reliable.²²

*12. Vortex flows. We will next describe some basic properties of vortex flows in an ideal fluid (Model #2 of Table 1). An understanding of these properties helps to bridge the gap separating the theory of potential flows from that of incompressible viscous flows, to be taken up in Chapter 2. The general theory of vortex flows is also fascinating in its own right.

Vorticity. In general, the vorticity of a three-dimensional velocity field $\underline{u}(\underline{x})$, with $\underline{u} = (u, v, w)$ and $\underline{x} = (x, y, z)$ both 3-vectors, is defined as

$$(12.1) \quad \underline{\omega}(\underline{x}) = (w_y - v_z, u_z - w_x, v_x - u_y) .$$

In another notation, the vorticity is the antisymmetric or skewsymmetric tensor with

$$(12.2) \quad \omega_i = \partial u_{i+2} / \partial x_{i-1} - \partial u_{i-1} / \partial x_{i+1} \quad (i = 1, 2, 3) ;$$

one easily verifies that the divergence of the vorticity of any velocity field $\underline{u}(\underline{x}) \in C^2(\Omega)$ is zero.

In any velocity field with nonzero $\underline{\omega}(\underline{x}) \neq 0$, one can define the notion of a vortex line. This stands in the same

²¹Von Mises included it in pp. 832-42 of the German edition of Lamb (2d ed., Teubner, 1931).

²²See [A2, §§8-9]; also R. von Mises, Am. Math. Monthly (1940), 673-85; and G. Birkhoff, Am. J. Math. 68 (1946), 247-56.

relation to a vorticity field $\underline{\omega}(\underline{x})$ that lines of force do to a force field and that streamlines do to a velocity field. Namely, a vortex line is a curve which is tangent at every point to the vorticity vector $\underline{\omega} = \nabla \times \underline{u}$ at that point.

In a path-breaking paper written in 1858,²³ Helmholtz derived two remarkable theorems from the preceding definitions and the Euler-Lagrange equations. These assert the following:

1. Vortex lines move with the fluid.
2. The product of the cross-section area and the angular velocity of a 'vortex filament' are invariant in time.

Both of these are consequences of the principle of the invariance of circulation derived in §10. The connection is provided by the following theorem of vector analysis.

Stokes' Theorem. Vorticity is related to circulation by Stokes' Theorem:

$$(12.3) \quad \Gamma = \oint_C \underline{u} \cdot d\underline{x} = \oint_C \sum u_k dx_k = \iint_S \underline{\omega} \cdot d\underline{S} ,$$

where S is any surface spanning the curve C . Hence, in a simply connected domain Ω , such as the exterior of a sphere, a flow has a velocity potential if and only if its vorticity is everywhere zero.

It follows from Stokes' Theorem that:

(A) the vorticity vector at a point is the intersection of all planes through the point which have, locally, zero circulation per unit area. By the invariance of circulation, this property is conserved in an inviscid fluid, proving #1. Moreover by (A), we know that the sheath surrounding any vortex tube has the property that the circulation is zero around any closed curve on this sheath contractible to a point in the sheath. Hence the 'circulation' around any vortex tube is the same for every circuit going around it once, from which #2 follows.

²³Crelle 55 (1858), 25-55; Wiss. Abh. i, 101- . Under hypotheses to be stated in Chapter 2, Kelvin extended Helmholtz's theorems to compressible flows in Edin. Trans., 1869; Papers iv, 13-68.

Vortex lines. As a (singular) limiting case, one can imagine flows in which all the vorticity is concentrated in a single vortex line, around which the circulation is constant. The simplest example is the straight vortex line along the z-axis, with velocity field $(y/r^2, -x/r^2, 0)$, $r^2 = x^2 + y^2$. As Helmholtz knew, the associated multiple-valued velocity potential $\phi = \arctan y/x = \theta$ is the magnetostatic potential of a stationary current flowing along the z-axis, and it may have been this physical analogy that originally suggested to Helmholtz his theory of vortex lines.

Vortex rings. An analogous circular distribution of vorticity is provided by a vortex ring, whose vorticity is distributed with constant density in a circle, say $x^2 + y^2 = a^2$, $z = 0$. Since there is no vorticity elsewhere, there is a multiple-valued velocity potential, identical with the magnetic potential induced by a current flowing around a circular wire.

Such vortex rings are commonly seen as smoke rings; they can be produced by taking a drum having a circular hole in the center, and filling it with smoke. When the side of the drum opposite the hole is tapped, smoke is ejected through the hole. A ring of concentrated, nearly uniform vorticity is formed near the rim of the hole where the flow 'separates', and rises majestically under its own self-action, much like the vortex-pair of Example 13.

The magnetic analogy. Since $\nabla \times \underline{\omega} \equiv 0$, one can associate with any velocity field $\underline{u}(\underline{x})$ a 'current' $\underline{\omega}(\underline{x})$ flowing along its vortex lines, the total current passing through any vortex tube being equal to the circulation $\Gamma = \oint \underline{u} \cdot d\underline{x}$ around any circuit going (once) around that tube. It is a remarkable fact that a steady (vector) electric current of vector intensity \underline{J} produces a magnetic field \underline{H} satisfying $\nabla \times \underline{H} = 4\pi \underline{J}$.²⁴ This law, discovered by Biot and Savart, was an early clue to

²⁴J. D. Jackson, "Classical Electrodynamics", first ed. p. 153. For simplicity, we are using here electromagnetic (relativistic) units, so that $c = 1$.

electromagnetic theory. They derived an integral formula which expresses \underline{H} in terms of \underline{J} , the analogue of which is

$$(12.5) \quad \underline{u}(\underline{x}) = \frac{1}{4\pi} \int \frac{\underline{r} \times \underline{\omega}(\underline{x}')}{r^3} dR(\underline{x}') \quad .^{25}$$

Perhaps inspired by this analogy, Helmholtz derived (12.5) under mild integrability assumptions; we will not derive it here. Instead, we will consider some special cases.

The simplest examples are provided by the straight vortex line $(0,0,z)$, corresponding to an electric current in a long straight wire, and a vortex ring, which corresponds to a uniform current going around a circular wire.

In the case of two-dimensional velocity fields $\underline{u}(\underline{x}) = (u(x,y), v(x,y), 0)$, with vector vorticity $\underline{\omega}(\underline{x}) = (0,0,\zeta)$, $\zeta = u_y - v_x$, formula (12.5) specializes to

$$(12.5') \quad \psi = \frac{1}{2\pi} \int \zeta(x',y') \ln r \, dx' dy' ,$$

where $r = [(x-x')^2 + (y-y')^2]^{1/2}$. This expresses the stream function in terms of the vorticity, as the solution of the two-dimensional Poisson equation $-\nabla^2 \psi = \zeta$ in an infinite plane. In this domain, $(\ln r)/2\pi$ is the Green's function of $-\nabla^2$.

Vortex sheets. A limiting case of (12.5') is provided by the free boundary (also called a 'slipstream') separating two adjacent uniform parallel flows, such as

$$(12.6) \quad \underline{u}(\underline{x}) = \begin{cases} (u,0,0) & \text{if } y > 0 , \\ (-u,0,0) & \text{if } y < 0 . \end{cases}$$

This corresponds to a uniform vortex sheet (hence a current) parallel to the z-axis in the (x,z) -plane.

Likewise, a limiting case of (12.5) is the 'vortex sheath' around a circular jet in an otherwise stationary fluid, with

²⁵Cf. Batchelor [B1, p. 87]. Chapter 7 of [B1] gives an excellent general discussion of vortex flows in an ideal fluid.

$$(12.7) \quad \underline{u}(\underline{x}) = \begin{cases} (u, 0, 0) & \text{if } y^2 + z^2 < a^2 \\ \underline{0} & \text{if } y^2 + z^2 > a^2 \end{cases}.$$

Induced drag.²⁶ A now classic application of the preceding ideas is the theory of induced drag, developed by Prandtl and others in the 1920's to help explain the drag of an airfoil of finite span. It is a very approximate theory, somewhat analogous to Lagrange's theory of long waves.

It assumes that the vorticity in the 'free stream' approaching an airfoil is negligible, and that the airfoil is streamlined so that its 'wake' consists of a thin sheet into which the boundary layer (see Chapter 2) flows as it is shed behind the airfoil, it follows from the invariance of circulation that all the vorticity in the flow field must be concentrated in this sheet, which is therefore properly called a vortex sheet.

If we accept the idea that the flow direction is nearly that of the free stream, and the Kutta-Joukowski formula $L = \rho U \Gamma$ in each vertical plane parallel to the free stream flow direction, then it follows that the spanwise variation in the lift $L = L(y)$ of the corresponding airfoil sections determines the vorticity of this vortex sheet (assumed to be nearly horizontal):
 $\omega(y) = L'(y)/\rho U$, approximately.

The simplest case is that of a rectangular wing, all of whose sections are the same. For such wings it seems reasonable to assume that $L = L(y) = L_0$ is independent of y . In this case, if the preceding reasoning is accepted, then the vorticity should be concentrated in vortex lines behind the wing tips [8, §107]; these are called tip vortices [8, §109]. The energy shed in these and analogous vortex sheets gives rise to an 'induced drag', which can be roughly estimated by making engineering approximations [8, §110]. Applied in the context of engineering experience and judgement, predictions based on such models can be very useful, but they are by no means part of exact science.

²⁶ See [8, Chapter VI, Part C]. Glauert's monograph "Elements of Airfoil and Airscrew Theory", 2d ed., Cambridge Univ. Press, 1947, gives an excellent survey of the ideas discussed briefly in §§10-13 of this chapter.

REFERENCES FOR CHAPTER 1

- [A1] G.K. Batchelor and R.M. Davies (eds.), "Surveys in Mechanics", Cambridge University Press, 1956.
- [A2] G. Birkhoff, "Hydrodynamics; A Study in Logic, Fact and Similitude", Princeton University Press, 2d ed., 1960.
- [A3] G. Birkhoff and R.E. Lynch, "Numerical Solution of Elliptic Problems", SIAM Publications, 1982.
- [A4] G. Birkhoff and E.H. Zarantonello, "Jets, Wakes, and Cavities", Academic Press, 1957.
- [A5] Sydney Goldstein (ed.), "Modern Developments in Fluid Dynamics", 2 vols., Oxford University Press, 1938.
- [A6] H. Lamb, "Hydrodynamics", 6th ed., Cambridge University Press, 1932.
- [A7] L. Prandtl and O.G. Tietjens, "Fundamentals of Hydro- and Aeromechanics".
- [A8] _____, "Applied Hydro- and Aeromechanics", McGraw-Hill, 1934.
- [A9] L.M. Milne-Thomson, "Theoretical Hydrodynamics", 4th ed., Macmillan, 196 .
- [A10] J.J. Stoker, "Water Waves", Interscience, 1957.
- [A11] V.L. Streeter, "Fluid Dynamics", McGraw-Hill, 1948 (later editions).
- [A12] Brian Thwaites (ed.), "Incompressible Aerodynamics", Oxford, Clarendon Press, 1960.

2. VISCOSITY and COMPRESSIBILITY.

1. Introduction. Euler's equations for fluid motion illustrate the lofty concept of reducing all physics to a handful of 'governing' differential equations. This idea has had an impressive history. It inspired Fourier, Kelvin, Kirchhoff, Maxwell, Poincaré, and many other 19th century mathematical physicists. In Chapter 1, we reviewed some of the successes and failures of Euler's equations, making the additional approximation of a homogeneous incompressible fluid of constant density $\rho = \rho_0$.

Ideal vs. real fluids. Although the model of an 'ideal' fluid studied in Chapter 1 is very useful, and we will consider it further in Chapter 4 below, it neglects two physical variables of fundamental importance: compressibility and viscosity. The present chapter will take up some mathematical models designed to account for their effect.

We will begin (in §§2-3) with the theory of sound waves, to which Chapter 5 will also be devoted. To a very good approximation, these can be considered as 'small oscillations' of Lagrangian dynamical systems, and many aspects of their mathematical theory can be best understood if so viewed. Those not familiar with the elementary theory of such systems may find it helpful to read Appendix A.

Indeed, the theory of sound waves arises if one linearizes Euler's equations, still assuming that there is a velocity potential. The concept of an incompressible, inviscid fluid is simply replaced by that of an elastic fluid, satisfying $p = f(\rho)$ (Euler's equation of 'state'). We will now try to explain its relation to Lagrange's ideas.

Lagrangian dynamics. In his classic Mécanique Analytique, Lagrange presented Euler's equations in a still more general context: that of a conservative dynamical system, envisaged by Lagrange. Denoting 'kinetic' and 'potential' energy by T and V , and assuming for simplicity a finite number of degrees of freedom, the evolution of such a system is determined by the

Euler-Lagrange variational equations

$$(1.1) \quad \frac{d}{dt} \frac{\partial L}{\partial \dot{q}_i} = \frac{\partial L}{\partial q_i}, \quad \dot{q}_i = dq_i/dt.$$

Here $L(q, \dot{q}) = T - V$ is called the Lagrangian; the 'generalized coordinates' q_1, \dots, q_r can be arbitrary.

Eq. (1.1) is the Euler-Lagrange variational equation for the condition that the action integral $\int L(q, \dot{q}) dt$ be stationary-- i.e., in Lagrange's notation, that $\delta \int L(q, \dot{q}) dt = 0$ for all infinitesimal variations $\delta q(t)$ in 'configuration space' having the same endpoints $q(t_0) = q_0$ and $q(t_1) = q_1$. Because of this, it is often called the Principle of Least Action.¹ It was used by Liouville, Hamilton, Jacobi, and others to 'geometrize' much of mechanics, and their concepts helped to inspire the theories of relativity and quantum mechanics in the early 20th century.

The reversibility in time of Euler's equations (Chap. 1, §7) expresses his faith in the idea that moving fluids could be treated as conservative (Lagrangian) dynamical systems having infinitely many degrees of freedom. For example, the potential flows of an ideal fluid satisfy a more complicated version of (1.1), with $T = (\rho_0/2) \iiint (\nabla \phi \cdot \nabla \phi) dR$ the Dirichlet integral and $V = mg\bar{y}(t)$ where \bar{y} is the height of the center of gravity.

Euler's formula $\rho = \rho(p)$ (Chap. 1, §2), obviously intended by him to express the elasticity of air and other fluids, clearly neglects the effect of temperature, T . But as everyone knows, gases expand when heated, and contract when they are cooled. The same is ordinarily true of liquids, although water, curiously, expands as it cools just above the temperature of freezing.² In reality, the (thermodynamic) state of any fluid depends on two variables (p and T , say), and not just on one as Euler assumed; he should have written

¹See C. Lanczos, The Variational Principles of Mechanics, Univ. of Toronto Press, 1949, esp. p. 115 ff.

²If water did not expand during freezing, ice would not float and ponds would freeze solid!

$$(1.2) \quad \rho = \rho(p, T)$$

in place of $\rho = \rho(p)$. Moreover the work of compression heats a fluid, converting mechanical energy into thermal energy according to the formula

$$p \, dV = C_{\rho} \, V \, dT ,$$

where $C = C(p, \rho)$ expresses the specific heat of the fluid in units of mechanical energy.

Thermodynamics. This conversion of mechanical to thermal energy is just one aspect of the 19th century subject of 'thermodynamics', of which Euler and Lagrange were unaware. To understand the influence of compressibility on fluid behavior, one must be aware of this and other 'thermodynamic' concepts, including that of 'absolute zero' (0°K), adiabatic flow, ideal gas, etc.

We will devote §§4-6 to various aspects of compressible fluid motion that depend on such thermodynamic concepts. We will begin with some topics in atmospheric meteorology that are basic for an understanding of the weather. We will then turn our attention to viscosity effects on fluid flows, trying to indicate their very different nature.

2. Sound Waves. In Chapter 1, we described a variety of idealized flows of an homogeneous, incompressible, inviscid fluid. These analytically defined flows are compatible with Euler's equations of motion for a fluid with $\rho = \rho_0$, an assumption that implies $\nabla \cdot \underline{u} = 0$. The rest of this chapter will be devoted to deriving analytical formulas for flows in which the effects of compressibility and/or viscosity are taken into account.

After potential flows, the simplest mathematical model of fluid motion is that used to treat sound waves of infinitesimal amplitude (acoustic or "linear" waves) in a homogeneous compressible, but still inviscid fluid. These are tractable because the velocity potential ϕ and the associated pressure perturbation $\delta p = p - p_0$ satisfy the linear, constant-coefficient wave equation

$$(2.1) \quad \phi_{tt} = c^2 \nabla^2 \phi = c^2 (\phi_{xx} + \phi_{yy} + \phi_{zz}), \quad c^2 = dp/d\rho .$$

This is deftly derived in Lamb [6, §§285, 287] from the Euler-Lagrange equations for irrotational flow, neglecting gravity.

In Lamb's derivation of (2.1), "linearization" is achieved by neglecting terms quadratic in the velocity (as in Lagrange's general theory of small oscillations). Thus it neglects the convection terms $\sum u_k \partial u_i / \partial x_k$, thus replacing D/Dt by $\partial/\partial t$. In the equation of continuity, this gives

$$\rho_t = -\text{div}(\rho \underline{u}) = -\rho \nabla \cdot \underline{u} - \sum u_k \partial \rho / \partial x_k .$$

Alternatively, one can replace $D\rho/Dt = -\rho \nabla \cdot \underline{u}$ by $\partial \rho / \partial t = \rho \cdot \underline{u}$, getting

$$(2.2) \quad \delta \rho_t = \rho_t = -\rho_0 \nabla \cdot \underline{u} = -\rho_0 \nabla^2 \phi, \quad \delta \rho = \rho - \rho_0 .$$

Linearizing Euler's equation of state, and setting $\delta p = p - p_0$, we have also

$$(2.3) \quad p = c^2 \delta \rho, \quad c^2 = dp/d\rho .$$

Combining (2.2) and (2.3):

$$(2.3') \quad (\delta p)_t = c^2 (\delta \rho)_t = -c^2 \rho_0 \nabla \cdot \underline{u} .$$

Finally, neglecting gravity and convection (linearizing the equations of motion):

$$(2.4) \quad \underline{u}_t \approx D\underline{u}/Dt = -\frac{1}{\rho_0} \nabla(\delta p) .$$

Therefore, differentiating (2.3'):

$$(2.5) \quad (\delta p)_{tt} = -c^2 \delta p_{tt} = -c^2 \rho_0 \nabla \cdot \underline{u}_t = c^2 \nabla^2 \delta p ,$$

which shows that δp , the 'linearized' (or 'infinitesimal') overpressure, also satisfies the wave equation (2.1).

Historical remark. Eqs. (2.1) and (2.5) were first derived by Euler in 1759, essentially by linearizing his equations of motion.³ Newton had previously deduced Eq. (2.5) from less general considerations. Assuming Boyle's Law for isothermal pressure variations at constant temperature, $p = k\rho$, he calculated $c \approx 900$ f/s in air under standard atmospheric conditions. This is about 20% too low, for reasons to be explained in §6.

Plane waves. In the one-dimensional case of so-called plane sound waves, with $\delta p = \delta p(x,t)$, $\vartheta = \vartheta(x,t)$, $\underline{u} = (u(x,t), 0, 0)$, Eqs. (2.1) and (2.5) reduce to

$$(2.6) \quad \vartheta_{tt} = c^2 \vartheta_{xx} \quad \text{and} \quad \delta p_{tt} = c^2 \delta p_{xx} ,$$

respectively. If the speed of sound, c , is taken as an empirical constant (it is about 1100 f/s in air under standard atmospheric conditions), a very good fit to a wide range of observations can be obtained. The general solution of (2.6), as for the DE $\eta_{tt} = c^2 \eta_{xx}$ satisfied by the elevation in 'long' gravity waves of infinitesimal amplitude (Chap. 1, §3), is

$$(2.6') \quad \vartheta = f(x+ct) + g(x-ct) ,$$

whence $u = \vartheta_x = f'(x+ct) + g'(x-ct)$. This clearly expresses the most general plane sound wave (of infinitesimal amplitude) as the superposition of two components, travelling without change of form at speed c in opposite directions.

Standing and progressive waves. As special cases of the f and g in (2.6'), we obtain the 'simply harmonic' progressive waves,

$$\delta p = A \begin{Bmatrix} \cos \\ \sin \end{Bmatrix} k(x \pm ct) = \begin{Bmatrix} \cos \\ \sin \end{Bmatrix} (kx \pm \omega t), \quad \omega = ck .$$

³Morris Kline, "Mathematical Thought from Ancient to Modern Times", p. 520. Actually, temperature variations in sound waves are very small (often $< 10^{-4}^\circ$ C).

By taking a linear combination ('superposition') of two such real progressive waves of equal amplitude travelling in opposite directions, we obtain the simply harmonic standing waves,

$$(2.7) \quad \delta_p = \begin{cases} \cos(kx+\omega t) + \cos(kx-\omega t) = 2 \cos kx \cos \omega t , \\ \sin(kx+\omega t) + \sin(kx-\omega t) = 2 \sin kx \cos \omega t , \end{cases}$$

whose frequency $f = \omega/2\pi = ck/2\lambda$. Algebraically, it is more convenient to treat real, simply harmonic waves as the real (or imaginary) parts of complex exponential functions

$$(2.8) \quad Ae^{i(kx-\omega t)} = Ae^{ik(x-ct)} = Ae^{ikx} e^{i\omega t} .$$

In the complex domain, the distinction between standing and progressive waves disappears.

Fourier integrals. In infinite space, a large class⁴ of plane wave solutions of (2.5) can be constructed as Fourier integrals

$$(2.9) \quad \delta_p = \int_{-\infty}^{\infty} \alpha(k) e^{i(kx-\omega t)} dk , \quad \omega = c|k|$$

of simply harmonic solutions of (2.5); the corresponding real Fourier integrals are described in the exercises.

Spherical waves. Other exact solutions of (2.5) include the incoming and outgoing spherical waves

$$(2.10) \quad \delta_p = \frac{A}{r} \begin{cases} \cos \\ \sin \end{cases} k(r \pm ct) .$$

From these exact solutions, Kirchhoff constructed by superposition an integral formula solving the general initial value problem.

Wave vectors. By rigid rotation, we obtain as special solutions of (2.5) in three-dimensional space, for any wave vector \underline{k} , the 'standing wave' solutions

⁴Essentially, all these that are of finite energy are (square-integrable), by Plancherel's Theorem.

$$\delta p = A \begin{Bmatrix} \cos \\ \sin \end{Bmatrix} \underline{k} \cdot \underline{x} \begin{Bmatrix} \cos \\ \sin \end{Bmatrix} \omega t, \quad \omega^2 = c^2 k^2,$$

where $k = |\underline{k}| = (k_1^2 + k_2^2 + k_3^2)^{1/2}$. By superposition, we can construct from these standing waves the 'progressive wave' solutions

$$(2.11) \quad \delta p = A \begin{Bmatrix} \cos \\ \sin \end{Bmatrix} [k(\underline{\kappa} \cdot \underline{x} - ct)],$$

where $\underline{\kappa} = \underline{k}/k$ is a unit vector. This obviously "progresses" with speed c in the direction of $\underline{\kappa}$, without change of form. Note that c is independent of \underline{k} : sound waves are non-dispersive.

Energy of sound waves.⁵ The kinetic energy of a system of plane waves, with $u = \phi_x = f'(x+ct) + g'(x-ct)$ from (2.6'), is

$$(2.12) \quad T = \frac{1}{2} \rho_0 \int u^2 dx.$$

Letting $\xi = \int u dt$ denote the displacement of a fluid particle from its equilibrium position, we then have for a simply harmonic train of progressive waves of amplitude a ,

$$(2.13) \quad \xi = a \cos \omega(t - \frac{x}{c}), \quad \omega = ck.$$

An elementary integration then gives

$$T = (\rho_0/2) \omega^2 a^2 \int \sin^2 \omega(t - \frac{x}{c}) dx,$$

the average value of whose integrand over any complete quarter-period in space or time is $1/2$. Hence the average kinetic energy density (in space instantaneously or time at any point) is

$$(2.14) \quad \bar{T} = \rho_0 \omega^2 a^2 / 4.$$

⁵See H. Lamb, "The Dynamical Theory of Sound", Art. 60. His n is our ω .

Since in general, for small sinusoidal oscillations of Lagrangian systems, the average kinetic energy is exactly equal to the average potential energy, it follows that the total energy per unit volume is

$$(2.15) \quad \bar{E} = \rho_0 \omega^2 a^2 / 2$$

3. Helmholtz equation. The phenomenon of resonance is associated with 'standing waves' of sound, whose pressure variations are of the general form⁶

$$(3.1) \quad \delta p(\underline{x}, t) = P(\underline{x}) e^{i\omega t}$$

where $P(\underline{x})$ is an eigenfunction of the Helmholtz equation

$$(3.2) \quad \nabla^2 p + (\omega^2/c^2)p = 0 ,$$

for the boundary condition $\partial P/\partial n = 0$ on Γ , the boundary of Ω .

Open tubes. From the standpoint of Natural Philosophy, the simplest illustration of the phenomenon of resonance is provided by a vertical open tube, above which a tuning fork is held to stimulate vibrations of given frequency. If the diameter d of the tube is small in comparison with the wave length λ , then plane waves with $\delta p = \delta p(\underline{x}, t)$ are excited. Letting k denote ω/c , so that $\omega = kc$, (3.2) therefore reduces to

$$(3.3) \quad d^2P/dx^2 + k^2P = 0 , \quad k = \omega/c .$$

If the water level is taken as $x = 0$, and the top of the tube is $x = \ell$, then the boundary condition $\partial(\delta p)/\partial n = 0 = \partial P/\partial n$ is satisfied (approximately) at $x = 0$ (the closed end). The open

⁶We adopt here the convenient complex representation, whereby both $\text{Re}\{P(\underline{x}) e^{i\omega t}\} = P(\underline{x}) \cos \omega t$ and $\text{Im}\{P(\underline{x}) e^{i\omega t}\} = P(\underline{x}) \sin \omega t$ are real solutions of the DE $u_{tt} = c^2 \nabla^2 u$.

end is at atmospheric pressure, so that $\delta p = 0$ (nearly) when $x = \ell$. The resulting Sturm-Liouville system is therefore (3.3) and $P'(0) = P(\ell) = 0$, with the eigenfunctions

$$(3.4) \quad P_j(x) = \cos[(2j-1)\pi x/\ell] , \quad j = 0, 1, 2, \dots ,$$

and the natural frequencies

$$(3.4') \quad f_j = \omega/2\pi = (j - \frac{1}{2})c/\ell , \quad j = 0, 1, 2, \dots .$$

These can be excited by a tuning fork having the same frequency; the corresponding wave-lengths for resonance are $\lambda_j = c/f_j$. Since middle C has the frequency 256 hz, and c is about 1100 f/s, giving $\lambda \approx 4.3$ ft., we see that this experiment is easy to realize physically.

Closed tubes. Similarly, for a long, narrow tube of length ℓ closed at both ends, the appropriate boundary conditions are $P'(0) = P'(\ell) = 0$, giving the eigenfunctions

$$(3.5) \quad P_j(x) = \cos(j\pi x/\ell) , \quad j = 0, 1, 2, \dots .$$

The case $j = 0$ corresponds physically to a permanent increase in the mean pressure, and not to a 'standing wave' at all. The natural frequencies of the pipe are therefore

$$(3.5') \quad f_j = \omega_j/2\pi = j\pi c/2\ell = jc/2\ell , \quad j = 1, 2, 3, \dots .$$

They are integral multiples of the fundamental frequency $f_1 = c/2\ell$, whereas those of an open tube are odd multiples $(2j-1)f_1$ of it.

Rectangular box. For a closed rectangular box with sides ℓ, ℓ', ℓ'' , the boundary condition $\partial P/\partial n = 0$ give similarly (by 'separation of variables') the eigenfunctions

$$(3.6) \quad p_j(\underline{x}) = \cos(j\pi x/\ell) \cos(j'\pi y/\ell') \cos(j''\pi z/\ell'') ,$$

where j, j', j'' are arbitrary intervals. Each of these satisfies the Helmholtz equation (3.2) with

$$\omega^2/c^2 = \pi^2 \left(\frac{j^2}{\ell^2} + \frac{j'^2}{\ell'^2} + \frac{j''^2}{\ell''^2} \right)$$

and so

$$(3.6') \quad f_j = \omega_j/2\pi = \left[\frac{j^2}{\ell^2} + \frac{j'^2}{\ell'^2} + \frac{j''^2}{\ell''^2} \right]^{1/2} c/2\ell .$$

where $J'_\nu(\beta) = 0$ have been tabulated, whence the eigenvalues are the $k^2 = k^2(\nu, j, \ell)$ with

$$(3.8) \quad k^2 = (\beta_{\nu, j}/b)^2 + \nu^2 + (\ell\pi/b)^2 .$$

Spherical jar. The natural frequencies of a spherical jar (of radius a) can be expressed similarly in terms of the spherical Bessel functions $j_n(r)$ (associated with Bessel functions of half-integral order) and spherical harmonics $S_{m,n}(\phi, \theta)$. The eigenfunctions are again products $j_n(kr)S_{m,n}(\phi, \theta)$, where the $k = k(n, j)$ are chosen to make $j'_n(ka) = 0$.

The resonance frequencies of a hemispherical jar can be found similarly, by selecting those eigenfunctions of a spherical jar which are symmetric in the equatorial plane so that, in terms of latitude ϕ and longitude θ , they satisfy $P(r, \theta, -\phi) = P(r, \theta, \phi)$.

Unfortunately, 'separations of variables' such as those used above to obtain the eigenfunctions of cylinders, spheres, and hemispheres do not exist for most shapes. All coordinate systems to which it can be applied were discovered already by 1850 or so, although the fact that the Laplace operator was not separable in any other coordinate systems was not proved until about 1930.

4. Equations of state. Euler's formula $\rho = \rho(p)$ (Chap. 1, §2), obviously intended by him to express the elasticity of air and other fluids, clearly neglects the effect of temperature, T . As everyone knows, gases expand when heated, and contract when they are cooled. The same is ordinarily true of liquids, although water, curiously, expands as it cools just above the temperature of freezing.⁶

As everyone knows, gases expand much more than liquids; whereas the density of air is doubled by a pressure of 2 atm. (psia), that of water is increased by less than .03%. Indeed, fortunately for mathematicians, the behavior of real gases is is stimulated very well by the equation

$$(4.1) \quad p = k \rho T ,$$

where T is the temperature above absolute zero (-273°C). Indeed, when rewritten in the form $pV = RT$, Eq. (4.1) is one definition of a perfect gas (see §5 below, and also Chap. 5).

More generally, the (thermodynamic) state of any fluid really depends on two variables (p and T , say), and not just on one as Euler assumed; he should have written

$$(4.2) \quad \rho = \rho(p, T)$$

in place of $\rho = \rho(p)$. Moreover the work of compression heats a fluid, converting mechanical energy into thermal energy according to the formula

$$p \, dV = \rho \, C_V \, dT ,$$

where $C = C(p, \rho)$ expresses the specific heat of the fluid in units of mechanical energy.

Before discussing the implications of the oversimplification $p = f(\rho)$ for the partial differential equations of fluid motion

⁶If water did not expand during freezing, ice would not float and ponds would freeze solid!

(and their solution), we will devote a few pages to some much simpler consequences of importance for understanding weather conditions ("meteorology").

The atmosphere. Indeed, the most familiar example of a nearly perfect gas is provided by air. This is a mixture of gases, consisting of about 75% of nitrogen molecules N_2 , 25% of oxygen molecules O_2 , and 1% of atomic argon. Most important for meteorology, real air also contains variable amounts of water vapor (H_2O), a small amount of carbon dioxide (CO_2), and traces of other chemicals (including dust particles). For convenient reference, we list in Table 2 some dimensional constants that are useful for treating atmospheric phenomena.

Table 2. Some Useful Dimensional Constants

Absolute zero	$T = -273^\circ C = 0^\circ K$
Standard atmosphere:	$T = 15^\circ C = 288^\circ K$
	$p = 1 \text{ Kg/cm}^2$ (approx.)
	$\rho = 1.2255 \text{ Kg/m}^3$
Mech. equivalent of heat for water is:	
	$1^\circ C = 427 \text{ meters}$
	$1^\circ F = 770 \text{ feet}$
Specific heat of air:	$C_p = .2375, C_v = .168.$

From the data of Table 2, it follows that the internal energy of air per unit mass at $288^\circ K$, being $C_v T$, converted from thermal to mechanical energy, is enough to raise it over 20 Km. against gravity.

Meteorological applications. The preceding considerations, which stand in stark contrast to Euler's hypothesis $\rho = \rho(p)$, have some important (if elementary) meteorological implications for the earth's atmosphere. The simplest of these concern the variations in pressure p and temperature T with altitude y , over a given area at a given time. They assume approximate hydrostatic equilibrium, which is very reasonable provided that

vertical components of wind velocity are small. See [A7, Chap. II] for fuller discussions of these implications.

Since $\underline{u}(\underline{x};t) = \underline{0}$ in hydrostatic equilibrium, Euler's equation of motion (Chap. 1, (2.1)) reduces to $\underline{0} = \underline{g} - \nabla p/\rho$, or $\text{grad } p = \rho \underline{g}$. It follows easily that, if $\underline{g} = -\nabla G$ is a gradient field (e.g., if $\underline{g} = (0,0,-g) = -\nabla(gy)$), then the pressure must be a function $p = F(G)$ of the gravitational potential G . Therefore, near the earth's surface, we must have $p = p(y)$ in hydrostatic equilibrium.

Since $\text{grad } p = \rho \underline{g} = (0, -\rho g, 0)$, evidently $\rho = -p'(y)/g = \rho(y)$ must also depend only on altitude in hydrostatic equilibrium. In particular, in dry air, which is nearly an ideal gas, the condition that T depend only on y , i.e., that

$$(4.3) \quad T = p(y)/R\rho(y) = T(y)$$

is also necessary for hydrostatic equilibrium. The function $T(y)$ describing the variation of (mean) temperature with altitude (the so-called temperature profile), at a given fixed time t , is however somewhat unpredictable. Three types of profile are especially noteworthy; in all cases, we have as above

$$(4.4) \quad dp/dy = -g\rho(y) ,$$

and so

$$(4.4') \quad p(y) = g \int_y^{\infty} \rho(p, T(y)) dy .$$

Physically, this asserts that the pressure at any point is due to the weight of the air above it. The preceding formulas apply in particular to the 'elastic fluids' defined by Euler's equations (Chap. 1 (2.1)-(2.3)).

Constant density. For an incompressible fluid of constant density ρ_0 (e.g., in an 'ideal fluid'), the pressure profile is therefore $p = p_s + \rho_0 g(y_s - y)$ where p_s is the surface pressure and $y_s - y$ is the depth below the surface (Pascal's

formula).⁷ In this model, the temperature profile is irrelevant; it approximates lake pressure profiles very well, and ocean pressure profiles fairly well.

Isothermal model. For an ideal gas at constant temperature T_0 , $p = k\rho$. Hence, differentiating (4.4) by Leibniz' rules we have:

$$dp/p = -g\rho dy/p = -gy/k .$$

Integrating, we get pressure and density profiles that decay exponentially with altitude:

$$(4.5) \quad p = p_0 e^{-gy/k} , \quad g/k = g\rho_0/p_0 .$$

At 'standard' atmospheric temperature, $15^\circ \text{C} = 288 \text{ }^\circ\text{K}$,

$$g\rho_0/p_0 = .00122 \frac{\text{gm}}{\text{cm}^3} \times 10^{-3} \frac{\text{cm}^2}{\text{gm}} \approx (8 \text{ Km})^{-1}$$

Since $.5 \approx e^{-.7}$, it follows that in an isothermal atmosphere at 15°C , the density (and pressure) would be halved in about 5.6 Km, or 17,000 feet.

Polytropic atmosphere. Mathematically, a 'polytropic' gas is by definition a fluid in which Euler's equation of state (2.3) holds with $p = k\rho^\gamma$. In a perfect gas with $T = p/R\rho$, this implies $T = (k/R)\rho^{\gamma-1}$, whence by (4.4),

$$(4.6) \quad dp/dy = k\rho^{\gamma-1} d\rho/dy = -g\rho(y) ,$$

and so $-gdy = k\rho^{\gamma-2} d\rho$. In turn, for any γ , this implies a linear variation of temperature with altitude: for some constant of integration y_a , the height of the atmosphere,

$$(4.6') \quad g(y_a - y) = [k\gamma/(\gamma-1)]\rho^{\gamma-1} = [\gamma/(\gamma-1)]RT .$$

Setting $y = 0$, this gives the atmospheric height as

⁷This is the "uniform atmosphere" of [A7, §11], while (4.5) is the "isothermal" atmosphere of [A7, §12].

$$y_a = [\gamma(\gamma-1)]RT_0/g = [\gamma(\gamma-1)](p/g\rho)_0 .$$

Dry air is very nearly a perfect gas with

$$(4.7) \quad \left(\frac{p}{g\rho}\right)_0 \approx \frac{1 \text{ Kg}}{\text{cm}^2} \times \frac{.00125 \text{ gm}}{\text{cm}^3} = 8 \times 10^5 \text{ cm} = 8 \text{ Km} .$$

Moreover, air expands nearly adiabatically; hence it behaves like a polytropic gas with $\gamma = 1.408$. If we substitute these numbers into (4.6'), we obtain a predicted atmosphere height of roughly

$$(4.7') \quad y_a \approx [8\gamma/(\gamma-1)] \text{ Km} - 28 \text{ Km} ,$$

and a negative temperature gradient of about 10° C/Km .

Actually, in the so-called troposphere, the bottom 5-8 miles of the atmosphere, the best mean fit of the polytropic model to data is given by $\gamma = 1.2$. This is about half-way between $\gamma = 1.408$, the exponent for adiabatic expansion of dry air, and the isothermal model with $\gamma = 1$.⁸ This gives $(\gamma-1)/\gamma = 1/6$ and $dT/dy = -6^\circ \text{ C/Km}$, or about $3^\circ \text{ F/1000 ft}$. The stratosphere above this troposphere is nearly isothermal.

Atmospheric stability. Much of the deviation from the isothermal model is due to daytime thermal 'convection cells', caused by solar radiation. When the negative temperature gradient exceeds 10° C/km substantially, buoyancy causes masses of air to rise more or less adiabatically, often forming cumulus clouds.

Water vapor. Such clouds form when rising air, cooling adiabatically, becomes supersaturated. Supersaturated air is far from a perfect gas! Saturated air at atmospheric pressure contains about 2.5% of H_2O at 30° C , and 0.15% at -10° C [A7, p. 57]. Because the latent heat of evaporation (boiling) is 550° C (550 gcal/gm), condensation releases large amounts of heat, a fact which dominates the thermodynamics of saturated and supersaturated air. See Chap. 8 for descriptions of some phenomena resulting from this fact.

⁸The main reason is daytime atmospheric instability due to solar heating.

5. Thermodynamic Effects. Compressible flows involves thermodynamic considerations in an essential way. For example, thermodynamics explains why the observed Eulerian equation of state of gases is nearly polytropic, of the form $p = k\rho^\gamma$ where $\gamma = C_p/C_v$ is the ratio of the specific heat at constant pressure to that at constant volume. The explanation, due essentially to Laplace (ca. 1820), depends on the 'adiabatic flow' concept. (As was explained in §2, if $p = k\rho^\gamma$, then $c^2 = dp/d\rho = k\rho/\rho$.)

Adiabatic flows. A gas is called perfect when its thermodynamic equation of state is $pV = RT$, and its internal energy $E = E(T)$ is a function of temperature alone. Air is a nearly "perfect" gas at ordinary temperatures and pressures; moreover considerations from the kinetic theory of gases suggests that all gases should be nearly "perfect" at low densities (i.e., when the molecular mean free path is many molecular diameters); see Appendix E.

In a perfect gas, clearly $p(\partial V/\partial T)_p = R$, where the subscript p signifies "at constant pressure". Moreover by the first law of thermodynamics (conservation of energy); the specific heat at constant pressure, C_p , satisfies

$$C_p dT = dE + p_0 dV = E'(T)dT + p_0 \left(\frac{\partial V}{\partial p}\right)_p dT .$$

On the other hand, the specific heat at constant volume, C_v , satisfies by definition $C_v dT = dE = E'(T)dT$. Combining the preceding equations with $p(\partial V/\partial T)_p = R$, we get

$$(5.1) \quad C_p = C_v + R .$$

Now define an adiabatic flow as one in which all the work of compression goes into local heat (heat transfer is negligible), so that

$$0 = dE + p dV = C_v dT + p dV ,$$

and $dT = -(p/C_v)dV$. Since $pV = RT$, $dp/p + dV/V = dT/T$, and so

$$\begin{aligned}\frac{dp}{p} &= \frac{dT}{T} - \frac{dV}{V} = -\frac{dV}{V} \left[1 + \frac{pV}{C_V T}\right] \\ &= \frac{1}{C_V} \frac{dV}{V} [C_V + R] = -\frac{C_p}{C_V} \frac{dV}{V}.\end{aligned}$$

The ratio $C_p/C_V = \gamma$ is called the adiabatic constant, and it is nearly constant over large ranges of temperature and pressure for most gases. When γ is constant, clearly

$$(5.2) \quad p = \exp\left(\int dp/p\right) = \exp(-\gamma \int dV/V) = kV^{-\gamma} = k\rho^\gamma,$$

where k is a constant of integration. This is the adiabatic equation of state.⁹

Note that the preceding derivation does not invoke the concept of entropy or the second law of thermodynamics.

Bernoulli equation. The preceding discussion is of interest primarily as relating the speed of sound in an ideal gas to static measurements of $\gamma = C_p/C_V$. Namely, differentiating $p = k\rho^{\gamma-1}$, we get $c^2 = dp/d\rho = k\gamma\rho^{\gamma-1} = \gamma p/\rho = pC_p/\rho C_V$.

We next derive the Bernoulli equation for steady compressible flows of any elastic fluid satisfying Euler's equations:¹⁰

$$(5.3) \quad \frac{1}{2} u^2 + \int dp/\rho + G = K, \quad K = \text{const.},$$

valid along any streamline. To derive (5.3), consider the tangential derivatives

$$\frac{d}{ds} \left(\frac{1}{2} u^2 \right) = u \frac{du}{ds} = -\frac{1}{\rho} \frac{\partial p}{\partial s} + \frac{\partial G}{\partial s}$$

the last equality simply expresses the tangential component of acceleration $du/dt = Du/Dt$ as the tangential component of force

⁹It is valid when the thermal diffusivity $\kappa = K/\rho C_V \ll c^2/\omega = \lambda c$ (K the thermal conductivity); see E.U. Condon, Am. J. Phys. 1 (1933), 18- .

¹⁰Thinking of flow in a stream tube as one-dimensional, we here write u for q .

per unit mass (Newton's Second Law).¹¹ Integrating along the streamline, we get (5.3).

We will call the function $h(\rho) = \int dp/\rho$ in (5.3) the Bernoulli function for the elastic fluid (adiabatically, expanding perfect gas)

$$(5.4) \quad h(\rho) = \int dp/\rho = \int \gamma k \rho^{\gamma-2} d\rho = \frac{\gamma k}{\gamma-1} \rho^{\gamma-1}$$

whence $h(\rho) = \gamma p/(\gamma-1)\rho$. Note also that $h = C_p T$, while $c^2 = dp/d\rho = \gamma h$. Finally, note that in (locally) irrotational flow, the constant K in (5.3) is the same for all streamlines. This because in all directions, not just the streamline direction:

$$\begin{aligned} d\left(\frac{1}{2}u^2\right) &= u \, du = d\left(\frac{1}{2}\sum u_k^2\right) = \sum u_k \, du_k \\ &= \sum_{k,i} u_k \frac{\partial u_k}{\partial x_i} dx_i = \sum_{k,i} u_k \frac{\partial u_i}{\partial x_k} dx_i, \end{aligned}$$

where the last equation holds by irrotationality. Since $\partial/\partial t = 0$ in steady flow, however, we have by Euler's equations of motion (Chap. 1, §2),

$$\sum_{k,i} u_k \frac{\partial u_i}{\partial x_k} dx_i = - \sum_i \left\{ \frac{\partial p}{\rho \partial x_i} + \frac{\partial G}{\partial x_i} \right\} dx_i = - \frac{dp}{\rho} - dG:$$

Transposing, we get

$$(5.5) \quad d\left(\frac{1}{2}u^2\right) + d\left(\int \frac{dp}{\rho}\right) + dG = 0,$$

which implies (5.3) in any connected domain.

Convergent-divergent nozzle. We now consider steady flows in convergent-divergent nozzles, such as are used in supersonic wind-tunnels and in steam turbines (de Laval nozzles). This theory is asymptotic, in the sense that it assumes nearly parallel flow (i.e.,

¹¹Most authors today give much more sophisticated derivations, and appeal to the concept of entropy and to the Second Law of Thermodynamics.

lateral velocities and accelerations are neglected, together with the boundary layer). We also neglect accelerations due to gravity, as is usual in high-speed gas dynamics.

In such flows, we have

$$(5.6) \quad \rho u A(x) = C, \quad C = \text{const.}$$

Moreover, under these assumptions, (10.3) simplifies to

$$(5.7) \quad u^2/2 + k\gamma\rho^{\gamma-1}/(\gamma-1) = K.$$

Combining (5.6) and (5.7) we get

$$(5.8) \quad \rho^2(2K - B\rho^{\gamma-1}) = C^2/A^2(x),$$

where $B = 2\gamma k/(\gamma-1) > 0$ if $\gamma > 1$ (an important assumption, always fulfilled physically).

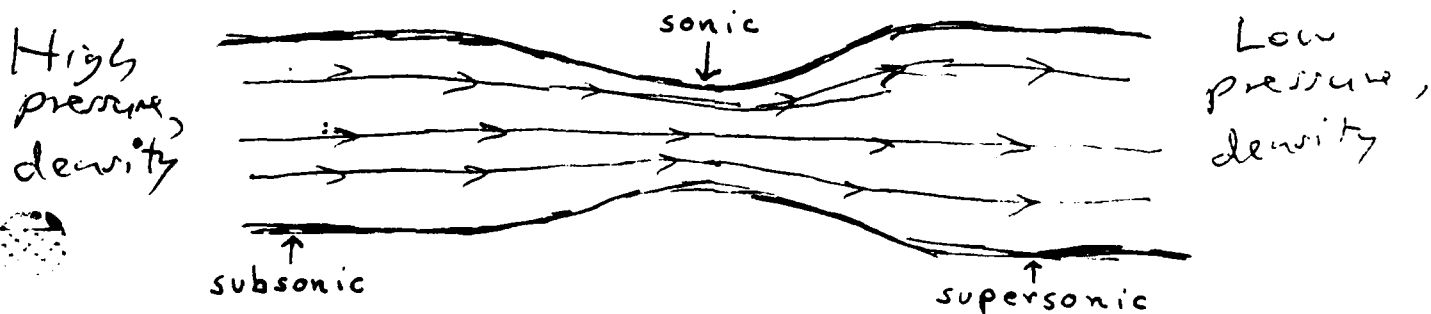
By graphing the function $F(\rho)$ on the left side of (5.8), one sees that it is convex and positive on the interval $[0, (2K/B)^{1/(\gamma-1)}]$. At its maximum, $dA = 0$ and hence, by (5.6),

$$d\rho/\rho + du/u = 0,$$

On the other hand, $u du + dp/\rho = u du + c^2 d\rho/\rho = 0$ by Bernoulli's equation (neglecting variations in G). Hence

$$c^2 d\rho/\rho = -u du = -u^2 (du/u) = u^2 d\rho/\rho,$$

and $c^2 = u^2$. Therefore, velocity is sonic at the "throat" (minimum $A(x)$). By the second law of thermodynamics, it is subsonic on the upstream side, and supersonic on the downstream side, as indicated in the attached sketch.



6. Mach number; adiabatic flow. The Mach number $M = U/c$ of a fluid flow is the ratio of the 'velocity at infinity', U , to the sound speed there. For $M < 0.8$ or so, Euler's concept of an elastic fluid, with the adiabatic equation of state $p = k\rho^{1.408}$ for air derived by Laplace, takes adequate care of most compressibility effects.

Similarity. Much more can be said. For a wide variety of mathematical models of compressible flow, linear and nonlinear compressibility effects and even shock waves are independent of size, so long as the medium, its 'state' (p , T , hence c and S), and velocities u are the same at corresponding points. This theoretical similarity principle applies to Euler's equations, for any equation of state $p = f(\rho)$. In particular, it applies to flows past two geometrically similar wings or bullets.

From a theoretical standpoint, therefore, if viscosity is neglected, predicted pressure distributions should agree with those observed on small-scale airfoil models suspended in a wind-tunnel as well as with those on full-scale airplanes. Likewise, if a theoretical prediction agrees with observation on a 0.44" rifle bullet, then it should agree with those on a 16" shell. In short, any such model provides a theoretical basis for performing model tests.

This idea was used already before 1750 by Benjamin Robins, who observed (using the ballistic pendulum invented by him) that the drag coefficient $C_D(M)$ of bullets increased by a factor of 2-3 near the speed of sound. (The phrase 'sonic barrier' is sometimes used to describe this phenomenon.) Euler edited a German translation of Robins' book, adding many comments that almost doubled its length. However, it was not until the 20th century that realistic mathematical models of supersonic flows past bullets and airfoils were constructed.

In a nearly perfect gas like dry air (not wet steam!), one can say much more. All phenomena depend only on γ and the Mach number $M = U/c$, where U is a representative flow speed. Mathematically speaking, for a given γ , if $u(x,t)$ is a solution

of the relevant DE's (essentially these of Euler), then so is $\underline{v}(\underline{x}, t) = \underline{u}(\lambda \underline{x}, \mu t)$, so long as the ratio U_∞/c_∞ ($c_\infty = (dp/d\rho)_\infty$) is the same.

Plane waves of finite amplitude. Many scientists have tried to treat the propagation of plane sound waves of finite amplitude (e.g., in air) 'exactly' by integrating Euler's equations for an adiabatic gas. One of the first questions asked was: what are the conditions (on the equation of state $p = p(\rho)$) under which a sound wave can propagate "without change of form" in a compressible fluid--i.e., be definable by

$$u = u(x - ct), \quad \rho = \rho(x - ct) .$$

This question is easily answered using Lagrangian coordinates.

In Lagrangian coordinates, writing $x = x(a, t)$ (where a is the cumulative mass), clearly $x_t = u$, x_{tt} is the acceleration, and $x_a = 1/\rho = V$ is the specific volume. Hence, the equation of motion for a plane wave reduces to

$$\begin{aligned} (6.1) \quad x_{tt} &= -\partial p / \partial a = -p'(\rho) \partial \rho / \partial a \\ &= -\frac{\partial p}{\partial} \left(\frac{1}{x_a} \right) = x_{aa} / x_a^2 = \rho^2 \frac{dp}{d} x_{aa} . \end{aligned}$$

In order that this reduce to $x_{tt} = c^2 x_{aa}$, it is necessary and sufficient that $\rho^2 dp/d\rho = c^2$, hence $dp/d(1/\rho) = -c^2$, whence

$$(6.2) \quad p = a - c^2/\rho$$

This is called the Chaplygin equation of state; unfortunately, it does not hold in any real fluid.

Linearized supersonic flow.¹² Another notable linear approximation to compressibility effects concerns supersonic flows around

¹²See G.N. Ward, "Linearized Theory of Compressible Flow", Cambridge Univ. Press, 1955; J.W. Miles, "Potential Theory of Unsteady Supersonic Flow", *ibid.*, 1947. For practical interpretations, see A.E. Puckett, *J. Aero. Sci.* 13 (1946), 475-84.

very slender airfoils. These are approximated quite well by a linearized model developed by Prandtl and Glauert. According to this model, the velocity potential of a 'slender body' moving parallel to the z-axis satisfies

$$(6.3) \quad (M^2 - 1)\phi_{zz} = \phi_{xx} + \phi_{yy}$$

In 1932, von Kármán and Moore used this model to estimate the drag coefficient $C_D(M)$ of a slender conical projectile, as a function of the Mach number. Their results explained qualitatively the large increase in $C_D(M)$ near $M = 1$, already observed (for bullets) by Robins around 1750.

7. Formation of shocks. We now turn our attention to time-dependent flows of an 'elastic' (inviscid but compressible) fluid of the kind postulated by Euler. We will first show that, to transmit plane waves of finite intensity without change of form, such a fluid must have a non-physical "Chaplygin" equation of state of the form $p = A + B/\rho$ (i.e., $\gamma = -1$). We will then take up so-called 'simple' waves, and explain why simple compression waves develop shock discontinuities.

Earnshaw paradox. Imagine an elastic fluid with equation of state $p = p(\rho)$ in which sound waves can propagate "without change of form"--i.e., satisfy

$$u = u(x - ct), \quad = (x - ct) .$$

By using Lagrangian coordinates, it is easy to determine the form that the function $p(\rho)$ must have.

In Lagrangian coordinates, writing $x = x(a, t)$ (where a is the cumulative mass), clearly $x_t = u$, x_{tt} is the acceleration, and $x_a = 1/\rho = V$ is the specific volume. Hence, the equation of motion for a plane wave reduces to

$$(7.1) \quad \begin{aligned} x_{tt} &= -\partial p / \partial a = -p'(\rho) \partial \rho / \partial a = -\frac{\partial p}{\partial \rho} \left(\frac{1}{x_a} \right) \\ &= x_{aa} / x_a^2 = \rho^2 \frac{dp}{d\rho} x_{aa} . \end{aligned}$$

In order that this reduces to $x_{tt} = c^2 x_{aa}$, it is necessary and sufficient that $\rho^2 dp/d\rho = c^2$, hence $dp/d(1/\rho) = -c^2$, whence

$$(7.2) \quad p = a - c^2/\rho ;$$

This is called the Chaplygin equation of state. Unfortunately, it does not hold in any real fluid; this is the 'Earnshaw paradox'. It was discovered in 1860.

Simple waves. A compressible fluid in which the pressure p is an increasing function $p = f(\rho)$ of the density ρ may be called an 'elastic' fluid. In adiabatic flow, a perfect gas is equivalent to an elastic fluid with $f(\rho) = k\rho^\gamma$, $\gamma = C_p/C_v$. Plane waves in an elastic fluid are called simple waves when isobars coincide with isovels (level lines of $u(x,t)$), i.e., when $u = g(\rho)$. In adiabatic flows of a perfect gas, isobars (level lines of p) coincide with isotherms (level lines of T), in any case.

After expressing all variables as functions of ρ (at least locally),¹³ it is easy to derive the properties of simple (plane) waves. With this assumption, Euler's equations of continuity and motion (Chapter 1, (2.1)-(2.2)), become

$$(7.3) \quad u_t + [u + \rho^{-1}(dp/d\rho)] u_x = 0$$

and

$$(7.4) \quad \rho_t + [d(\rho u)/d\rho] = 0 .$$

On the other hand, since isovels and isobars coincide, we must have $u_t = -\lambda u_x$ and $\rho_t = -\lambda \rho_x$ for the same λ . Substituting into (7.3) and (7.4), we get

$$(u-\lambda)u_x = -c^2 \rho_x/\rho \quad \text{and} \quad (u-\lambda)\rho_x = -\rho u_x ,$$

¹³This is the approach of Landau and Lifschitz [B6, §94], whose exposition is similar.

respectively. In turn, these imply that

$$u_x/\rho_x = -c^2/\rho(u-\lambda) = (u-\lambda)/\rho ,$$

whence $(u-\lambda)^2 = c^2$, $u-\lambda = \pm c$, and so, finally, $\lambda = u \pm c$. This proves the following result: in any simple wave, each isobar (isovel or isotherm) has a constant slope $\lambda(\rho)$: it is therefore a straight line in the (x,t) -plane.

Conversely, given a family of straight lines in the (x,t) -plane with smoothly varying slope λ , by choosing the density $\rho(\lambda)$ so as to make $u \pm c = \lambda$ for the specified equation of state, we obtain a simple wave. Moreover as long as $|u(0,t)| < c(0,t)$, we can generate such a simple wave in a fluid initially at rest by a 'moving piston' with velocity at one end (for which $a = 0$).

A more difficult argument, presented in Courant-Friedrichs [B3, §29], shows that the boundary of any region of constant state must also satisfy $dx/dt = u \pm c$. Moreover [B3, p. 95], forward-moving simple plane waves in a perfect gas (isentropic flow) satisfy

$$(7.5) \quad u + c = u_0 + c_0 + \frac{\gamma+1}{2}(u - u_0) .$$

It follows that characteristic lines containing faster moving particles gain on those with smaller u if $\gamma > -1$, which is always the case in real gases. This conclusion is commonly rephrased in the statement that the density profiles of compression waves steepen with time, whereas those of rarefaction waves flatten [B6, p. 97]. Here by a 'compression wave' is meant one in which u is a decreasing function of x , so that $\rho_t = -\rho u_x$ is increasing in time, whence by (7.5) $u+c$ is also a decreasing function of x .

Riemann's equations. For any system of plane waves, the two families of curves in the (x,t) -plane defined by

$$(7.6) \quad dx/dt = u+c \quad \text{and} \quad dx/dt = u-c ,$$

respectively, are called 'characteristic curves' or simply characteristics. They have an elegant formulation due to Riemann (1859).¹⁴ For $p = k\rho^\gamma$ defined as in (5.5), let

$$\int \frac{dp}{\rho} = \int k\gamma\rho^{\gamma-1} = \frac{k\gamma}{\gamma-1} \rho^{\gamma-1} = \omega$$

Then Euler's equations [(2.1)-(2.2) of Chapter 1] are equivalent to

$$(7.7) \quad u_t + uu_x = -c\omega_x, \quad \omega_t + u\omega_x = -cu_x.$$

Adding and subtracting, we obtain

$$(7.8) \quad \left\{ \frac{\partial}{\partial t} + (u+c) \frac{\partial}{\partial x} \right\} (\omega+u) = 0$$

and

$$(7.9) \quad \left\{ \frac{\partial}{\partial t} + (u-c) \frac{\partial}{\partial x} \right\} (\omega-u) = 0$$

In a 'simple' wave, therefore, either $\omega+u$ or $\omega-u$ is constant.

Conclusion. We have constructed in §§6-7 two important families of inviscid compressible flows by analytical methods: self-similar flows and simple flows. In both families, however, the flows depend on functions of one variable only. In Chapter 6, we will show why numerical methods are not subject to this limitation.

8. Viscosity. In real fluids, the Helmholtz-Kelvin Principle of Permanence of Circulation fails to hold because of tangential stresses due to viscosity, or 'internal friction'. As we will show in Chapter 7, the net effect of these in an incompressible fluid is to add a term $\nu \nabla^2 \underline{u}$ to the Euler-Lagrange equations of motion,

¹⁴See Lamb [A6, p. 482], whose exposition we summarize here. Riemann's analysis was clarified by Rayleigh (Papers, vol. V, p. 573).

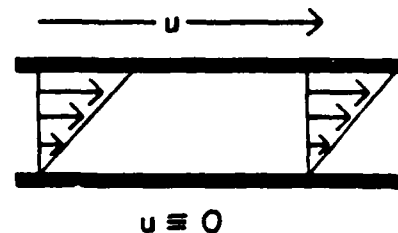
thus replacing Eq. (2.1) of Chapter 1 by

$$(8.1) \quad \begin{array}{l} \text{compensates for} \\ \text{incompressibility} \end{array} \quad \begin{array}{l} \text{diffusion} \\ \text{diffusion} \end{array} \\ Du_i/Dt = -\partial p/\rho \partial x_i + g_i + \nu \nabla^2 u_i ,$$

where ν is a material constant depending on the fluid,¹⁵ and called its kinematic viscosity. Physically, $\nu \nabla^2 \underline{u}$ represents diffusion of momentum by molecular wandering.

The vector partial DE (8.1), together with $\nabla \cdot \underline{u} = 0$ and $\rho = \rho_0$, defines Model 3 of Table 1. In this section, we will try to motivate it and describe its significance, by applying it to the two families of time-independent vortex flows described in Examples 10 and 11 of Chapter 1, §10.

Parallel flow. Consider first a steady parallel flow with velocity field $(0,0,w(x,y))$. One naturally guesses (with Newton) that an internal shear stress will arise across any plane parallel to the streamlines, proportional to the velocity gradient perpendicular to that plane. Thus the tangential stress acting on the sides of a rectangular cylinder will be as in the adjacent drawing.



The resultant force per unit distance in the z-direction will be

$$\begin{aligned} & \mu \int [w_x(x+\Delta x, y) - w_x(x, y)] dy + [w_y(x, y+\Delta y) - w_y(x, y)] dx \\ & = \mu \iint [(w_x)_x + (w_y)_y] dx dy , \end{aligned}$$

where the last equation follows by Stokes' Theorem.

To balance this resulting force and keep the flow in equilibrium requires an opposite longitudinal pressure gradient of

¹⁵ Actually $\nu = \mu/\rho$ and the viscosity $\mu = \rho \nu$ depend on the temperature and pressure, especially in liquids. In gases, μ is nearly independent of the density (pressure).

$-\partial p/\partial z$ acting on the ends of the cylinder. Moreover, since there is no lateral acceleration, we must have $\partial p/\partial x = \partial p/\partial y = 0$, whence $p = p(z)$. We conclude the condition for equilibrium:

$$(8.2) \quad p'(z) = \mu \nabla^2 w(x,y) ,$$

where p decreases as z increases and so $\nabla^2 w < 0$. Finally, since the left side of (8.2) depends only on z , and the right side only on x and y , both must be constant. That is, in parallel flow we must have¹⁶

$$(8.3) \quad \nabla^2 w = C , \quad p = \mu C z .$$

No slip boundary condition. Now consider flow parallel to the z -axis in a cylindrical pipe whose cross-section in the (x,y) -plane is S . To determine the 'velocity profile' $w(x,y)$, the DE (8.3) must be supplemented by a stronger boundary condition than the boundary condition $u_n = 0$ of non-viscous flow theory. Since any finite shear stress implies a finite velocity gradient, and a finite velocity gradient makes a discontinuity in w impossible, the natural boundary condition is the no slip condition $w \equiv 0$ on ∂S .

Poiseuille flow. The most important case is that of a circular pipe of radius a , $S: x^2 + y^2 = a^2$. In that case,

$$(8.4) \quad w = C(r^2 - a^2)/4 , \quad r^2 = x^2 + y^2 ;$$

the velocity profile is parabolic. The discharge rate (total volume flowing per unit time), is

$$Q = \iint w(x,y) dx dy = \frac{-2\pi C}{4} \int_0^a (a^2 - r^2) r dr = -\pi C a^4/8$$

Substituting into (8.3), we get

¹⁶The 'membrane equation' $\nabla^2 w = C$ of constant linearized mean curvature arises also in the torsion problems of elasticity.

$$(8.4') \quad -\frac{\partial p}{\partial z} = -\mu C = 8\mu Q/\pi a^4 ,$$

$$\text{or } Q = \pi a^4 (-dp/dz)/8\mu. \text{ }^{17}$$

Couette flow. We next consider the equilibrium of pure plane swirl, with $u_r = 0$ and $u_\theta = f(r)$, under the action of viscous forces. Since the angular velocity at radius r is $\omega(r) = f(r)/r$ the rate-of-strain matrix has an angular shear component of

$$\lim_{\Delta r \rightarrow 0} [f(r+\Delta r) - (r+\Delta r)f(r)/r]/\Delta r ,$$

or $f'(r) - f(r)/r$. Hence the viscous shear stress is $\mu[f'(r) - f(r)/r]$ per unit length; the total viscous force acting on a circle is $\mu[rf'(r) - f(r)]$, and the torque exerted is $\mu[r^2f'(r) - rf(r)]$. This torque must be a constant in steady flow, so that

$$(8.5) \quad r^2f'(r) - rf(r) = K \quad \text{in equilibrium .}$$

Since $(f/r)' = f'/r - f/r^2$, clearly $1/r^3$ is an integrating factor, and the general solution is

$$(8.6) \quad \omega(r) = f(r)/r = K \int dr/r^3 = C - K/2r^2 ,$$

where C is a constant of integration and μK is the torque. This gives, finally,

$$(8.7) \quad u_\theta(r) = Cr - K/2r .$$

Flows satisfying (8.7) are called Couette flows; given two concentric rotating cylinders of radii a and $b > a$, rotating with angular velocities $\omega(a)$ and $\omega(b)$, there is just one Couette flow between them which satisfies the no slip boundary condition.

Measuring viscosity. Formula (8.5) makes it easy to measure viscosity. Let the clearance between two (exactly) concentric

¹⁷See [A5, §138]. Note that the distance from the inlet required to establish a parabolic velocity profile in a circular pipe is considerable; see [A5, §139].

cylinders be δ , and let the inner cylinder of radius a be held stationary by a measured torque N . Then, by (8.5),

$$(8.8) \quad N = 2\pi\mu K = \mu[a^2 f'(a) - af(a)] .$$

Now let the outer cylinder of radius $a+\delta$, be rotated with angular velocity ω . By (8.6) and the 'no slip' condition on the inner cylinder, $Ca = K/2a$, whence $K = 2a^2 C$. By (8.7) and the 'no slip' condition on the outer cylinder

$$\frac{K(a+\delta)}{2a^2} - \frac{K}{2(a+\delta)} = (a+\delta)\omega .$$

A little algebraic manipulation gives from this

$$K = \frac{a^2(a+\delta)^2}{2(2a\delta + \delta^2)} ,$$

whence

$$(8.9) \quad \mu = N/2\pi K = \frac{(2a\delta + \delta^2)}{\pi a^2(a+\delta)^2} \frac{N}{\omega} ,$$

and μ is about $2\delta N/\pi a^3 \omega$.

Plane viscous flows. The effect of viscosity on the vorticity $\zeta = v_x - u_y$ in plane viscous flows is very simple. Taking the curl of the Navier-Stokes equation (8.1), the terms $\nabla \times (\nabla p)$ and $\nabla \times (\nabla G)$ drop out, in three dimensions also. Moreover, expanding $\nabla \times (D\underline{u}/Dt)$:

$$(u_t + uu_x + vu_y)_y - (v_t + uv_x + vv_y)_x ,$$

and deleting $u_y(y_x + v_y) - v_x(u_x + v_y)$ because $u_x + v_y = 0$, we get

$$(v_x - u_y)_t + u(v_x - u_y)_x + v(v_x - u_y)_y ,$$

which is just $D\zeta/Dt$. In summary, we have the following result.

THEOREM. The vorticity in any plane time-dependent incompressible viscous flow satisfies the DE

$$(8.10) \quad D\zeta/Dt = \nu \nabla^2 \zeta .$$

9. Reynolds number. Model #3 of Table 1 assumes the Navier-Stokes Equations (8.1); we rewrite them in vector form as:

$$(9.1) \quad D\mathbf{u}/Dt = -\nabla p/\rho + \mathbf{q} + \nu \nabla^2 \mathbf{u} , \quad \nu = \mu/\rho .$$

It also assumes $\nabla \cdot \mathbf{u} = 0$ and $\rho = \rho_0$; and finally, it assumes the 'no slip' boundary condition $\mathbf{u} = 0$ on stationary solid surfaces--and continuity of velocity on moving solid surfaces.¹⁸ We will refer to flows that satisfy these conditions as incompressible viscous flows, or flows of an incompressible viscous fluid.

Remark 1. Even in a moving fluid of constant density ρ_0 , the effect of a conservative gravity field $\mathbf{q} = \nabla G$ is simply to decrease the hydrostatic pressure by $\rho_0 G$, where G is the gravitational potential.

Remark 2. As was noted before, any 'potential flow' satisfies (9.1)--though rarely the boundary condition of 'no slip'.

If we compensate for gravity effects by Remark 1, Eq. (9.1) reduces to¹⁹

$$(9.2) \quad \frac{\partial u_i}{\partial t} + \sum u_k \frac{\partial u_i}{\partial x_k} + \frac{1}{\rho} \frac{\partial p}{\partial x_i} = \nu \nabla^2 u_i , \quad i = 1, 2, 3 .$$

We now consider the possibility of obtaining 'similar' incompressible viscous flows with scale models, in which distance, time, density, and viscosity are transformed by specified 'scale factors' as follows:

$$(9.3) \quad \begin{aligned} x_i &\rightarrow \alpha x_i , & t &\rightarrow \beta t , \\ \rho &\rightarrow \gamma \rho , & \mu &\rightarrow \delta \mu , \end{aligned}$$

¹⁸We postpone a discussion of what conditions to impose on free (e.g., liquid-air) surfaces until Chapter 8, liquid-liquid interfaces are even more complicated.

¹⁹Since we will discuss only fluids of constant density in the rest of this chapter, we will omit the subscript on $\rho_0 = \rho$.

whence $v \rightarrow \delta v/\gamma$. Suppose also that the pressure is allowed to change by $p \rightarrow \kappa p + \lambda$, where κ and λ are unspecified constants, not controlled experimentally. Then the four terms of (9.2) are multiplied by factors

$$\alpha/\beta, \quad \alpha/\beta^2, \quad \kappa/\alpha\gamma, \quad \delta/\alpha\beta\gamma$$

respectively. Clearly, (9.2) still holds if and only if these factors are all the same. This is evidently the case if and only if $\alpha^2\gamma/\beta\delta = 1$; the pressure will then adjust so that $\kappa = \alpha^2\gamma/\beta^2$ -- i.e., it will be multiplied by the same factor as ρU^2 , where U is a representative velocity.

These conclusions are most conveniently restated in terms of the Reynolds numbers

$$(9.4) \quad Re = \rho U d/\mu = U d/\nu$$

of the flows. Since the Reynolds number is multiplied by $\gamma\alpha^2/\beta\delta$ under the specified changes of scale, we have the following basic result.

THEOREM. Two flows of incompressible viscous fluids determined by geometrically similar constraints are themselves similar under the changes of scale (9.3), if and only if they are at the same Reynolds number Re .

COROLLARY. Similar bodies held in uniform streams of two incompressible viscous fluids with the same orientation must have the same drag coefficient at any given Re . In symbols, $C_D(Re)$ is a single-valued function for objects having given shape.

Discussion. As Prandtl-Tietjens explain vividly in [A8, Chapter II], the Reynolds number of a flow past a solid is a rough measure of the ratio

$$(\text{inertial forces})/(\text{viscous forces})$$

Hence, if it were not for the fact that the Navier-Stokes equations are a singular perturbation of Euler's equations, one would expect that above a sufficiently large Re , incompressible viscous flows

past any obstacle would deviate arbitrarily little from the potential flow past the same obstacle.

And indeed, this expectation is fulfilled except has passed very near the in a thin boundary layer that is dominated by the no-slip boundary condition dominates. This boundary layer is shed into a wake behind the obstacle, and the high concentration of vorticity in the boundary layer is transported with it, creating vortices or "eddies" which are a conspicuous feature of most wakes. Although these real wakes are quite different from the imaginary 'stagnant' wakes that we investigated in [A9, Chapter 1], they do lead to drag coefficients $C_D(\text{Re})$ having the same order of magnitude.

Cylinders. The prediction of the preceding corollary has been confirmed in countless experiments; we will now consider in some detail the observed flows past a circular cylinder held broadside. In this case, as the Reynolds number increases from 0.001 (say) to 10^7 , a remarkable series of metamorphoses takes place.²⁰

When $\text{Re} < 0.1$, a large mass of fluid around and behind the cylinder is retarded. As Re increases from 0.1 to 30 or so, two stationary vortices form symmetrically behind the cylinder, becoming more and more elongated as the Re increases.

When $\text{Re} > 50$ or so, steady flow (though presumably possible mathematically) becomes unstable. Indeed, in the range $50 < \text{Re} < 500$, vortices of opposite sign are shed from opposite sides in alternation. A very suggestive (if inaccurate!) approximation to the flow is a vortex sheet consisting of two semi-infinite rows of staggered point-vortices; their spacing ratio is determined by approximate stability. When Re exceeds 1000, the wake becomes increasingly turbulent. Plots of $C_D(\text{Re})$ are shown in [A8, p. 96] and [A5, p. 419]; although not totally consistent, they are the same for air as for water.

²⁰ For much more detailed descriptions of flows past circular cylinders, see [A5, pp. 417-39] and [A4, Chapters XI-XIII]. A vivid and realistic general overview of viscous flows past "bluff bodies" is in [A5, Chapter 5].

Some idea of the range of Re of practical importance may be had by noting that an airplane wing whose chord length is 5 meters, when moving through air ($\nu \approx 0.1$) at 720 Km/hr, has a Re of the order of 10^8 . When $Re > 2 \times 10^5$, the boundary layer becomes turbulent, and the observed pressure distribution (plotted in dimensionless form as $C_D(\theta)$) bears a fair resemblance to that for potential flow (see the Figure, xeroxed from [A5, p. 422]).

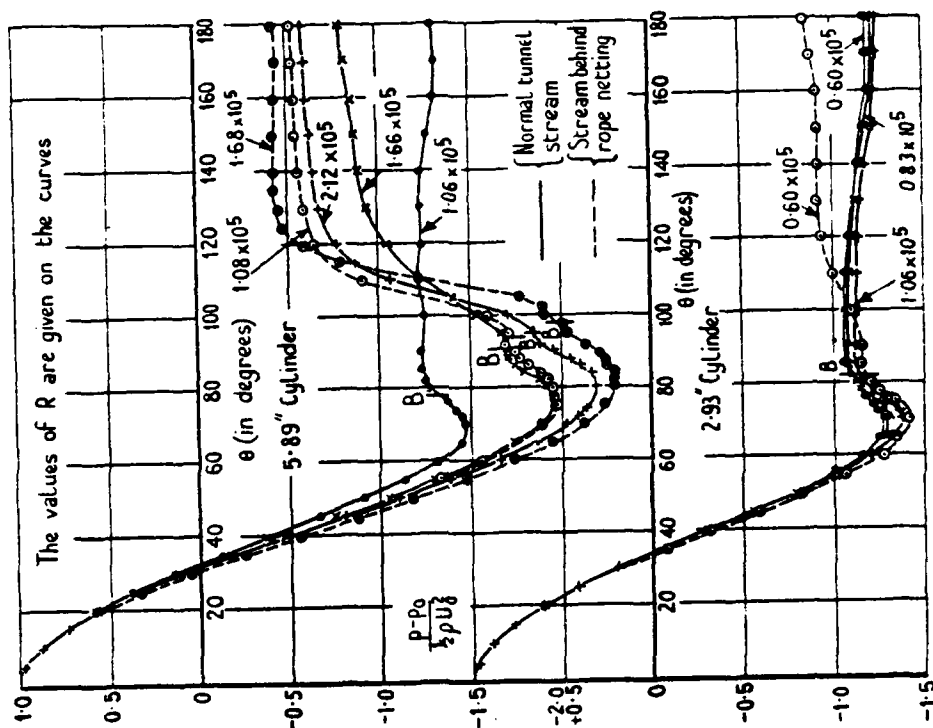


FIG. 152.

Spheres. The flow past a sphere held fixed in a uniform stream exhibits analogous qualitative variations with the Re . When $Re < 50$ or so, a time-dependent or "steady" flow is obtained, as one might expect intuitively. However, when $Re > 50$, the steady flow apparently becomes unstable; a "boundary layer" (see §10) then separates from the sphere near its equator, and flows into a "wake" consisting of possibly turbulent (when $Re > 500$) vortices.

Stokes flow past sphere. In more detail, if inertial forces (the convection terms $\sum u_k \partial u_i / \partial x_k$) are neglected, the Navier-Stokes equations reduce to Stokes' DE for "creeping" flow in cylindrical coordinates:

$$(9.5) \quad \left[\frac{\partial^2}{\partial r^2} - \frac{1}{r} \frac{\partial}{\partial r} + \frac{\partial^2}{\partial z^2} \right]^2 \psi = 0 .$$

Stokes succeeded in integrating this DE by separating variables in spherical coordinates. Namely, the substitutions $z = R \cos \theta$, $r = R \sin \theta$, $\psi = f(r) \sin^2 \theta$ reduce (9.5) as in [A6, §338] to:

$$(9.6) \quad \left[\frac{\partial^2}{\partial R^2} - \frac{2}{R^2} \right]^2 f(R) = 0 .$$

This is a special case of Euler's homogeneous DE, and has a basis of solutions of the form R^ν ($\nu = -1, 1, 2, 4$). The hypotheses of no slipping at the surface $R = a$ and asymptotically uniform velocity U at ∞ give the solution

$$(9.7) \quad \psi = (3UaR/4) \left(1 - \frac{1}{3} \frac{a^2}{R^2} \right) \sin^2 \theta .$$

Denoting the net (axial) force on the sphere by D , and defining the dimensionless drag coefficient by

$$(9.8) \quad C_D = 2D/\pi \rho U^2 a^2 ,$$

we have $C_D = 24/Re$.

Assuming an asymptotic approximation of Oseen, S. Goldstein obtained the asymptotic series²¹

$$(9.9) \quad C_D = 24Re^{-1} \left\{ 1 + \frac{3}{16} Re - \frac{19}{1280} Re^2 + \frac{71}{20480} Re^3 - \dots \right\} ,$$

which exceeds the measured drag by less than 10% when $Re < 10$.

²¹[A5, §215]. The 1965 Dover edition corrects an error in Goldstein's original formula.

10. Boundary layer theory. It is usual to contrast "bluff" bodies like a sphere, circular cylinder, or broadside plate or disc, with "streamlined" shapes like a well-designed airfoil, whose "dividing streamline" separates at the "trailing edge". Loosely speaking, bluff bodies are followed by a broad wake, and their drag is primarily due to wake underpressure ("form drag"). In contrast, the drag of streamlined bodies is primarily due to skin friction.²² We will devote this section to a more careful analysis of skin friction, introducing Prandtl's boundary layer equations in the process.

Prandtl's concept [A8, p. 59] was that the flow field around a streamlined body "splits up into two regions:

1. Surrounding the surface of the solid body there is a thin layer where the velocity gradient $\partial w/\partial n$ generally becomes very large, so that even with very small values of the velocity w the shear stresses $\tau = \mu \frac{\partial w}{\partial n}$ assume values which cannot be neglected.

2. The region outside of this layer, where the velocity gradient does not become so large, so that the influence of viscosity is negligible. Here the streamline picture is entirely determined by the action of pressure, i.e., it is the picture of a potential flow."

In his celebrated paper of 1904, Prandtl gave intuitive arguments to justify neglecting all terms of the Navier-Stokes equations in the boundary layer of a flat plate (parallel to the x-axis) except the following [A8, p. 62, (2)]:

$$(10.1) \quad \frac{\partial u}{\partial t} + u \frac{\partial u}{\partial x} + v \frac{\partial u}{\partial y} = - \frac{1}{\rho} \frac{\partial p}{\partial x} + \frac{1}{Re} \frac{\partial^2 u}{\partial y^2} .$$

This contains, in addition to the terms of the DE for parallel flow, $y_t = u_{yy}/Re$, the convection term $uu_x + vu_y$ and a term $-p_x/c$ representing the effect of pressure variations outside the boundary layer.

The transverse velocity component $v(x,y)$ is determined by $u(x,y)$ from the incompressibility condition $u_x + v_y = 0$, as

²²See again Prandtl-Tietjens [A8, pp. 86-96]; also Goldstein [5, Chapter II].

$$(10.1') \quad v(x,y) = \int_0^y u_x(\eta,y) dy .$$

Alternatively, we can take the stream function ψ as unknown. This makes the equations of motion (13.1) reduce to

$$(10.2) \quad \psi_{ty} + \psi_y \psi_{xy} - \psi_x \psi_{yy} = -\frac{1}{\rho} p_x + \frac{1}{\text{Re}} \psi_{yyy} .$$

Blasius solution. In 1908, Blasius derived an exact self-similar solution of the boundary layer equations, starting from the observation that (by Rayleigh's analogy with the heat equation) the boundary layer should grow like $(vx)^{1/2}$. Assuming that the flow velocity U outside the boundary layer is constant (the case of a parallel plate in a uniform stream), we then have for $\xi = (vx/U)^{1/2}$ and $\eta = y/2\xi$, setting

$$(10.3) \quad \psi = U \xi f(\eta) ,$$

whence $u = \frac{1}{2} U f'$, $u_y = U f''/4\xi$, $u_{yy} = U^2 f'''(\eta)/8\xi^2$. The function f is characterized by the DE

$$(10.4) \quad f''' + ff'' = f'^2 - 1$$

and the boundary conditions $f(0) = f'(0) = 0$, $f''(\infty) = 2$.

In 1930, Falkner and Skan generalized the preceding result to the case that the flow velocity $U(x)$ outside the boundary layer was of the form $U = cx^m$. In this case, (10.4) is replaced by

$$(10.5) \quad f''' + m + \frac{1}{2}(m+1)ff'' = mf'^2$$

[A5, p. 140].

Today, boundary layers and their mathematical analysis constitute a major topic in fluid mechanics. For this reason, after a descriptive chapter on boundary layers [A5, Chapter II], Goldstein devotes another chapter [A5, Chapter IV] to their

mathematical theory, while Schlichting devotes an entire book [B9] to them.

Discussion. Obviously, the boundary layer approximation to the Navier-Stokes equations assumes that the flow near any surface is nearly parallel to that surface, because boundary layers are so thin, by definition. For the same reason, it assumes that the pressure inside the boundary layer near any point on the surface differs negligibly from that just outside the boundary layer. Outside the boundary layer, however, Bernoulli equation holds by #2 above, and so

$$(10.6) \quad p = p_0 - \frac{1}{2} \rho U^2(x) ,$$

where $U(x)$ denotes the flow speed just outside the boundary layer.²³ In boundary layer theory proper, this is assumed to be a known function.

The general mathematical problem of boundary layer theory is therefore to solve the nonlinear partial DE

$$(10.7) \quad uu_x + vu_y = UU'(x) + vu_{yy} ,$$

where v is determined by (10.1'), and the boundary conditions $u(x,0) \equiv 0$, $\lim_{y \rightarrow \infty} u(x,y) = U(x)$.

²³It is usually better to write $U_1(x)$ rather than $U(x)$, to avoid confusion with the "free stream velocity" of the main stream.

11. Turbulence. We have already described the physical breakdown at high Reynolds numbers, in pipes (§9) and in boundary layers (§10), of the mathematical model of "steady flow" definable from the Navier-Stokes equations by setting $\partial/\partial t = 0$. When the diffusion of momentum by viscous stresses becomes small enough in comparison with inertial convection, steady flow becomes unstable. We tried to relate this breakdown to the fact that the Navier-Stokes equations constitute a singular perturbation of the Euler-Lagrange equation, as $\nu \downarrow 0$. In this section, we will replace the deterministic model obtained by setting $\partial/\partial t = 0$ in the Navier-Stokes equation by a very different probabilistic model.

Flow in pipes. To clarify the meaning of this model, we will reconsider first some empirical facts about flows through straight cylindrical pipes. The "hydraulic radius" b of any such pipe is defined by

$$(11.1) \quad b = (\text{area})/(\text{circumference}) ,$$

so that $b = (\pi a^2)/(2\pi a) = a/2$ for a cylindrical pipe of radius a . Next, we define the dimensionless friction coefficient γ for a "steady" flow through such a pipe as in [A5, §137] by

$$(11.2) \quad \gamma = \frac{P_1 - P_2}{\frac{1}{2} \rho u_m^2} \frac{b}{\ell} , \quad \ell = \text{length} .$$

This represents the fraction of the kinetic energy of the mean flow that is converted to potential energy during flow through one hydraulic diameter.

In laminar Poiseuille flow $\gamma = 16/Re$, and this theoretical prediction has been generally confirmed experimentally for $Re < 2,000$. However, for $Re > 2,000$, the observed values of γ cease to decline, and may even increase in "smooth" pipes. Associated with this phenomenon is the fact that visual and

photographic evidence shows that the flow ceases to be parallel or "laminar", and becomes "turbulent", i.e., eddies instead. Careful experiments by Nikuradse, reproduced in the attached figures, xeroxed from [A5, p. 379], show asymptotic values of γ ranging from about .005 to about .015.

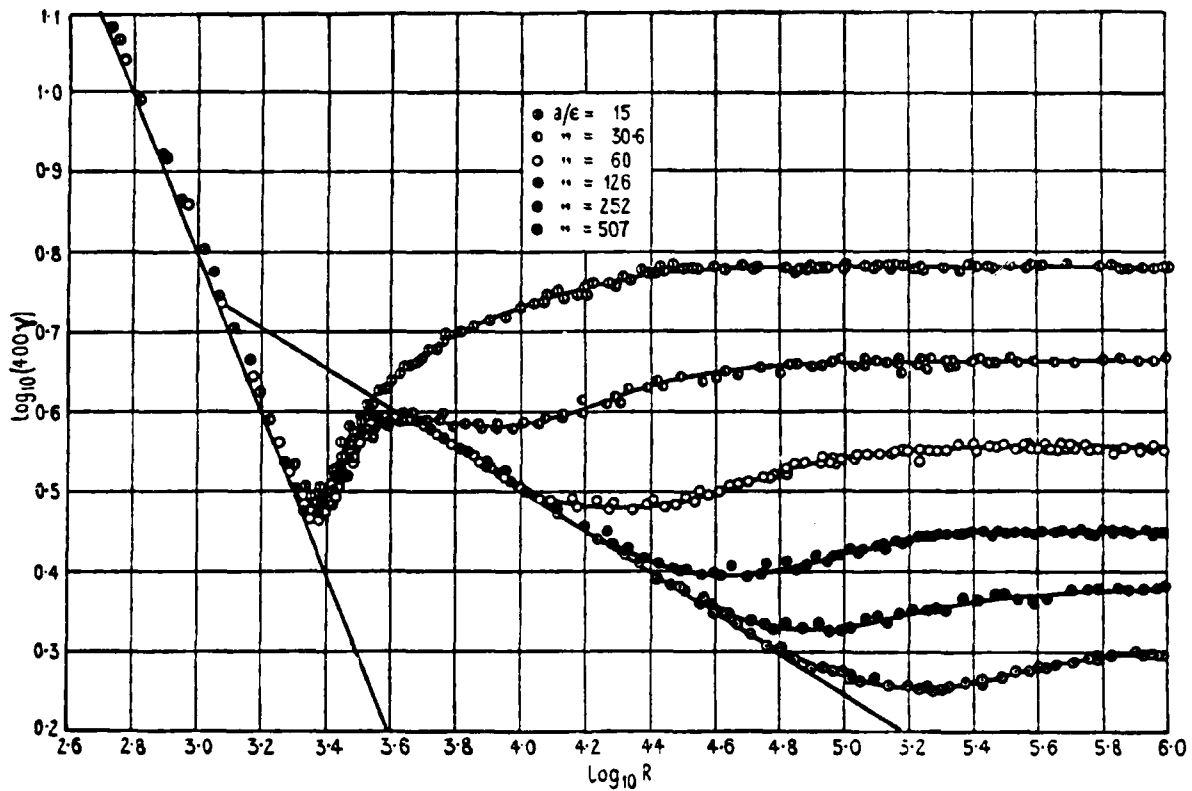


FIG. 121.

Boundary layers. We will next consider the separation point (or "zone") where the boundary layer "separates" from a cylindrical or spherical obstacle. Prandtl originally (1904) proposed predicting this by calculating (from $P(x)$) the point at which $\partial u/\partial y$ changed sign in the calculated boundary layer. Blasius used this criterion in 1908, to predict the separation point for slightly viscous flow past a circular cylinder, with reasonable success.³³ Although a more careful study by D. Meksyn³⁴ reveals many small discrepancies between "separation points" predicted by such methods and their observed positions, this criterion gives fairly good results at intermediate Re , $10^2 < Re < 10^5$ (say).

However, at a variable point in the range $10^5 < Re < 10^6$, the boundary layer in the flow around a sphere becomes turbulent, separation is delayed, contracts dramatically, and the drag coefficient decreases by 50% or so. The attached figure, reproduced from [5, p. 495] indicates the complexity of the phenomena. As a result, Prandtl's asymptotic boundary layer theory (which predicts an asymptotically constant C_D) becomes totally inapplicable.

Random velocity-fields. In order to obtain an adequate mathematical description of turbulent flows such as the preceding, it is agreed by experts that one must consider a "sample space" Ω of random velocity fields $\underline{u}(\underline{x};t;w)$. Moreover $\Omega = (\Omega, B, \mu)$ must assign a 'countably additive' probability measure $\mu(S)$ to each 'Borel subsets' $S \subset \Omega$.

In such a sample space, one can define the mean velocity field

$$(11.3) \quad \underline{u}_m(\underline{x}) = \int_{\Omega} \underline{u}(\underline{x};t;w) d\mu(w).$$

³³H. Blasius, Zeits. Math. Phys. 56 (1908), 1- .

³⁴D. Meksyn, "New Methods in Laminar Boundary Layer Theory", Pergamon, 1961.

The ergodic hypothesis is that this "sample average" will agree with the time average

$$(11.4) \quad \lim_{T \rightarrow \infty} \frac{1}{2T} \int_{-T}^T \underline{u}(\underline{x}; t; \omega) d\mu(\omega) .$$

Statistical models defined in this way are evidently entirely unlike any of the continuum models discussed previously in this book.

12. Analytical Fluid Dynamics in 1940. By 1940, the concept of Euler and Lagrange, of developing analytical fluid dynamics as a deductive science from the Euler-Lagrange equations, had become badly fragmented. As we have explained earlier, at least six very different initial-boundary value problems had been developed as analytical 'models' for fluid flows arising under different circumstances. An overview of these was given in Table 1 of p. 1-3. To this list should probably be added Prandtl's asymptotic model of "potential theory with boundary layers and vortex sheets". The model of "compressible inviscid flow with shocks" will be described in Chapter 6.

The inviscid 'fluid' defined mathematically by the Euler-Lagrange equations was renamed an 'ideal' fluid, and no longer believed in. Although it was recognized that "ideal fluid theory ... has been developed into an instrument of great elegance and power", and that "fairly close agreement with observation has been realized ... for tides and waves", it was considered "perhaps surprising, not that the results of theory and observation often disagree violently, but that they sometimes agree fairly well ..." [A5, p. 21].

Worse than that, by 1940 most experts thought of fluid mechanics as a complex web of theory and experiment, in which mathematics by itself should not be taken too seriously. For

AD-A135 900

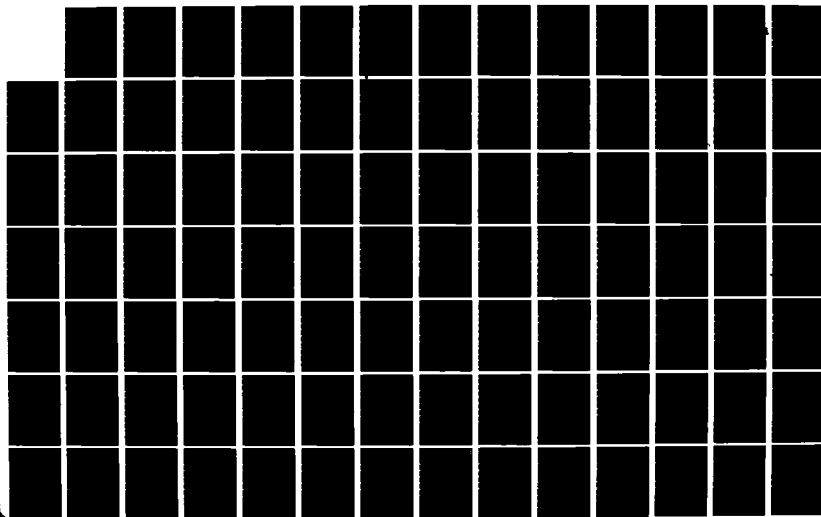
NNMERICAL FLUID DYNAMICS(U) HARVARD UNIV CAMBRIDGE MA
G BIRKHOFF 1983 N00014-75-C-0596

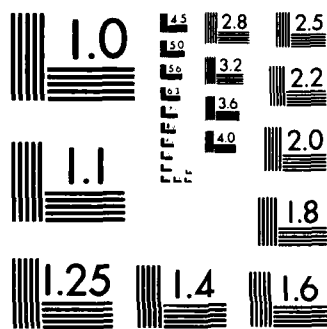
2/4

UNCLASSIFIED

F/G 20/4

NL





MICROCOPY RESOLUTION TEST CHART
NATIONAL BUREAU OF STANDARDS-1963-A

example, partial differential equations do not appear at all in Goldstein's influential "Modern Developments in Fluid Dynamics" [A5] until the third chapter, and the treatment becomes more and more empirical as the treatise progresses, so much so that it seems almost incredible that Lamb was originally to be the chief editor!

The same can be said of most other books and research articles on fluid mechanics written since 1940. Instead of deducing facts systematically from a consistent set of partial differential equations and boundary conditions, the authors pick and choose freely from a large collection of mathematical 'models', justifying their choice in each case by the tolerable 'fit' it gives to empirical data over some specified range of physical conditions.³⁵

Thus, the noble vision of Euler and Lagrange, together with its modification by Stokes, has been largely abandoned in contemporary analytical fluid dynamics. The basic reason for this relapse has been, of course, the inability of mathematicians to solve analytically the initial-boundary wave problems posed by the partial DE's of fluid mechanics.

In the 1940's, inspired by faith in the potentialities of programmed computers, John von Neumann proposed a new vision. Observing that approximate numerical methods were, in principle, free from the limitations to special geometries and linear DE's that generally characterize formal analytical solutions, he proposed using high-speed computers to make the "arithmetization of analysis" achieved theoretically in the 19th century into a practical reality.

The next chapter will try to give a clearer idea of von Neumann's vision. Our later chapters will then give case studies of the extent to which, in specified areas, this new vision is realizable today, and will try to predict how much more is likely to be achieved in the foreseeable future.

³⁵ Even this procedure is more justifiable philosophically than the use of empirical "constitutive equations" obtained by fitting empirical data over very limited ranges.

REFERENCES FOR CHAPTER 2

- [B1] George Batchelor, An Introduction to Fluid Dynamics, Cambridge Univ. Press, 1967.
- [B2] G. Birkhoff, "Numerical fluid dynamics", SIAM Review 25 (1983), 1-34.
- [B3] R. Courant and K. Friedrichs, Supersonic Flow and Shock Waves, Interscience, 1948.
- [B4] Collected Works of Th. von Kármán, 1902-1951,
- [B5] H.W. Liepmann and A.E. Puckett, Aerodynamics of a Compressible Fluid, Wiley, 1947.
- [B6] L.D. Landau and E.M. Lifschitz, Fluid Mechanics, Addison-Wesley, 1959.
- [B7] Ludwig Prandtl, Gesammelte Werke, 3 vols.
- [B8] Rayleigh (J.W. Strutt, Baron), Theory of Sound, 2 vols., 2d ed., Macmillan, 1926; Dover, 1945.
- [B9] H. Schlichting, Boundary Layer Theory, McGraw-Hill, 1955.
- [B10] G.G. Stokes, Mathematical and Physical Papers, Cambridge Univ. Press, 1880-
- [B11] G.I. Taylor, Scientific Papers, 4 vols. Cambridge Univ. Press, 1958-71.
- [B12] G.B. Whitham, Linear and Nonlinear Waves, Wiley, 1974.

3. VON NEUMANN'S INFLUENCE

1. Background. In Chapters 1 and 2, we summarized some basic facts about analytical fluid dynamics, from its initial mathematical formulation by Euler to its status as of 1940, giving historical perspective where feasible. Lamb's Hydrodynamics [A6], and Pradtl-Tietjens' Hydro- and Aeromechanics ([A7],[A8]) are the most helpful references for amplifying this summary.¹

We now turn to the revolutionary concept of numerical fluid dynamics, which developed in the first two decades after World War II into a major scientific and engineering effort. Although numerical fluid dynamics deals with the same physical phenomena as analytical fluid dynamics, its mathematical tools are entirely different. Whereas analytical fluid dynamics relies on separations of variables, conformal mappings, superpositions of solutions, and other special methods of classical analysis, numerical fluid dynamics is based on general existence, uniqueness and convergence theorems. Its cornerstone is the principle that all constructive mathematics can be reduced to the performance of arithmetic operations and suitably defined 'passages to the limit': the so-called Arithmetization of Analysis.

The successful 'arithmetization of Analysis', based on strict adherence to "Weierstrassian rigor" was a major theoretical achievement of 19th century mathematicians. Its importance was clearly and prominently expressed by Henri Poincaré, himself the leading rigorizer of the partial DE's of classical mathematical physics, in his keynote address to the 1900 International Mathematical Congress.

Although Weierstrass, Poincaré, and other 19th century mathematicians may have succeeded in 'arithmetizing Analysis' in principle, large-scale, high-speed supercomputers are needed to 'arithmetize' Fluid Dynamics in any practical sense. John von Neumann (1903-1955) was one of the first scientists to

¹See also [B2], which gives a less technical overview.

appreciate the potentialities of such computers, and most of this chapter will be concerned with his ideas and influence.

It is a relevant but easily overlooked fact that, when the first edition of Lamb's classic book was published in 1879, the theory of partial DE's was virtually non-existent. The first edition of Rayleigh's Theory of Sound [B8] had just been published (1877), and it is not surprising that Lamb and other specialists in analytical fluid mechanics relied on the methods of Lagrange, Laplace, Fourier, Stokes, Helmholtz, Kelvin, and other earlier mathematicians, as interpreted by Rayleigh and in Thomson and Tait's Principles of Natural Philosophy (1870).

However, between 1879 and 1932, the publication date of Lamb's sixth edition, the theory of partial differential equations developed enormously. It also became widely disseminated through texts and monographs written by such outstanding research figures (or pairs of figures) as Poincaré, Hadamard, Courant-Hilbert, Frank-von Mises, Kellogg, Riemann-Weber, and Sommerfeld. However, Lamb seems to have considered none of these books to be helpful for solving problems in analytical fluid dynamics.

On the contrary, he explicitly remarks [All, p. 61]: "The formal proof of 'existence-theorems' of this kind is not attempted in the present treatise. For a review of the literature of this part of the subject the reader may consult [Encyc. der math. Wiss. ii (1900)]." Indeed, the emphasis on general theorems of existence, uniqueness, and convergence which characterized "Weierstrassian rigor" seems to have had little influence on developments in analytical fluid dynamics right up to the present time. Thus, after a polite paragraph distinguishing hyperbolic from elliptic and parabolic DE's, Whitham [1974, p. 142] simply refers the reader "to the many excellent texts on the general theory of partial differential equations".

In sharp contrast, von Neumann's concept of mathematical physics was dominated by the ideas expounded in the books listed above. Throughout his career, he was primarily concerned with fundamental general principles and general formulas, similar to

those which had preoccupied Dirichlet, Riemann, Helmholtz, Kirchhoff, Poincaré, Hadamard, and Hilbert.² Like Hilbert, moreover, he was strongly attracted to axiomatic foundations of mathematics and mathematical physics, and had himself made notable contributions to these foundations during the years 1925-41. In this spirit, during the years 1927-40 he had been a pioneer in the reformulating ideas about partial differential equations in terms of function space concepts, thereby facilitating a much more general 'arithmetization of analysis' than had been achieved by his predecessors.

Most mathematicians having this background and taste (and I am one of them), believe that a truly rigorous science of numerical continuum physics should (ideally) be developed along the following lines:

1. Specification of a system of assumed partial DE's and other auxiliary equations (e.g., initial and boundary conditions) which take into account all the relevant physical variables.
2. Convincing deductive proof that these assumptions define well-posed initial and/or boundary value problems.
3. Convincing experimental proof that, this exact mathematical solution is, in general, physically realistic.
4. In each case, specification of a directed set of systems of approximate equation (E_h), called (full) discretizations of the exact problem, each of which is also well-set and can be solved to any desired accuracy $\epsilon > 0$ in a finite number of arithmetic operations.
5. Provision of algebraic and/or combinatorial algorithms and a computer, which together make it possible to perform these operations at a cost $\$ = \(h, ϵ) less than the benefit to be derived from knowing the solution.

From a practical engineering standpoint, it is not necessary that these algorithms should converge for arbitrarily small h . But ideally, Steps #1-4 should be feasible; this is precisely what Poincaré and others meant in referring to the 'arithmetization of analysis'. Only Step 5 depends on computing hardware.

²Hilbert was even more rigorous than Poincaré!

Accordingly, in Chapters 4-6, we will try to conform to the ideal of Steps 1-5 outlined above. It will only be in Chapters 7 and 8 that we will compromise these lofty principles in describing how numerical fluid dynamics has been successfully applied to scientific and engineering problems.

2. Progress before 1930. Von Neumann was by no means the first person to solve fluid flow problems by direct calculation ('arithmetic'). Already in 1889, the Flemish engineer Massau had used the method of characteristics to predict the progress of flood waves (Stoker [A10, p. 482]).

Similarly, L.F. Richardson (1881-1953) had made determined efforts to solve problems involve the Laplace and biharmonic operators ∇^2 and ∇^4 by numerical methods before World War I.³ For this purpose, he used the now standard 5-point difference approximation to $\phi_{xx} + \phi_{yy} = 0$ on a square mesh.

$$(2.1) \quad \phi_{i,j} = \frac{1}{4}[\phi_{i-1,j} + \phi_{i+1,j} + \phi_{i,j-1} + \phi_{i,j+1}] = \frac{1}{4} \diamond \phi_{i,j},$$

on a square mesh. Twenty-five years later (see §4), Southwell was to demonstrate the fruitfulness of Richardson's methods.

In the following decade, he tried his hand at numerical weather forecasting, publishing a book on the subject in 1922.⁴ This, too, had a lasting influence.

Likewise, Stan Ulam once told me (personal communication) that Marcel Brillouin was provided with a computing assistant, for some years around 1900, to help him calculate ocean tides numerically from first principles. After two years, alas, he

³See Phil. Trans. A210 (1911), 307-57, and Proc. Phys. Soc. London 23 (1911), 449-88. For historical perspectives, see the article, "Solving Elliptic Problems: 1930-1980" by one of us in [24]. The difference approximation (2.1) was known to Runge (1906).

⁴"Weather Prediction by Numerical Process", Cambridge University Press, 1922; Dover Reprint (with an introduction by Sydney Chapman) 1965. For a thoughtful analysis of its contents, see George W. Platzmann, Bull. Am. Meteor. Soc. 48 (1967), 514-50 and 49 (1968), 495-500.

discovered that his assistant had made a mistake in the first three months that vitiated all their subsequent calculations!

The 'arithmetization' of the solution of partial DE's continued to make progress during the years 1900-1930. Thus in 1917, R.G.D. Richardson proposed using properties of the 5-point difference approximation (2.1) on square nets to deduce not only "well-known results...for...elliptic partial equations", but also as a research tool for investigating "the new boundary problem for the hyperbolic equation". In 1922, Phillips and Wiener made a more rigorous application of the same idea to the Dirichlet problem.⁵ Historians of science will doubtless find many other precursors of modern numerical methods written before 1925, such as the 1924 paper of Hardy Cross on his 'moment distribution' method, which foreshadowed the 'relaxation method' of Southwell (see below).

But the most notable pre-1930 paper on the numerical solution of partial DE's was written in 1927 by Courant, Friedrichs, and Lewy [C3]. This path-breaking article begins by rederiving the main conclusions of R.G.D. Richardson, Phillips, and Wiener about the Dirichlet problem in the plane. It points out that analogous methods can be applied to the 7-point difference approximation to $\phi_{xx} + \phi_{yy} + \phi_{zz} = 0$ on a cubic mesh,

$$(2.2) \quad \phi_{i,j,k} = \frac{1}{6}[\phi_{i-1,j,k} + \phi_{i+1,j,k} + \phi_{i,j-1,k} + \phi_{i,j+1,k} \\ + \phi_{i,j,k-1} + \phi_{i,j,k+1}]$$

It then analyzes difference approximations to the diffusion equation $u_t = \alpha \nabla^2 u$ and the wave equations $u_{tt} = c^2 \nabla^2 u$, this time on uniform rectangular meshes with mesh-length h in space and $k = \Delta t$ in time.

For the diffusion equation in one space dimension, it proposes the forward difference scheme⁶

⁵R.G.D. Richardson, Trans. Am. Math. Soc. 18 (1917), 489-518; H.B. Phillips and N. Wiener, J. Math. and Phys. 2 (1923), 105-24.

⁶This scheme had been proposed earlier by E. Schmidt, Föppl Festschrift, Springer, 1924, p. 123.

$$(2.3) \quad u_j^{i+1} = u_j^i + r[u_{j+1}^i - 2u_j^i + u_{j-1}^i], \quad \text{where } r = \alpha\Delta t/h^2.$$

For the wave equation, it proposes the 5-point approximation

$$(2.4) \quad u_j^{i+1} = 2u_j^i - u_j^{i-1} + r^2[u_{j+1}^i - 2u_j^i + u_{j-1}^i],$$

where $r = \alpha\Delta t/h$. This is exact at mesh-points when $r = 1$. More generally, in m dimensions, it proposes using

$$(2.5) \quad u_j^{i+1} = 2u_j^i - u_j^{i-1} + r^2 \nabla_h^2 u_j^i,$$

where $\nabla_h^2 u_{j,j}^i = \diamond u_{j,j}^i - 2mu_j^i$ is the discrete $(2m+1)$ -point Laplacian.

These difference approximations have obvious applications to fluid mechanics. Thus the diffusion equation applies to parallel flows (Chap. 1, §11), while the wave equation applies to sound waves, which will be our major concern in Chapter 4. However the authors of this famous paper do not seem to have been seriously interested in these or any other applications at the time.

3. Stability conditions. Instead, they were interested primarily in the convergence of the approximate solutions to a (limiting) exact solutions, when r is fixed and $h \downarrow 0$. To this end, they made a notable analysis of the stability of the preceding difference approximations. They showed there that, in order to prevent the solutions from 'blowing up' in finite time, one had to limit the time-step t in terms of the spatial mesh-length Δx , by the formulas

$$(3.1) \quad r = \Delta t/\alpha\Delta x^2 \leq \frac{1}{2} \quad \text{for } u_t = \alpha u_{xx},$$

and

$$(3.2) \quad r = \Delta t/c\Delta x \leq 1 \quad \text{for } u_{tt} = c^2 u_{xx},$$

The dimensionless ratios r occurring in (3.1) and (3.2) are called the Courant numbers of the uniform rectangular meshes on which Courant and his collaborators proposed to solve initial-boundary value problems. More precisely, they proved

THEOREM 1. For fixed $r > 1/2$ and a uniform rectangular mesh in (x,t) -space, the ΔE (difference equation) (2.3) is violently unstable, in the sense that, for almost all initial data, solutions of (2.3) are unbounded as $\Delta x \downarrow 0$. Likewise, the DE (2.4) is violently unstable if $r > 1$.

Proof. As regards (2.3), we will consider solutions of the special form

$$(3.3) \quad u_j^i = (-1)^j \gamma^i, \quad \gamma = 1 - 4r.$$

We omit the verification that such functions do indeed satisfy (2.3).

Likewise, $u_j^i = \gamma^i (-1)^j$ satisfies (2.4) if and only if

$$(3.4) \quad \gamma^2 = 2\gamma(1 - 2r^2) - 1.$$

The roots γ_1, γ_2 of (3.4) satisfy $\gamma_1 \gamma_2 = 1$. Hence, if the discriminant $4r^2(1 - r^2)$ of the equation is negative, one of the $|\gamma_i|$ must exceed 1, and again the rate of growth of solutions of (2.4) must be unbounded as $h \downarrow 0$ with fixed r .

Conversely, we have

THEOREM 2. If $r \leq 1/2$, then the solutions of (2.3) for any continuous initial $u(x,0)$ converge to a solution of $u_t = u_{xx}$, as $h \downarrow 0$. Likewise, if $r \leq 1$, then the solutions of (2.4) for any continuous $u(x,0)$ converge to a solution of $u_{tt} = c^2 u_{xx}$.

If r satisfies the inequality (3.3), then $u_j^i = \gamma^i e^{ikj}$ satisfies (2.3) if and only if

$$\gamma = 1 - 2r(1 - \cos kh).$$

Since any set of initial values can be expanded in Fourier series, and $1 - \cos kh \geq 2$, this implies stability if $\gamma \leq 1/2$. Likewise, if $r \leq 1$ in (3.4), then $|\gamma| = 1$ for any solution $u_j^i = \gamma^i e^{ikj}$ of (2.4), since

$$\gamma^2 = 2\gamma - 2r^2(1 - \cos kh) - 1$$

has a positive discriminant. Hence we have neutral stability.

Remark. The preceding proofs are only sketched. In particular, we do not distinguish sharply enough between the cases of an infinite domain, $(-\infty, \infty)$, a semi-infinite domain such as $(0, \infty)$, and a finite interval $[0, b]$. We will make these distinctions, and discuss which boundary conditions give rise to well-set initial value problems, in Chapter 5 (for $u_{tt} = c^2 u_{xx}$) and in Chapter 7 (for $u_t = \alpha u_{xx}$).

4. Southwell and 'relaxation' methods. The idea of solving partial DE's by numerical methods continued to gain momentum in the 1930's. Mention should be made of ingenious calculations by Bickley and Thom in England, from the 1920's on, which determined various properties not only of potential flows, but also of incompressible viscous flows past obstacles of various special shapes. We shall review these briefly in Chapters 4 and 7, respectively.

Next, one should cite the brilliant work of Gershgorin on numerical conformal mapping, and on estimating the truncation errors of approximate solutions of the Dirichlet problem obtained by difference methods. These and many other theoretical results concerned with the numerical solution of elliptic boundary value problems are ably summarized in the scholarly book by Kantorovich and Krylov [C6].⁷ This lists many highly accurate approximations for the Laplace operator, and gives a number of general recipes for solving the Dirichlet and Neumann problems.

⁷The first edition of this book was published in 1936, in Russian.

However, these pioneer publications devoted little attention to numerical algebra: the practical question of actually solving the large systems of linear algebraic equations to which difference approximations give rise. This question had deeply interested Gauss, Jacobi, Seidel, and other 19th century mathematicians,⁸ but had become unfashionable in most academic circles by 1930.

The first person to develop a practical procedure for solving such systems, and apply it successfully to a wide variety of elliptic problems involving hundreds of unknowns, was R.V. Southwell.⁹ Southwell was the spiritual heir of L.F. Richardson, whose ideas formed the starting point of Southwell's book [C10]. Motivated by mechanical analogy, he developed relaxation methods, similar to the Gauss-Seidel method, for approaching equilibrium and determining normal modes of vibration in systems governed by variational principles. In the years 1935-40 these relaxation methods were applied mainly to problems from structural mechanics.

By 1946, however, Southwell and his collaborators had also solved many fluid flow problems which were intractable by analytical methods, typically using difference 'nets' containing 300-1000 mesh points, and concentrating the latter near singularities. Most of these problems involved second-order linear or quasilinear DE's of the form

$$(4.1) \quad \nabla \cdot (p \nabla \Psi) + f(x,y) = 0 ,$$

preferably on a square mesh.

The first fluid flow problem solved in [C10] (by D.G. Christopherson) was that of determining the pressure distribution in a slider bearing, as predicted by Reynolds' hydrodynamical theory

⁸ See the bibliography of Forsythe-Wasow [C4], the historical notes in R.S. Varga's "Matrix Iterative Analysis", Prentice-Hall, 1962, or H.H. Goldstine's "Numerical Analysis from the 15th through the 19th Century". For a 50 year overview, see [C9, pp. 17-38].

⁹ For the mathematical theory of relaxation methods, see G. Temple, Proc. Roy. Soc. A169 (1939), 476-500, and Leslie G. Fox, Quar. J. Mech. Appl. Math. 1 (1948), 253-80.

of lubrication, whose basic DE is

$$(4.2) \quad \frac{\partial}{\partial x} \left(\frac{h^3}{\mu} \frac{\partial p}{\partial x} \right) + \frac{\partial}{\partial y} \left(\frac{h^3}{\mu} \frac{\partial p}{\partial y} \right) = 6 \left\{ \frac{\partial}{\partial x} (hu) + \frac{\partial}{\partial y} (hv) \right\} ,$$

(Chapter 2, §10). Notable features of Christopherson's solution of this problem include his approximate determination of the free boundary (at 'zero' pressure), and of temperature effects on viscosity. For details, see [C10, pp. 172-80] or Christopherson's original paper cited there.

Another problem treated was the flow of gas through a convergent-divergent nozzle. The domain of interest was first mapped conformally onto a rectangle by relaxation methods described (and successfully applied to many problems) in [C10, Chapter IV].¹⁰ The governing DE's

$$(4.3) \quad \frac{\partial}{\partial x} \left(\rho \frac{\partial \psi}{\partial x} \right) + \frac{\partial}{\partial y} \left(\rho \frac{\partial \psi}{\partial y} \right) = 0$$

and

$$(4.3') \quad \frac{\partial}{\partial x} \left(\frac{1}{\rho} \frac{\partial \psi}{\partial x} \right) + \frac{\partial}{\partial y} \left(\rho \frac{\partial \psi}{\partial y} \right) = 0$$

with the constraint

$$(4.4) \quad \int \frac{dp}{\rho} + \frac{1}{2} q^2 = \text{const.}$$

were then solved successfully for subsonic flow, but not for subsonic-supersonic flow. See [C10, pp. 180-91], or J.R. Green and R.V. Southwell, Phil. Trans. A239 (1944), 367-86 for more details.

Still other applications to percolation through porous media were treated in [C10, Chapter VI], while solutions of free streamline problems conclude the book.

¹⁰ Any DE of the form (4.2) in a simply connected domain can be transformed into one of the same form on a rectangle by a suitable conformal transformation; cf. Chapter 1, §§7,9.

However, the solution of even one such problem by hand (or using a desk calculator) was a tedious job in 1945, requiring weeks or months of work by a skilled specialist, concentrating full time on it. Convergence was accelerated by intuition and experience, rather than on underlying mathematical principles. Numerical fluid dynamics was still in a very primitive state, and only a few scientists foresaw the revolutionary changes that electronic computers would make possible in the next two decades.

5. Von Neumann's vision. The man who most clearly envisioned numerical fluid dynamics as we know it today was John von Neumann. It was an electrifying experience to hear him propose in 1945, in a lecture given at the First Canadian Mathematical Congress, that computers might be used instead of wind-tunnels to simulate the flow of air around airplanes. In one sense, this was a bold reaffirmation of the thesis of Euler and Lagrange, that fluid dynamics could be treated as a mathematical science. However, it also radically revised this thesis, which had gradually disintegrated in the two centuries 1740-1940. It proposed complementing analytical fluid dynamics by numerical fluid dynamics.

Specifically, von Neumann's lecture emphasized the limitations of the classical methods of Analysis, such as separation of variables and expansions in series to special geometries and linear problems.

He observed that numerical methods are relatively free from these limitations. As we explained in §1, this follows in principle from the theoretical arithmetization of Analysis achieved in the 19th century, when it was demonstrated that all of Analysis can be reduced to arithmetic and skillful passage to the limit (i.e., to Algebra and Topology). In principle, one can approximate many linear and nonlinear differential equations by stable suitable difference schemes on a sufficiently fine mesh, and then solve these in a finite number of steps with arbitrarily high accuracy.

Von Neumann's idea was that by carrying out these arithmetic operations at electronic speeds with 10-15 digit accuracy (an accuracy unattainable by analog computers), large-scale digital computers could solve the resulting difference equations with negligible roundoff error, thus converting the theoretical arithmetization of analysis into a practical reality.

It is a pity that no written version of von Neumann's talk seems to exist.¹¹ However, I can vouch for the correctness of the preceding statements, because I was there and it was my unenviable task to be the next speaker. My chosen topic of "Universal Algebra" had seemed imaginative enough beforehand, but it paled into insignificance when presented just after von Neumann had finished! (See Proc. First Canadian Math. Congress, Univ. of Toronto Press, 1946, pp. 310-26 and p. xxii.) The next talk (pp. 327-37) was by Douglas Hartree, on the solution of partial differential equations by the differential analyzer. The leading computer at that time, it was an analog machine!

His previous work. Though he had published nothing about his ideas in the unclassified literature, von Neumann had already performed some interesting numerical experiments. Because of World War II, he had been vitally concerned with shock and blast waves from 1941 on. To these, he had applied the standard mathematical model developed by Rankine, Hugoniot, Hadamard, and others. This model, which is Model #5 of the list on p. 3 of Chapter 1, and which we will discuss in greater depth in Chapter 6, makes essential use of thermodynamics. It assumes that Newtonian space-time is cut up into a finite number of regions by one or more moving two-dimensional 'shock waves' (alias shock fronts').¹² In each region, the flow is assumed to be isentropic, while the equation of continuity $D(\ln \rho)/Dt = \text{div } \underline{u}$ and the Euler-Lagrange equations of motion are assumed to hold globally. However, the

¹¹The most relevant quotations come near the beginning of his paper with H.H. Goldstine, published posthumously in his Collected Works [C8, esp. pp. 2-4]. See also [C5, pp. 179-80].

¹²Somewhat as Kirchhoff, cut space up into a main stream and a stagnant 'wake', separated from it by a vortex sheath.

entropy or 'adiabat' of each particle, hence its equation of state in Lagrangian coordinates, $p = k(\underline{a}, t)\rho^\gamma$, depends on the 'strengths' of the shocks that it has passed through.

During the late war years of 1944-45, poring intermittently with von Neumann over spark shadowgraph pictures of projectiles in flight, I got a vivid sense of his interest in mathematical formulations and results, and of his realistic skepticism as to their validity. Some idea of the scope and content of his work in this area can be gleaned from his reports and papers, collected in [C8'] as items ##19-29.

His initial studies (§§19-26), made in 1941-43, used analytical methods to predict: (a) "the laws of decay of a blast wave due to a point explosion of energy E_0 " using "the so-called similarity property of the solution",¹³ (b) "the origin of explosions and the propagation of their effects" in plane shock waves including "when the so-called Chapman-Jouguet hypothesis is true, and what formulas are to be used when it is not" (##19,20). (Cf. [B3, §§86-96] for a contemporary assessment of this work.)

Brilliant, essentially algebraic studies of interactions between two or more plane shock waves were a by-product of the studies of (b); ##22-23 describe this work, which is unrelated to the purpose of the present book, and led him to the famous Triple Shock Paradox [B2, §17].

Particle model. It was not until 1944, in #27, that von Neumann initiated his first direct numerical attack on the non-linear wave equation $x_{tt} = H'(x_a)x_{aa}$ of Chapter 2, (6.1). For this purpose, he proposed using a 'molecular' model of equally spaced beads on a line, connected by springs, similar to Lagrange's model of a laterally vibrating string constructed 175 years earlier. Specifically, he proposed dividing the a-axis into

¹³ #21, taken from Chapter II of Los Alamos Report LA-200 (1947); see [C8', p. 200] for background dates. The basic ideas stem from G.I. Taylor, Report RC-10 and J. von Neumann Report AM-9, both dated June, 1941. For comparable Russian work, see L.I. Sedov. Similarity and Dimensional Methods in Mechanics, Academic Press, 1959, Ch. IV, §11.

intervals of equal mass by a uniform mesh, and "lumping" the mass in each interval into a bead. One can then make each spring just stiff enough to accelerate the j -th bead, of mass $m = \Delta a_j$, according to the postulated 'equation of state'. The result is to replace $x_{tt} = -H'(x_a)x_{aa}$ by the system

$$(5.1) \quad x_j''(t) = P(x_j - x_{j-1}) - P(x_{j+1} - x_j) ,$$

where $P(\Delta x) = \frac{1}{m}H(\frac{\Delta x}{\Delta a})$ simulates $H(V)$. More precisely (see Chapter 6), given any smooth solution $x(a,t)$ of $x_{tt} = -H'(x_a)x_{aa}$, one can show that as $m \rightarrow 0$, the solutions of the semi-discretized model defined by (5.1) will tend to $x(a,t)$.

Since one can 'arithmetize' the solution of the system (5.1) by any of several methods (e.g., fourth-order Runge-Kutta), we can say that von Neumann's molecular model constituted a true 'arithmetization' of his physical model, at least in the absence of shock waves.

As von Neumann remarked [C8', p. 367]: "this system...is clearly a reasonable physical approximation of the substance which the hydrodynamical equation (15) describes. It corresponds to a quasi-molecular...substance, where the mass ascribed to one 'bead'...is the mass of a 'molecule'....Clearly this is not the 'true' molecular description of the substance....Thus the true number of molecules in [a gram-mol of a real substance] is Loschmidt's number $N \approx 6 \times 10^{23}$, while for a practical computing scheme some number of 'molecules' N between 10 and 100 will be appropriate. However, the actual value of Loschmidt's number N never figures in hydrodynamics; all that is required is that N should be a great number."

In summary, von Neumann's first idea was to semi-discretize the non-linear, second order, hyperbolic DE $x_{tt} = -H'(x_a)x_{aa}$, i.e., to replace it by a large system of ordinary DE's. He then proposed integrating these DE's by a nonlinear generalization

$$(5.2) \quad x_j^{n+1} - 2x_j^n + x_j^{n-1} = (\Delta t)^2 [p(x_j^n - x_{j-1}^n) - p(x_{j+1}^n - x_j^n)]$$

of the CFL (Courant-Friedrichs-Lewy) 5-point difference approximation (2.4). Finally, he optimistically proposed "completely ignoring the possibility of shocks,"¹⁴ because mass, momentum, and total (particle) energy are conserved in the limit $\Delta a \rightarrow 0$ of this model. He recognized the oscillations which arise behind shocks as analogous to the thermal agitation of molecules in a heated gas, and he proposed using this analogy to simulate shock behavior, since the Rankine-Hugoniot conditions (cf. Chapter 6) conform to the same conservation laws.

It was evident to von Neumann and to later workers that discontinuities, and even steep fronts, would be hard to locate precisely if one used difference equations like (5.2), or even by a semi-discretization, and that this makes it difficult to solve the underlying partial differential equation $x_{tt} = -H'(x_a)x_{aa}$ accurately by any numerical method on a discrete mesh. Indeed, artificial oscillations do propagate from shock discontinuities if the most natural difference approximations are used. To damp these out, von Neumann and Richtmyer later introduced an "artificial viscosity" (see §6). Although this does not simulate the real thickness of the shock, which is a small fraction of the mesh-length, it does reduce the thickness to a few mesh lengths, and largely eliminates the oscillations.

6. Von Neumann's influence. Von Neumann's unpublished Montreal talk heralded a new era for fluid dynamics. The revolution which it initiated is still in full course, and this monograph is intended in part to clarify and chronicle some of its progress in the 40 years since it began.

Von Neumann's personal influence in precipitating this revolution was enormous, for at least three quite different reasons. First, he was one of the most brilliant mathematicians of this century and was deeply interested in fluid mechanics as such.

¹⁴He also suggested that " $14^2 \approx 200$ and $14^3 \approx 3000$ [particles] may be needed in truly two- or three-dimensional problems."

Second, his activity came just when modern large-scale, high-speed computers were about to become available.

And finally, he participated personally in several major projects, at a time when the scale of scientific activity in the United States was growing by an order of magnitude, and his ideas contributed substantially to their success. He was not only a key figure at the Los Alamos Scientific Laboratory (LASL), and later an A.E.C. Commissioner, but he was also a potent adviser to the Army (through the Ballistic Research Center at Aberdeen), the Navy (through the Office of Naval Research), and the Air Force (through the Rand Corporation). In addition, he was in close contact with top scientists at IBM, the Standard Oil companies, RCA, and other leading industrial firms whose success depended on continuing technological innovation.

Von Neumann's fame, his scientific optimism, his ideas, and his influence quickly ushered in a new era in scientific computing. Within five years, his prophetic vision had become so widely accepted that C.B. Thompkins could write:¹⁵

Many of the problems presented were problems involving partial differential equations. The solution...was to be brought about...by: (1) buying a machine; (2) replacing the differential equation by a similar equation with a fine but otherwise arbitrary grid; (3) closing the eyes, mumbling something about truncation error and roundoff error, and (4) pressing the button to start the machine.

Computing costs. Von Neumann's optimism was based, of course, on his belief that computing would become several orders of magnitude faster and cheaper. He was concerned with this question from the start; see [C8, pp. 10-15]. Later, in his 1948 reports to the Standard Oil Development Co., von Neumann began by comparing an estimated cost of 12.5¢ per multiplication for a trained operator using a desk computer, with a cost of 1.4¢ on the IBM SSEC calculator [C8, p. 665]. His reports concluded by describing a "small" problem as having 10 space

¹⁵ From Tompkins' preface to Dorothy Bernstein, Existence Theorems in Partial Differential Equations, Annals of Math. Study No. 23, Princeton University Press, 1950.

intervals Δx and 20 time intervals Δt , and a "large" problem as having 25 space intervals and 120 time intervals [C8, p. 750].

Around 1956, I made estimates similar to those of von Neumann [A3, pp. 205-6]. My corresponding cost estimates were 2.5¢ and .002¢, using efficient Harvard graduate students and "second generation" computers.

It is amusing to compare these estimates of computing costs with those of L.F. Richardson (op. cit., in §2, p. 325), written around 1910. Richardson "paid piece rates for the operation $\Delta x^2 + \Delta y^2$ of about $n/18$ pence per coordinate point, n being the number of digits...one of the quickest boys averaged 2,000 operations $\Delta x^2 + \Delta y^2$ per week" for $n = 3$. For $n = 6$, this comes to about 0.5¢ per point.

Von Neumann's own contributions. In the decade 1945-55, fascinated by their potential for advancing engineering science, von Neumann devoted a substantial fraction of his prodigious mental energy to advancing computer architecture and component design, and to software development. His fundamental contributions to these subjects have been described by H.H. Goldstine [C5, Part Three], his co-worker in this area from 1944 on and later Vice-President of IBM. We can sum them up by saying that he played a prominent role in fulfilling his own prophecy: that the cost of scientific computing would decrease by many orders of magnitude within a few decades.

The next four sections of this chapter (§§7-10) will contain rather sketchy and superficial accounts of one central part of these von Neumann post-war attempts to solve basic problems of fluid dynamics by numerical methods. These summaries, and the later material in this lecture, will attempt to relate his ideas and methods to contemporary and later work. Although he had access to the best computing machines existing in his lifetime, such as the Univac and the IBM-704, these were quite puny by modern standards. Hence it is his ideas about numerical fluid dynamics, rather than any specific computing achievements, that are of the greatest significance today.

These summaries of von Neumann's contributions will be followed (in §11) by an analysis of molecular models of matter. I have included this analysis partly because von Neumann himself thought of the Maxwell-Boltzmann kinetic theory of gases as a logical alternative to the basic continuum models invented by Euler and Stokes. Moreover he realized clearly that, in principle, discrete models were, in some fundamental sense, better suited than continuum models to digital computers (in abstract terms, to 'automata' having only a finite number of 'states'). Thus he often speculated as to how many 'molecules' would be needed to simulate macroscopic gas motions adequately. This speculation seems especially timely today, when one can imagine a parallel computer containing a million identical 'chips', each dedicated to computing the trajectory of one molecule, and another million chips dedicated to monitoring different regions of space, each of which contain up to 10 molecules at any one time!

Finally, in §12, I will discuss briefly some of the most notable computing schemes developed at Los Alamos in the years 1960-75. I will do this because, in my opinion, they constitute significant extensions of von Neumann's ideas about numerical fluid dynamics.

7. Von Neumann's Legacy, I. Von Neumann had only 10 years after his Montreal talk in which to develop his ideas. The boldness of his imagination becomes especially impressive when we consider the limited capabilities of the leading digital computer of 1945: the ENIAC with its negligible "memory" and Howard Aiken's slow electromechanical Selective Sequence Calculator.

Today, 40 years after his Montreal talk and 30 years after his premature death, it seems timely to review von Neumann's papers and reports on numerical hydrodynamics, and to reevaluate his vast legacy of ideas with the wisdom of hindsight. In making this review, we should remember that his ideas were engendered during World War II (against Hitlerism) and the Cold War that followed it almost immediately. In those years, the design of

atomic (U-235 or plutonium) and hydrogen bombs were given top priority by the American and Russian governments.¹⁶

Shock and blast waves. Largely for this reason, the problem of simulating (and predicting) the evolution of shock and blast waves continued to interest von Neumann after World War II. Soon after 1945, he abandoned the kinetic theory analogy, and replaced it by an 'artificial viscosity', whose purpose was to 'smooth out' the calculations, and not to simulate Nature. This artificial viscosity did not simulate the real thickness of the shock, which is a small fraction of the mesh length h , but did reduce it to about $5h$.

Von Neumann used artificial viscosity to simulate plane shocks in a joint paper (#28) with R.D. Richtmyer, published in 1950, and to simulate spherical shocks in a second paper (#29) with H.H. Goldstine, published in 1955.¹⁷ In these papers, he continued to use Lagrangian coordinates, whereas most later writers have used 'Eulerian' coordinates (as did Riemann); cf. Chapter 2, §6. Therefore, for convenient reference, we will reproduce his equations here, even though the paper has been analyzed by Richtmyer and Morton in [C11, §§12.8-12.13], and we will discuss it again in Chapter 6, §3.

In Lagrangian coordinates, letting $x(a,t)$ denote the position at time t of the particle with cumulative mass-coordinate a , we will have as in Chapter 2, §6, $u = x_t$ and $V = 1/\rho = x_a$. The equation of continuity (conservation of mass) reduces to the identity $x_{at} = x_{ta}$, true automatically if $x(a,t) \in C^2$. There remain the (one-dimensional) equation of motion (conservation of momentum), and the equation of energy conservation. For these, von Neumann and Richtmyer proposed using

¹⁶ See my comments in *Historia Mathematica* 10 (1983), pp. 243-8. Much of von Neumann's work during these years was classified, for reasons of national security.

¹⁷ The preceding papers were originally published in *J. Appl. Phys.* 21 (1950), 232-7, and *Comm. Pure Appl. Math.* 8 (1955), 327-53. For spherical shocks, see also Sedov, op. cit., supra, and G.I. Taylor, *Proc. Roy. Soc.* A201 (1950).

$$(7.1) \quad u_t = -(p+q)_x$$

and

$$(7.2) \quad E_t = -(p+q)V_t, \quad V = 1/\rho.$$

Here $E = C_V T$ is the internal energy; it is $pV/(\gamma-1)$ in a perfect gas; von Neumann and Richtmyer use $U, X,$ and x where we use $u, x,$ and a ; moreover they let $a = \int \rho_0(\xi) d\xi$, where ξ is any mass-coordinate.

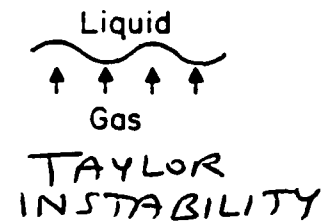
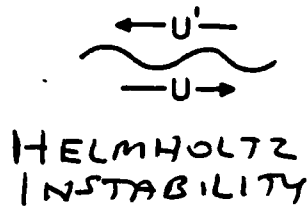
It is stated that "The dissipation [term] q is introduced for purely mathematical reasons. Therefore, q may be taken as any convenient function of $p, V,$ etc., and their derivatives," provided that the mechanical energy dissipated by it is converted into heat, so that the Rankine-Hugoniot conditions are satisfied across it.

Taylor instability. Von Neumann was also interested in nonlinear Helmholtz-Taylor instability. Before taking this up, we summarize the basic formulas that govern linear Helmholtz-Taylor instability, treated as a perturbed Lagrangian dynamical system. The mathematical model assumes a nearly plane interface (vortex sheet or 'shear layer') separating two incompressible fluids, of densities ρ and ρ' , and moving with speeds U and $-U'$ in opposite directions.

In the linearized approximation, a small initial perturbation can be resolved by Fourier theory into sinusoidal components. Moreover, relative to 'moving axes' making $\rho U + \rho' U' = 0$, these will be normal modes. They govern equations of such a normal mode, having spatial variation $\begin{pmatrix} \cos \\ \sin \end{pmatrix} kt$ and of amplitude $A_k(t)$ is $\ddot{A}_k(t) = S(k)A_k(t)$. Letting g signify the downward gravitational force per unit mass, a a downward acceleration and γ the interfacial surface tension, the equation of motion reduces to:¹⁸

¹⁸See G. Birkhoff, Proc. Symp. Appl. Math. 13 (1960), 55-76.

$$(7.3) \quad S(k) = \frac{\rho \rho' k^2}{(\rho + \rho')^2} (U - U')^2 - \frac{\rho - \rho'}{\rho + \rho'} (g - a) k - \frac{\gamma k^3}{\rho + \rho'}$$



When $S(k) < 0$, we have neutral stability, and $A_k(t) = \alpha_k \cos \omega t + \beta_k \sin \omega t$, where $\omega_k^2 = S(k)$. However, when $S(k) \geq 0$, $A_k(t) = \alpha_k e^{\omega_k t} + \beta_k e^{-\omega_k t}$, and we have instability. It follows from (7.3) and these formulas, that the condition for stability is [B8, p. 378]:

$$(7.4) \quad 4g(\rho - \rho') > \rho^2 \rho'^2 (U - U')^4 / (\rho + \rho')^2 .$$

Three other important and qualitatively correct conclusions also follow [A4, p. 252]:

- I. The relative tangential velocity $|U - U'|$ is always a *destabilizing* influence (Helmholtz instability).
- II. Acceleration from a light towards a dense fluid is also *destabilizing* (Taylor instability); it may be counteracted by gravity.
- III. Surface tension is always a *stabilizing* influence; it always makes extremely short ripples stable, thus keeping the surface from getting too irregular.

When $\rho = \rho'$, as in a shear layer ('vortex sheet') in an otherwise homogeneous fluid, we have Helmholtz instability and exponential breakdown of the plane interface separating otherwise parallel flows. When $\rho \gg \rho'$ (wind over water) and $g > a$, we have neutral stability, even though wind does generate waves. When k is very large, we have capillary waves. G.I. Taylor and D.J. Lewis made a famous experimental study of the unstable case $a > g$. They reported observing:

- (1) an exponential increase in amplitude as given by the first-order theory until the amplitude is about 0.4λ ;
- (2) a transition stage during which the amplitude increases from 0.4λ to 0.75λ , and the surface disturbance changes to the form of round-ended columns of air penetrating into the liquid, which forms narrow up-standing columns in the interstices;
- (3) a final stage of penetration through the liquid of the air columns at a uniform velocity proportional to $\sqrt{a-g}$.

Many schemes were proposed in the 1950's for rationalizing these observations.

Von Neumann's interest in Taylor instability gave rise to two Los Alamos Reports:¹⁹ AECU-2979, written in 1953 and reproduced as [C8', #31], and LA-2165, written in collaboration with A. Blair, N. Metropolis, A.H. Taub, and M. Tsingou. Whereas the former, written with Fermi, was very short and analytical in character, his second (joint) paper constituted a substantial computational achievement at the time. A shortened version of it was published (posthumously) in MTAC 13 (1959), 145-84, and later reprinted as [C8, pp. 611-51].

His second paper takes the stream function Ψ and the pressure p as primary dependent variables, from which fluctuations in the density can be computed through the DE

$$(7.1) \quad \rho_t = U\rho_x + V\rho_y = \Psi_y\rho_x - \Psi_x\rho_y.$$

The simplest stable difference approximation to (7.1) causes some (spurious) numerical pseudo-diffusion of mass, reminiscent of the diffusion of momentum caused by 'artificial viscosity'. In 60 time steps, on a 15×38 grid, the initially sharp density discontinuity broadened into a band about $2h$ in width. This is very acceptable from a practical standpoing. Taylor and Helmholtz instability will be discussed further in Chapter 4, §§9-10.

¹⁹ See also H.H. Goldstine's remarks in [C8', pp. 435-6].

8. Von Neumann's stability test. We next turn to von Neumann's ideas about the stability of difference approximations to initial value problems. These generalize the analysis of Courant-Friedrichs-Lewy [C3], already discussed in §2 above. As A. Taub explains in [C8, p. 664], von Neumann never wrote a systematic exposition of his ideas about stability. He applied them to the numerical solution of the nonlinear diffusion equation

$$(8.1) \quad u_t = (pu_x)_x + g(x,t) ,$$

in a Los Alamos Report with Richtmyer [C8, 652-63]. He also authorized their inclusion in a well-known paper by G.C. O'Brien, M. Hyman and S. Kaplan [1950], based on a lecture that he had given at the Naval Ordnance Laboratory in August, 1947.²⁰ This extends to general linear, constant-coefficient DE's the results of Courant, Friedrichs and Lewy mentioned in §2 above.

What is often called the "von Neumann stability test" for a difference approximation to an initial-boundary value problem, consists in applying Fourier analysis to the linear, constant-coefficient ΔE on a uniform mesh most closely approximating the DE actually used, and verifying that the rates of exponential growth of the solution of this ΔE remains uniformly bounded, as the mesh length $h \rightarrow 0$, for all wave vectors k .

The first substantial rigorization of this idea, in the limited context of linear, constant-coefficient DE's and ΔE 's on a torus (with uniform meshes), was given by Lax and Richtmyer in 1956.²¹ They summarized their main conclusion as follows.

Lax Equivalence Theorem. Given a well-posed initial-boundary value problem and a finite-difference approximation to it that satisfies the consistency condition, stability is necessary and sufficient for convergence.

²⁰J. Math. Phys. 29 (1951), 223-51. A résumé of von Neumann's lecture had been written up by Human in 1947, as a technical note.

²¹Comm. Pure. Appl. Math. 9 (1956), 267-93.

This result was rederived by Richtmyer a year later, with many important applications, in his classic book whose second edition [C9] is still widely used today. There the "von Neumann condition" for stability is carefully explained in [C9, §4.7].

In 1965, Varga and I obtained more precise and somewhat more general results.²² Thus we showed that one can construct a stable difference approximation having an arbitrarily high order of accuracy, to any linear, constant-coefficient DE which defines an initial value problem satisfying the Hadamard stability criterion.

The von Neumann test for the stability of difference approximations is well illustrated by the following example.

Example 1. The DE of a vibrating beam is

$$(8.2) \quad u_{tt} = -E^2 u_{xxxx} .$$

First, we use the Plancherel Theorem to show that (8.2) satisfies the Hadamard stability criterion, and so defines a well-set IV problem. In particular, we show that for the 'small oscillations' to which (8.2) refers, energy is conserved.

Sketch of proof. Formally, from

$$(8.3) \quad u(x,t) = \int_{-\infty}^{\infty} g(k,t) e^{ikx} dk ,$$

we get by Leibniz' Rule that

$$(8.4) \quad u_{xxxx} = \int_{-\infty}^{\infty} k^4 g(k,t) e^{ikx} dx .$$

Hence, the Fourier transform $g(k,t)$ of $u(x,t)$ satisfies

$$(8.5) \quad g_{tt} = -E^2 k^4 g$$

²²J. Math. and Phys. 44 (1965), 1-23. See also H.O. Kreiss, Numer. Math. 1 (1959), 186- , and other papers cited in [C9].

Therefore, the general solution of (8.2) is

$$(8.6) \quad u = \int_{-\infty}^{\infty} \{a(k)e^{i(kx+Ek^2t)} + b(k)e^{i(kx-Ek^2t)}\} dk .$$

We now consider the energy integral

$$(8.7) \quad \epsilon(t) = \frac{1}{2} \int_{-\infty}^{\infty} [u_t^2 + (Eu_{xx})^2] dx .$$

Again formally, we have

$$\epsilon'(t) = \int_{-\infty}^{\infty} [u_t u_{tt} + Eu_{xx} u_{xxt}] dx = E \int_{-\infty}^{\infty} [-u_t u_{xxxx} + u_{xx} u_{xxt}] dx$$

But $-\int u_t u_{xxxx} dx = -[u_t u_{xxx}] + \int u_{tx} u_{xxx} dx$, integrating by parts. Assuming that $\lim_{|x| \rightarrow \infty} u_t u_{xxx} = 0$, this gives

$$\begin{aligned} \epsilon'(t) &= E \int_{-\infty}^{\infty} [u_{tx} u_{xxx} + u_{xx} u_{xxt}] dx \\ &= E \lim_{X \rightarrow \infty} [u_{xx} u_{tx}]_{-X}^X = 0 . \end{aligned}$$

Hence the energy ϵ is constant.

9. The wave equation. Especially relevant to fluid mechanics is the application of the ideas discussed in §8 to the wave equation $u_{tt} = c^2 \nabla^2 u$. To fix ideas, we will treat specifically the three-dimensional case relevant to sound waves in space:

$$(9.1) \quad u_{tt} = c^2 (u_{xx} + u_{yy} + u_{zz}) .$$

Again, we consider a uniform space mesh with $x = jh$, $y = j'h$, $z = j''h$ (j, j', j'' integers), and set

$$(9.2) \quad u_j^m = u^m e^{i \underline{k} \cdot \underline{x}} = u^m e^{i(kj+k'j''+k''j''')h} .$$

For (9.1), the simplest central difference approximation leads to a 9-point formula. Letting $\underline{j} = (j, j', j'')$, and with $r = c\sqrt{t}/h$

the Courant number, an elementary computation gives the 9-point formula

$$(9.3) \quad u_j^{m+1} - 2u_j^m + u_j^{m-1} = \frac{c^2 \Delta t^2}{h^2} \nabla_h^2 u ,$$

as in [C3]. Setting $u = e^{i\mathbf{k} \cdot \mathbf{x}} e^{i\omega t}$, after verifying that

$$\nabla_h^2 u_j^m = 6 \cos kh - 6 = -12 \sin^2(kh/2) ,$$

we get the 'consistency' condition

$$(9.4) \quad \alpha - 2 + \alpha^{-1} = 12r^2 \sin^2(kh/2) .$$

We now derive $r^2 \leq 1/3$ as the von Neumann condition (generalized Courant condition) for the stability of the difference approximation (9.3). Since the amplification factor tends to ∞ as $h \rightarrow 0$ if (9.4) has even one root α with $|\alpha| < 1$, and since $\alpha_1 \alpha_2 = 1$ (the coefficient of α^{-1} in (9.4)), (9.3) is stable (neutrally) if and only if $\alpha_1 = e^{i\theta}$, $\alpha_2 = e^{-i\theta}$ for some θ . In the stable case, $|\alpha| = |\alpha^{-1}| = |\alpha|^{-1}$, the left side of (9.4) ranges from 4 to 0 and the right side from $-12r^2$ to 0. Hence the von Neumann condition for stability is $r^2 \leq 1/3$.

A similar discussion applies to the n-dimensional wave equation (n space variables, to give a (2n+3)-point central difference approximation that is stable (for fixed r) if and only if $r^2 \leq 1/n$.

Energy conservation. The total energy at time t of a solution of (9.1) is

$$(9.5) \quad \varepsilon(t) = \frac{1}{2} \int_{\Omega} [u_t^2 + c^2(u_x^2 + u_y^2 + u_z^2)] dR .$$

Then, by Leibniz' Rule

$$(9.6) \quad \varepsilon'(t) = \int_{\Omega} [u_t u_{tt} + c^2(u_x u_{xt} + u_y u_{yt} + u_z u_{zt})] dR .$$

Since $u_{tt} = c^2 \nabla^2 u$, it follows that

$$(9.7) \quad \begin{aligned} \epsilon'(t) &= c^2 \int_{\Omega} [(u_t u_{xx} + u_x u_{xt}) + (u_t u_{yy} + u_y u_{yt}) \\ &\quad + u_t u_{zz} + u_z u_{zt}] dR \\ &= c^2 \int_{\Omega} \operatorname{div}(u_t \nabla u) dR = c^2 \int_{\Omega} u_t \frac{\partial u}{\partial n} dR . \end{aligned}$$

For $\Gamma = \partial\Omega$ is a large sphere or cube expanding to ∞ , the last integral tends to zero if u dies out rapidly. This proves that Model #4 for sound waves (the standard 'acoustic approximation') is energy-conserving in free space.

Plancherel Theorem. The Divergence Theorem is the essence of the preceding proof. A very different proof can be based on the Plancherel Theorem, a general duality theorem relating square-integrable functions defined throughout free space to the square-integrals of their Fourier transforms. Its essence consists in the assertion that if for $\Omega = \mathbb{R}^n$, the (multiple) integral

$$(9.8) \quad \int_{\Omega} |\phi(\underline{x})|^2 dx_1 \cdots dx_n < +\infty ,$$

then ϕ has a Fourier transform $F(\underline{x})$, defined in the 'dual space' $K = \mathbb{R}^n$ by

$$(9.8') \quad F(\underline{k}) = \pi^{-n} \int_{\Omega} e^{-i\underline{k} \cdot \underline{x}} \phi(\underline{x}) dx_1 \cdots dx_n ,$$

for 'almost all' \underline{k} . Moreover

$$(9.9) \quad \phi(\underline{x}) = \int_K e^{i\underline{k} \cdot \underline{x}} F(\underline{k}) dk_1 \cdots dk_n$$

for almost all \underline{x} , and (finally):

$$(9.10) \quad \int_K |F(\underline{k})|^2 dk_1 \cdots dk_n = \int_{\Omega} |\phi(\underline{x})|^2 dx_1 \cdots dx_n .$$

The exercises listed on the attached sheet give a few applications of the preceding formulas; others may be found in Chapter 5.

10. Von Neumann's Legacy, II. Von Neumann was also keenly interested in industrial applications of scientific computing, and we shall conclude our brief résumé of von Neumann's legacy to "numerical hydrodynamics as a mathematical science" by calling attention to three of his other papers.

Petroleum reservoir exploitation. The first two of these [C8, #19-20], written for the Standard Oil Development Company in 1947-48, were concerned with petroleum reservoir exploitation. They deal with parabolic systems, and suggest in Part III generalizations, already discussed in §6, of the classic Courant-Friedrichs-Lewy analysis of the stability of difference approximations. To circumvent the $\Delta t \leq \Delta x^2/2\alpha$ stability bound on the explicit (forward time-step) solution of $u_t = \alpha u_{xx}$ that had been proposed by Courant, Friedrichs, and Lewy, von Neumann proposed using implicit different approximations.

At about the same time, J. Crank and P. Nicolson²³ proposed approximating $u_t = \alpha u_{xx}$ by

$$(10.1) \quad u_j^{m+1} = u_j^m + r[\delta^2 u_j^{m+1} + \delta^2 u_j^m]/2 ,$$

$r = \alpha \Delta t / \Delta x^2$. This has $O(h^2)$ accuracy and is unconditionally stable. Although the system (10.1) of linear algebraic equations is implicit, its coefficient-matrix is tridiagonal (with the natural ordering of unknowns and equations). Hence it can be solved very rapidly and accurately by Gaussian elimination.

Unfortunately, this ceases to be true in two space dimensions. However, within 10 years, by the time that large-scale, high-speed computers were becoming available for determining how to enhance petroleum reservoir exploitation, improved algebraic algorithms for solving the parabolic difference equation

$$(10.2) \quad u_j^{m+1} = u_j^m + r[\nabla_h^2(u_j^{m+1}) + \nabla_h^2(u_j^m)]$$

²³Proc. Camb. Phil. Soc. 43 (1947), 50-67. For details, see Forsythe-Wasow, [C4], pp. 141-3, and Varga, "Matrix Iterative Analysis", Chapter 8.

had been invented, which made possible the efficient solution of systems like (10.2). Most notable were the (now classic) parabolic ADI methods invented for this purpose by Peaceman, Rachford, Douglas, and others. These new methods, and the IBM-704 computers which had by then become available, revolutionized the science of petroleum reservoir exploitation.

Numerical weather prediction. Von Neumann was also fascinated by the possibility of basing weather forecasting on differential equations describing the motion of the atmosphere, with the help of a computer. In more exuberant moments, he even suggested that enormous "payoffs" might come from weather control, and his ideas have stimulated a major activity whose current status is hard to assess scientifically.²⁴

The clearest record of von Neumann's fascination with the possibilities of numerical weather prediction consists of his paper [C8', pp. 413-30] with Charney and Fjörtoft on "Numerical integration of the barotropic vorticity equations". Vivid accounts of von Neumann's attempts at achieving substantial progress in the years 1946-50, with very meager computing facilities, have been written by Goldstine [C5, pp. 300-5] and Platzmann (Bull. Am. Met. Soc. 60 (1979) 302-12). Charney (Proc. Nat. Acad. Sci. 41 (1955) 798-802) has reviewed progress to 1955.

Von Neumann regarded the calculations discussed in this paper as only "an essential first step in the general program"; he was greatly limited by the small size and speed of the computers then available. His solution on the ENIAC in 1950 of the crude model and approximation used in these calculations must, indeed, be regarded as a brilliant achievement in both theoretical hydrodynamics and computer science!

We will limit our discussion of this work to a few superficial remarks, made primarily for purposes of orientation. First,

²⁴Cf. [B2, §14]. Good reviews of the subject of numerical weather prediction are: N.A. Phillips, Rev. Geophys. 1 (1963), 123-76, and Ann. Rev. Fluid Mech. 2 (1970), 251-89; also G.J. Haltiner and R.T. Williams, "Numerical Prediction and Dynamic Meteorology", Wiley, 1980.

the model used the one-level "quasi-geostrophic, non-divergent vorticity equation, in which the sole dependent variable is the height z of a fixed isobaric surface"; specifically, the 500 mb level. Thus it is a 'one-level' model.

The simplest such model is provided by the so-called barotropic equation

$$(10.1) \quad d\zeta/dt = -u \cdot \nabla(\zeta + f) ,$$

where f is the Coriolis effect. This can be derived by adapting to spherical atmospheres the laws of two-dimensional vortex motion first formulated by Helmholtz (to a rotating atmosphere).

Von Neumann and his collaborators used a sophisticated variant of this model, designed to take account of pressure variations. Their objective was to see how well their numerical experiments predicted the evolution in time of observed isobars. These isobars and their correlation with cyclonic and anticyclonic wind patterns constitute one of the most conspicuous features of weather maps.

Turbulence. Finally, von Neumann gave much thought to turbulence. In 1949, he wrote down his tentative conclusions in a long manuscript [C8', pp. 437-72], which he never had time to polish for publication. However, posthumous reviewers judged it (in 1963) to be "one of the most illuminating discussions of turbulence extant". In it, he identified turbulence as a problem stemming from the nonlinear instability of the Navier-Stokes equations for an incompressible fluid, equations whose validity he took for granted.

After briefly reviewing the previous mathematical ideas about turbulence, von Neumann's manuscript concentrates on "statistical" models of turbulence. Actually, von Neumann's review does not mention explicitly the most conspicuous feature of modern statistical formulations: the notion of a random velocity-held $u(x, t, \omega)$, where ω designates an element of a probabilistic sample space $\Omega = [V, \Sigma, \mu]$, V being a function space (perhaps a Sobolev space) of velocity fields, Σ a Borel algebra of 'measurable' subsets

of V (perhaps its Borel sets), and μ is a probability measure. Averages then refer to integrals $\int f(\underline{x}, \omega) d\mu(\omega) = \bar{f}(\underline{x}, \underline{u}, t)$ over this sample space,²⁵ weighted by μ .

From the standpoint of numerical fluid dynamics, most relevant are von Neumann's comments concerning "Computational Possibilities" (his Part XI). Here he reached the somewhat pessimistic conclusion [C8', p. 469] that:²⁶

...there might be some hope to 'break the deadlock' by extensive, but well-planned computational efforts. It must be admitted that the problems in question are too vast to be solved by a direct computational attack, that is, by an outright calculation of a representative family of special cases...however, one could name certain strategic points... where relevant information must be obtainable by direct calculations. If this is properly done, and the operation is then repeated..., etc., here is a reasonable chance of effecting real penetration into this complex of problem and gradually developing a useful, intuitive relationship to it. This should, in the end, make an attack with analytical methods, so that it is truly more mathematical, possible.

We will defer further discussion of von Neumann's ideas about turbulence until Chapter 7.

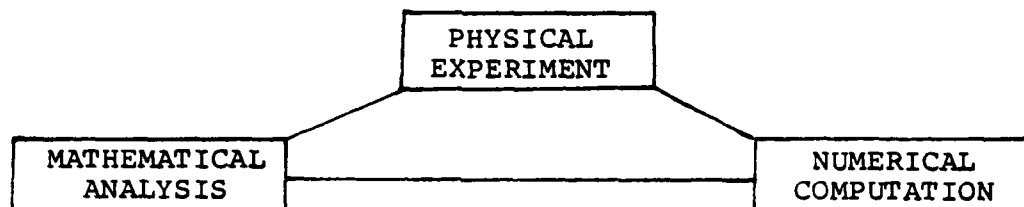
Conclusion. We have here italicized the word "analytical" for emphasis; von Neumann was always mindful of there being three different tools of scientific investigation: physical experiment, mathematical analysis, and numerical computation.²⁷ He also realized that, although any one of these can lead to a new scientific or engineering insight, all three should give consistent quantitative results before a scientific theory can be accepted as valid. Cf. the distinction made in §1 of Chapter 1 between

²⁵This definition avoids (in principle) von Neumann's criticism [C8', p. 447] that: "there is considerable uncertainty regarding the nature of the averages that are involved".

²⁶This contrasts with his optimistic prediction, made 3 years earlier [C8, p. 13], that to solve the Navier-Stokes equations by a "direct numerical attack" "may in the less involved cases be satisfactorily handled with about 2,500 mesh points", and 'turbulent' solutions...would probably require about 100 successive values of t ...about 10^6 multiplications are involved'. As we have seen, to perform 10^9 multiplications costs only a modest amount today.

²⁷See the discussion in [C8', pp. 348-56].

philosophical (i.e., qualitative), approximate engineering, and exact scientific models. The following diagram is intended to stress the importance of this realization.



Finally, he was supremely aware of the fact that analytical and numerical methods should both be rigorously justifiable from the same basic assumptions, in the same way that Analysis can be 'arithmetized'. And his ultimate aim was clearly to make fluid dynamics into a mathematical science.

11. Molecular models of fluids. Von Neumann was a frequent visitor to Los Alamos, and his initial approach to computational fluid dynamics through molecular models was developed there into an effective tool for solving many different kinds of problems. We will conclude this chapter by a brief survey of some of the methods developed by other Los Alamos scientists in this spirit.

Newton's model of ballistics. Of course, von Neumann was by no means the first to use molecular models to treat fluid flow problems. Newton constructed a mathematical theory of projectile drag, based on a very naive such model, 60 years before Euler tried to reduce fluid mechanics to a mathematical science by postulating the partial DE's of Chapter 1, §2. Newton's model led him to theorize that the drag D of a bullet should be

$$(11.1) \quad D = \rho U^2 \iint \sin^2 \theta \, dS ,$$

integrated over its head-- θ being the angle of inclination of an element dS of surface to its trajectory. Though grossly incorrect in several respects, this model did predict correctly

the approximate proportionality of the drag to the cross-section area A , the air density ρ , and the square of the speed U , for bullets of given shape. In other words, its conformity to the principle of inertial similarity (Chapter 1, §7) was valuable.

Moreover, Newton's model approximates fairly well the air resistance to the motion of a satellite moving through a rarefied gas, in which the Knudsen number (the ratio λ/L of the molecular mean free path to the obstacle diameter) exceeds one.²⁸ The biggest deviation from this model comes from the fact that the reflection of molecules bounding off solid surfaces is not ordinarily 'specular' but 'diffuse': the angle of reflection does not equal the angle of incidence, but is nearly independent of it.

Molecular models have played several important roles in the historical evolution of fluid mechanics, some of which are reviewed briefly in [B2, §12]. From a physical standpoint, Newton's crude model has long since been superseded by Maxwell's kinetic theory of gases. This provides a satisfactory explanation for many properties of perfect gases (and anomalies!), which would otherwise be inexplicable. Moreover it enables one to correlate such material constants as density, specific heats, molecular and thermal diffusivities, etc., in a very enlightening way.

Naturally, von Neumann had Maxwell's kinetic theory very much in mind in his pioneer work on numerical fluid dynamics. However, since the explanations alluded to in the preceding paragraph are peripheral to the main theme of this book, they have been deferred to Appendix E.

Instead, this chapter will be concluded by a review of some numerical experiments made at Los Alamos, motivated by ideas similar to those which inspired von Neumann's original report on the numerical simulation of shock waves.

²⁸ See W.D. Hayes and R.F. Probst, "Hypersonic Flow Theory", Academic Press, 1959, Chapter X. Newton assumed that the gas particles bounced elastically when hit by the missile.

12. Particle-in-cell Codes. The talented group at the Los Alamos Scientific Laboratory (LASL) has been making a sustained effort for nearly 30 years to realize von Neumann's idea of 'arithmetizing' fluid dynamics. Three notable landmarks in their progress were the development of families of PIC codes, of MAC codes, and of ALE codes (all acronyms) for treating large classes of flows. Each of these families of codes was applied to a variety of fluid flow problems, and the results evaluated from an empirical standpoint. We will discuss them here from a scientific standpoint.²⁹

A thoughtful 1959 article by Pasta and Ulam sheds considerable light on the evolution of LASL thinking.³⁰ It describes a computational approach initiated in 1952, and its application to simulate the Taylor instability of two fluids, with density ratio $\rho'/\rho = 2$. It comments that very many particles would be needed to define an accurate density function by the usual (mass)/(volume) definition. Instead, it used an assembly of 128+128 particles of masses m and $2m$, free to move in a gravity field while repelling each other with force $1/r$ up to a specified cutoff distance, beyond which the repulsion is negligible.

The PIC or particle-in cell method for solving problems in fluid dynamics was developed at LASL by F.H. Harlow and M.E. Evans in the late 1950's³¹ (a cheaper variant exists, called FLIC). It is basically a quasi-molecular model, which was designed to simulate (rather crudely, to be sure) flows involving substantial compression ratios (say 2:1 or 4:1). In concept, it relies on von Neumann's idea ([C8', p. 368]) that "the classical derivations of hydrodynamics from molecular-kinetic models have established that...details of the intramolecular forces are immaterial for this part...of hydrodynamics".

²⁹ See also R.W. MacCormack and H. Lomax, Annual Rev. Fluid Mech. 11, (1979), p. 289-316, whose conclusions we will review in Chapter 7.

³⁰ Math. Comp. 13 (1959), 1-13.

³¹ M.E. Evans and F.H. Harlow, LASL Report LA-2139 (1957). For a more polished exposition, see F.H. Harlow, Proc. Symp. Appl. Math. XV (1963), p. 269-88, and Methods Comp. Phys. 3 (1964), p. 319-45.

Space is divided into rectangular cells in the PIC method, each of which contains a variable number of particles, typically ranging from 4 to 16. These are accelerated by the 'pressure' gradient, the 'pressure field' being estimated from the number of particles (local 'density') in each cell. Because the number of particles is an integer, the pressure and density change by relatively large jumps, as do particle accelerations (but not velocities).

Harlow and his LASL collaborators developed empirically many special techniques for 'smoothing out' flows simulated by the PIC method. By utilizing them, they were able to simulate convincingly many flows (e.g., the hyper-velocity impact of a cylinder on a laminated plate) that had not previously been simulated as successfully by any other method. The PIC method treats large distortions and the opening and closing of 'voids' without special modifications. On the other hand, it is time-consuming, and cannot treat nearly incompressible flows.

"A continuum method which evolved out of the PIC code is the Fluid in Cell or FLIC code of Gentry, Martin and Daly (1966), based on earlier work by Rich (1963). They departed from the finite particle approach of PIC but retained most of the other aspects".³²

Marker-and-cell codes. In the early 1960's, the marker-and-cell (or MAC) method was developed at LASL for treating nearly incompressible ('low Mach number') flows, with special emphasis on 'free surface' motions.³³ For this purpose, it included 'markers' to keep track of the locations of free surfaces and other interfaces. It had capabilities somewhat similar to those of the famous Fromm-Harlow code for simulating vortex

³²Roache [C9', p. 241]. The references cited are M. Rich, Rep. LAMS-2826, and R.A. Gentry, R.E. Martin, and R.J. Daly, J. Comp. Phys. 1 (1966), 87-118.

³³F.H. Harlow and J.E. Welch, Physics of Fluids 8 (1965), 2182-9; and 9 (1966), 842-51; J.E. Welch, F.H. Harlow, J.P. Shannon, and B.F. Daly, "The MAC Method", LASL Report LA-3425, 1966.

streets, which we will discuss in Chapter 7. But unlike the latter, it did not utilize the Helmholtz equations for plane vortex flows. Hence it could not be regarded in principle as a general purpose code for solving (approximately) the Navier-Stokes equations.

Because it was actually applied mostly to potential flows with free boundaries, we shall postpone detailed discussion of the MAC method until Chapter 4, where we will analyze in depth typical problems for which published solutions were obtained with its help.

REFERENCES FOR CHAPTER 3

- [C1] G. Birkhoff and R.E. Lynch, "Numerical Solution of Elliptic Problems", SIAM Publications, 1981.
- [C2] L. Brillouin, "Wave Propagation in Periodic Structures", Dover, 1953.
- [C3] R. Courant, K. Friedrichs, and H. Lewy, "Uber die partielle D'gleichungen der mathematischen Physik", Math. Annalen 100 (1928), 32-74.
- [C4] G.E. Forsythe and W. Wasow, "Finite Difference Methods for Partial Differential Equations", Wiley, 1960.
- [C5] H.H. Goldstine, "The Computer from Pascal to von Neumann", Princeton University Press, 1972.
- [C6] L.V. Kantorovich and V.I. Krylov, "Approximate Methods for Higher Analysis", Nordhoff-Interscience, 1958.
- [C7] N. Metropolis, J. Howlett, G.-C. Rota (eds.), "A History of Computing in the Twentieth Century", Academic Press, 1980.
- [C8] John von Neumann, "Collected Works", (A.H. Taub, ed.), vol. V, Pergamon Press, 1963.
- [C8'] Ibid., vol. VI.
- [C9] R.D. Richtmyer and K.W. Morton, "Difference Methods for Initial-Value Problems", 2nd ed., Interscience, 1967.
- [C10] Martin Schultz (ed.), "Elliptic Problem Solvers", Proc. of a Conference in Santa Fe, NM, Academic Press, 1981.
- [C11] R.V. Southwell, "Relaxation Methods in Theoretical Physics", Clarendon Press, Oxford, 1946.
- [C12] John von Neumann, 1903-57. Special issue of Bull. Am. Math. Soc. (1958), devoted to reviews of his life and work.
- [C13] Peter D. Lax, Hyperbolic Systems of Conservation Laws and the Mathematical Theory of Shock Waves, SIAM Publications, 1973.
- [C14] Patrick J. Roache, Computational Fluid Dynamics, Hermosa Publ., 1972.
- [C15] Norman Zabusky, "Computational Synergetics and Mathematical Innovation", J. Comp. Phys. 43 (1981), 195-249.

4. POTENTIAL FLOWS

1. Introduction. Chapters 4-6 will deal with three relatively simple classical models of fluid motion: potential flows, sound waves, and nonlinear 'one-dimensional' waves (including "plane waves of finite amplitude"). We have selected these because of their (comparative) mathematical simplicity: the first two are the best understood partial DE's of mathematical physics. Nevertheless, it is far from easy to treat even these accurately and reliably by rigorously justified methods, especially in three-dimensional space and time! And until at least relatively simple flow problems can be so handled, one surely cannot regard numerical fluid dynamics as a mathematical science!

This chapter will be concerned with potential flows. In §4 of Chapter 1, we defined an n -dimensional potential flow ($n = 2, 3$) as a flow whose velocity field $\underline{u}(\underline{x}; t)$ has a scalar 'velocity potential' $\phi(\underline{x}; t)$ such that, at all points of the flow domain Ω ,

$$(1.1) \quad \underline{u} = \nabla\phi = (\partial\phi/\partial x_1, \dots, \partial\phi/\partial x_n) .$$

We also assumed the fluid to be incompressible, and of constant density $\rho = \rho_0$, from which it follows that ϕ must be a harmonic function:

$$(1.2) \quad \nabla^2\phi = \sum \partial^2\phi/\partial x_j^2 = 0 ,$$

(loc. cit., formula (4.2)). The Euler-Lagrange equations of motion then hold if and only if variations in the pressure p satisfy the Bernoulli equation (ibid., (3.1)):

$$(1.3) \quad \frac{1}{2} \nabla\phi \cdot \nabla\phi + \partial\phi/\partial t + \frac{p}{\rho} = \frac{P(t)}{\rho} - G$$

Here $G(\underline{x})$ is the gravitational potential (G is gy where y is the elevation in most applications), and $P(t)$ is some ambient stagnation pressure level depending only on time.

In this chapter, we will analyze the numerical techniques that have proved most successful (to date) in solving various boundary value and initial-boundary value problems associated with potential flows. The precision of our analysis will be aided by the fact that classical analysis has provided many exact analytical solutions of potential flow problems. Moreover the ideas of classical analysis usually enable one to greatly reduce the cost of computing potential flows. Indeed, some classes of potential flows can be treated more effectively by classical analytic methods than by modern numerical techniques.

Our discussion deals with three cases. First come potential flows bounded by impermeable solid walls, possibly with 'circulation'. Then come time-independent potential flows with free boundaries at constant pressure. Finally, we take up time-dependent flows with free boundaries, including gravity waves.

In an ideal incompressible, nonviscous fluid initially at rest and bounded by solid walls (no "free boundaries"), the velocity field at any instant depends only on the instantaneous normal velocity components along the walls. Its determination reduces to solving a Neumann problem for the velocity potential ϕ and it is therefore independent of the previous motion of the walls (i.e., of the past history). Thus the velocity field is the same for an impulsive acceleration from rest, when the fluid inertia is felt as "added mass", as it is in steady flow caused by moving the same obstacle at the same constant velocity through the (ideal) fluid.

Added mass. As Kirchhoff pointed out, theory actually says much more about the dynamics of a rigid body in an infinite ideal fluid, initially at rest. Such a body has six degrees of freedom in space: three of translation, and three of rotation. It is usually mathematically convenient to take these as parallel to and around three coordinate axes through the centroid of the body, taken as the origin of coordinates.

Now let $\phi_i(\underline{x})$, where $i = 1, \dots, 6$, denote the velocity potentials of the potential flows induced by translation with unit

linear velocity, resp. rotation with unit angular velocity, along and around the axes mentioned above. Define the added mass coefficients of the body as the Dirichlet inner products

$$(1.4) \quad m_{ij} = D\langle \phi_i, \phi_j \rangle = \iint_{\Omega} [\nabla \phi_i \cdot \nabla \phi_j] dR .$$

There are 15 of them in space, and 6 in the plane; note that the m_{ii} are kinetic energy integrals.

Relative to suitable 'principal axes', we can reduce the number of nonzero added mass coefficients to 6 in space (3 of translation and 3 of rotation), and to 3 in the plane (two of translation and one of rotation). Moreover, by applying Lagrange's equations to the (purely inertial) Lagrangian function $L = T = \frac{1}{2} \sum m_{ij}(\underline{q}) \dot{q}_i \dot{q}_j$, one can deduce a complete theory of the motion of a solid of arbitrary shape and density through an ideal (incompressible, inviscid) fluid.¹ Here we only give two illustrations of the power of Kirchhoff's theory.

THEOREM. The added mass coefficient m_{ij} in (1.4) is the j -th component Q_j of force resisting unit acceleration in the i -th direction. For a cylinder moving broadside, Q_1 is the horizontal component of thrust, Q_2 the vertical component of thrust, and Q_3 the torque resisting acceleration.

Because of the mathematical elegance and many practical applications of this theory, we will devote §§2-5 below to explaining various numerical techniques for computing the added mass coefficients m_{ij} defined by (1.4), and their effectiveness in various cases. Throughout this discussion, we will assume the fluid to be (asymptotically) stationary at infinity (in symbols, $\lim_{|\underline{x}| \rightarrow \infty} \underline{u}(\underline{x}) = \underline{0}$). This choice of stationary axes is needed to make the m_{ij} finite.

¹See Lamb [6, Chapter VI] or, for a more modern exposition, G. Birkhoff [2, Chapter VI].

2. Inverse methods. For a few shapes, such as the sphere and circular cylinder treated in Chapter 1, §§4-5, the velocity potentials $\phi_i(\underline{x})$ have simple analytical expressions and the 'Dirichlet inner products' $D\langle\phi_i, \phi_j\rangle$ in (1.4) can be calculated in closed form. Thus for the unit sphere with center at the origin, with the fluid at rest at ∞ , the velocity potentials for translation are as in Chapter 1, (4.6):

$$(2.1) \quad \phi_i(\underline{x}) = x_i/r^3, \quad i = 1, 2, 3,$$

The m_{ii} are $2\pi/3$, and the m_{ij} with $i \neq j$ all vanish. Moreover the $\phi_i(\underline{x})$ for rotation ($i = 4, 5, 6$) all vanish, so the computation of added mass coefficients involving rotation is trivial.

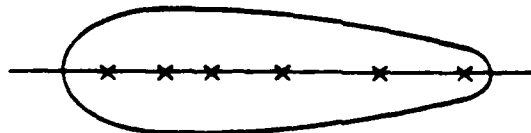
Cylinder. Similar formulas hold for a (circular) cylinder. Treating this as plane flow in the (x, y) -plane, we have:

$$(2.2) \quad \phi_1 = \frac{-x}{x^2 + y^2}, \quad \phi_2 = \frac{-y}{x^2 + y^2}, \quad \phi_3 = 0.$$

Hence the added mass matrix has the simple form indicated to the right.

$$\rho \begin{bmatrix} \pi a^2 & 0 & 0 \\ 0 & \pi a^2 & 0 \\ 0 & 0 & 0 \end{bmatrix}$$

Although analytical methods are only applicable to special shapes, as von Neumann emphasized (it was not a new discovery!) they can be used to compute added mass coefficients of elliptic cylinders, ellipsoids, and various other shapes. In particular, by superposing suitable linear combinations of sources and sinks, of the same total strength, on a uniform flow, one can construct the velocity potentials and stream functions of flows past a variety of axially symmetric solids and cylinders. The method is due to the British engineer Rankine, and bodies constructed in this way are called Rankine bodies. A typical Rankine body is sketched to the right.



Computational procedure. For example, one might superpose on a uniform flow (with $\psi = r^2$), sources of strength e and e' at $(1,0,0)$ and $(\frac{1}{2},0,0)$, equal and opposite sinks at $(-1,0,0)$ and $(-\frac{1}{2},0,0)$, and a dipole of moment μ at the origin. This will give²

$$(2.3) \quad \psi = r^2 + e(\cos \alpha - \cos \beta) + e'(\cos \alpha' - \cos \beta') \\ + \frac{\mu}{r} \sin^2 \theta .$$

By adjusting the three free parameters e , e' , and μ , one can construct potential flows around dirigible-like bodies with fore-and-aft symmetry having variable slenderness, nose taper, and mid-section roundness.

As von Kármán pointed out in a well-known 1928 paper [B4], the method can be applied to any axially symmetric body, the analytic continuation of whose velocity potential ϕ to the axis of symmetry has no singularities.

3. A potential flow problem. We next present a simple plane potential flow problem, one that could be solved numerically by hand (in a month?) using Southwell's 'relaxation methods' (Chapter 3, §4). As usual with plane flows, we can think of them as arising when cylinders parallel to the z -axis having the specified profiles are moved broadside in the (x,y) -plane.

Example 2. Consider the resistance to broadside acceleration of a square cylinder in a stationary concentric square container parallel to it. Without loss of generality, we can assume that the inner cylinder is the square $[-1,1]^2$; and that the outer cylinder bounds the square $[-M,M]^2$, where M is an integer.

Those wishing to compute added masses might well begin with this example ($M = 5$ is a good choice), which is relatively easy to program. Because of the flow symmetry, it suffices to compute

²Since the stream function for a simple source is $-\cos \theta$ (or $1 - \cos \theta$), where θ is colatitude.

one quadrant of the flow, which greatly reduces the cost (for given h). It has only one major source of error: the singularities at the corners of the square. There the flow velocity would be infinite if we really had potential flow.

The error can be estimated empirically by comparing computer outputs for different values of h ; it will be analyzed theoretically in §4. Theoretically, it would be $O(h^2)$ except at the corners, if one solved exactly the difference equations $\nabla_h^2 \psi = 0$, i.e.,

$$(3.1) \quad \psi_{i,j} = \frac{1}{4}[\psi_{i+1,j} + \psi_{i,j+1} + \psi_{i-1,j} + \psi_{i,j-1}]$$

at all interior mesh points.

In the first quadrant, the boundary conditions are $\psi = 0$ on the outer square and the x-axis, $\psi = y$ (for unit acceleration) on the inner square, and $\partial\psi/\partial h = 0$ on the y-axis. Expressing this as the symmetry condition $\psi_{-i,j} = \psi_{i,j}$, and substituting into (3.1), we get

$$(3.2) \quad \psi_{0,j} = \frac{1}{4}[\psi_{0,j-1} + \psi_{0,j+1}] \quad \text{if } x = 0.$$

For $h = 1/5$, this problem gives about 600 equations in as many unknowns. The matrix has band half-width 25, and so to solve these equations by direct band Cholesky elimination requires performing about $24 \times 25^3 = 4 \times 10^5$ multiplications! To perform these in 1940, even with the desk machines for doing arithmetic that were then available, would take a skilled computer on the order of a year.

Using quasi-iterative relaxation methods and human ingenuity, this time was reduced by Southwell's students to about a month. Today, using a high-speed computer and a well-designed package of 'debugged' subprograms such as ELLPACK, it has been reduced to seconds!

ELLPACK. Basically, ELLPACK is a very simple program statement language which enables users to call a large variety of

carefully checked Fortran subprograms for solving second-order elliptic boundary value problems on a rectangular grid such as the one proposed above. A brief summary of its methods and capabilities is given in Chapter 9 of Birkhoff-Lynch [A3].

Difference approximations. Although the 5-point difference approximation (3.1) is widely used in practice, and has $O(h^2)$ accuracy at all interior points, it is by no means the only or generally the best 'discretization' (alias 'arithmetization') of the Laplace equation.

Actually, ψ is analytic except at the corners, and there is an ingenious 9-point approximation

$$(3.3) \quad 20 \psi_{i,j} = 4[\psi_{i+1,j} + \psi_{i,j+1} + \psi_{i-1,j} + \psi_{i,j-1}] \\ + \psi_{i+1,j+1} + \psi_{i-1,j+1} + \psi_{i-1,j-1} + \psi_{i+1,j-1}$$

which has $O(h^4)$ accuracy, also except near corners. But unfortunately, as we will show, the actual error is more nearly $O(h^{4/3})$ for the flow around a square, because of the singularities at the corners. Moreover it is not obvious how to compute the Dirichlet integral from values at mesh points.

Bilinear finite elements. For these reasons, it is preferable to approximate ψ by piecewise bilinear finite elements. For this finite element approximation,³ the nodal values which minimize the Dirichlet integral $D\langle\psi,\psi\rangle$ in the associated 'finite element' space satisfy Pólya's 9-point difference equation

$$(3.4) \quad 8 \psi_{i,j} = \psi_{i+1,j} + \psi_{i,j+1} + \psi_{i-1,j} + \psi_{i,j-1} \\ + \psi_{i+1,j+1} + \psi_{i-1,j+1} + \psi_{i-1,j-1} + \psi_{i+1,j-1}$$

For corner (nodal) values $\psi_0, \psi_1, \psi_2, \psi_3$ on any mesh square S , the contribution $D_S\langle\psi,\psi\rangle$ from S to the Dirichlet integral is

³Methods of solving elliptic problems based on finite element approximations are usually called finite element methods (FEM).

$$(3.5) \quad \frac{2}{3} \sum_{j=0}^3 \psi_j^2 - \frac{1}{3}(\psi_0 + \psi_2)(\psi_1 + \psi_3) - \frac{2}{3}(\psi_0 + \psi_1\psi_3) .$$

The algebraic equation (3.4) is equivalent to the statement that $\psi_{i,j}$ minimizes the sum of the partial Dirichlet integrals $D_S \langle \psi, \psi \rangle$ taken over the squares ('cells') in the 2×2 square S^* with vertices at $(x_{i\pm 1}, y_{j\pm 1})$. Essentially, it applies the Rayleigh-Ritz method to the 'approximating subspace' of continuous, piecewise bilinear functions on the subdivided domain $[\Omega, \pi_h]$: the domain Ω subdivided into squares of side h .

'Conforming' elements. Note that if discontinuous approximating functions were allowed, we could easily reduce $D \langle \psi, \psi \rangle$ to zero by defining ψ to be piecewise constant: equal at each point to the value ψ_{ij} computed (by any method!) at the nearest mesh point--or to the average of all such values when there is more than one 'nearest' mesh point. This is possible because Kelvin's minimum energy principle only applies to continuous, piecewise differentiable functions. In this context, globally continuous piecewise polynomial functions are said to be 'conforming', because they conform to the underlying variational principle.

For second-order elliptic DE's all continuous, piecewise analytic functions are 'conforming': within this class, $|D \langle U, U \rangle - D \langle u, u \rangle| < \delta$ implies that $|U(x, y) - u(x, y)| < \varepsilon(\delta)$, where $\lim_{\delta \rightarrow 0} \varepsilon(\delta) = 0$. For fourth order DE's, such as are associated with 'creeping' flow, 'conforming' elements must be continuously differentiable (and piecewise smooth).

4. Corner singularity. The difference equations and finite elements described in §3 approximate potential flows very well in the interior of the flow very well, because the stream function (being harmonic) is analytic. However, the fit near the corners of a square obstacle is very poor. Thus the velocity of the (idealized) potential flow considered is infinite at the corner; as Helmholtz observed, this would imply infinite negative pressure

by the Bernoulli equation, and so lead to cavitation. Likewise, a real (slightly) viscous flow would tend to separate at the corner, if it did not cavitate there.

More relevant to our immediate concerns is the fact that, although the methods described in §3 have a local relative error which is $O(h^2)$ or smaller at interior points there is an error (with uniform mesh) that is $O(h^{4/3})$ associated with each corner singularity. We will now derive this result.

The local singularity of the flow around a 90° corner is easily found by elementary conformal mapping. The transformation $\zeta = z^{2/3}$ maps the flow in the three-quadrant domain depicted in Figure 2a onto uniform flow with stream function η and velocity potential ξ (complex potential $W = \xi + i\eta$) in the upper half of the complex ζ -plane. Since $W = \zeta = z^{2/3}$, $dW/dz = 2/3z^{-1/3}$, but this is the complex conjugate of the velocity (see for example Chapter 1). Hence the magnitude of the velocity near the corner is proportional to $1/\sqrt[3]{r}$, and tends to infinity as $r \rightarrow 0$.

The preceding flow is typical in the sense that, up to constant factor, all flows past a 90° corner not having a stagnation point there have the same asymptotic velocity distribution--the complex potential being given by

$$(4.1) \quad W = c_1 z^{2/3} + c_2 z^{4/3} + c_3 z^2 + \dots, \quad c_1 \neq 0.$$

It is evident that the ingenious finite element described in §3 does not have anything like this asymptotic behavior. Specifically, the true contribution to the Dirichlet (kinetic energy) integral from a circular sector of radius h centered at the corner will be of the order of

$$(4.2) \quad \int_0^h \int_0^{3\pi/2} |dW/dz|^2 r \, dr \, d\theta = (3M/2) \int_0^h r^{1/3} \, dr = M_1 h^{4/3}.$$

Hence, assuming that the 'pollution' is asymptotically confined to a fixed number of mesh cells, the error made in estimating the

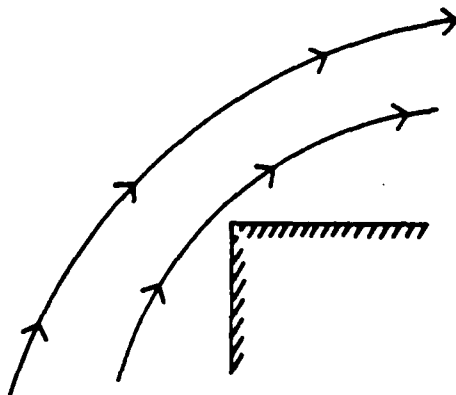


Fig. 2a. Flow around corner.

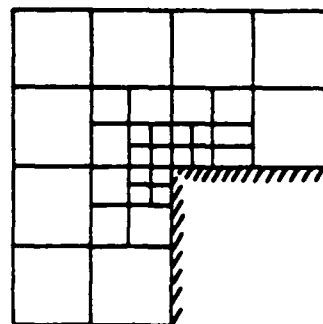


Fig. 2b. Local mesh refinement.

energy (or equivalently, the added mass) can be expected to be of the order of $h^{4/3}$. This expectation is confirmed in numerical experiments. More generally, for flows around convex obstacles having a corner where the tangent direction changes abruptly by $k\pi$ radians, the transformation $z - z_0 = t^{1+k}$ maps the z -domain locally onto a half-plane. Since the ψ -domain is also a half-plane, we have $|\nabla\psi| = O(r^{-k/(1+k)})$, $r = |z - z_0|$. Since the singularity is not matched, the error $\nabla e \cdot \nabla e = O(r^{-2k/(1+k)})$. Integrated over a disc of radius h , therefore

$$D(e, e) = O\left(\int_0^h r^{1-\nu} dr\right) \quad \text{where } \nu = 2k(1+k), \quad D\langle e, e \rangle = O(h^{2-\nu}) \\ = O(h^{2/(1+k)}).$$

(At a reentrant corner, k is negative; at a reentrant square corner, $k = -1/2$ and $t = (z - z_0)^2$; hence there is no singularity there.)

Singular elements. One way to obtain higher-order accuracy near protruding corners is to introduce additional "singular elements" into the approximating subspace, capable of reproducing the first two terms of the series (4.1). Since the third term is filled automatically (being analytic), the asymptotic error in the velocity can be presumed to be of the order of

$d(z^{8/3})/dz = O(z^{5/3})$. The error in the kinetic energy in a circular sector of radius h should correspondingly be of the order of

$$\int_0^h r^{5/3} r dr \sim h^{11/3},$$

giving nearly $O(h^4)$ accuracy.

Blending edge values. As Southwell realized [C11], already in the 1940's, a good way to reduce the total error in solving elliptic problems is to refine the mesh locally near singularities, and also in regions where gradients are steep. A technique proposed in [B*] for improving accuracy in solving elliptic problems, is to combine local mesh refinement with bilinear blending of the edge values⁴ in each 2-cell. This has been successfully applied by J.C. Cavendish, using only piecewise linear edge functions. Presumably higher-order accuracy could be achieved by using piecewise quadratic edge values.

Smooth obstacles. It is hard to avoid corners if one restricts attention to quadrilateral and triangular elements, which can describe only the exterior of a polygon. However, many important obstacles are smooth--i.e., without corners. For flows past smooth obstacles, ψ is also smooth. By using higher-order FEM or difference methods, the latter available in ELLPACK, one can therefore also hope to achieve high-order accuracy in the nodal values $\psi_{i,j}$. We next consider the problem of computing $D\langle\psi, \psi\rangle$ accurately from the $\psi_{i,j}$. We know of three local schemes for doing this which, when filled in by bilinear blending, are exact for quadratic harmonic functions; see [C*, p. 294]. The first of these proceeds as follows.

Scheme A. At the center of each mesh square, interpolate the average of the four corner values. Next, at the midpoint of

⁴ See [C1, Chapter 7]. Ref. [B*] is to Birkhoff-Gordon-Cavendish. Ref. [C*] is to G. Birkhoff and R.E. Lynch, Math. and Computers in Simulation 22 (1980), pp. 291-7; see also their note with John Brophy in [D4].

each interior edge, interpolate the average of the four adjacent values on the rotated (through 45°) mesh which results. Thus

$$(4.3) \quad \psi_{1,j+\frac{1}{2}} = \frac{1}{4}[\psi_{i,j} + \psi_{i,j+1} + \psi_{i-\frac{1}{2},j+\frac{1}{2}} + \psi_{i+\frac{1}{2},j+\frac{1}{2}}] .$$

Equivalently, using subscripts as in Fig. 3a below, we define

$$(4.4) \quad \psi(P) = [6\psi_0 + \psi_1 + \psi_2 + 6\psi_3 + \psi_4 + \psi_5]/16 .$$

Having bisected each interior mesh segment in this way, we have a unique quadratic interpolant to the three specified values (e.g., to $\psi_{i,j-1}$, $\psi_{1,j-\frac{1}{2}}$, $\psi_{i,j}$). This gives the desired 'conforming' interpolant on interior mesh lines; for Dirichlet problems, the values on boundary mesh segments are known.

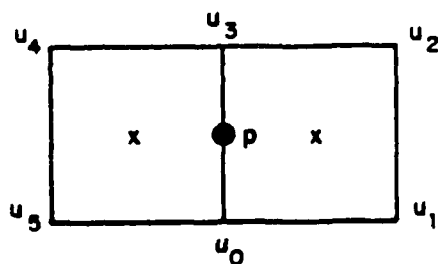


Fig. 3a

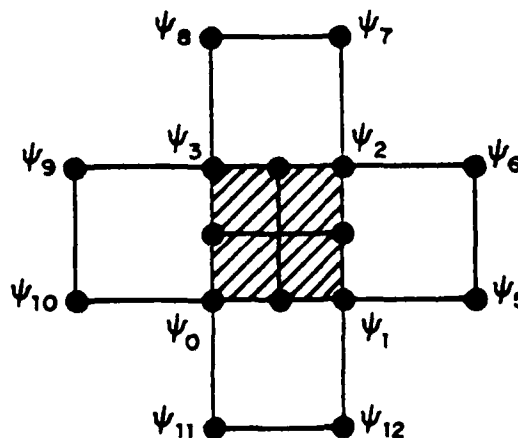


Fig. 3b

5. Added mass.⁵ The true added mass problem differs from the simplified problem discussed in §§3-4, in that the object accelerated is assumed to be in an infinite fluid (no wall effects). We next consider the added mass coefficients for an infinite cylinder of general cross-section, moving broadside in pure translation (angular velocity $\omega = 0$). In every (x,y) -plane perpendicular to the axis of the cylinder, this flow has the same harmonic velocity potential $\phi(x,y)$ satisfying the DE $\nabla^2 \phi = 0$ and the Neumann boundary condition

$$(5.1) \quad \frac{\partial \phi}{\partial n} = U \frac{\partial x}{\partial n} + V \frac{\partial y}{\partial n} \quad \text{on } \Gamma ,$$

where (U,V) is the vector (broadside) velocity of the cylinder. Moreover

$$(5.1') \quad \lim_{|\underline{x}| \rightarrow 0} |\nabla \phi| = 0 .$$

The complex potential of the flow can therefore be written in the form

$$(5.2) \quad W = c_1/z + c_2/z^2 + c_3/z^3 + \dots ,$$

where the $c_k = a_k + ib_k$ are appropriate complex constants. Moreover the Neumann boundary condition (5.1) is equivalent to the Dirichlet boundary condition on the stream function:

$$(5.3) \quad \psi = Uy - Vx \quad \text{on } \Gamma .$$

The case of a square obstacle (Example 2) is typical.

Inversion. Clearly, the numerical procedures of §§3-4 do not suffice to treat exterior Dirichlet or Neumann problems in an infinite fluid, because they would require the solution of an infinite system of linear equations inaccessible by computer. One can circumvent this difficulty by using a 'singular element'

⁵For the concept of added mass, see Chapter 1, §8. For a survey of what was known about added mass in 1960, see [A2, Chapter 6].

at infinity, perhaps of the form (5.2). To make this 'conforming', one can interpolate a buffer element constructed using 'blending functions' [C1, Chapter 7].

Conformal mapping. One can also use the technique of conformal mapping. This is especially easy to apply to cylinders with square or rectangular cross-sections, because Schwarz-Christoffel transformations reduce to elliptic integrals. Using this approach, W.G. Bickley [D1] computed the added mass of a square very accurately in 1934. For general cylinders, one can apply the methods of [A3, Chapter 8, §7].

In general, however, it is preferable to make a different appeal to complex analysis. The substitution $z \rightarrow 1/2$ carries solutions (5.2) of exterior Dirichlet or Neumann problems into solutions of interior Neumann problems. For example, it carries the solution of the exterior Dirichlet problem for the square $S: -1 \leq x, y \leq 1$, with boundary condition $\psi = y$ on $\Gamma = \partial S$, into the solution of an interior boundary value problem on a domain shaped somewhat like a four-leaved clover.

This method of computing added masses of cylinders has been discussed recently in the references cited in footnote 4; these discussions will not be reviewed here. Instead, we will turn our attention to a much more difficult topic: the computation of added mass coefficients of solids.

Added mass of solids. We determined the added mass of a sphere analytically in Chapter 1, §8. That of a sphere in a concentric spherical container can be obtained similarly, by considering the velocity-fields associated with potentials of the form

$$(5.4) \quad \phi = \left[ar + \frac{b}{r} \right] \cos \theta = ax + \frac{bx}{r^3}.$$

By applying Kelvin transformations, one can obtain from these the resistance to the acceleration of a sphere in an arbitrary concentric spherical container [D9, pp. 123-33].

However, to compute the added mass of (or velocity field) associated with general solids numerically, with reasonable accuracy, is a formidable task. For axially symmetric solids, one can take Stokes' stream function as the unknown. This satisfies the DE

$$(5.5) \quad \psi_{rr} - \frac{1}{r} \psi_r + \psi_{zz} = 0 ,$$

in cylindrical (r,z) -coordinates, $r = \sqrt{x^2 + y^2}$. Recently, R.E. Lynch has constructed an unpublished difference approximation to (5.5) having $O(h^6)$ accuracy.

Boundary element methods. Instead of putting sources and sinks on the axis, one can locate them in 'source panels' on the surface of the body.⁶ As in the two-dimensional case, it may be convenient to assume the solid to be at rest, and immersed in a moving fluid. This method leads to a Fredholm integral equation called the integral equation of potential theory [D9, Chapter X]. For a comprehensive discussion of the "calculation of potential flows about arbitrary bodies", see also J.M. Hess and A.M.O. Smith, Progress Aero. Sci. 8 (1966), 1-138. A very readable introduction to this method is also given in Chow [D5].

Inversion. Perhaps the most promising approach to the problem of computing the added mass of general solids is again provided by inversion, but using the transform of the velocity potential ϕ as the unknown function. This is

$$(5.6) \quad F(x,y,z) = \frac{1}{r} \phi \left[\frac{x}{r^2}, \frac{y}{r^2}, \frac{z}{r^2} \right], \quad r^2 = x^2 + y^2 + z^2 .$$

This is harmonic; moreover since inversion is a conformal transformation, it carries normals to the boundary into normals to the boundary. But since distances ds are multiplied by r^{-2} , normal derivatives are multiplied by a factor r^2 , the dot

⁶We will discuss this method thoroughly after we have experimented with it.

product $\nabla\phi \cdot \nabla\phi$ is multiplied by r^4 , and volumes correspondingly by r^6 . Therefore

$$(5.6') \quad \nabla\phi \cdot \nabla\phi \, dR = r^2 \nabla F \cdot \nabla F \, dx \, dy \, dz ,$$

where $F(x,y,z)$ is the solution of the Neumann problem for the Laplace equation and the boundary condition $\partial F / \partial n = r^{-2} \partial\phi / \partial v$.

Although the transformed stream function, which only exists in the axially symmetric case, has the advantage of having its boundary values known, and not just its normal derivatives, it is the solution of a much more complicated differential equation than $\nabla^2 F = 0$. Therefore, to use it seems impractical.

However, the preceding remarks are purely conjectural. Still another approach consists in using a formula due to G.I. Taylor, and extended by the author, Schiffer-Szegö, and John Brophy.⁷ This states that the added mass for translation is $4\pi\rho\mu_1' - \rho \text{vol}(\Sigma)$, where μ_1' is the "polarization". Using this approach, John Brophy has actually calculated the added mass of a cube, to three significant figures.

6. Container effect. The estimation of 'wall effects' and 'container effects' is very important, not only for many problems of numerical fluid dynamics, but also in experimental fluid dynamics. Much as computers can only handle a finite number of unknowns (most commonly from 300 to 20,000 of them in solving partial DE's today), so wind-tunnels, water tunnels and the like are necessarily of finite extent. For potential flow problems, both fixed and free boundary corrections are of interest, the latter being typically much smaller.

The substantial magnitude of the fixed wall container effect on added masses is evident from the following simple calculation. Let the container be a concentric square $\Gamma_1: \max(|x|, |y|) = R$

⁷G.I. Taylor, Proc. Roy. Soc. A120 (1928), 13-22 and 260-83; M. Schiffer and G. Szegö, Trans. AMS 67 (1949), 130-205; [A2, p. 154] (and p. 16) of the first ed.); and John Brophy, Ph.D. Thesis, Purdue University, 1983.

having R^2 times the area enclosed by Γ . Since $\gamma \cdot \gamma$ decays like $O(r^{-4})$ in an infinite fluid, and $\int r^{-4} r dr = \frac{1}{2} R^2$, it is plausible that the 'container effect' is asymptotically proportional to $1/R^2$. One can presumably correct for this (to within 0.2% or so) by asymptotic (Richardson) extrapolation, a method to be described later in this section. The following simple example gives further evidence for the preceding conclusion.

Example 3. We will next determine the fluid resistance to acceleration of a cylinder of radius a surrounded by an ideal fluid in a concentric cylindrical container of radius R . By choice of units, we can assume that $a = 1$.⁸ To determine this resistance, it suffices to consider complex potentials $W = \phi + i\psi$ of the special form

$$(6.1) \quad W = kz + kR^2/z.$$

Since with (5.4), $\psi = k(r - R^2/r) \sin \theta$, evidently the 'stream function' $\psi(x, y) \equiv 0$ on the circle $r = R$. Therefore the fluid in the annulus $1 \leq r \leq R$ can be regarded as constrained externally by a circular container (cylindrical in R^3), $|z| = R$, and impelled internally by the disk $|z| \leq 1$ (a solid cylinder in R^3).

Also, $\phi = k(r + R^2/r) \cos \theta$, and so

$$(6.2) \quad \frac{\partial \phi}{\partial n} = \frac{\partial \phi}{\partial r} = \frac{\partial \psi}{r \partial \theta} = k \left(1 - \frac{R^2}{r^2}\right) \cos \theta$$

is identically $-\cos \theta$ on the unit circle $r = 1$ if and only if $k(R^2 - 1) = 1$. With these formulas in hand, it is a straightforward (if tedious) exercise to compute the kinetic energy integral $\frac{1}{2} m = \frac{1}{2} m U^2 = \frac{1}{2} \rho D \langle \nabla \phi, \nabla \phi \rangle$. This computation we now summarize.

The squared velocity at any z is

$$(6.3) \quad q^2 = |dW/dz|^2 = u^2 + v^2 = |\zeta|^2 = k^2 \left(1 - R^2/z^2\right)^2.$$

⁸This argument is an application of the principle of inertial similarity (Chapter 1, §7).

Hence $u = k[1 - (R^2 \cos 2\theta)/r^2]$, $v = k(R^2 \sin 2\theta)/r^2$. Therefore

$$q^2 = k^2 [1 + (R^4/r^4) - 2(R^2 \cos 2\theta)/r^2]$$

This formula, combined with $dx dy = r dr d\theta$, makes it easy to evaluate the double integral $D\langle\phi, \phi\rangle = \langle\nabla\phi, \nabla\phi\rangle$ in polar coordinates. Integrating q^2 from $\theta = 0$ to $\theta = 2\pi$, we get $k^2\pi$ times $1 + (R^4/r^2)$. The (iterated) integral of this from $r = 1$ to R gives, finally

$$\begin{aligned} m &= \rho D\langle\phi, \phi\rangle = \pi k^2 \int_1^R [1 + (R^4/r^4)] r dr \\ &= \pi \rho k^2 [r^2/2 - R^4/2r^2]_1^R \\ &= (\pi \rho k^2/2) [(R^2-1) + (R^4-R^2)] = \pi \rho k^2 [R^4-1] . \end{aligned}$$

Since $k^2 = 1/(R^2-1)^2$, this gives finally

$$(6.4) \quad m = \pi \rho (R^2 + 1)/(R^2 - 1) = \pi \rho (1 + \frac{2}{R^2} + O(\frac{1}{R^4})) .$$

Alternative derivation. An alternative derivation of the 'container correction' (6.4) goes as follows. The velocity potential $\phi = x + x/r^2 = (r + r^{-1}) \cos \theta$ not only describes the plane potential flow with $U = 1$ around the unit disk, $r \leq 1$, but its 'analytic continuation' inside the disk represents the potential flow induced by the translation of any smaller concentric disk $r \leq a$ ($a < 1$) in a cylindrical container. This is easily verified since, on $r = a$,

$$u_r = u_n = \partial\phi/\partial r = (-a^{-2}) \cos \theta .$$

This matches the normal velocity component on the boundary of a disk of radius $a < 1$, translating with speed $U = (1 - a^{-2})$ in the container $r = 1$.

By Bernoulli's formula, therefore, if this disk undergoes horizontal acceleration $\alpha = U$, the horizontal component of force is

$$\begin{aligned}
 X &= -\rho \int (\cos \theta) \phi(a) d\theta \\
 &= -\rho(a + a^{-1}) \int \cos^2 \theta d\theta = \pi \rho(a + a^{-1}) .
 \end{aligned}$$

Setting $X = m\alpha$, therefore, we get

$$m = \pi \rho a^2 [(1 + a^2)/(1 - a^2)] .$$

Extrapolation. Knowing that the container effect (or 'wall effect') is asymptotically proportional to $1/R^2$, where R is the radius of the container, we can estimate and partially correct for the error. Let m_1 be the added mass computed in a container of radius R ; then it is usually much easier to compute m_θ in a container of radius θR , where $\theta < 1$ is some fraction, say $\theta = \frac{1}{2}$.

If the asymptotic formulation were exact, we would then have both

$$m_1 = m_0 + k \quad \text{and} \quad m_\theta = m_0 + k/\theta^2 .$$

Hence we would have

$$(6.5) \quad m_1 + \theta^2(m_1 - m_\theta)/(1 - \theta^2) = m_0 .$$

Similarly, suppose that the error of a difference or finite element approximation is known to be asymptotically proportional to h^2 . Then by calculating a quantity with mesh lengths h and θh ($\theta < 1$), with resulting values m_θ and m_1 , the value

$$(6.5') \quad m_0 = m_\theta + \theta^2(m_\theta - m_1)/(1 - \theta^2) ,$$

should be an improved approximation to m_0 , better than either m_0 or m_θ alone. By definition, Richardson extrapolation consists in using a formula like (6.5') to obtain a (hopefully improved) approximation to m_0 .

7. Two-dimensional airfoil computations. A thoughtful reconsideration of the methods and results of §§1-6 brings out two basic but often ignored facts. First, although the determination of the well-defined potential flows discussed there had been arithmetized in principle by 1900, thanks to the genius of Poincaré and others, their computation in practice is still far from having been automated. Second, classical analysis often suggests several competing methods for arithmetizing (digitizing) the accurate determination of such potential flows. The choice of the 'optimal' method may depend on what is being computed: a single number or vector (the net force), the pressure distribution, on a profile or solid, or the velocity field as a whole.

These facts seem to be much less widely appreciated than the shortcomings of the potential flow model, some of which have been commented on in Chapter 2.

The rest of this chapter will be devoted to various more general classes of potential flows whose definition is much less straightforward, whose computation (especially in three dimensions) is correspondingly more difficult, but whose study is justified because their determination is still so much simpler than that of the compressible and viscous flows to be treated in later chapters.

A classic family of two-dimensional potential flows has played an important role in the design of wing sections (or 'profiles') for airplanes. This family of flows has already been described in Chapter 1, §11, and their underlying analytical theory is summarized in Appendix C, for convenient reference. We will refer freely to this summary in explaining the relevant computational issues in the present section.

The basic model assumes that, for any (reasonably small) angle of attack α , the flow around an airfoil section adjusts itself so as to produce 'finite velocity at the trailing edge' (S' in the figure). For given $\alpha = \arctan(V/U)$, there is exactly one conformal mapping of the exterior of an airfoil with a sharp trailing edge S' onto the exterior of a given circle,

which maps S' onto $T' = (1,0)$. Perhaps the most powerful technique of two-dimensional airfoil theory consists in computing this map, say $w = f(z)$ with inverse $z = f^{-1}(w)$.

The prototype of such mappings is provided by Joukowski airfoils, with

$$(7.1) \quad w = \frac{1}{2}[z + \sqrt{z^2 - 4}] \quad \text{and} \quad z = w + w^{-1}.$$

The relevant numerical procedures for this case are described at length by Chow in [D5, Section 2.7],⁹ and we will just summarize a few relevant facts here. Under (7.1), the circle $|w| = 1$ corresponds to the slit of all $(x,0)$ with $x \in [-2,2]$. Less obviously, circles through $w = \pm 1$ correspond to circular arcs through $z = \pm 2$. Slightly larger circles through $w = 1$ correspond to Joukowski airfoils whose mid-section is nearly a circular arc, a cusp at the trailing edge, and whose leading 'edge' is nearly semicircular.

Analytically, any Joukowski airfoil can be specified (up to similarity) by prescribing the center $(-\delta, \epsilon)$ of the circle in the w -plane which is mapped onto it. The camber (mean curvature of the section midline) is nearly proportional to ϵ , and the mean thickness to δ . It is easy to write a computer program

⁹Chow treats the more general case of mappings $z = w + b^2/w$, $2w = [z + \sqrt{z^2 - 4b^2}]$, but this obviously reduces to $z/b = w/b + b/w$, hence by (7.1), to a simple change of scale.

which will plot the profile of the Joukowsky airfoil corresponding to given ϵ and δ , and to verify visually (at an interactive terminal with graphics capability) the statements at the end of the last paragraph.

Quantities of interest. Many quantities and functions are of aerodynamic interest, such as the lift L , the moment M (or center of pressure, C.P.), the pressure (coefficient) distribution $C_p(x)$, and the streamlines and equipotentials. We next consider the computation of these in the special case of Joukowsky airfoils.

For given $\alpha, \gamma, \delta, \epsilon$, we will have

$$(7.2) \quad W = e^{i\alpha} w + e^{-i\alpha} w^{-1} + i\gamma \ln w - \gamma \ln \alpha.$$

Hence, given any subroutine for plotting streamlines $\psi = \text{const}$ (with constant $\Delta\psi$) and equipotentials $\phi = \text{const}$ (with constant $\nabla\phi$) in the w -plane for given α and γ , with $w = 1$ as a stagnation point, $z = w + w^{-1}$ maps the $w_{j,k} = w(\phi_j, \psi_k)$ into the mesh points of a network of streamlines and equipotentials in the z -plane. (This is because, in \mathbb{R}^2 and in its extension to the complex sphere, conformal maps preserve streamlines and equipotentials.)

In the limiting case $\delta = 0$ of a circular arc Joukowsky profile, for any camber $\epsilon > 0$, the circulation Γ which will produce finite velocity at the leading as well as the trailing edge is uniquely determined. Curiously (and unrealistically), the resulting lift is produced at a mean angle of attack $\alpha = 0$, while (undesirably) the center of pressure is at the midpoint.

Pressure distribution. The main use of two-dimensional airfoil theory is for predicting the pressure coefficient distribution $C_p(x)$ on the upper ('suction') and lower ('pressure') side of the airfoil. This is easily computed from the Bernoulli equation, and the relation

$$(7.3) \quad q^2 = |dW/dz|^2 = |(dW/dw)(dw/dz)|^2 = |dW/dw|^2 \cdot |dw/dz|^2$$

The distribution of $|dW/dw|^2$ as a function of w (and hence of $z = w + w^{-1}$) was already determined in Chapter 1, §11.

8. Free surfaces. In hydrodynamics, a 'free surface' usually means simply a surface at constant pressure. These arise most notably in the mathematical theory of gravity waves; as Lamb wisely observes [A6, p. 231]: "One of the most interesting and successful applications of hydrodynamical theory is to the small oscillations, under gravity, of a liquid having a free surface". Lamb then expands on this theme for two chapters, each 110 pages long.

The first of Lamb's chapters is concerned with 'tidal waves', which Lamb defines [A6, §169] as waves in which "the vertical acceleration of the fluid particles may be neglected or, more precisely, ... the pressure at any point (x, y) is sensibly equal to the static pressure $[p = p_0 + \rho g(y_0 + \eta - y)]$ due to the depth $[y_0 - y]$ below the free surface $[y = \eta(x, z)]$ ".

Lamb's second chapter on gravity waves is concerned with 'surface waves' of which "the most important case... is that of waves in relatively deep water". By applying the method of separation of variables to solutions $\phi(x, y; t)$ of the Laplace equation $\phi_{xx} + \phi_{yy} = 0$ in a vertical plane, that are sinusoidal in time (normal modes), he is led to look for solutions of the form

$$(8.1) \quad \phi = A \cosh k(y+h) \cos kx e^{i(\omega t + \alpha)} .$$

He shows that, under the hypothesis of small oscillations, Kelvin's "free surface" condition (our Chapter 1, (6.9))

$$(8.2) \quad \phi_{tt} + g \frac{\partial \phi}{\partial y} = 0, \quad (\text{Chapter 1, (6.12)})$$

which reduces when $\phi(\underline{x}; t) = \phi(\underline{x}) e^{i\omega t}$ to

$$(8.2') \quad \omega^2 \phi = g \frac{\partial \phi}{\partial y}, \quad [\text{A6, p. 364, (8)}]$$

is satisfied if and only if

$$(8.3) \quad \omega^2 = gk \tanh kh .$$

In the limit, as $h \rightarrow \infty$, (8.1) reduces to $\phi = Ae^{-ky} \cos kx \cos(\omega t + \alpha)$, and (8.3) to $\omega^2 = gh$. In the opposite limit as $h \rightarrow 0$, of 'long' or 'shallow water' waves, the elevation $\eta(x, z)$ of the free surface of any time-dependent potential flow satisfies the linear, constant-coefficient wave equation

$$(8.4) \quad \eta_{tt} = gh(\eta_{xx} + \eta_{zz}).^{10}$$

The numerical integration of this DE will be the central concern of Chapter 5; in this chapter, we will look at other aspects of the free surface condition.

From the periodic 'small oscillations' satisfying (8.1), (8.3') derived by Lamb in [A6, Chapters VIII and IX], the general solution of many wave problems in 'oceans' of constant (or infinite) depth can be obtained by superposition as Fourier integrals of these 'normal modes'. That this is possible for 'small' oscillations (in space and time) is guaranteed by general "completeness" theorems of modern harmonic analysis.

Harmonic analysis in time is always applicable to 'small oscillations' (i.e., to waves of 'infinitesimal' amplitude), of 'free surfaces' satisfying (8.2) of time-dependent potential flows with stationary solid boundaries. Moreover, the formulas become especially simple in 'oceans' of infinite or constant finite depth, as we have seen. Since the approximation of infinite depth is valid whenever all relevant wave lengths are small in comparison with the depth (in symbols, whenever $\lambda \ll h$), these analytical methods are widely applicable.

However, since potential theory is only indirectly involved, and since analytical considerations usually dominate numerical

¹⁰ See Chapter 1, §4. Note that the instantaneous normal velocity $\eta_t(y, z, t)$ depends on the entire history of the motion, and not just on the instantaneous normal velocities of the walls.

considerations in these applications, we will simply refer the reader to Chiang C. Mei's excellent "Applied Dynamics of Ocean Surfaces", Wiley, 1983, for a comprehensive survey of what can be derived by these "wave packet" methods.

The situation is very different as regards waves of finite amplitude and waves in oceans (or lakes) of variable depth. Such waves have been treated successfully for a large variety of conditions by the MAC and related methods developed at Los Alamos. A number of such solutions obtained there, are described in [D6] and in the references listed in its bibliography. In computing these time-dependent flows with free boundaries, a Dirichlet (and/or Poisson) type boundary value problem for the velocity potential (and/or vorticity) must be solved at each time step. This makes the "computational complexity" of solving such problems an order of magnitude greater than that of computing added mass. Three-dimensional calculations (see [D8],[D10]) are therefore especially impressive. Necessarily, in making them, the emphasis must be on expediency rather than on mathematical rigor.

We again refer the reader to the original publications for descriptions and analyses of the algorithms that were found most effective in solving these problems. Moreover, we will do the same for the ingenious calculations by Michael Longuet-Higgins of the evolution of two-dimensional 'breaking waves'.¹¹

9. Ship wave resistance. Being less transient, flows having stationary free boundaries tend to have greater intrinsic interest. This is especially true of the 'free surface' around a ship moving at constant speed through calm water of constant depth. The prediction and reduction of the 'wave resistance' encountered by a ship under these circumstances is a classical problem of naval architecture.

As with most other wave phenomena, the 'small amplitude' theory of ship waves is the part most amenable to analytical methods,

¹¹Proc. Roy. Soc.

and it is the only one that will be discussed here. From a scientific standpoint, even the quantitative computation of the wave resistance of 'thin' ships producing 'linear' waves has not yet been developed to the point of routine rigorous application, and we shall take this problem up next.

Linear theory.¹² As was first shown by J.H. Michell (Phil. Mag. 45 (1898), 106-23), the assumptions of potential flow under gravity and a 'free surface' at constant pressure head, in the linearized 'small amplitude' approximation, to a formula expressing the dimensionless wave resistance coefficient C_w as a quintuple integral, as follows.

If R_w is the (theoretical) wave resistance of a (thin) ship having length $L = 2\ell$ and beam $2B$, moving dead ahead into smooth water with constant speed v , we define $F = gL/v^2$ as the squared reciprocal $F = f^{-2}$ of the nautical Froude number $f = v/\sqrt{gL}$.

We let $y = \eta(x, z)$ be the equation of the submerged portion of the hull, which is supposed symmetric about a longitudinal centerline plane. The longitudinal section is not generally rectangular, but we enclose it in a convenient rectangle S' , as in Figure 7: the origin is on the water surface amidship, z goes vertically down, and x lengthwise, positive forward. In order to obtain a dimensionless representation, we introduce $\xi = x/L$, $\zeta = z/L$. Then, if $y = \eta(x, z)$ is the (dimensional) hull offset at the point (x, z) of the longitudinal section, we define the dimensionless offset $G(\xi, \zeta)$ by

$$(9.1) \quad G(\xi, \zeta) = \frac{1}{B} \eta(L\xi, L\zeta)$$

$G(\xi, \zeta)$ is defined on the scaled longitudinal sect which is contained in the scaled rectangle

$$S: \quad -(1/2) \leq \xi \leq (1/2), \quad 0 \leq \zeta \leq D/L .$$

¹²We base this discussion largely on G. Birkhoff, B.V. Korvin-Kroukowsky, and J. Kotik, Trans. Soc. Naval Arch. Marine Eng. (1954), 339-96.

The dimensionless horizontal slope of the l surface is given by

$$(9.2) \quad h(\xi, \zeta) = \partial G / \partial \xi .$$

Then Michell's integral is

$$(9.3) \quad R_w = \frac{1}{2} \rho v^2 B^2 C_w ,$$

where

$$(9.4) \quad C_w = \frac{8F^2}{\pi} \int_S \int_S d\xi d\zeta \int_S \int_S d\xi' d\zeta' h(\xi, \zeta) h(\xi', \zeta') \\ \int_1^\infty e^{-\lambda^2 F(\zeta + \zeta')} \cos \lambda F(\xi - \xi') \frac{\lambda^2 d\lambda}{\sqrt{\lambda^2 - 1}}$$

The salient feature of Equation (9.4) is that the wave resistance is due to pairs of hull elements, an element at ξ, ζ and another element at ξ', ζ' contribute

$$(9.4') \quad h(\xi, \zeta) h(\xi', \zeta') d\xi d\zeta d\xi' d\zeta' \int_1^\infty e^{-\lambda^2 F(\zeta + \zeta')} \\ \cos \lambda F(\xi - \xi') \frac{\lambda^2 d\lambda}{\sqrt{\lambda^2 - 1}}$$

The integral depends on the horizontal spacing $\xi - \xi'$ and the sum of the depths $\zeta + \zeta'$. The wave resistance coefficient C_w is obtained from Eq. (10.4) by integrating (summing) over all pairs. The integral in (10.4) is "absolutely convergent"; hence the integrations with respect to $\xi, \xi', \zeta, \zeta', \lambda$ may be taken in any order, yielding a variety of expressions.

Sink and trim. In general, forward motion tends to raise the bow of a ship, causing it to tilt upward at some 'angle of trim', and to lift its C.G. These changes affect the wave resistance, and so an exact prediction of wave resistance requires calculating the hydrodynamic thrust for enough values of sinkage

and trim (for given speed) to determine which are in dynamic equilibrium.

To be meaningful, the wave resistance of a ship must also be combined with its 'wake' or 'eddy-making' resistance (and 'skin friction'), to determine its total power requirements (in calm water) at each speed.

10. Interfacial instability. Helmholtz, Kelvin, and Rayleigh all recognized the natural tendency of waves to form on stationary 'free boundaries' of fluids in motion. Moreover they all realized that in an 'ideal' inviscid fluid, such surface waves have no tendency to get 'damped out'. For example, on the two-dimensional flow under a sluice gate depicted in Figure , one can superimpose a periodic wave train downstream. Again, the 'hydraulic jump' that forms downstream of the flow over a spillway is another familiar wave-like phenomenon. Likewise, by exploring the effects of surface tension, Rayleigh uncovered a fascinating range of phenomena associated with interfacial waves on capillary jets.

This tendency of waves to form or instability is especially easy to predict mathematically in the case of (nearly) parallel flows with straight streamlines of discontinuity, such as the jet from a straight tube (Figure 7a), already mentioned in Chapter 1, § , or of a uniform wind over a horizontal plane surface (Figure 7b). Other examples of potential flows enveloping an idealized 'cavity' or stagnant 'wake' at constant pressure will be discussed in Chapter 8.

Helmholtz instability.¹³ Helmholtz showed that although such 'discontinuous' potential flows might be in equilibrium, this equilibrium was in general strictly unstable. His demonstration, like its subsequent generalizations by Kelvin and Rayleigh, considered the stability of sinusoidally perturbed interfaces. Specifically, he solved the Euler-Lagrange equations

¹³H. Helmholtz, op. cit.

for the 'slip flow' associated with two ideal fluids having the configuration of Figure 8, with

$$(10.1) \quad u(y) = \begin{cases} U & \text{if } y < 0, \\ U' & \text{if } y > 0; \end{cases} \quad \rho(y) = \begin{cases} \rho & \text{if } y < 0, \\ \rho' & \text{if } y > 0, \end{cases}$$

in the unperturbed state.

To this he applied the theory of small oscillations for the interface $y = \eta(x,t)$, which has eigenfunctions $\eta(x,t) = A(t) \sin kx$. For each wave number k , relative to axes moving with velocity

$$(10.2) \quad \bar{U} = (\rho U + \rho' U') / (\rho + \rho'),$$

the amplitude $A(k)$ of each sinusoidal component in the Fourier expansion of $\eta(x;t)$ satisfies a second-order ordinary DE of the form

$$(10.3) \quad d^2 A / dt^2 = S(k) A.$$

This remains true (because the relevant DE is invariant under horizontal translation) when surface tension and gravity are taken into account. As Kelvin showed,¹⁴ the coefficient $S(k)$ in the DE (10.3) is given in general by

$$(10.4) \quad S(k) = \frac{\rho \rho' k^2}{(\rho + \rho')^2} (U - U')^2 - \frac{\rho - \rho'}{\rho + \rho'} gh - \frac{\gamma k^2}{\rho + \rho'},$$

where γ is the interfacial tension. It follows that perturbations are neutrally stable for all wavelengths $\lambda = 2\pi/k$ if and only if $g(\rho - \rho') > 0$ (heavier liquid below), and

$$(10.5) \quad 2\sqrt{g(\rho - \rho')\gamma} > \rho \rho' (U - U')^2 / (\rho + \rho');$$

otherwise, the interface is strictly unstable.

¹⁴ Math. and Phys. Papers, vol. 4, pp. 76-100; Rayleigh, Theory of Sound, 2d. ed. §365. This section is based on the article by one of us in Proc. Symp. Appl. Math. XIII, pp. 55-76.

Taylor instability. As G.I. Taylor pointed out in a series of classic papers,¹⁵ acceleration a of the fluids (assumed to be incompressible) normal to the interface can be combined with gravity, thus replacing g by the 'net gravity' or 'effective gravity' $g-a$ in (10.4) and (10.5). When $(a-g)(\rho-\rho') > 0$ (the acceleration dominates and is from the lighter toward the heavier fluid), we have the pure 'Taylor instability' of a heavy liquid separated by a horizontal plane from a pressurized gas which holds it up.

Three important qualitative conclusions follow from the preceding formulas [B6, p. 252]:

- A) Relative tangential velocity $U - U'$ is always destabilizing. (Helmholtz instability)
- B) Acceleration from a light towards a denser fluid also destabilizing; (Taylor instability)
- C) Surface tension is always stabilizing, and always makes sufficiently short ripples stable--hence making the initial value problem well-set.

Nonlinear effects. Philosophically, Helmholtz instability has been invoked to explain the 'generation of waves by wind' qualitatively, within the framework of discontinuous potential flow models. It has also been proposed to explain qualitatively the flapping of flags, and the formation of 'mackerel' clouds in the sky. Unfortunately, these attractive philosophical explanations have not, even after a century of ingenious speculation, led to a precise quantitative explanation of the observed sizes of gravity waves as functions of the wind speed and duration.

Nonlinear effects. Although viscosity and turbulence are obvious factors which have been neglected, and which may have an important influence on the generation of the neutrally stable waves mentioned in §9, it is primarily nonlinear effects that limit the applicability of formulas (10.1)-(10.5) to the strictly unstable interfaces of primary concern to us here. As Helmholtz

¹⁵Proc. Roy Soc. London A201 (1950), 192-6; D.J. Lewis, *ibid.* A202 (1950), 81-96. See also R. Bellman and R.H. Pennington, *Quar. Appl. Math.* 12 (1954), 151-62.

realized, vortex flows have a curious nonlinear evolution; we shall take this up in Chapter 7.

11. Free streamlines. Time-independent flows bounded by free streamlines at constant pressure provide potential flow models for a variety of fluid motions. Classic examples include the steady two-dimensional potential flows with free streamlines, of the kind discussed in Chapter 1, §9. These were proposed by Helmholtz, Kirchhoff, and others as models for jets and wakes, in homogeneous, incompressible fluids of constant density. In such fluids, one can eliminate the effect of gravity by considering the difference $P = p - \rho G$ between the total pressure and the hydrostatic pressure, as in Chapter 1, §7. By Bernoulli's equation, if stagnant fluid with $P = \text{const.}$ is on one side of the free streamline, such a 'free' streamline will be in equilibrium if and only if the flow speed q is constant on the free streamline.

This observation makes it possible to apply conformal mapping techniques to relate the complex potential $W = \phi + i\psi$ to the conjugate velocity $\zeta = u - iv$ for a variety of plane flows past plates and wedges, so as to predict the shape of a wake or jet; see Chapter 1, §9, for some examples.

In a notable 1906 paper, Levi-Civita reduced the determination of plane flows with free streamlines past curved obstacles to the solution of an integral equation. However, to determine the separation point mathematically is difficult.¹⁶ One must consider a one-parameter family of integral equations, and see which of these satisfies the Brillouin-Villat condition of 'finite' curvature of the separation point. How to do this will be explained in Chapter 8.

The literature on the subject prior to 1920 is summarized by Lamb in [A6, §§73-8]; for a more thorough treatment, see [A4, Chapters I-VI]. A brief but lively account of the state of the subject in 1940 was given by von Kármán in Bull. AMS 46 (1940),

¹⁶As Lamb remarks dryly [A6, p. , footnote]: "The working out of particular cases presents great difficulties".

613-82. Deep existence and uniqueness theorems for such flows with free streamlines of constant flow speed have been proved by Levay, Weinstein, Lavrentsen, Paul Garabedian and others; several of them are in [A4, Chapter VIII].

Since 1940, it has become customary to apply the preceding mathematical model to describe air- and vapor-filled cavities which form behind cylinders and solids moving at high speeds through water. At high speeds (if $U^2 \gg gd$), gravity can again be neglected. Moreover, the free streamline separating the liquid from the gas phase is much less unstable than in the case of wakes.

Finally, it should be observed that Villat was able to apply conformal mapping techniques to reduce the determination of a free streamline under gravity to a nonlinear integral equation.¹⁷

¹⁷See G. Birkhoff, Proc. Am. Soc. Civ. Eng. (1961), [A4, Chapter VIII, §11], 17-22; G. Birkhoff and David Carter, J. Rat. Mech. Anal. 6 (1957), 769-80.

REFERENCES FOR CHAPTER 4

- [D1] W.G. Bickley, "Two-dimensional potential problems for the space outside a rectangle", Proc. Lond. Math. Soc. 37 (1934), 82-105.
- [D2] G. Birkhoff, H.H. Goldstine and E.H. Zarantonello, "Calculation of Plane Cavity Flows", Rend. Sem. Mat. Torino 13 (1954), 205-24.
- [D3] G. Birkhoff, B.V. Korvin-Kroukovsky, and J. Kotik, "Wave resistance of ships", Trans. Soc. Nav. Arch. Marine Eng. (1954), 359-96.
- [D4] G. Birkhoff and A. Schoenstadt (eds.), Elliptic Problem Solvers, II. Academic Press, 1983.
- [D5] Chuen-Yen Chow, "An Introduction to Computational Fluid Dynamics", Wiley, 1979.
- [D6] S. Goldstein, "Low drag and suction airfoils", J. Aer. Sci. 15 (1948), 189-214.
- [D7] F.H. Harlow and A.A. Amsden, Fluid Dynamics, Report LA-4700 (UC-34), Los Alamos Scientific Laboratory, 1971.
- [D8] F.H. Harlow and J.E. Welch, "Numerical study of large amplitude free surface motions", Physics of Fluids 9 (1965), 842-
- [D9] O.D. Kellogg, Potential Theory, Springer, 1929.
- [D10] B.D. Nichols and C.W. Hirt, "Calculating three-dimensional free surface flows...", J. Comp. Phys. 12 (1973), 234-46. (See also their earlier article, ibid. 8 (1971), 434-
- [D11] L.I. Sedov and G.Y. Stepanov (eds.), "Non-steady Flow of Water at High Speeds", Proc. IUTAM Symposium held in Leningrad, 1971, Nauka, Moscow, 1973.
- [D12] Joanna W. Schot and Nils Salvesen (eds.), First Int. Congr. Numerical Ship Hydrodynamics, U.S. Naval Ship R&D Center, 1975.
- [D13] J.V. Wehausen, "The wave resistance of ships", Advances in Appl. Mech. 13 (1973), 93-245.
- [D14] J.V. Wehausen and Nils Salvesen (eds.), Sec. Int. Conf. Numerical Ship Hydrodynamics, University Extension Publications, Berkeley, CA.

5. SOUND WAVES¹

1. Introduction. The wave equation in m space dimensions,

$$(1.1) \quad u_{tt} = c^2 \nabla^2 u = c^2 \sum_{j=1}^m \partial^2 u / \partial x_j^2$$

is one of the best understood differential equations (DE's) of mathematical physics. As we have seen, it arises in the theory of 'long' gravity waves (Chapter 1, §§3-4), and it plays a central role in the theory of sound (Chapter 2, §2). For more detailed derivations, see the treatises of Lamb [A6, Chapter 10], Morse and Ingard [E12, Chapter 6] and Whitham [B12, Chapter 7].

In the theory of sound, as was explained in Chapter 2, §2, it is satisfied (approximately) by $u = \delta\phi$, δp , and all components of $\nabla(\delta\phi)$ such as δu . This chapter will be mainly devoted to schemes for its (approximate) numerical integration, including (in §4) the difference approximation (of Courant-Friedrichs-Lewy) already mentioned in Chapter 3, §2.

Our analysis of these schemes will be based on mathematical properties of the plane wave solutions of (1.1), of the form

$$(1.2) \quad u = \exp[i(\underline{k} \cdot \underline{x} + \omega t)] = \exp[i(\sum_{j=1}^m k_j x_j \pm \omega t)] ,$$

where $\underline{k} = (k_1, \dots, k_m)$ is a real wave vector and $\omega = ck$, where

$$(1.2') \quad k = |\underline{k}| = (\sum_{j=1}^m k_j^2)^{1/2} .$$

The progressive waves defined by (1.2)-(1.2') are simply harmonic in time and space; for algebraic convenience, we have presented them in complex form.

Standing waves. For any given wave vector $\underline{k} = (k_1, \dots, k_m)$, there are four related linearly independent real standing wave solutions of (1.1), namely

¹Chapters 5 and 6 have been co-authored by Prof. V.A. Dougalis of the University of Tennessee. Chapter 5 is a slightly modified copy of the first half of [E5]

$$(1.3) \quad u = \begin{Bmatrix} \cos \\ \sin \end{Bmatrix} \underline{k} \cdot \underline{x} \begin{Bmatrix} \cos \\ \sin \end{Bmatrix} \omega t, \quad \omega = ck.$$

The wave equation is reversible in time and space, and the subspace spanned by these is unchanged if \underline{k} is replaced by $-\underline{k}$ and/or ω is replaced by $-\omega$.

For any fixed wave vector \underline{k} , the DE (1.1) and the initial conditions

$$(1.4) \quad u(\underline{x};0) = a \cos \underline{k} \cdot \underline{x} + b \sin \underline{k} \cdot \underline{x}$$

and

$$(1.4') \quad u_t(\underline{x};0) = a' \cos \underline{k} \cdot \underline{x} + b' \sin \underline{k} \cdot \underline{x}$$

are satisfied in R^m by the linear combination

$$(1.5) \quad u(\underline{x};t) = [a \cos \underline{k} \cdot \underline{x} + b \sin \underline{k} \cdot \underline{x}] \cos ckt \\ + \left[\frac{a'}{ck} \cos \underline{k} \cdot \underline{x} + \frac{b'}{ck} \sin \underline{k} \cdot \underline{x} \right] \sin ckt$$

of the four real solutions listed in (1.3). This suggests that the general free space (or 'pure') initial value problem specified by the DE (1.1) and initial conditions of the form

$$(1.6) \quad u(\underline{x};0) = \int [a(\underline{k}) \cos \underline{k} \cdot \underline{x} + b(\underline{k}) \sin \underline{k} \cdot \underline{x}] dK$$

and

$$(1.6') \quad u_t(\underline{x};0) = \int [a'(\underline{k}) \cos \underline{k} \cdot \underline{x} + b'(\underline{k}) \sin \underline{k} \cdot \underline{x}] dK,$$

where $dK = dk_1 dk_2 \cdots dk_m$ has the solution

$$(1.7) \quad u(\underline{x};t) = \int \left\{ [a(\underline{k}) \cos \underline{k} \cdot \underline{x} + b(\underline{k}) \sin \underline{k} \cdot \underline{x}] \cos \omega t \right. \\ \left. + \left[\frac{a'(\underline{k})}{ck} \cos \underline{k} \cdot \underline{x} + \frac{b'(\underline{k})}{ck} \sin \underline{k} \cdot \underline{x} \right] \sin \omega t \right\} dK,$$

where $dK = dk_1 dk_2 \cdots dk_m$.

Plancherel's Theorem. Many existence theorems for the initial value problem in free space can be based on the preceding formulas.

Underlying them is Plancherel's Theorem, which establishes an isometric isomorphism between the space of square integrable functions $u(x)$ and the space of square integrable Fourier transforms $c(k)$. For algebraic simplicity, we will only write down the formulas for the univariate case, and we will write them in complex notation. These formulas

$$(1.8) \quad u(x) = \int_{-\infty}^{\infty} e^{ikx} f(k) dk$$

and

$$(1.8') \quad f(k) = \frac{1}{\pi} \int_{-\infty}^{\infty} e^{ikx} u(x) dx ,$$

define isometric isomorphisms between the complex Hilbert space $L^2(-\infty, \infty)$ of all Lebesgue square-integrable functions $u(x)$ and that of all (Lebesgue) square-integrable Fourier transforms $f(k)$.

The initial value (or 'Cauchy') problem for (1.1) (with $m = 1$) has a simple solution in terms of the resolution (1.8) - (1.8'). Namely, given

$$(1.9) \quad u(x, 0) = \int_{-\infty}^{\infty} e^{ikx} f(k) dk$$

and

$$(1.9') \quad u_t(x, 0) = \int_{-\infty}^{\infty} e^{ikx} g(k) dk ,$$

this solution is

$$(1.10) \quad u(x, t) = \int_{-\infty}^{\infty} e^{ikx} A(k, t) dk$$

where

$$(1.10') \quad A(k, t) = f(k) \cos ckt + [g(k)/ck] \sin ckt .$$

As is explained in Appendix C, these formulas and their generalizations permit one to analyze the accuracy of many difference and finite element schemes for integrating the wave equation (1.1) numerically, in terms of their accuracy for simply

harmonic waves of the form $\exp[i(\underline{k}\cdot\underline{x} \pm ckt)]$, $k = |\underline{k}|$. This analysis is based on a simple general principle: errors having different wave vectors (and hence in components coming from non-overlapping regions of the 'spectrum', propagate independently.² See also Vichnevetsky-Bowles [E14], which presents a similar analysis with many carefully chosen illustrations.

WAVPACK. For $m = 1$ and 2 , most of the algorithms described in this chapter, together with some others on nonlinear one-dimensional waves (see Chapter 6), are being incorporated into a collection of FORTRAN programs called WAVPACK. This includes subprograms for treating initial and boundary conditions (mostly of Dirichlet or Neumann type). This effort supplemented with starting procedures and treatment of boundary conditions (usually for Dirichlet or Neumann data), have been incorporated, together with some others on nonlinear waves, into a collection of FORTRAN programs called WAVPACK. This effort began in 1975 at Harvard University and is now continuing at the University of Tennessee, Knoxville, with the added participation of Professors M.D. Gunzburger, Ohannes Karakashian, and S.M. Serbin. Having started with rectangles and constant coefficients we are now in the process of including programs with more general domains and variable coefficients. When documented, this collection might serve as a pilot model for a package for solving hyperbolic problems at modest cost. We realize that such programs cannot compete with the far more sophisticated programs developed at major laboratories for solving practical problems. However we hope that the simplicity and economy of WAVPACK will make it generally useful as a tool for an introduction to the subject.

2. Boundary conditions. Clearly, the simple and elegant solution of the initial value problem for the wave equation presented in §1 can only be used in an infinite fluid occupying all of space. We will next describe some simple boundary conditions, present in most applications.

² Provided that the difference and finite element approximations are made on a uniform mesh.

Fixed boundaries. On solid or liquid boundaries enclosing a room or other domain Ω full of a gas such as air, the fluid acceleration normal to the boundary $\partial\Omega = \Gamma$ is negligible because of the low density of gases. Hence sound waves in gases satisfy the fixed boundary condition

$$(2.1) \quad \delta p_n \equiv \delta \phi_n \equiv 0 \quad \text{on } \Gamma ,$$

of purely tangential acceleration on the boundary.

Simplest is the one-dimensional case, $m = 1$, in which Ω can be assumed to be an interval $[0, \lambda]$ and (2.1) to reduce to

$$(2.2) \quad \phi_x(0) = \phi_x(\lambda) = 0 .$$

By proper choice of units of length, we can make $\lambda = \pi$, and hence assume that

$$(2.3) \quad \phi(x, 0) = \sum_{k=1}^{\infty} a_k \cos kx ,$$

and

$$(2.3') \quad \phi_t(x, 0) = \sum_{k=1}^{\infty} a'_k \cos kx ,$$

from the theory of Fourier series. The initial-boundary value problem can be solved for the DE (1.1), the boundary conditions (2.2), and the initial conditions (2.3)-(2.3'), by setting

$$(2.4) \quad \phi(x, t) = \sum A(k, t) \cos kx ,$$

where

$$(2.5) \quad A(k, t) = a_k \cos ckt + (b_k/ck) \sin ckt .$$

The preceding separation of variables is analogous to the classical theory of "small oscillations" about stable equilibrium of a Lagrangian dynamical system having a finite number of degrees of freedom (see Appendix A). In "generalized coordinates" q , the energy of such a system is the sum

$$(2.6) \quad \frac{1}{2}[\sum a_{jk} \dot{q}_j \dot{q}_k + \sum b_{jk} \dot{q}_j \dot{q}_k] = \frac{1}{2}[\dot{q}^T A \dot{q} + \dot{q}^T B \dot{q}]$$

of two quadratic forms. The "mass" or "inertial" matrix $B = ||b_{jk}||$ is symmetric and positive definite, while the symmetric "stiffness" matrix $A = ||a_{jk}||$ may only be positive semidefinite. This system's equations of motion are

$$(2.7) \quad B\ddot{q} + Aq = 0 ,$$

while its normal modes are the eigenvectors Q of the generalized eigenvalue problem

$$(2.8) \quad A Q = \omega^2 B Q ,$$

whose eigenvalues ω^2 are all nonnegative. The simply harmonic oscillations are the real and imaginary parts, $Q \cos \omega t$ and $Q \sin \omega t$, of

$$(2.9) \quad q(t) = Q e^{i\omega t} ,$$

Hence the "standing waves" defined by Eqs. (2.4)-(2.5) can be viewed as generalized "normal modes" of oscillation.

3. Dispersion analysis: plane waves. We now illustrate the preceding general remarks about numerical dispersion by considering the simple case $m = 1$ of plane waves.³ To this end, we recall from Chapter 2, §§2-3 and §5, Lagrange's semi-discretization (by "beads on a string") of the one-dimensional wave equation

$$(3.1) \quad u_{tt} = c^2 u_{xx} ,$$

for the initial conditions

$$(3.2) \quad u(x,0) = e^{ikx}, \quad u_t(x,0) = -i\omega e^{ikx}, \quad 0 \leq x \leq 1 ,$$

³For a general discussion of this phenomenon, see [E16].

To avoid the complications introduced by most boundary conditions, we will choose as our domain Ω either $(-\infty, \infty)$ or the periodic case.⁴

As previously, the initial value problem defined by (3.1)-(3.2) has the obvious exact solutions

$$(3.3) \quad u(x,t) = e^{i(kx \pm \omega t)},$$

provided $\omega = kc$. Here $k = 2\pi/\lambda$, where λ is the wave length. In the spatially periodic case most tractable by computer, the spatial period must be integral multiples $J\lambda$ of the wave length. For mathematical simplicity, we will use λ as the unit of length, thus making $\lambda = 1$.

The case of initial-boundary value problems on a finite interval $[0, a]$, with the boundary conditions $u_x(0) = u_x(a) = 0$ appropriate to sound waves, can easily be reduced to the periodic case by setting (multiple reflections)

$$(*) \quad u(x,t) = u(-x,t) = u(2a-x,t) = u(x+4a,t).$$

For the boundary conditions $u(0) = u(a) = 0$ appropriate to a vibrating string, one sets instead

$$(**) \quad u(x,t) = -u(-x,t) = -u(2a-x,t) = u(x+4a,t).$$

Consider now Lagrange's finite difference semi-discretization of (3.1) by a three-point central space difference on a uniform mesh. I.e., let $x_j = jh$, $0 \leq j \leq J$, $Jh = 1$ be a uniform partition of $[0, 1]$ and $v_j(t)$ be an approximation to $u(x_j, t)$ satisfying the second-order system of ordinary differential equations

$$(3.4) \quad \ddot{v}_j(t) = \frac{c^2}{h^2}(v_{j+1}(t) - 2v_j(t) + v_{j-1}(t)), \quad 1 \leq j \leq J,$$

with the periodic boundary conditions $v_0(t) = v_1(t)$, $v_{J+1}(t) = v_1(t)$.

⁴This corresponds to the 'equatorial canal' mentioned in Chapter 1, §3. Vertical walls at the ends of $[a, b]$, which make $\partial/\partial n = 0$ there give periodic waves with period $2(b-a)$.

Now suppose that the initial conditions $v_j(0)$, $\dot{v}_j(0)$ are exact at the nodes, i.e., let

$$(3.5) \quad v_j(0) = e^{ikjh}, \quad \dot{v}_j(0) = -i\omega e^{ikjh}.$$

By inspection, (3.4) has solutions of the form $v_j = e^{i(kjh - \omega_h t)}$, where by substitution in (3.4), we have

$$(3.6) \quad \omega_h^2 = \frac{4c^2}{h^2} \sin^2 \frac{kh}{2}.$$

Defining now $c_h = \omega_h/k$, the discrete wave speed, and

$$(3.7) \quad \gamma_h = \frac{c_h}{c} = \frac{\omega_h}{\omega},$$

it is seen by (3.6) that γ_h is given by

$$(3.8) \quad \gamma_h = \frac{\sin \sigma}{\sigma} = 1 - \frac{\sigma^2}{6} + O(\sigma^4),$$

where $\sigma = kh/2 = \pi h/\lambda$.

Now, the initial value problem (3.4)-(3.5) may be solved explicitly by assuming solutions of the form $\phi(t)e^{ikjh}$ and determining $\phi(t)$ from the initial data (3.5). It is straightforward to verify that its solution is

$$(3.9) \quad v_j(t) = (\cos \gamma_h \omega t - \frac{i}{\gamma_h} \sin \gamma_h \omega t) e^{ikjh},$$

with γ_h given by (3.7).

Consider next the relative error at the node x_j at time t of the semi-discretization (3.4)-(3.5), defined by $\varepsilon = \varepsilon_j(t) = (u(x_j, t) - v_j(t))/u(x_j, t)$, where $u(x, t)$, the solution of (3.1)-(3.2), is given by (3.3). The relative error is independent of j and is given by

$$(3.10) \quad \varepsilon = 1 - e^{i\omega t} (\cos \gamma_h \omega t - \frac{i}{\gamma_h} \sin \gamma_h \omega t).$$

Letting now $Q = \omega t$, (where $Q/2\pi$ is the number of time periods computed up to time t), it is seen by (3.10) that, for $(\gamma_h - 1)Q$ small,

$$(3.11) \quad \left| \frac{\epsilon}{Q} \right| \cong |\gamma_h - 1| \left| 1 - \frac{\sin Q}{Q} e^{iQ} \right| .$$

Note that the second factor in the right-hand side of the above is bounded for all $t \geq 0$ and tends to 1 as $t \rightarrow \infty$. Hence, the significance of keeping the dispersion $|\gamma_h - 1|$ small is evident from (3.11), since it is reasonable to require that an accurate approximation to (3.1) have for each $t > 0$ a small relative error per node per time step, computed up to time t .

As remarked above, the periodic initial value problem treated above can be treated by computer. In this case, A and B are cyclic (circulant) symmetric matrices with B positive definite and A positive semidefinite. Setting $v_0(t) = v_j(t)$ and $v_{j+1}(t) = v_1(t)$, the problem is easily handled using WAVPACK.

Full discretization. Much as was done by Courant-Friedrichs-Lewy, one can further discretize (3.4) in time as well as space, setting $\Delta t = r\Delta x/c$. Substituting the trial solution $e^{i(kjh - \omega_h n \Delta t)}$ into the fully discrete schemes gives formulas for ω_h and γ_h (as functions of Δt too) analogous to (3.6), (3.7). By solving an initial value problem for a system of difference equations (analog of (3.4)-(3.5)), the relative error may be computed again at time $t = n\Delta t$, and its dependence on $|\gamma_h - 1|$ exhibited. For example, in the case of the standard 5 point-approximation to (3.1) discussed in Chapter 3, §§2-3,

$$(3.12) \quad v_j^{n+1} - 2v_j^n + v_j^{n-1} = r^2 (v_{j+1}^n - 2v_j^n + v_{j-1}^n) ,$$

with exact initial conditions and with $r = c\Delta t/h \leq 1$, it can be shown that (3.11) is replaced (at $t = n\Delta t$, $n > 0$) by

$$(3.13) \quad \left| \frac{\epsilon}{Q} \right| \cong |\gamma_h - 1| \left| 1 - O\left(\frac{1}{n}\right) \right| .$$

In the next section, we will consider in detail (3.12) and other full discretizations of (3.1).

4. Second-order accuracy: plane waves. We consider next simple finite difference approximations of the (pure) initial-value problem for $u_{tt} = c^2 u_{xx}$ on a uniform rectangular mesh in space and time with mesh lengths $\Delta x = h$ and Δt , respectively. Denoting first by $u_j(t)$ the semi-discrete approximation to $u(jh, t)$, already discussed in the previous section, we have as before the Lagrange semi-discretization, equivalent to the molecular model discussed in Chapter 2,

$$(4.1) \quad \ddot{u}_j(t) = \frac{c^2}{h^2} \delta_x^2 u_j(t) ,$$

where $\delta_x^2 u_j = u_{j+1} - 2u_j + u_{j-1}$.

Approximating d^2/dt^2 in (4.1) by a 3-point central difference quotient, we again obtain the 5-point explicit scheme

$$(4.2) \quad u_j^{n+1} = r^2(u_{j-1}^n + u_{j+1}^n) + (2-2r^2)u_j^n - u_j^{n-1} ,$$

where $r = c\Delta t/h$. This scheme, whose stability we analyzed in Lecture 1', §2, has a local discretization error of $O(\Delta t^2 + h^2)$. If $r \leq 1$, and the initial approximations u_j^0, u_j^1 are taken to be $f(jh, 0)$ and⁵

$$(4.2') \quad u_j^1 = f(jh) + \Delta t g(jh) + r^2 \delta_x^2 u_j^0 ,$$

respectively, and if $f, g \in C^2(-\infty, \infty)$, then the global discretization error is also $O(\Delta t^2 + h^2)$.

In the case of an initial-boundary value problem with given Dirichlet-type endpoint conditions $u(0, t) = \alpha(t)$, $u(1, t) = \beta(t)$, the same is also true for $f, g \in C^2[0, 1]$, provided that the compatibility conditions $\alpha(0) = f(0)$, $\alpha'(0) = g(0)$, $\beta(0) = f(1)$, and $\beta'(0) = g(1)$ are satisfied.

⁵Formula (4.2') can be derived by expanding $u(x, t)$ in a Taylor series and using the identity $u_{tt} = c^2 u_{xx}$.

For $r = 1$ (4.2) reduces to

$$(4.3) \quad u_j^{n+1} = u_{j+1}^n + u_{j-1}^n - u_j^{n-1}.$$

It is easy to see that if u_j^0, u_j^1 are exact, then (4.3) will provide, for $n \geq 1$ the exact values of the solution of the initial-value problem for $u_{tt} = c^2 u_{xx}$ at the nodes (x_j, t^n) . This follows from the fact that for $r = 1$ both the solution and the fully discrete approximation admit the d'Alembert decomposition--the latter at mesh points-- $u(x_j, t^n) = \phi(x_j + ct^n) + \psi(x_j - ct^n)$.

However, this "exact" simulation property of (4.3) does not generalize in the presence of approximate initial and boundary conditions, variable coefficients or, more importantly, to higher dimensions. Hence, one is justified in investigating other schemes. For example, Richtmyer and Morton [26, Chapter 10] in addition to (4.2) study a 9-point implicit full discretization of (4.1), [26, (10.7), p. 263]. Both schemes are special cases of a general implicit method suggested by von Neumann [64, p. 231, (10)]:

$$(4.4) \quad \delta_t^2 u_j^n = r^2 [\alpha \delta_x^2 u_j^{n+1} + (1-2\alpha) \delta_x^2 u_j^n + \alpha \delta_x^2 u_j^{n-1}], \quad \alpha \geq 0.$$

The scheme has again a discretization error of $O(\Delta t^2 + h^2)$. For $\alpha = 0$ it reduces to (4.2) and the case $\alpha = 1/4$ is considered by Richtmyer and Morton. For $\alpha = 1/12$ we obtain the Størmer-Numerov method of $O(\Delta t^4 + h^2)$ accuracy. It is straightforward to verify that for $\alpha \geq 1/4$ the scheme is unconditionally stable, but for $\alpha < 1/4$ the stability condition on r is $r \leq 1/\sqrt{1-4\alpha}$. The solution of (4.4) for the values of the vector u^{n+1} (given $u(0,t)$ and $u(1,t)$) requires the decomposition of a tridiagonal matrix (once) and for each n , the formation of the right-hand side and two backsolves. The operation count is 7 multiplications and 8 additions per mesh point (x_j, t^{n+1}) . Of course, larger time steps are permitted by the less stringent (or non-existent) stability restrictions on r .

We determine the numerical dispersion of the schemes (4.1), (4.2), (4.4). As in §3, substituting the trial solution

$u_j = e^{i(kjh - \omega_h t)}$ into (4.1) gives, with $c_h = \omega_h/k$, $\sigma = \pi h/\lambda$, $\gamma_h = c_h/c$, much as in §3,

$$(4.5) \quad \gamma_h = \sin \sigma / \sigma = 1 - \frac{\sigma^2}{6} + \frac{\sigma^4}{120} + O(\sigma^6).$$

For the explicit fully discrete scheme (4.2), substituting the solution $u_j^n = e^{i(kjh - \omega_h n \Delta t)}$ in (4.2) gives the numerical dispersion relation

$$(4.6) \quad \sin(r\sigma\gamma_h) = r \sin \alpha.$$

In series form, (4.6) gives

$$(4.6') \quad \gamma_h = 1 - \frac{\sigma^2}{6}(1 - r^2) + O(\sigma^4).$$

The analogous equation for the implicit scheme (4.4) is

$$(4.7) \quad \sin(r\sigma\gamma_h) = r \sin \sigma (1 + 4\alpha r^2 \sin^2 \sigma)^{-1/2},$$

giving the series

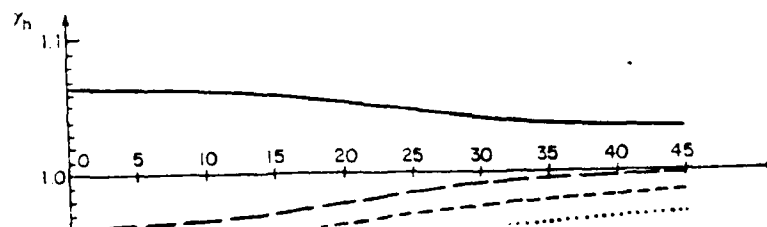
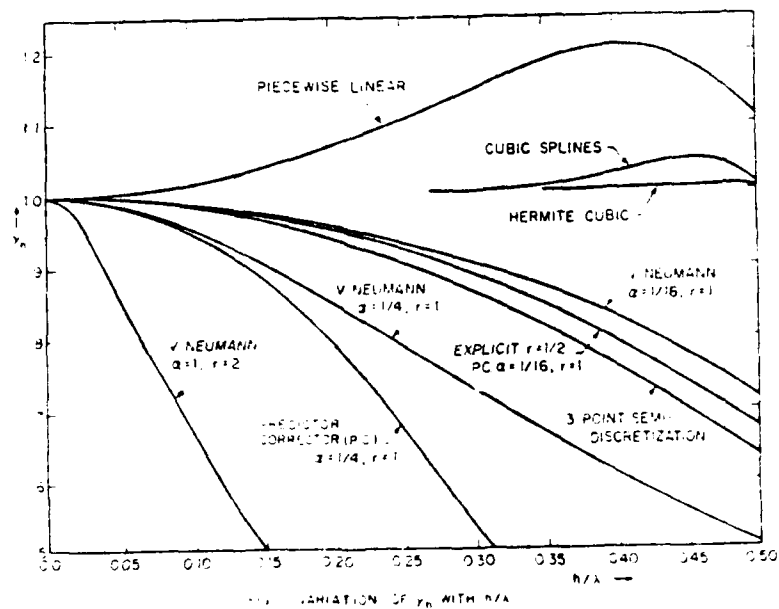
$$(4.7') \quad \gamma_h = 1 - \frac{\sigma^2}{6}[1 + r^2(12\alpha - 1)] + O(\sigma^4).$$

From (4.6'), (4.7') we conclude that the explicit scheme (4.2), even when $r \neq 1$, has always the least numerical dispersion $|1 - \gamma_h|$ among the one-parameter family of schemes given by (4.4). Table 3.1 shows the variation of γ_h with h/λ as computed from formula (4.7) for $\alpha = 0, 1/4$ and for $r = 0.5, 0.7$. We see that the explicit scheme ($\alpha = 0$) gives better results. Figure 3.1 also makes this point quite clear.

Finally, Table 3.2 shows the numerical results for a test problem given $u(0,t)$ and $u(1,t)$ with exact solution $u(x,t) = \cos \pi(x+t) + \sin \pi(x+t)$, $0 \leq x \leq 1$, $0 \leq t \leq 10$. The solution is approximated by three schemes ($\alpha = 0, 1/12, 1/4$) with exact starting conditions.

Table 3.1

Scheme h/λ	$r = 0.5$		$r = 0.7$	
	$\alpha = 0$	$\alpha = 1/4$	$\alpha = 0$	$\alpha = 1/4$
0.5	.6667	.5903	.7052	.5554
0.2	.9495	.9099	.9641	.8875
0.1	.9876	.9759	.9915	.9687
0.05	.9969	.9939	.9979	.9919
0.02	.9995	.9990	.9997	.9987
0.01	.9999	.9997	.9999	.9997



The column e denotes the maximum error at $t = 10$ and the column T the computing time (in seconds, double precision, FORTRAN H compiler of the Harvard-MIT IBM 370/168).

Table 3.2

h	Δt	$\alpha = 0$		$\alpha = 1/12$		$\alpha = 1/4$	
		e	T	e	T	e	T
.1	.2	unstable	-	unstable	-	3.95-1	.04
.1	.1	exact	.04	1.20-1	.07	3.06-1	.06
.1	.05	9.25-2	.07	1.20-1	.12	1.74-1	.12
.05	.1	unstable	-	unstable	-	2.45-1	.09
.05	.05	exact	.09	3.17-2	.15	9.20-2	.16
.05	.025	2.40-2	.16	3.17-2	.31	4.72-2	.29

5. Second-order accuracy: cylindrical waves. We now take up the two-dimensional analogs for equation (1.1) of the difference schemes discussed in the previous section. On a uniform square space mesh with mesh length h , denoting by $u_{j\ell}(t)$ the (semi-discrete) approximation to $u(jh, \ell h, t)$ we obtain the following semi-discretization, analogous to (4.1)

$$(5.1) \quad \ddot{u}_{j\ell}(t) = \frac{c^2}{h^2} \Delta u_{j\ell}(t) ,$$

where

$$(5.1') \quad \Delta u_{j\ell} \equiv u_{j+1,\ell} + u_{j,\ell+1} + u_{j-1,\ell} + u_{j,\ell-1} - 4u_{j\ell} .$$

This system of ordinary DE's expresses the equations of motion of a square array of molecules of mass m , supported by a network of strings under uniform tension T . Here $c^2 = T/\rho$, as for a vibrating string, where $\rho = m/h^2$ is the mean density per unit area. Thus $c^2 = h^2 T/m$.

Likewise, the analog of (4.2) is the 7-point fully discrete explicit scheme

$$(5.2) \quad \delta_t^2 u_{j\ell}^n = r^2 \Delta u_{j\ell}^n .$$

This scheme is stable if $r \leq 1/\sqrt{2}$. It has a discretization error of $O(h^2 + \Delta t^2)$ provided that the stability condition is satisfied, and the initial data $\underline{u}^0, \underline{u}^1$ are sufficiently accurate.

Initial data. The accurate determination of $u(\underline{x}, \Delta t)$ from given $u(\underline{x}, 0) = f(\underline{x})$ and $u_t(\underline{x}, 0) = g(\underline{x})$ is nontrivial in general. In this special case $g(\underline{x}) \equiv 0$ of release from rest, one can use symmetry: $u(\underline{x}, -t) = u(\underline{x}, t)$. Therefore, in one dimension, if we use the exact 4-point formula, (4.2) with $r = 1$,

$$u_j^1 = u_j^{-1} = \frac{1}{2}[u_{j+1}^0 + u_{j-1}^0] .$$

The opposite case $f(\underline{x}) \equiv 0$ is more difficult; only $(u_t)_j^n$ can be computed exactly from $(u_t)_j^0$ and the DE.

To treat the general case (in 1D), with arbitrary accuracy, one can use d'Alembert's decomposition to derive an exact analytical formula for computing $u(\underline{x}, \Delta t)$,⁶ with arbitrary accuracy. In two-dimensional sound wave propagation theory, if $u(x, y, 0) = f(x, y)$, $u_t(x, y, 0) = g(x, y)$ we may take, if f, g are sufficiently smooth, $u_{j\ell}^0 = f_{j\ell}$, $u_{j\ell}^1 = f_{j\ell} + \Delta t g_{j\ell} + \frac{r^2}{2} \Delta^2 f_{j\ell}$. For Dirichlet boundary conditions on a rectangle, say, (5.2) is straightforward to use and requires 2 multiplications per meshpoint.

The analog of the one-dimensional von Neumann scheme (4.4) is the 15-point implicit scheme

$$(5.3) \quad \delta_t^2 u_{j\ell}^n = r^2 [\alpha \delta_x^2 u_{j\ell}^{n+1} + (1-2\alpha) \delta_x^2 u_{j\ell}^n + \alpha \delta_x^2 u_{j\ell}^{n-1}], \quad \alpha \geq 0 .$$

This also has formal accuracy $O(\Delta t^2 + h^2)$ (and reduces to (5.2) for $\alpha = 0$). It is straightforward to verify that for $\alpha \geq 1/4$ (5.3) is unconditionally stable, the restriction on r for $\alpha < 1/4$ being $r \leq [2(1-4\alpha)]^{-1/2}$. For $\alpha > 0$, instead of solving the banded linear system (5.3) for the $u_{j\ell}^{n+1}$, one can implement this scheme in a predictor-corrector form, as follows:

⁶H. Weinberger, "Partial Differential Equations", Chapter 1.

$$(5.4) \quad \text{Predictor: } \tilde{u}_{j\ell}^{n+1} = 2u_{j\ell}^n - u_{j\ell}^{n-1} + r^2 \Delta u_{j\ell}^n,$$

$$(5.4') \quad \text{Corrector: } \delta_t^2 u_{j\ell}^{n+1} = r^2 [\alpha \Delta \tilde{u}_{j\ell}^{n+1} + (1-2\alpha) \Delta u_{j\ell}^n + \alpha \Delta u_{j\ell}^{n-1}].$$

This predicts by the explicit scheme (5.2) and corrects using the implicit scheme (5.3). Moreover, (5.4)-(5.4') can be combined into the single equation

$$(5.5) \quad \delta_t^2 u_{j\ell}^n = r^2 [\Delta u_{j\ell}^n + \alpha r^2 \Delta (\Delta u_{j\ell}^n)].$$

This predictor-corrector scheme is still accurate of $O(\Delta t^2 + h^2)$; however, the unconditional stability of (5.3) is lost. It can be shown that, for $\alpha \geq 1/16$, (5.4)-(5.4') is stable if $r \leq 1/\sqrt{8\alpha}$. The operation count for (5.4)-(5.4') is 8 multiplications per meshpoint per time step.

To find the numerical dispersion for the semidiscretization (5.1) we substitute the trial function $u_{j\ell} = e^{i(pjh+q\ell h-\omega ht)}$ into (5.1) and, recalling from §2 the notation $k = \sqrt{p^2 + q^2} = 2\pi/\lambda$, $p = k \cos \theta$, $q = k \sin \theta$, $\sigma = \pi h/\lambda$, $\gamma_h = c_h/c = \omega_h/\omega$, we obtain

$$(5.6) \quad \gamma_h = [\sin^2(\alpha \cos \theta) + \sin^2(\alpha \sin \theta)]^{1/2}/\sigma \equiv \sqrt{A(\sigma, \theta)}/\sigma,$$

or, in series form,

$$(5.6') \quad \gamma_h = 1 - \frac{1}{6} \sigma^2 (\cos^4 \theta + \sin^4 \theta) + O(\sigma^4).$$

Note that the two-dimensional case reduces to the one-dimensional (4.5) for $\theta = 0$. Also the phenomenon of numerical anisotropy, already discussed in §2, (i.e., different numerical dispersion along different directions θ) is evident from (5.6).

The corresponding relations for the explicit scheme (5.2), obtained by substituting $u_{j\ell}^n = e^{i(pjh+q\ell h-\omega h n \Delta t)}$ in (5.2), become (with $A = A(\sigma, \theta)$ defined by (5.6))

$$(5.7) \quad \sin(r\sigma\gamma_h) = r\sqrt{A},$$

$$(5.7') \quad \gamma_h = 1 - \frac{\sigma^2}{6}(\cos^4 \theta + \sin^4 \theta - r^2) + O(\sigma^4) .$$

For the implicit model (5.3) we obtain

$$(5.8) \quad \sin(r\sigma\gamma_h) = r[A/(1 + 4\alpha A)]^{1/2} ,$$

$$(5.8') \quad \gamma_h = 1 - \frac{\sigma^2}{6}[\cos^4 \theta + \sin^4 \theta + r^2(12\alpha - 1)] + O(\sigma^4) .$$

Finally, the predictor-corrector scheme (5.4)-(5.4') has numerical dispersion given by the formula

$$(5.9) \quad \sin(r\sigma\gamma_h) = r[A(1 - 4\alpha A)]^{1/2} ,$$

where γ_h is given in series form by an expression agreeing with (5.8').

Table 3.3 (cf. also Fig. 3.2) shows the variation of γ_h as a function of h/λ and θ for $r = .5$ and $r = .7$ for the explicit scheme (5.2) and the implicit scheme corresponding to $\alpha = 1/4$ in (5.3). Clearly the explicit scheme is more accurate.

The results are confirmed by numerous test problems. For example, considering Dirichlet boundary conditions on the unit square for an exact solution given by $u(x,y,t) = \sin \pi(x+y+\sqrt{2}t)$, $0 \leq x, y \leq 1$, $0 \leq t \leq 5$ and computing with the explicit scheme ($\alpha = 0$) and the predictor-corrector scheme (5.4)-(5.4') with $\alpha = 1/16$ we obtain the results of Table 3.4 (e is the maximum error at $t = 5$, T is the computing time in seconds).

We see that the doubling the time step that the use of the predictor-corrector scheme permits does not result in any cost savings. Moreover the errors, as expected, are a bit larger.

We finally briefly discuss the application of alternating direction methods for the solution of (1.1) in two space dimensions. Lees, [61], noticed that the von Neumann scheme (5.3) can be perturbed (preserving second-order accuracy) to

r = 0.7

h/λ	0.5		0.2		0.1		0.05		0.02		0.01		
Scheme θ deg	ExpI	ImoI											
0	.7052	.5554	.9641	.8875	.9915	.9697	.9979	.9919	.9997	.9986	.9999	.9997	
5	.7135	.5594	.9652	.8883	.9917	.9689	.9980	.9920	.9997	.9987	↓	.9997	
10	.7373	.5704	.9683	.8907	.9924	.9696	.9981	.9922	.9997	.9987		.9997	
15	.7377	.5863	.9730	.8944	.9936	.9707	.9984	.9924	.9997	.9988		.9997	
20	.8188	.6045	.9788	.8989	.9949	.9719	.9987	.9928	.9998	.9988		.9997	
25	.8677	.6223	.9849	.9036	.9964	.9733	.9991	.9931	.9998	.9989		↓	
30	.9150	.6379	.9906	.9080	.9977	.9746	.9994	.9935	.9999	.9989			
35	.9551	.6499	.9952	.9115	.9989	.9756	.9997	.9937	.9999	.9989		↓	
40	.9824	.6574	.9982	.9139	.9996	.9763	.9999	.9939	.9999	.9990			.9998
45	.9921	.5990	.9993	.9147	.9998	.9765	.9999	.9940	.9999	.9990			.9998

r = 0.5

h/λ	0.5		0.2		0.1		0.05		0.02		0.01	
Scheme θ deg	E	I	E	I	E	I	E	I	E	I	E	I
0	.6657	.5903	.9495	.9099	.9876	.9759	.9969	.9939	.9995	.9990	.9999	.9978
5	.6735	.5950	.9505	.9108	.9878	.9762	.9970	.9949	.9995	.9990	↓	↓
10	.6928	.6082	.9535	.9134	.9886	.9768	.9972	.9941	.9995	.9991		
15	.7218	.6275	.9580	.9173	.9897	.9779	.9974	.9944	.9996	.9991		
20	.7563	.6477	.9635	.9221	.9910	.9792	.9978	.9947	.9996	.9991		
25	.7920	.6718	.9693	.9272	.9924	.9806	.9981	.9951	.9997	.9992		
30	.8247	.6913	.9747	.9320	.9940	.9819	.9985	.9954	.9998	.9993		
35	.8509	.7063	.9791	.9358	.9949	.9830	.9987	.9957	.9998	.9993		
40	.8678	.7158	.9820	.9383	.9956	.9836	.9989	.9958	.9998	.9993		
45	.8737	.7191	.9830	.9392	.9958	.9839	.9990	.9959	.9998	.9993		

Table 3.3

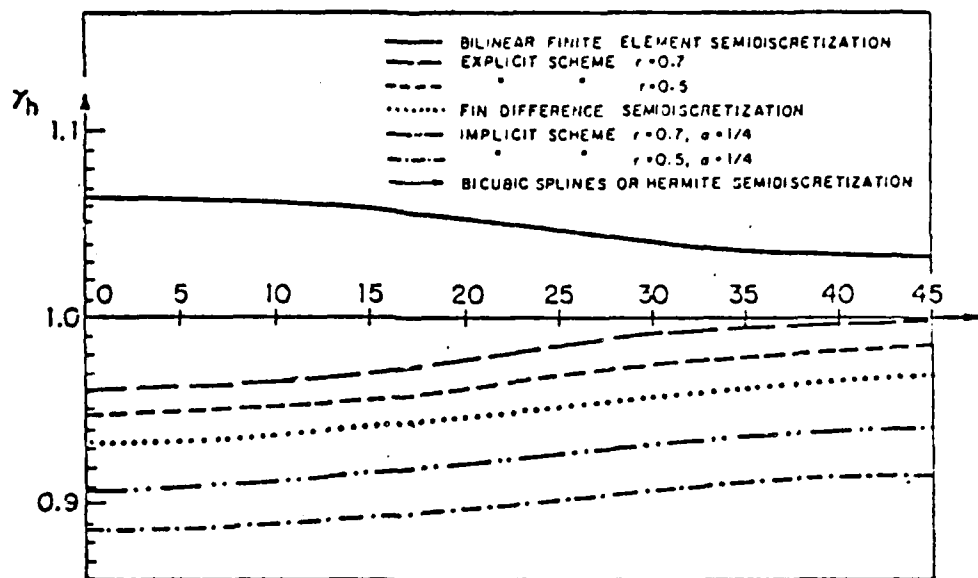


FIG. 2 VARIATION OF γ_h WITH θ FOR $n/\lambda = 0.2$

Scheme	h	r	e	T
$\alpha = 0$.1	.7	1.78-3	.30
	.05	.7	4.42-4	1.30
P.C. $\alpha = 1/16$.1	1.4	3.64-3	.33
	.05	1.4	5.58-4	1.56

Table 3.4

$$(5.10) \quad \delta_t^2 u_{jl}^n = r^2 \alpha [u_{jl}^{n+1} + (1-2\alpha)u_{jl}^n + \alpha u_{jl}^{n-1}] - r^4 \alpha^2 \delta_x^2 \delta_y^2 (\delta_t^2 u_{jl}^n) .$$

The advantage of (5.10) is that it is equivalent to a two-step scheme, each step of which requires the solution of one tridiagonal system of difference equations in the x-, resp. y-, direction; following the implementation of Fairweather and Mitchell [57] we may rewrite (5.10) as

$$(5.11) \quad \tilde{u}_{jl}^{n+1} - 2u_{jl}^n + u_{jl}^{n-1} = r^2 \delta_x^2 [\alpha \tilde{u}_{jl}^{n+1} + (1-2\alpha)u_{jl}^n + \alpha u_{jl}^{n-1}] + r^2 \delta_y^2 u_{jl}^n ,$$

$$(5.11') \quad u_{jl}^{n+1} = \tilde{u}_{jl}^{n+1} + \alpha r^2 \delta_y^2 (u_{jl}^{n+1} - 2u_{jl}^n + u_{jl}^{n-1}) .$$

Lees, [61] shows that the perturbed von Neumann scheme (5.10) is also unconditionally stable if $\alpha > 1/4$. It can be easily checked that the dispersion of (5.10), up to $O(\sigma^2)$ terms, is given by the series (5.8'). In addition to (5.10) Lees also analyzes another perturbation of (5.3) that factors in ADI form.⁷ Somewhat more generally we remark, following [57] that any scheme of the form

$$(5.12) \quad \delta_t^2 u_{jl}^n + \alpha (a u_{jl}^{n+1} + b u_{jl}^n + c u_{jl}^{n-1}) + \delta_x^2 \delta_y^2 (d u_{jl}^{n+1} + e u_{jl}^n + f u_{jl}^{n-1}) = 0 ,$$

may be factored in the equivalent two-tridiagonal system form

$$(5.13) \quad \begin{aligned} \tilde{u}_{jl}^{n+1} - 2u_{jl}^n + u_{jl}^{n-1} + \delta_x^2 (a \tilde{u}_{jl}^{n+1} + b u_{jl}^n + c u_{jl}^{n-1}) \\ + \delta_y^2 [(b - \frac{e}{a}) u_{jl}^n + (c - \frac{f}{a}) u_{jl}^{n-1}] = 0 , \end{aligned}$$

$$(5.13') \quad u_{jl}^{n+1} = \tilde{u}_{jl}^{n+1} - \delta_y^2 [a u_{jl}^{n+1} + \frac{e}{a} u_{jl}^n + \frac{f}{a} u_{jl}^{n-1}] ,$$

provided $d = a^2$.

⁷ADI is an abbreviation for "alternating direction implicit"-- a procedure which solves for the (tridiagonal) horizontal and vertical components of ∇_h^2 on successive 'half-iterations'.

REFERENCES FOR CHAPTER 5

- [E1] J.H. Bramble (ed.), Numerical Solution of Partial Differential Equations, Academic Press, 1966.
- [E2] M. Ciment and S.H. Leventhal, "Higher order compact implicit schemes for the wave equation", *Math. Comp.* 29 (1975), pp. 985-994.
- [E3] L. Collatz, "Hermitean methods for initial value problems in partial differential equations", pp. 41-61 in J.J. Miller (ed.), Topics in Numerical Analysis, Academic Press, 1973.
- [E4] V.A. Dougalis and G. Birkhoff, "A comparison of numerical methods for solving wave equations", pp. 231-51 of J.W. Schot and N. Salvesen (eds.), Proceedings First International Conference on Numerical Ship Hydrodynamics, N.S.R.D.C., 1975.
- [E5] G. Birkhoff and V.A. Dougalis, "Sound Waves", Report issued in 1980 by the Mathematics Department of the University of Tennessee.
- [E6] G. Fairweather and A.R. Mitchell, "A high accuracy alternating direction method for the wave equation", *J. Inst. Math. Applics.* 1 (1965), pp. 309-316.
- [E7] H.O. Kreiss and J. Oliger, Methods for the Approximate Solution of Time Dependent Problems, GARP Publication No. 10, 1973.
- [E8] P.D. Lax and B.S. Wendroff, "Systems of conservation laws", *Comm. Pure Appl. Math.* 13 (1960), pp. 217-237.
- [E9] P.D. Lax and B.S. Wendroff, "Difference schemes for hyperbolic equations with high order of accuracy", *Comm. Pure Appl. Math.* 17 (1964), pp. 381-398.
- [E10] M. Lees, "Alternating direction methods for hyperbolic differential equations", *J. SIAM* 10 (1962), pp. 610-616.
- [E11] Warren P. Mason, Physical Acoustics: Principles and Methods, many volumes, Academic Press, 1964-
- [E12] P.M. Morse and K.U. Ingard, Theoretical Acoustics, McGraw-Hill, 1968.
- [E13] G.G. O'Brien, M.A. Hyman, and S. Kaplan, "A study of the numerical solution of partial differential equations", *J. Math. and Phys.* 29 (1951), 223-51.

- [E14] E.G. Richardson (ed.), Technical Aspects of Sound, 3 vols., Elsevier, 1953-1962.
- [E15] B. Swartz and B.S. Wendroff, "The relative efficiency of finite difference and finite element methods I. Hyperbolic problems and aplines", SIAM J. Num. Anal. 11 (1974), pp. 979-993.
- [E16] Robert Vichnevetsky and John B. Bowles, Fourier Analysis of Numerical Approximations of Hyperbolic Equations, SIAM Publications, 1982.

6. NONLINEAR ONE-DIMENSIONAL WAVES¹

1. Introduction. Wave propagation has fascinated mathematicians for a very long time. An outstanding and comprehensive general reference is the recent book by Whitham [D23]. Here one will find well-motivated and authoritative explanations of the phenomena of shock formation, diffusion and dispersion. To give more structure to an exceedingly broad subject, Whitham distinguishes two main classes of waves: hyperbolic waves, whose theory is "formulated mathematically in terms of partial differential equations", and dispersive waves, which "cannot be characterized as easily", but are usually thought of as waves whose velocity (or "celerity") c depends on the wave length λ .

In this chapter, we will consider only waves in one space dimension; even for these the nonlinearity of the convection term uu_x leads to formidable difficulties, which we will try to elucidate. We will first take up "plane waves of finite amplitude" in a gas, a subject whose analytical theory was well developed by 1910. A scholarly review of what was known then may be found in Lamb [A6, Arts. 281-4]. For later developments, see Courant-Friedrichs [B3].

Our main concern will be with the computer simulation of nonlinear waves, a subject that has been treated previously in the well-known book by Richtmyer and Morton [C9, Chapter 12], and in the valuable compendium by Roache [C13]. We will extract from these and other references the results which are most relevant to the computer simulation of one-dimensional nonlinear wave propagation, describe and analyze theoretically some effective algorithms for achieving this simulation, and summarize our experience with these algorithms. Our discussion will differ from the expositions in [C9] and [C13] in its emphasis on analytical and philosophical considerations. It will also attempt to provide an up-to-date and reasonably complete survey of recent progress on the topics treated.

¹Chapter 6 is a revision of the first half of a report by V.A. Dougalis and the author, issued by the University of Tennessee in January, 1980.

The mathematical theory of plane waves of finite amplitude is based on three first-order partial differential equations. The first two:

$$(1.1) \quad \rho_t + (\rho u)_x = 0 \quad (\text{continuity})$$

and

$$(1.2) \quad (\rho u)_t + (\rho u^2 + p)_x = 0, \quad (\text{motion})$$

are due to Euler; they can be interpreted as expressing conservation laws for mass and momentum. The third, which replaces the Newton-Euler-Laplace 'equation of state' $p = k\theta^\gamma$ for a gas, is

$$(1.3) \quad E_t + [(E+p)u]_x = 0.$$

Here $E/\rho = e(p,T) + \frac{1}{2}u^2$ is the specific energy per unit mass of the fluid, e being its thermal 'internal' energy (see §2) and $u^2/2$ its (mechanical) kinetic energy. Hence (1.3) expresses the conservation of energy, in a way which would not have been meaningful before Joule determined the 'mechanical equivalent of heat' around 1850.

In §2, we will review some mathematical properties of the system (1.1)-(1.3), including the notions of characteristic, simple wave, shock wave, and the Rankine-Hugoniot equations; see Chapter 2, §§5-6, for an informal and intuitive introduction to the same concepts. Next, in §3, turning to the Lagrangian formulation of these equations (Chapter 3, §7), we will discuss the von Neumann-Richtmyer scheme for solving them numerically.

We will then study the mathematical significance of the fact that the quasilinear hyperbolic system of first-order partial DE's can be written in conservation law form, as

$$(1.4) \quad \frac{\partial v_i}{\partial t} + [f_i(\underline{v})]_x = 0, \quad i = 1, 2, 3,$$

for some vector $\underline{v} = (v_1, v_2, v_3)^T$.

AD-A135 900

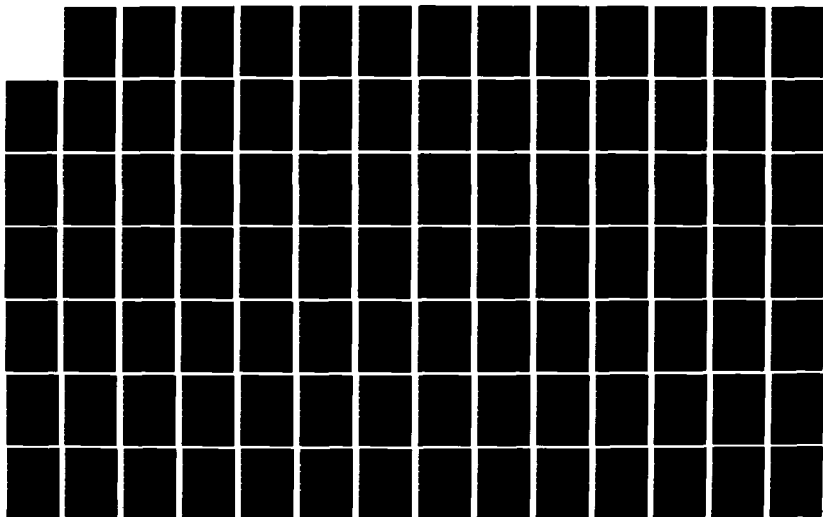
NNMERICAL FLUID DYNAMICS(U) HARVARD UNIV CAMBRIDGE MA
G BIRKHOFF 1983 N00014-75-C-0596

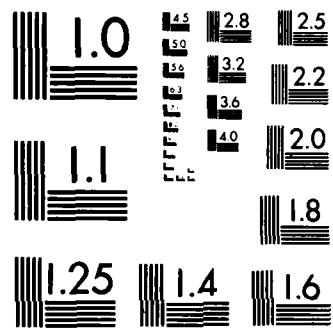
3/4

UNCLASSIFIED

F/G 20/4

NL





MICROCOPY RESOLUTION TEST CHART
NATIONAL BUREAU OF STANDARDS-1963-A

As a simple model of such conservation laws we will also consider the single equation

$$(1.5) \quad u_t + [f(u)]_x = 0 ,$$

which illustrates many features and mathematical problems associated with the system (1.4). Our discussion of 'plane waves of finite amplitude' will be concluded, in §§5-8, with a review of some recent numerical methods for the solution of these systems and an analysis of some relevant numerical experiments.

The rest of this chapter is concerned with solving the Burgers-Korteweg-de Vries equation

$$(1.6) \quad u_t + uu_x = \nu u_{xx} + \alpha u_{xxx} , \quad \nu, \alpha \text{ constants, } \nu > 0 .$$

This illustrates the interaction of convection (uu_x) with diffusion (νu_{xx}) and dispersion (αu_{xxx}). We shall consider the two interactions separately. For a unified point of view cf. [F17, Chapter 4].

In §§9-10, we consider the Burgers equation,

$$(1.7) \quad u_t + uu_x = \nu u_{xx} , \quad \nu > 0 ,$$

which simulates some properties of viscous compressible flow. We briefly review its existence and uniqueness theory, and summarize our experience with some schemes for its numerical solution.

In §§11-12 we consider the Korteweg-de Bries equation. Originally proposed [F12] as an approximation to long unidirectional gravity waves, (cf. [F27]), the DE is

$$(1.8) \quad u_t + uu_x + u_{xxx} = 0 ,$$

it has since arisen in many other contexts. We shall consider some of its variants, as well as their theory and methods for their numerical solution.

2. Isentropic flows. We have already touched on some of the most important aspects of the theory of 'plane waves of finite amplitude' in Chapter 2, §§6-7 (where we discussed physical and analytical aspects), and in Chapter 3, §7 (where we discussed numerical methods). We will now consider such waves more systematically.²

The basic equations for such waves, in a compressible, inviscid fluid are (1.1)-(1.3). These express the conservation of mass, linear momentum and energy, respectively; ρ is the density, u the velocity and p the pressure of the fluid. E denotes the total energy per unit volume, given by $E = \rho e + \rho u^2/2$; where e is the internal energy per unit mass:

$$(2.1) \quad e = e(p, T)$$

This supplements the equation of state of a perfect gas

$$(2.1a) \quad pV = RT, \quad V = 1/\rho.$$

In a perfect gas, Eq. (2.1) also simplifies to

$$(2.1b) \quad e = C_V T.$$

From (1.3) and (2.1a)-(2.1b), one can derive the internal energy formula for a polytropic gas (perfect gas with constant specific heats):

$$(2.2) \quad e = p/\rho(\gamma-1),$$

where $\gamma = c_p/c_v$ is a constant greater than 1. Air under normal conditions is approximately polytropic with $\gamma = 1.4$.

Isentropic flows. In classical thermodynamics,³ the entropy S is defined by the equation $dS = (de + pdV)/T$, where T is

²For a more detailed discussion, from which we have drawn freely, see a 1980 University of Tennessee Report on "One-dimensional nonlinear waves", by V.A. Dougalis and the author.

³The kinetic theory of gases (see Appendix E) can be viewed as an attempt to derive thermodynamic laws from a mechanistic model.

the absolute temperature. Then, eliminating e , we can replace (1.1)-(1.3), (2.1) by the equivalent system

$$(2.3) \quad \begin{aligned} \rho_t + (\rho u)_x &= 0, & (\rho u)_t + (\rho u^2 + p)_x &= 0, \\ S_t + uS_x &= 0, & p &= p(\rho, S). \end{aligned}$$

For polytropic gases, the last equation becomes $S = C_V \log(p/\rho^\gamma)$. Also, the third equation of (2.3) implies that S is constant on each particle path in the x,t -plane, i.e., that

$$(2.4) \quad \frac{dS}{dt} = 0 \quad \text{when} \quad \frac{dx}{dt} = u.$$

If the fluid is initially at rest with a constant entropy S_0 , Eq. (2.4) implies that $S = S_0$ throughout the flow; such flows are called isentropic.

Physically, flows are isentropic when there is no 'dissipation' of mechanical energy into heat. For this reason, to 'derive' the preceding equations from the general Navier-Stokes equations, one must not only assume that there are no external body forces, but one must also neglect viscosity and heat conduction. For this derivation, we refer the reader to [A9, §6.3].

Characteristics. In 1858, Riemann made a classic study of the isentropic case that $p = f(\rho)$. Physically, this is the case in which the purely mechanistic model of Euler-Lagrange is valid. Mathematically, the model assumes a quasilinear hyperbolic system of two first-order equations (1.1)-(1.2), supplemented by $p = f(\rho)$. Each solution therefore has two families of characteristics, $r = \text{const.}$ and $s = \text{const.}$, relative to which the system can be rewritten as a single hyperbolic DE in normal form:

$$\partial^2 u / \partial r \partial s = F(r, s, u, u_r, u_s).$$

Historically, it was Riemann's analysis that led to the theory of characteristics.

In Riemann's problem, the characteristics are the two families of curves in space-time

$$C^+: dx/dt = u + c, \quad C^-: dx/dt = u - c,$$

corresponding to 'wave fronts' moving relative to the fluid with the 'signal' (sound) velocity $\pm c = (dp/d\rho)^{1/2}$. On each of these, we have an invariant integral, called a Riemann invariant. Specifically,

$$\int \frac{c(\rho)}{\rho} d\rho + u = \text{const. on } C^+: \frac{dx}{dt} = u + c$$

and

$$\int \frac{c(\rho)}{\rho} d\rho - u = \text{const. on } C^-: \frac{dx}{dt} = u - c.$$

In the case of a polytropic gas, where $c^2 = \gamma p/\rho$, these equations become

$$\frac{2c}{\gamma-1} \pm u = \text{const. on } C^\pm: \frac{dx}{dt} = u \pm c.$$

Simple waves. Evidently, the independent variables $x - ct = r$ and $x + ct = s$ of the d'Alembert decomposition $u = f(x+ct) + g(x-ct)$ of the linear⁴ wave equation $u_{tt} = c^2 u_{xx}$ are characteristics, since $dx/dt = -c$ if $s = \text{const.}$ Waves of the form $u = f(x+ct)$ or $u = g(x-ct)$ are evidently especially 'simple'; in them, the level lines $u = \text{const.}$ and $\rho = \text{const.}$, (hence $p = f(\rho) = \text{const.}$) are all characteristics; hence $u = g(\rho)$.

Analogously, in a general isentropic flow, a simple wave is one in which all physical variables are constant along the characteristics of one family. Such solutions of (1.1)-(1.3) are produced by a moving piston in a semi-infinite tube of initially quiescent fluid; they represent a disturbance moving in one

⁴In Lagrangian coordinates (see §3), this is the case $\gamma = -1$ of $p = A - B/\rho$, and also of the linearized approximation treated in Chapter 5.

direction. They were discovered by Poisson (1807) and Earnshaw (1858), before Riemann wrote his paper, by assuming that $u = V(\rho)$, where $V(\rho)$ is now an arbitrary function. Substituting into (1.1), this gives

$$(2.5) \quad (\rho_t + V\rho_x)V' + c^2\rho_x/\rho = 0$$

and

$$(2.5') \quad \rho_t + (V + \rho V')\rho_x = 0 .$$

Multiplying (2.5') by $\rho V'$ and subtracting the result from (2.1), we get

$$\rho[c^2/\rho - \rho V'^2] = 0 .$$

As this shows, $V' = \pm c/\rho$. For the equation of state $p = k\rho^\gamma$, this gives

$$(2.6) \quad u = V(\rho) = \pm \int [c(\rho)/\rho] d\rho = \frac{\pm 2}{\gamma-1} \{c(\rho) - c_0\}, \quad \gamma \neq 1 .$$

For $p = k\rho$, we have $u = k \ln \rho$ instead.

3. Shocks; von Neumann-Richtmyer scheme. The theory of isentropic flows can be based on Euler's equations for an 'elastic fluid' (Chapter 1, §2); Riemann's brilliant investigations made no use of thermodynamic considerations, and indeed did not need them. This is because in differentiable flows of a perfect gas, initially at rest as in the Lagrange problem, these equations are satisfied with $p = k\rho^\gamma$, and determine the evolution of such flows.

However, when two of Riemann's 'characteristics' meet and coalesce, as they must in any 'simple' compression wave, discontinuities arise as mathematical 'singularities'. As a result, the initial value problem as stated literally has no solution valid for $t > T$, some finite length of time.

Rankine-Hugoniot equations. We have already pointed this out in Chapter 2, §§6-7; the resulting difficulty was resolved by the

British engineer Rankine (1870) and the French ballistician Hugoniot (1903), by making a second appeal to thermodynamics. By combining the conservation laws of mass, momentum and energy with the thermodynamic equation of state $p = R\rho T$, they were able to predict the observed jumps in p , ρ , T across the near-discontinuity or shock wave that results. In a perfect gas, these jumps are given by

$$(3.1) \quad \frac{\rho_2}{\rho_1} = \frac{1 + \gamma^*(p_2/p_1)}{\gamma^* + (p_2/p_1)} = \frac{u_1}{u_2}, \quad \gamma^* = \frac{\gamma+1}{\gamma-1} \approx 6 \quad \text{in air.}^5$$

To satisfy the Second Law of Thermodynamics, the shock must be a compression shock.

Spark shadowgraphs of bullets in flight and measurements of supersonic flows in wind tunnels amply confirm these predictions. Rayleigh's calculations (1910) predict a shock wave thickness, of the order of 10^{-5} cm. in air; cf. Lamb [A6, Art. 360a].

To derive these equations,⁶ it is simplest to transform to axes moving with the velocity of the shock front, and then to use conservation of mass and momentum to derive

$$\rho_1 u_1 = \rho_2 u_2 = m \quad \text{and} \quad p_1 + \rho_1 u_1^2 = p_2 + \rho_2 u_2^2.$$

One can eliminate the first of these by rewriting the second as

$$p_2 + \rho u_2^2 = p_1 + \rho u_1^2 = \text{const.}$$

The adiabatic law becomes $p_2 u_2^\gamma = p_1 u_1^\gamma = m^{-\gamma} k$. Solutions of these two simultaneous equations can be found graphically.

Von Neumann-Richtmyer scheme. The first serious attempt to calculate the evolution of non-isentropic one-dimensional compressible time-dependent flows was made by von Neumann and

⁵ See again Lighthill in [A1, pp. 250-352], for an authoritative reassessment.

⁶ See H.W. Liepmann and A.E. Puckett, "Aerodynamics of a Compressible Fluid," Wiley, 1947, p. 39. The ratio p_2/p_1 satisfies

$$(p_2 - p_1)/p_1 = 2\gamma(M^2 - 1)/(\gamma + 1);$$

see *ibid.*, p. 40.

Richtmyer, in a 1949 paper already discussed in Chapter 3, §7. They used Lagrangian coordinates, and we will now describe their procedure in a different notation.⁷

Let a denote the cumulative mass (the Lagrangian space variable), and let $\xi = \xi(a, t)$ be the position of the plane (fluid element) of cumulative mass a at time t . Then the specific volume of the flow is $\xi_a = 1/\rho = V(a, t)$, the velocity is $u = \xi_t$, whence the conservation of mass ("continuity equation") follows automatically since $u_a = \xi_{ta} = \xi_{at} = V_t$.

Conservation of momentum (the "equation of motion") can now be expressed by

$$(3.2) \quad u_t + p_a = 0 ,$$

while conservation of energy takes the form

$$(3.3) \quad e_t + pV_t = 0 .$$

Von Neumann and Richtmyer [C8, vol. vi, pp. 380-5] based their numerical treatment on the preceding equations, supplemented by a term $q = -\mu u_a$, acting as a dissipative "viscous stress". They proposed letting the "artificial viscosity" (or "pseudo-viscosity") be a function of the flow variables, and depend on the meshlength $h = \Delta x$ of the space discretization. They modified (3.2), (3.3) to

$$(3.4) \quad u_t + (p+q)_a = 0 ,$$

$$(3.5) \quad e_t + (p+q)V_t = 0 .$$

Quoting from their paper, q is required to have the properties:

1. The equations [our (3.2)-(3.5)] must possess solutions without discontinuities.

⁷For simplicity, we have also assumed that $\rho_0(a) \equiv 1$, which we can do without loss of generality in a homogeneous medium.

2. The thickness of the shock layers must be everywhere of the same order as the interval length Δx used in the numerical computation, independently of the strength of the shock and of the condition of the material into which it is running.
3. The effect of the terms containing q in [(3.4) and (3.5)] must be negligible outside of the shock layers.
4. The Hugoniot equations must hold when all other dimensions characterizing the flow are large compared to the shock thickness.

Von Neumann and Richtmyer assumed the artificial or pseudo-viscosity to be given by

$$(3.6) \quad \mu = Kh^2 |u_a|/V ,$$

where K is a dimensionless constant of order 1, and verified that it satisfied the above requirements (their #4 refers to steady plane shocks). Setting $r = \Delta t/\Delta x$, they proposed computing the four vectors $\underline{u}^{n+1/2}$, \underline{v}^{n+1} , $\underline{q}^{n+1/2}$, and \underline{p}^{n+1} in turn on a staggered mesh. Writing $n-1/2$ as n' , $n+1/2$ as n'' , $j-1/2$ as j' and $j+1/2$ as j'' , their equations become

$$(3.7) \quad u_j^{n''} - u_j^{n'} = r[p_j^{n''} - p_j^{n'} + q_j^{n'} - q_j^{n''}] ,$$

$$(3.8) \quad v_j^{n+1} - v_j^n = r[u_{j+1}^{n''} - u_j^{n''}] ,$$

$$(3.9) \quad q_j^{n''} = 2c^2 \left\{ \frac{(u_{j+1}^{n''} - u_j^{n''}) u_{j+1}^{n''} - u_j^{n''}}{v_j^n + v_j^{n+1}} \right\} ,$$

and

$$(3.10) \quad \begin{aligned} & [\gamma(p_j^{n+1} + p_j^n) + 2(\gamma-1)q_j^{n''}](v_j^{n+1} - v_j^n) \\ & = -(v_j^{n+1} + v_j^n)(p_j^{n+1} - p_j^n) \end{aligned}$$

The accuracy is $O(h^2)$ except for (3.7), which has only $O(h)$ accuracy. However (3.7) is small except across shocks.

4. Lax-Wendroff scheme; shock 'capturing'. Many authors have suggested alternative "artificial viscosity" formulas, with the aim of approximating Rankine-Hugoniot transitions across shock fronts in the fewest possible mesh lengths. Most of them have adopted 'Eulerian' coordinates instead of the 'Lagrangian' coordinates adhered to by von Neumann. This change necessitates the integration of three instead of two first-order DE's, since the conservation of mass (implied by the identity $\xi_{ta} = \xi_{at}$ in Lagrangian coordinates) is no longer 'built in' automatically.

An important, relatively early proposal along these lines was made by Lax and Wendroff [F16] in 1960. This scheme has second-order accuracy in space and time; moreover, it has the attractive feature of bringing out applicability to general systems of first-order (hyperbolic) DE's expressing conservation laws.

Conservation laws. We will discuss 'conservation laws' systematically in some depth in §7; for the present, we note only that they refer mathematically to systems of first-order DE's of the following general form:

$$(4.1) \quad \frac{\partial u_i}{\partial t} + \frac{\partial f_i}{\partial x} = 0, \quad i = 1, \dots, r,$$

where $u_i = u_i(x, t)$ and $f_i = f_i(u_1, \dots, u_r)$. We let $\underline{u} = [u_1, \dots, u_r]^T$ and $A = A(\underline{u})$ be the Jacobian $r \times r$ matrix given by $A_{ij} = \partial f_i / \partial u_j$. Then we can rewrite (4.1) in vector form as

$$(4.2) \quad \frac{\partial \underline{u}}{\partial t} + A(\underline{u}) \frac{\partial \underline{u}}{\partial x} = 0.$$

The quasilinear system (4.2) is said to be (strictly) hyperbolic, [F15, p. 24] if for each \underline{u} the matrix A has r real, distinct eigenvalues $\lambda_1, \dots, \lambda_r$. Then the solution \underline{u} of (4.2) has r distinct real characteristics defined by $dx_i/dt = \lambda_i(\underline{u})$.

For example, let us consider the equations of isentropic flow in Lagrangian coordinates considered in §3. Denoting the Lagrangian position variable a by x , and assuming that

$\rho_0 \equiv 1$ we can write equations (3.2) and (3.3) in the form

$$(4.3) \quad \frac{d}{dt} \begin{bmatrix} u \\ v \end{bmatrix} + \begin{bmatrix} 0 & p'(V) \\ -1 & 0 \end{bmatrix} \begin{bmatrix} u_x \\ v_x \end{bmatrix} = \begin{bmatrix} 0 \\ 0 \end{bmatrix},$$

where $p = p(V)$ is the equation of state, which for a polytropic gas is of the form $p = kV^{-\gamma}$, for some positive constant k . The eigenvalues of the 2×2 matrix A are

$$(4.4) \quad \lambda_1 = \sqrt{-p'(V)}, \quad \lambda_2 = -\sqrt{-p'(V)}$$

and therefore the system is hyperbolic if $p'(V) < 0$, which is true for polytropic gases.

For any system of the form (4.2), writing \underline{v} in place of \underline{u} (since V will no longer appear), the Lax-Wendroff scheme consists in setting

$$(4.5) \quad \underline{v}_j^{n+1} = \underline{v}_j^n - r(\underline{f}_{j+1}^n - \underline{f}_{j-1}^n)/2 \\ + r^2 [A_{j''}^n (\underline{f}_{j+1}^n - \underline{f}_j^n) - A_j^n (\underline{f}_j^n - \underline{f}_{j-1}^n)]/2,$$

where $r = \Delta t/\Delta x$ and

$$(4.5') \quad \underline{f}_j^n = \underline{f}(\underline{v}_j^n), \quad A_j^n = A(\frac{1}{2}\underline{v}_{j+1}^n + \underline{v}_j^n).$$

Often, the Lax-Wendroff scheme is implemented as a two-step procedure, equivalent to (4.5) in the linear case $\underline{f}(\underline{v}) = A\underline{v}$, for a constant matrix A . One such two-step variant, due to Richtmyer, [C9, p. 303], is given by

$$(4.6a) \quad \underline{v}_j^{n''} = \frac{1}{2}(\underline{v}_{j+1}^n + \underline{v}_j^n) - \frac{r}{2}(\underline{f}_{j+1}^n - \underline{f}_j^n),$$

$$(4.6b) \quad \underline{v}_j^{n+1} = \underline{v}_j^n - r(\underline{f}_j^{n''} - \underline{f}_j^n).$$

To apply this two-step method to the equations of gas dynamics for a polytropic gas, we first rewrite (1.1)-(1.3) and

(2.2) in the following form:

$$(4.7a) \quad \rho_t + m_x = 0, \quad (4.7b) \quad m_t + \left(\frac{m^2}{\rho} + p\right)_x = 0,$$

$$(4.7c) \quad E_t + \left(\frac{m}{\rho}(E+p)\right)_x = 0, \quad (4.7d) \quad p = (\gamma-1)\left(E - \frac{1}{2}\frac{m^2}{\rho}\right),$$

Here $m = \rho u$ is the momentum density; for computation, it is also convenient to introduce the intermediate variables $P = p + m^2/\rho$ and $F = m(E+p)/\rho$. The system (4.7) (4.7c) is now in the 'conservation law' form of (4.2), with $n = 3$, $\underline{v} = (\rho, m, E)$, and $\underline{f}(\underline{v}) = (m, P, F) = (m, p + m^2/\rho, m(E+p)/\rho)$.

In this notation, the two-step Lax-Wendroff-Richtmyer scheme has as its first step:

$$(4.8a) \quad \rho_j^{n''} = \frac{1}{2}(\rho_{j+1}^n + \rho_j^n) - \frac{r}{2}(m_{j+1}^n - m_j^n),$$

$$(4.8b) \quad m_j^{n''} = \frac{1}{2}(m_{j+1}^n + m_j^n) - \frac{r}{2}[P_{j+1}^n - P_j^n],$$

$$(4.8c) \quad E_j^{n''} = \frac{1}{2}(E_{j+1}^n + E_j^n) - \frac{r}{2}[F_{j+1}^n - F_j^n],$$

$$(4.8d) \quad P_j^{n''} = (\gamma-1)[E_j^{n''} - (m^2/2\rho)_j^{n''}],$$

the first step, followed by

$$(4.9a) \quad \rho_j^{n+1} = \rho_j^{n''} - r(m_j^{n''} - m_j^{n''}),$$

$$(4.9b) \quad m_j^{n+1} = m_j^{n''} - r[P_j^{n''} - P_j^{n''}],$$

$$(4.9c) \quad E_j^{n+1} = E_j^{n''} - r[F_j^{n''} - F_j^{n''}],$$

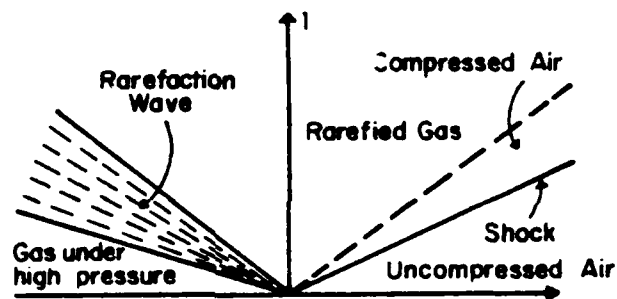
$$(4.9d) \quad P_j^{n+1} = (\gamma-1)[E_j^{n+1} - (m^2/2\rho)_j^{n+1}].$$

A (linearized) von Neumann stability analysis for the Lax-Wendroff scheme applied to the system (5.3) gives [C9, p. 304] the

following restriction on the Courant number $r = \Delta t/\Delta x$:

$$(4.10) \quad r < (|u| + c)^{-1} = [|m|/\rho + (\gamma p/\rho)^{1/2}]^{-1}$$

We used the scheme (4.8)-(4.9) to simulate the evolution in time of an initial step function of p and ρ , such as arises in a "shock tube". Given the initial values p_0, ρ_0 , on one side of a membrane, and p_1, ρ_1 on the other, with $u = 0$ on both sides, a sudden rupture of the membrane causes a shock to travel down the tube, and a centered rarefaction wave to travel upstream, as indicated in Figure 2; see [B3, p. 182], and [F23, p. 184].



Von Neumann and many others have compared calculated with experimental values of the variables listed, and we did so, too.

We used the scheme (4.8)-(4.9) to simulate the evolution in time of a discontinuous step initial profile of p, ρ and u . This "shock tube problem", cf. [B3, p. 182], [F23, p. 184], has been extensively studied in gas dynamics experiments. Specifically, for $\gamma = 1.4$ we considered the following initial values

$$(4.11a) \quad \text{For } x < 1: \quad p_4 = 1, \quad \rho_4 = 1, \quad u_4 = 0 .$$

$$(4.11b) \quad \text{For } x > 1: \quad p_1 = 0.25, \quad \rho_1 = 0.25, \quad u_1 = 0 .$$

Exact solutions for p , ρ , u , E for $t > 0$ can be easily obtained, cf. [F23, pp. 184-186]. In this case we obtain the following solution: For $t > 0$ there are four regions, denoted by 1 through 4 in Figure 5.1, in each of which the flow quantities are constant. Regions 3 and 4 are connected by a centered rarefaction wave (fan) through which the flow quantities are continuous. In Regions 1 and 4 the gas is at rest and the values of p and ρ are identical to their initial values for $x > 1$ and $x < 1$, respectively. Regions 1 and 2 are separated by a shock travelling to the right with speed 1.586 and across which all flow quantities are discontinuous. In region 2 we have $p_2 = .482$, $\rho_2 = .396$, $u_2 = .586$. Regions 2 and 3 are separated by a contact discontinuity travelling to the right with speed .586 and across which p and u are continuous but ρ is discontinuous; we have that $\rho_3 = .594$. Finally, the front and the end of the rarefaction wave travel with speeds -1.183 and $-.481$, respectively. The exact solution in the rarefaction wave region is found by an iterative method due to Godunov (cf. §7) implemented in a program that Dr. Gary Sod kindly sent us.

To compute the numerical solution of this problem by (4.8)-(4.9) we used 200 space intervals on $[0,2]$ so that $\Delta x = 0.01$ and a constant $\Delta t = 0.001$, a value well within the stability limit prescribed by (5.5). We show in Figures 5.2 and 5.3 the exact and the obtained numerical values of p and ρ , respectively, at 350 time steps, i.e., at $t = .35$. (All computations were done in single precision using the FORTRAN G compiler of the IBM 360-65 at the University of Tennessee, Knoxville.) We observe the well-known oscillations, especially in the vicinity of the shock and the contact discontinuity (for ρ) but also in the interior of the regions 2 and 3. The shock transition takes place over approximately 5 Δx -intervals. The contact discontinuity (Figure 5.3) extends over approximately 10 Δx -intervals. The overshoot before the shock is approximately 20% for both p and ρ . The transition from region 4 into the rarefaction wave is smoothed.

5. Artificial viscosity; recent developments. As we have pointed out before (cf. §?), various formulas for 'artificial viscosity' have been used since the pioneering work of von Neumann and Richtmyer; cf. [F16]. We made numerical experiments using the Lax-Wendroff method of §4 and an artificial viscosity originally introduced by Lapidus [F14] for a two-dimensional problem.⁸ According to Lapidus' recipe, artificial viscosity terms of the form

$$\nu r \Delta (|\Delta u_{i+1}^{n+1}| \Delta v_{i+1}^{n+1}) ,$$

where $\Delta u_i^n = u_i^n - u_{i-1}^n$, $\underline{v} = [\rho, m, E]^T$, are added as a final (fractional) step to the values of ρ_i^{n+1} , m_i^{n+1} , E_i^{n+1} obtained by (4.9). Here ν is a constant whose value can be chosen to match a particular problem and the amount of artificial dissipation desired.

Formula (4.8) and (4.9) are therefore supplemented by a third set of equations:

$$(5.1a) \quad \tilde{\rho}_i^{n+1} = \rho_i^{n+1} + \nu r \Delta (|\Delta u_{i+1}^{n+1}| \Delta \rho_{i+1}^{n+1}) ,$$

$$(5.1b) \quad \tilde{m}_i^{n+1} = m_i^{n+1} + \nu r \Delta (|\Delta u_{i+1}^{n+1}| \Delta m_{i+1}^{n+1}) ,$$

$$(5.1c) \quad \tilde{E}_i^{n+1} = E_i^{n+1} + \nu r \Delta (|\Delta u_{i+1}^{n+1}| \Delta E_{i+1}^{n+1}) ,$$

$$(5.1d) \quad \tilde{p}_i^{n+1} = p_i^{n+1} ,$$

and the values $\tilde{\rho}_i^{n+1}$, \tilde{m}_i^{n+1} , \tilde{E}_i^{n+1} , \tilde{p}_i^{n+1} represent then the flow quantities at $t = (n+1)\Delta t$. We used formulas (5.1) with the value $\nu = 1$, recommended by G. Sod [F22]. The results for p and ρ are shown in Figures 5.4 and 5.5, respectively, again at $t = .35$, i.e., at 350 time steps. Note that most oscillations have been damped out. The shock transition occupies 6 to

⁸ Pointed out to us by A. Harten in 1975; cf. also [F22].

7 Δx -intervals. The contact discontinuity is again spread over 10 Δx -intervals. The overshoot to the left of the shock has been reduced to approximately 8%. The rounded transition zone from region 4 to the rarefaction wave has slightly increased.

We conclude this section with a brief review of some developments in the literature on "shock capturing" methods subsequent to Lax-Wendroff. There are other two-step variants of the Lax-Wendroff method which reduce to it in the linear case; we cite for example schemes due to MacCormack and to Rubin and Burstein.⁹ We also mention the higher order methods of Rusanov and of Burstein and Mirin.¹⁰ Most of these methods typically approximate shocks by a transition 3-5 Δx -intervals wide (there is more spread in the case of contact discontinuities). Moreover, nongrowing oscillations appear in the vicinity of discontinuities. Lerat and Peyret discuss systematically the (numerical) shock width and the amplitude and location of the oscillations of such methods.¹¹

Recent developments have concentrated in producing sharp resolutions of discontinuities without oscillations. Among these we note the "antidiffusion" method of Boris and Book and the "artificial compression" method due to Harten [F10]. The latter can be applied to standard difference schemes and gives significantly improved resolution of both shocks and contact discontinuities, cf. [F10], [F22]. A "random choice" method, due to Chorin and based on Glimm's existence proof will be reviewed in §8.

Several comparisons of numerical methods for the solution of the initial-value problem of the one-dimensional gas dynamics equations have appeared in the literature. A recent survey by Sod [F22] is especially valuable. Sod considers many modern

⁹For Rubin and Burstein, see J. Comp. Phys. 2 (1967), 178-96; for McCormack, see [A17, pp. 151-63] and [A25, p. 253].

¹⁰J. Comp. Phys. 5 (1970), 507-16 and 547-71; *ibid.* 11 (1973), 38-68.

¹¹See [A24, pp. 251-6].

schemes and compares them based on their performance on a typical "shock tube" problem. He points out that two schemes, due to Godunov and Hyman (for references see Sod, op. cit.) behaved better than the others without corrective procedures.

6. Shock fitting; Moretti's program. The purpose of the preceding numerical experiments was to develop and justify theoretically a computer program to be included in WAVPACK which would solve Riemann's initial value problem accurately and efficiently, even when shock waves were present initially or were formed during the time interval of calculation. Essentially, our aim was thus to realize von Neumann's original ambition by a procedure available (for example) to energetic college seniors. We are still trying to realize this objective, and §§6-8 will explain some of the difficulties that we have encountered!

Following Richtmyer [C9, §12.9], we will term "shock fitting" or "shock locating" techniques those schemes which, in contrast with "shock capturing" techniques, divide the computational region into subregions by lines of discontinuity in the (x,t) -plane. These lines can be shocks or contact discontinuities, for example. Unlike the "shock capturing" methods discussed in §§4-5, "shock fitting" methods produce piecewise smooth solutions in the regions bounded by lines of discontinuity. Thus they use Model #5 of Chapter 1, §3, at a very basic level.

Here we consider the application of shock-fitting methods to the Riemann initial value problem for the equations of gas dynamics for a polytropic gas and also the easier piston problem of §2, namely to compute the 'simple flow' created in a tube of length L containing gas initially at rest by a moving piston at end.

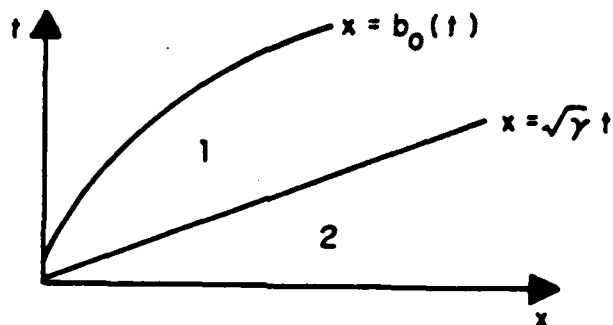
Professor G. Moretti of the Polytechnic Institute of New York has worked extensively on shock fitting for one- and multi-dimensional problems of gas dynamics. For the one-dimensional case that we will consider here, see his reports [F18] and

[F19].¹² He has kindly sent us a FORTRAN program (5C1) implementing his shock fitting technique in one-dimensional problems in tubes of variable cross section; in our tests we used only the constant cross section option.

In this program an approximate solution at the interior mesh points of the smooth flow regions is computed by a Lax-Wendroff type scheme [F18, p. 34] with variable time step that satisfies the usual stability condition (5.5). As soon as a shock is "detected" (by an appropriate test on the slope of the profile of the solution, [F18, p. 56]), it is treated as a computational boundary (interface) between adjacent regions of smooth flow. The shock trajectory is computed by the Rankine-Hugoniot across it and the information reaching the discontinuity along the characteristics from the two adjacent subregions. So, nonlinear systems of algebraic equations have to be solved at every time step. Within each region (a maximum of 10 regions can be handled with a maximum of 50 grid points per region) the mesh size is constant but Δx may differ from region to region as points are created or deleted, automatically, to describe in more or less detail, respectively, the nonsmooth or smooth portions of the flow. A part of the program eliminates shocks if they are too weak. More complications arise in the case of contact discontinuities, shock reflections at boundaries, shock coalescence and interactions, etc.

Using single precision on the Fortran G compiled, and the IBM 360-65 of the University of Tennessee at Knoxville, we first calculated (in 1978) flows induced in a gas at rest by the motion of a piston at the left end. The flow can be divided in two regions as in the figure below (x, t are dimensionless as in [F18, p. 22]). In region 1, bounded by the piston path and the characteristics through the origin, the solution is a simple wave [B3, p. 92]. Exact solutions can be found in this region [F18, p. 24]. In region 2, the gas is at rest. We ran a few test problems with different paths $b_0(t)$. The first two

¹² See also his reports "The choice of a time-dependent technique in gas dynamics," PIBAL Rept. 69-26, PIB 1969, "Thoughts and afterthoughts about shock computations," PIBAL Rept. 72-37, PIB 1972 in which he further expands on his philosophy on numerical methods for gas dynamics.



were rarefaction waves produced by the following piston paths

$$(6.1) \quad x = -t^3$$

and

$$(6.2) \quad x = -t^2,$$

previously used by Moretti as test problems in [F18]. The solution corresponding to (6.1) has continuous velocity gradients; whereas if (6.2) is used, there is an initial discontinuity in u_x which dissipates with increasing time. In both problems a right-hand side computational boundary $x = 1$ for $0 \leq t \leq 1/\sqrt{\gamma}$ was used and 25 x -intervals so that, initially, $\Delta x = 0.04$. (Subsequently the mesh is "stretched" automatically between the piston path and the right-hand boundary.) For $\gamma = 1.4$, Table 6.1 shows the behavior of the error in the velocity (appropriately dimensionless as in [F18, p. 22]). In the table t denotes time, x the x -mesh length and ϵ the maximum absolute error in the velocity.

The numerical profiles were smooth and the maximum error usually occurred at the first characteristic $x = \sqrt{\gamma}t$. The numerical "noise" of nonzero values extended one mesh length into region 2 for problem (6.1) and three mesh lengths for (6.2). Of course the piston path (6.2) gives larger errors in the vicinity of the first characteristic.

(6.1)			(6.2)		
t	Δx	ϵ	t	Δx	ϵ
.222	.040	.002	.190	.041	.010
.394	.042	.003	.332	.044	.013
.527	.046	.004	.457	.048	.014
.639	.050	.006	.574	.053	.021
			.688	.059	.019

TABLE 6.1 Rarefaction waves.

Subsequently, we considered compression waves with different piston paths. For example let $b_0(t)$ be given by

$$(6.3) \quad x = b_0(t) = t^3 ,$$

a problem also considered in [F18]. This piston path (with zero initial acceleration) will produce a shock which originates (for $\gamma = 1.4$) at $x = .842$, $t = .844$ where the characteristics C^+ will first merge. A right-hand side computational boundary $x = 1.5$ for $0 \leq t \leq .95$ was used and 45 x -intervals so that initially $\Delta x = 1/30$. The shock was predicted accurately and after its occurrence ($t \geq .844$) the program concentrated on the region of non-zero flow to the left of the shock where it reduced the number of mesh points to 12. When the flow became nearly uniform, for $t \geq .928$, the number of mesh points was reduced to 6. Table 6.2 shows the behavior of the error of the velocity.

t	Δx	ϵ	t	Δx	ϵ	t	Δx	ϵ
.186	.033	.001	.724	.025	.018	.892	.010	.012
.329	.032	.003	.759	.024	.036	.902	.003	.013
.435	.032	.003	.791	.022	.060	.911	.007	.005
.516	.030	.004	.819	.021	.099	.918	.006	.006
.582	.029	.005	.844	.019	.296	.928	.009	.009
.637	.028	.006	.864	.015	.043	.936	.006	.007
.684	.026	.011	.880	.012	.033	.942	.005	.004

TABLE 6.2 Compression wave.

7. Conservation law form. In his well-known monograph [C13], Peter Lax has explained lucidly how to obtain 'generalized solutions' of initial value problems for first-order hyperbolic systems of the form $\underline{u}_t + [f(\underline{u})]_x = 0$. The class of such systems includes the Euler-Rankine-Hugoniot equations for 'plane waves of finite amplitude' that we have been studying in this chapter. For purposes of orientation, we now consider the case that the vector $\underline{u}(x,t)$ is a scalar--i.e., the case of

$$(7.1) \quad u_t + [f(u)]_x = 0$$

with $f \in C^1(-\infty, \infty)$, for differentiable initial data

$$(7.1') \quad u(x,0) = g(x) , \quad g \in C^1(-\infty, \infty) .$$

The prescription consists in looking at the 'characteristics' defined parametrically in the upper half-plane by

$$(7.2) \quad x(\xi,t) = \xi + tf'(g(\xi))$$

These will cover an open neighborhood of the x-axis $t = 0$; in this neighborhood, u is constant along each characteristic, so that

$$(7.2') \quad u(x(\xi,t), t) = g(\xi)$$

where nearby characteristics merge into a discontinuity of u , the slope s of the resulting 'shock' is required to satisfy

$$(7.3) \quad s = [f]/[u] ,$$

in conformity with the basic 'conservation principle' that the integral relation

$$(7.3') \quad \frac{d}{dt} \left[\int_a^b u \, dx \right] = f(a) - f(b)$$

is equivalent to (7.1) for continuously differentiable functions. Above, f may be thought of as the local rate of flux of the substance whose 'density' is u , from left to right.

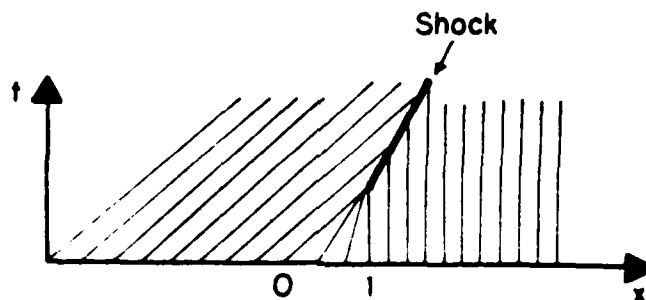
Thus, for the familiar self-convection equation

$$(7.4) \quad u_t + uu_x = 0$$

with $f(u) = u^2/2$, for the jump from u_1 to u_2 , the prescription (3) consists in setting $u_s = (u_1 + u_2)/2$. For example [Cl3, (3.11)], if we set

$$(7.4') \quad u(x,0) = g(x) = \begin{cases} 1 & \text{for } x \leq 0 , \\ 1-x & \text{for } 0 \leq x \leq 1 , \\ 0 & \text{for } x \geq 1 , \end{cases}$$

the solution has the characteristics shown in Figure 1.



Unfortunately, there is a subtle but very basic flaw in the derivation of the shock velocity formula (7.3) as has been pointed out by Whitham, in [Bl2, p. 40].

Namely, let $v = \psi(u)$ be any continuously differentiable function with continuously differentiable inverse, $u = \phi(v)$, so that $\psi'(u) \neq 0$ and $\phi'(v) = 1/\psi'(u) \neq 0$. Then the DE (7.1) is equivalent to

$$\phi'(v)\{v_t + f'(\phi(v))v_x\} = 0 ,$$

as one discovers by setting $u = \phi(v)$ (7.1) and hence to

$$(7.5) \quad v_t + [F(v)]_x = 0 ,$$

where

$$(7.5') \quad F(v) = \int f'(\phi(v))dv .$$

For example, setting $u = v^3 + v$, we obtain as equivalent to (7.4) the DE

$$(7.6) \quad v_t + [v^4/4 + v^2/2]_x = 0 .$$

This has exactly the same characteristics, for any (continuously differentiable) $g(x)$ in (7.1') and corresponding v with

$$(7.7) \quad v^3(x) + v(x) = g(x) ,$$

or, equivalently,

$$(7.7') \quad v = \frac{2}{\sqrt{3}} \sinh \left[\frac{1}{3} \sinh^{-1} (3\sqrt{3} g(x)/2) \right] .$$

This is because level lines of u are level lines of v , and vice-versa.

However, the shock velocity prescribed by (7.3) is not the same for (7.6) as it is for (7.4). An easy calculation gives for $F(v) = v^4/4 + v^2/2$,

$$(7.8) \quad s' = \left[\left(\frac{v_2^4}{4} + \frac{v_2^2}{2} \right) - \left(\frac{v_1^4}{4} + \frac{v_1^2}{2} \right) \right] / (v_2 - v_1)$$

$$= (v_2 + v_1) [2 + v_2^2 + v_1^2] ,$$

which is not equivalent to

$$(7.9) \quad s = (u_1 + u_2)/2 = (v_1^3 + v_1 + 3v_2^3 + v_2)/2$$

Self-convection DE. We next consider in detail the problem of integrating numerically the self-convection equation (7.4). This can be thought of as a limiting case of Euler's equation of motion for an elastic fluid, in which the pressure is nearly independent of the density.

For a given initial velocity distribution $u(x,0) = \phi(x)$, the DE (7.4) can be integrated by the method of characteristics, as follows. Consider the level lines $u(x,t) = \lambda$ of any solution of (7.4). By definition, on each such level line we have

$$0 = du = u_x dx + u_t dt = u_x (dx - u dt) ,$$

whence $dx/dt = u = \lambda$ is a constant (unless $u_x = 0$) and so u is constant. This shows that each level line $u = \lambda$ of any solution of (7.4) must have constant slope in the (x,t) -plane, in a region of non-constant u .

Conversely, we can use this fact to solve (7.4) locally, for given $u(x,0) = \phi(x) = C^1$, as follows. Define the characteristic through $(\xi, 0)$ parametrically by

$$(7.10) \quad x = \xi + \phi(\xi)t .$$

By what was shown above, any solution $u(x,t)$ of (7.4) satisfying $u(x,0) = \phi(x)$, must satisfy

$$(7.11) \quad u(\xi + \phi(\xi)t, t) = \phi(\xi) ,$$

and have the lines $\xi = \text{const.}$ must be level lines.

Moreover since $f \in C^1$, the derivative $(\partial x / \partial \xi)_t = 1 + tf'(\xi)$ is positive provided that

$$|t| < 1/|\phi'(\xi)|_{\max} = 1/L,$$

where $L = |f'(\xi)|_{\max}$ is the (local) Lipschitz constant of $\phi(x) = u(x,t)$. Hence the mappings $x \rightarrow \xi$ are diffeomorphisms for $|t| < 1/L$, and the equation $u(\xi + tf(\xi), t) = \phi(\xi)$ defines $u(x,t)$ as a differentiable, single-valued function in this neighborhood. In it,

$$(7.12) \quad u_t + uu_x = u_t + \phi(\xi)u_x = 0,$$

since the second expression is just the total derivative

$$du/dt = \partial u / \partial t + (\partial u / \partial x)(dx/dt)$$

along this characteristic. We conclude

THEOREM. For any initial velocity distribution $u(x,0) = \phi(x) \in C^1$, the DE (7.4) has a continuously differentiable solution, given by (2), valid for $|t| \leq 1/L$.

Piecewise linear solutions. The following lemma is easily verified; accents (primes) denote derivatives.

LEMMA. The affine function $c(t) + \lambda(t)x$ satisfies (7.4) if and only if $\lambda'(t) = -\lambda^2$ and $c'(t) = -c(t)\lambda$.

This is immediate, since $u_t = c' + \lambda'x$ and $uu_x = (c + \lambda x) = c\lambda + \lambda^2 x$. Since $-d\lambda/\lambda^2 = d(1/\lambda)$, it follows that $\lambda = \lambda_0/(1 + \lambda_0 t)$ and

$$(7.13) \quad \frac{d}{dt}(\ln c) = -\lambda_0/(1 + \lambda_0 t) = -\frac{d}{dt}[\ln(1 + \lambda_0 t)]$$

Since the steps are reversible, this has the

COROLLARY. The affine functions

$$(7.14) \quad u = (c_0 + \lambda_0 x)/(1 + \lambda_0 t)$$

are solutions of (7.4), for any c_0, λ_0 .

Note that for $\lambda_0 > 0$ (a so-called rarefaction wave), (7.14) is well-defined for all $t > 0$, whereas a compression wave with $\lambda_0 < 0$ blows up in time $(-1)/\lambda_0$, forming a shock.

Numerical integration.¹³ By combining the preceding results, we are led to a very efficient scheme for integrating (7.4) numerically, along characteristics. Namely, approximate the initial velocity distribution $u(x,0) = \phi(x)$ by a piecewise linear function

$$(7.15) \quad U(x) = \phi(\xi_i) + \frac{\phi(x_{i+1}) - \phi(x_i)}{x_{i+1} - x_i} (x - x_i) ,$$

on (x_i, x_{i+1}) . For $t > 0$, consider the characteristics

$$(7.15') \quad x_i(t) = x_i + \phi(\xi_i)t = \xi_i + U_i t .$$

This can be done until $t = 1/(U_i)_{\min}$.

¹³The scheme proposed here evolved in the course of discussions with Prof. Sun Jingyou of Jinan University, People's Republic of China.

REFERENCES FOR CHAPTER 6

- [F1] T.B. Benjamin, J.L. Bona and J.J. Mahony, "Model equations for long waves in nonlinear dispersive systems," *Phil. Trans. Roy. Soc. London A272* (1972), 47-78.
- [F2] J.L. Bona and R. Smith, "The initial-value problem for the Korteweg-de Vries equation," *Phil. Trans. Roy. Soc. London A278* (1975), 555-604.
- [F3] A.J. Chorin, "Random choice solution of hyperbolic systems," *J. Comp. Phys.* 22 (1976), 517-533.
- [F4] J.D. Cole, "On a quasilinear parabolic equation occurring in aerodynamics," *Quar. Appl. Math.* 9 (1951), 225-236.
- [F5] R. Courant and D. Hilbert, Methods of Mathematical Physics, vol. 2, Wiley-Interscience, New York, 1962.
- [F6] J. Douglas and B.F. Jones, "On predictor-corrector methods for nonlinear parabolic differential equations," *J. SIAM* 11 (1963), 195-204.
- [F7] J. Douglas and T. Dupont, "Galerkin methods for parabolic equations," *SIAM J. Numer. Anal.* 7 (1970), 575-626.
- [F8] J. Glimm, "Solutions in the large for nonlinear hyperbolic systems of equations," *Comm. Pure Appl. Math.* 18 (1965), 697-715.
- [F9] S. Godunov, "A finite difference method for the numerical computation and discontinuous solutions of the equations of fluid dynamics," *Mat. Sbornik*, 47 (1959), 271-
- [F10] A. Harten, "The artificial compression method for computation of shocks and contact discontinuities I: single conservation laws," *Comm. Pure Appl. Math.* 30 (1977), 611-638.
- [F11] E. Hopf, "The partial differential equation $u_t + uu_x = \mu u_{xx}$," *Comm. Pure Appl. Math.* 3 (1950), 201-230.
- [F12] D.J. Korteweg and G. de Vries, "On the change of form of long waves advancing in a rectangular canal and on a new type of long stationary waves," *Phil. Mag.* (v), 39 (1895), 422-443.
- [F13] M.D. Kruskal et al., "A method for solving the Korteweg de Vries equation," *Phys. Rev. Lett.* 19 (1967), 1095-1097.
- [F14] A. Lapidus, "A detached shock calculation by second-order finite differences," *J. Comp. Phys.* 2 (1967), 154-177.

- [F15] P.D. Lax, "Almost periodic solutions of the KdV equation" (with computational Appendix by J.M. Hyman), *SIAM Review* 18 (1976), 351-375.
- [F16] P.D. Lax and B. Wendroff, "Systems of conservation laws," *Comm. Pure Appl. Math.* 13 (1960), 217-237.
- [F17] S. Leibovich and A.R. Seebass, eds., Nonlinear Waves, Cornell University Press, Ithaca, N.Y., 1974.
- [F18] G. Moretti, "A critical analysis of numerical techniques-- the piston-driven inviscid flow," PIBAL Rept. 69-25, Polyt. Inst. of Brooklyn, 1969.
- [F19] G. Moretti, "Complicated one-dimensional flows," PIBAL Rept. 71-25, Polyt. Inst. of Brooklyn, 1971.
- [F20] A.C. Newell, ed., *Nonlinear Wave Motion*, Proc. Summ. Seminar, Potsdam, N.Y. 1972, *Lectures in Appl. Math.* vol. 15, Amer. Math. Soc., 1974.
- [F21] O.A. Oleinik, "Discontinuous solutions of nonlinear differential equations," *Uspekhi Mat. Nauk (N.S.)*, 12 (1957), No. 3 (75), pp. 3-73 (*Amer. Math. Soc. Transl.*, Ser. 2, 26, pp. 95-172).
- [F22] G. Sod, "A survey of several finite difference methods for systems of nonlinear hyperbolic conservation laws," *J. Comp. Phys.* 27 (1978), 1-31.
- [F23] M. Ablowitz and H. Segur, Solitons and the Inverse Scattering Transform, SIAM Publications, 1982.
- [F24] A. Jeffrey and T. Kakutani, "Weak nonlinear dispersive waves: a discussion centered around the Korteweg-de Vries equation," *SIAM Review*, 14 (1972), pp. 582-643.
- [F25] O.A. Karakashian, Galerkin methods for some nonlinear equations in Hydrodynamics, Ph.D. Thesis, Harvard University, 1979.
- [F26] H.B. Keller (ed.), *Computational Fluid Dynamics*, (Proc. Symp. in Applied Math., AMS-SIAM, New York, 1977), A.M.S., Providence, R.I., 1978.
- [F27] J.W. Miles,
J. Fluid Mech. 106 (1981), 131-147.
- [F28] R. Miura, "The KdV equation: a survey of results," *SIAM Review*, 18 (1976), 412-459.

7. INCOMPRESSIBLE VISCOUS FLOWS

1. Introduction. In this chapter, we will study the (approximate) numerical solution of problems involving (idealized, incompressible) viscous fluids of constant density $\rho = \rho_0$. We recall from Chap. 2, §8, that the motion of such fluids is governed by $\nabla \cdot \underline{u} = 0$ and the Navier-Stokes equations

$$(1.1) \quad \rho D\underline{u}/Dt + \nabla P = \mu \nabla^2 \underline{u} ,$$

where $P = p - \rho G$ is the 'potential pressure'. This equation is approximately valid in air and water when $M < 0.1$.¹ If $\underline{\omega} = \nabla \times \underline{u}$ denotes the vorticity, then after taking the curl of Eq. (1.1) to eliminate P , we get:

$$(1.2) \quad \rho \{ D\underline{\omega}/Dt + \underline{\omega} \cdot \nabla \underline{u} \} = \mu \nabla^2 \underline{\omega} ,$$

as in Lamb [A6, p. 578, (8)]. Landau and Lifschitz [B6, p. 50, (15.10)] give the alternative, equivalent formula

$$(1.2') \quad \partial \underline{\omega} / \partial t = \nabla \times (\underline{u} \times \underline{\omega}) + \nu \nabla^2 \underline{\omega} .$$

In plane flows, $\underline{\omega} = (0, 0, \zeta(x, y))$ is orthogonal to $\nabla \underline{u} = (\nabla u, \nabla v, 0)$, and so $\underline{\omega} \cdot \nabla \underline{u} \equiv 0$. This simplifies (1.2) to

$$(1.3) \quad \rho D\zeta/Dt = \mu \nabla^2 \zeta \quad (\text{plane flows}) ,$$

as in [A6, p. 578, (2)]. This is called by Roache [C14] the vorticity equation.

Steady plane flows. For simplicity, we will first consider the case of 'steady' plane flows, having a time-independent velocity field $(u(x, y), v(x, y))$. In terms of the stream function $\psi(x, y)$, we have as in Chap. 1 $\underline{u} = (\psi_y, -\psi_x)$ and $\partial/\partial t = 0$. Hence we can rewrite (1.3) as

¹In problems involving lubrication, variations in μ with temperature can cause major deviations from theory.

$$(1.4) \quad \mu_y \nabla^2 \mu_x - \psi_x \nabla^2 \psi_y = \nu \nabla^4 \psi .$$

Eq. (1.4) encapsulates into a single fourth-order, nonlinear elliptic DE, the Navier-Stokes equations of motion and the incompressibility condition $\nabla \cdot \underline{u} = 0$ governing the motion of fluids of constant density.²

Another interesting area problem concerns the decay of the three-dimensional velocity field $\underline{u}(\underline{x})$ of a "liquid filling a closed vessel" whose boundary Γ consists of stationary walls on which $\underline{u} \equiv \underline{0}$ (no-slip boundary condition). A little skillful formula manipulation shows that the rate of kinetic energy dissipation, F , defined by $F = -\dot{T}$ where

$$(1.5) \quad 2T = \rho \int_{\Omega} q^2 dR, \quad q^2 = u^2 + v^2 + w^2 ,$$

satisfies

$$(1.5') \quad 2F = \mu \int_{\Omega} (\xi^2 + \eta^2 + \zeta^2) dR = \mu \int_{\Omega} |\underline{\omega}|^2 dR .$$

Since the integrand is identically nonnegative, we see that $F > 0$ unless $\underline{\omega} \equiv \underline{0}$. Hence the kinetic energy decreases continuously. Actually, it decreases exponentially:³

$$(1.6) \quad T(t) \leq e^{-\alpha t} T(0) ,$$

where $\alpha = \min\{\int_{\Omega} |\underline{\omega}|^2 dR / \int_{\Omega} |\underline{u}|^2 dR\} > 0$. The number α is like the minimum of a Rayleigh quotient; it is a monotonically decreasing function of the domain.

Kinds of problems. A far greater variety of problems will be taken up in this chapter than were touched on in the preceding three chapters. Broadly speaking, they fall into three main classes: (1) initial value problems (with or without boundaries),

²Because of conservation of mass, constant density implies the incompressibility condition $\nabla \cdot \underline{u} = 0$.

³See Batchelor [B1, p. 212], where (2.1) is derived.

(2) equilibrium problems, and (3) problems with stationary driving forces and boundary conditions whose solutions, nevertheless, fluctuate in time. Vortex streets behind cylinders and turbulent flows in pipes are two classic examples of such flows.

In general, problems of class (3) arise at higher Reynolds numbers (e.g., $Re > 100$), and are presumed to occur because, as $Re \uparrow \infty$ ($\nu \downarrow 0$), the governing Navier-Stokes equations constitute a singular perturbation of the lower-order 'ideal fluid' equations. Practically speaking, the solution of such problems at the present time requires a much greater degree of empiricism than was adopted in Chapters 4-6; this is especially true in the theory of turbulent flows.

As a small partial compensation, the distinction between liquids and gases is much less important than it was for 'plane waves of finite amplitude' (Chap. 6), for example. Although viscous heating can produce important variations in the viscosity of lubricants, the mathematical theory (which assumes μ and ρ to be constant) is applicable to air and water under most circumstances. In particular, as Stanton and Pannell showed in a classic series of experiments,⁴ the 'critical Reynolds number' Re_{crit} for the onset of turbulence seems to be about the same in the two fluids, different as they are in most physical respects (including molecular structure).

⁴Phil. Trans. A214 (1914), 119-24.

2. Parallel flows. In general, solutions of the Navier-Stokes equations represent a balance between viscous diffusion and inertial convection, with the latter dominating at higher Reynolds numbers. We begin by discussing the numerical simulation of diffusion effects in a class of time-dependent 'parallel flows' in which convection effects are absent (i.e., in which $D/Dt = \partial/\partial t$). These include as limiting cases the steady Poiseuille flow already treated analytically in Chap. 2, §8; time-dependent Couette flows generalizing the steady Couette flow treated in Chap. 2, §8, can be handled by similar methods.

By definition, a parallel flow is one in which all velocity vectors point in the same direction, which we choose to be that of the x_3 -axis. This makes $u_1 \equiv u_2 \equiv 0$, and reduces the incompressibility condition $\nabla \cdot \underline{u} = 0$ to $\partial u_3 / \partial x_3 = 0$, which implies $u_3 = u(x_1, x_2; t)$. In turn this implies that $\sum u_k \partial u_i / \partial x_k = 0$ ($i = 1, 2, 3$), thus eliminating the convection terms from the Navier-Stokes equations (i.e., making $D\underline{u}/Dt = \partial \underline{u} / \partial t$). In summary, the Navier-Stokes equations

$$(2.1) \quad D u_i / Dt = \partial u_i / \partial t + \sum u_k \frac{\partial u_i}{\partial x_k} = \nabla^2 u_i - \frac{1}{\rho} \frac{\partial P}{\partial x_i},$$

with $P = p + \rho G$ and $\underline{g} = \nabla G$, are greatly simplified. Changing notation (writing $u_3 = u$, $x_1 = x$, $x_2 = y$), we obtain the following example. (Note that the Poiseuille flow of Chap. 2, §8, is obtained as a special case.)

Example 1. For flow parallel to the z -axis with velocity $u(x, y; t)$, we have

$$(2.2) \quad u_t = \nu(u_{xx} + u_{yy}) + f(t),$$

where $f(t) = g_3 - \rho^{-1} \partial p / \partial z$. (To maintain the flow parallel to the z -axis, the pressure field must satisfy

$$p = p_0(t) + p_1(t)z + \rho G, \quad p_1 = f(t)/\rho.$$

In a rigid vertical pipe whose boundary Γ has the cross-section γ in the (x, y) -plane, the flow must also satisfy the boundary

condition

$$(2.3) \quad u(x,y;t) = U(t) \quad \text{on } \gamma ,$$

where $U(t)$ is the vertical velocity of the pipe (typically $U(t) \equiv 0$), with $f(t) = 0$.

Heat conduction analogy.⁵ Formulas (2.2) and (2.3), also govern the cooling of a rod, and it has been intensively studied in that connection. Readers familiar with the treatment of this problem should be able to supply most of the methods reviewed below. The 'channel' to be treated first corresponds to a 'slab'.

For simplicity, we consider first the special case of a 'channel' or purely two-dimensional flow with $u = u(y,t)$ and $f(t) = 0$ in (2.2). This reduces (2.2) to the one-dimensional diffusion equation $u_t = u_{yy}$. Assuming a uniform rectangular mesh, and letting r denote the usual stability ratio $r = v\Delta t/\Delta y^2$, we are led to the Courant-Friedrichs-Lewy difference approximation of Chap. 3, §3

$$(2.4) \quad u_j^{n+1} = u_j^n + r[u_{j+1}^n - 2u_j^n + u_{j-1}^n]$$

on a 4-point stencil. Eq. (2.4) reduces for $r = 0.5$ to the Liebmann method

$$(2.5) \quad u_j^{n+1} = (u_{j-1}^n + u_{j+1}^n)/2 ,$$

invented in 1918. This optimal mesh-ratio uses a 3-point stencil, and makes the domain of dependence a staggered mesh. We next recall a few well-known facts about the difference schemes (2.4) and (2.5).⁶

Like the analytical theory of the diffusion equation $u_t = u_{yy}$, the theory of (2.5) is simplest on an infinite line. When

⁵The article by G.I. Taylor in [H1] shows how to use the soap film analogy to obtain the steady flow through a pipe.

⁶For a fuller account, see Richtmyer and Morton [C9, Ch. 8]. Chap. VI of Richtmyer's original book contains a very readable account; Varga is also excellent.

iterated, it gives rise for the 'delta-function' initial data

$$u_0^0 = 1 \quad \text{and} \quad u_j^0 = 0 \quad \text{for} \quad j \neq 0$$

to the binomial probability distribution. Hence, for general initial data, the approximate solution is given by the convolution of the initial data with this distribution. Using Stirling's asymptotic formula for factorials, we can deduce the result that, for $r = 1/2$, the approximate solution indeed converges as $\Delta y \rightarrow 0$ to the exact solution of $u_t = \nu u_{yy}$, which is the convolution of the Laplace kernel with the initial data, the kernel being $t^{-1/2} \exp(-y^2/4\nu t)$ up to a constant factor.

Unfortunately, the Courant stability restriction $\Delta t \leq \Delta y^2/2\nu$ imposed on the time step of the Liebmann method is very severe with a fine mesh. If we set $u_j^0 = (-1)^j$, then $u_j^n = (1-4r)^n u_j^0$, which grows exponentially in magnitude with oscillating sign if $r > 1/2$. In fact, the solution "explodes", in the sense that the rate of exponential growth in time tends to infinity as $\Delta y \rightarrow 0$. --On a finite interval, the solution of (2.5) for the initial data $u_j^0 = (-1)^j \sin(j\pi/n)$ behaves similarly, but the growth factor no longer has a simple mathematical expression.

Neglecting possible turbulence effects (i.e., at low Reynolds numbers), the 'coast-down' of parallel flow in a pipe of general cross-section can be treated similarly. Instead of (2.5), the optimal choice of r for the explicit (CFL) difference approximation to (2.2) is:

$$(2.6) \quad u_{j,k}^{n+1} = \frac{1}{4} [u_{j+1,k}^n + u_{j,k+1}^n + u_{j-1,k}^n + u_{j,k-1}^n] .$$

This approximates (2.2) with $f = 0$ for $\Delta t = h^2/4\nu$, with $\Delta x = \Delta y = h$. On the boundary profile γ , one sets $u \equiv 0$.

Crank-Nicolson method. One can circumvent the time-step limitation, and at the same time achieve a higher (trapezoidal) order of accuracy in Δt , by replacing (2.4) by the implicit Crank-Nicolson approximation

$$(2.7) \quad u_j^{n+1} = u_j^n + r(\delta^2 u_j^n + \delta^2 u_j^{n+1})/2 .$$

This ΔE is stable for all positive r ; moreover because the coefficient-matrix of the unknown vector \underline{u}^{n+1} is tridiagonal, the system of equations (2.7) can be solved with only a moderate amount of extra work (a factor three).

The one-dimensional equation $u_t = \nu u_{xx}$ provides excellent illustrations of the principles of error analysis and stability analysis summarized in Appendices F and G. Richtmyer-Morton [C9, pp. 189-91] lists 14 different approximations to this DE, and discusses a few of their properties. Some of these are stated in the Exercises at the end of this section. However, the two-dimensional case is far more typical (and challenging!).

Square pipes. Parallel flows in pipes having a square (or rectangular) cross-section can be approximated similarly, and have an almost identical error analysis. (This is because the matrix A_h for the semi-discretization, $u_t = A_h u$, is the tensor product of two tridiagonal matrices, with eigenfunctions $\sin(k\pi x/a)\sin(k\pi y/b)$.) Again, their error analysis provides an excellent source of exercises, and the 'explicit' CFL method of Chap. 3, §3, applies with trivial modifications.

However, implicit schemes like the Crank-Nicolson method can no longer be simply and efficiently combined with band elimination in two or more space dimensions; the operation count with $h = 1/n$ becomes $O(n^4)$. For a rectangular pipe, one can use Fast Fourier Transforms or direct ("tensor product") factorization.

Iterative methods can also be used. One can make a good initial guess by extrapolation in time (secant or parabolic); moreover the relevant matrix is strictly diagonally dominant; and one can store its LU-decomposition.

Another practical alternative is to use parabolic ADI; still another alternative (but more complicated in practice), is to achieve higher-order accuracy in time by using Padé

approximations. For these procedures, we refer the reader to the literature.⁷

Circular pipe. The case of a pipe with circular cross-section brings out another class of difficulties, associated with optimizing difference (or finite element) approximations to (self-adjoint) elliptic operators on plane domains with curved boundaries. This optimization problem is discussed at length in a forthcoming paper with R.E. Lynch, and only one simple procedure will be described here.

This consists in overlaying the first quadrant with a square mesh with mesh length $h = a/n$, and selecting a suitable $r = \nu \Delta t / h^2$. The difficulty with the 'irregular stars' on the boundary can be handled by using the analogy with a D.C. electrical resistance network.

Electrical analogy. In this analogy, each mesh segment \overline{PQ} is represented by a wire of suitable conductance κ and the value of u at each mesh-point ("node") is interpreted as the voltage there. Kirchoff's node law then states the algebraic sum $\sum_{\lambda=1}^4 \kappa_{\lambda} (u_0 - u_{\lambda})$ of the currents into and out of each node must be zero. At strictly interior mesh-points, where four mesh segments of lengths h meet, as in Fig. 1a, this reduces to

$$4u_0 = u_1 + u_2 + u_3 + u_4 ,$$

For the 'irregular stars' of Figs. 1b and 1c, respectively, the

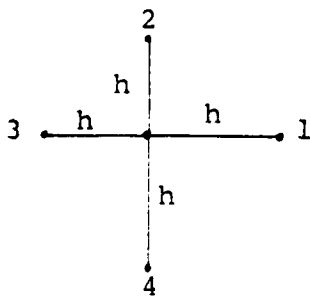


Fig. 1a

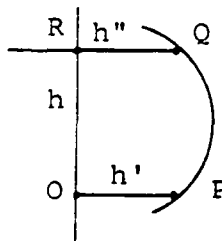


Fig. 1b

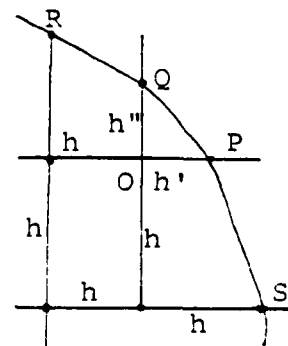


Fig. 1c

⁷ See Forsythe-Wasow, Chaps. 11-17; Richtmyer-Morton [C9, Chap. 8]; Varga, Chap. 8; Jim Douglas, Jr., and Todd Dupont, SYNSPADE 1970, pp. 130-214.

conductances should be (taking the conductance of a strictly interior mesh point as unit): $\kappa(\overline{OP}) = h/h'$ and $\kappa(\overline{OR}) = (2h+h'+h'')$ in Fig. 1b, for example.

3. Nearly parallel flows. Nearly parallel flows arise in a variety of circumstances: as boundary layers, as flows in straight pipes at Reynolds numbers in the range $500 < Re < 2000$, and in lubricating films. We will discuss lubricating films first.

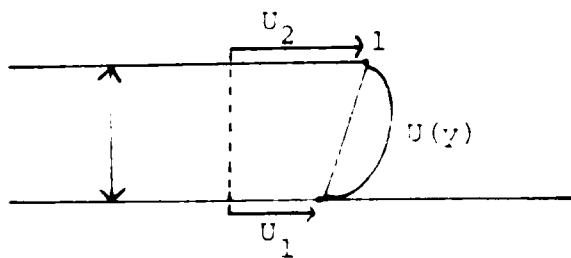
Hydrodynamics of lubrication. Although it is natural to think of lubrication primarily as the art of reducing friction (i.e., shear stress), a little reflection makes it obvious that in order to support heavy rotating machinery, the pressure in lubricating oils must in fact be much greater than the shear stress.

If $h(x,z)$ denotes the clearance separating the two surfaces whose sliding past each other is to be lubricated, then one can derive the relevant differential equation

$$(3.1) \quad \frac{\partial}{\partial x} [h^3 \frac{\partial p}{\partial x}] + \frac{\partial}{\partial z} [h^3 \frac{\partial p}{\partial z}] = 6\mu (U_1 + U_2) \frac{\partial h}{\partial x},$$

using a quite simple intuitive argument due to Osborne Reynolds. It assumes that ρ and μ are constant, that the solid surfaces move parallel to the (vertical) (x,y) -plane, and that U_1 and U_2 are the speeds at which the surfaces are moving in the x -direction.

When the solid surfaces bounding the lubricating film have radii of curvature $R_1(x,z)$ much larger than $h(x,z)$, it seems reasonable to assume that the flow near any point is essentially a parallel flow between the walls $y = 0$ and $y = h$. This pressure gradient must be essentially parallel to the (x,z) -plane, since there is negligible room for transverse acceleration. If it were zero, the flow would be the pure 'shear' flow with linear velocity profile $(U_2 + [U_1 - U_2]y/h, 0, 0)$ and constant shear stress $\mu(U_1 - U_2)/h$. The local pressure gradient will cause a parabolic deviation from this of $[y(h-y)/2\mu](\partial p/\partial x, \partial p/\partial z)$, inducing a flux of volume equal to



$$\underline{F} = \frac{1}{2\mu} \int_0^h \{y(h-y) dy\} (\partial p/\partial x, \partial p/\partial z) = (-h^3/12\mu) (\partial p/\partial x, \partial p/\partial z)$$

On the other hand, the linear velocity profile will cause a net flux of $(h[U_1+U_2]/2, 0)$. Because of incompressibility, the divergence of the total flux must be zero, giving (3.1).

In an unusually rigorous derivation of Eq. (3.1) from the Navier-Stokes equations, Pinkus and Sternlicht [G8, p. 6] point out that they make use of the following assumptions:⁸

1. The height of the fluid film y is very small compared to the span and length x, z . This permits us to ignore the curvature of the fluid film, such as in the case of journal bearings, and to replace rotational by translational velocities.
2. Negligible variation of pressure across the fluid film. Thus

$$\frac{\partial p}{\partial y} = 0$$

3. The flow is laminar; no turbulence occurs anywhere in the film.
4. Gravity forces on the film are negligible.
5. Fluid inertia is small compared to the viscous shear.
6. Only velocity gradients (nearly) perpendicular to the solid surfaces need be considered. They also remind their readers of the general assumptions underlying Model #3.
7. No slip at the solid surfaces.
8. Viscosity is isotropic and independent of the rate of shear.

From these approximations, (3.1) can be derived by the following argument.

The flow in the gap between two sliding surfaces is the vector sum of the flows (both nearly parallel to these surfaces) due to: (i) the pressure gradient, and (ii) the tangential motion of the surfaces, respectively. The flow due to the pressure gradient has a locally parabolic profile: $u = U_y(h-y)$, $v = V_y(h-y)$. From this it follows that

⁸So as to be able to treat gas lubrication, they allow ρ to be variable. They derive our (3.1) as the special case $\rho = \text{const.}$

$$\nabla p = -2 (U,V) \quad (\text{Navier-Stokes}) .$$

Moreover since $\int_0^h y(h-y)dy = h^3/6$, the rate of volume flux is $\underline{Q}' = [h^3/6](U,V)$. Combining, we get $\underline{Q}' = -(h^3/12\mu)\nabla p$, as in (3.2).

In almost all cases, the two surfaces bounding a lubricating film are moving parallel to each other, with velocities $(U_1,0)$ and $(U_2,0)$. Their motion induces an average velocity of $(U_1+U_2,0)$ and a linear velocity profile. Hence the additional volume flux is

$$\underline{Q}'' = (h/2)(U_1+U_2,0) .$$

Setting $\underline{Q} = \underline{Q}' + \underline{Q}''$, (3.1) follows since, because of volume conservation, $\text{div } \underline{Q} = 0$. Q.E.D.

Our concern here is primarily with solving Eq. (3.1), not with deriving it. In the one-dimensional case of no side leakage of the lubricant, classic analytical solutions refer to a plane 'slider' bearing sliding over a plane, and a cylindrical 'journal' of radius R resting on a cylindrical bearing of radius $R+\delta$.

Slider bearing. In this case, by suitably locating the origin, we can assume that $h = cx$. We can then substitute into (3.1) and integrate, getting [G1, p. 125]

$$(3.3) \quad p'(x) = -6\mu U_1 \left(\frac{1}{h^2} - \frac{h_1}{h^3} \right) = - \frac{6\mu U_1}{c^2} \left(\frac{1}{x^2} - \frac{x_1}{x^3} \right) ,$$

where $h_1 = h(x_1)$ is the clearance h where $p'(x) = 0$ --i.e., where the pressure is a maximum.

If the slider extends from $x = a$ to $x = b$, we must have $p(a) = p(b) = p_{\text{atm}}$. Solving (3.3) and choosing h_1 so as to make these boundary conditions compatible, we get as in [G1, pp. 126-7]:

$$(3.4) \quad p - p_{\text{atm}} = \frac{6\mu U}{c^2(a+b)} \left(\frac{a+b}{x} - \frac{ab}{x^2} - 1 \right) ,$$

where we have set $U_2 = 0$ and $U_1 = U$, the natural assumptions. The mean pressure is

$$\bar{p} - p_{\text{atm}} = \frac{6\mu U}{c^2} \left\{ \frac{1}{b-a} \ln \frac{b}{a} - \frac{2}{b+a} \right\}$$

and the friction is $(\mu U/c) \ln (b/a)$.

The case of a cylindrical journal of radius r , resting on a semi-cylindrical bearing of radius $r+\delta$, is much more complicated algebraically. The journal will find equilibrium with its center O at a distance ϵ from the center O' of the bearing, where OO' makes an angle ψ with the vertical. The equilibrium position will make the vector thrust (O,Y) , where Y is the total load.

In this particular case, the solution can be expressed in closed form by elementary functions.⁹ However in most cases, one must integrate (3.1) numerically. Since (3.1) is the DE of a linear source problem, this is easy using ELLPACK.

⁹ Sommerfeld gave the classic formulas in Zeits. Math. Phys. 50 (1904), 97- .

4. Two time-dependent examples. In this section, we will study two time-dependent plane flows that illustrate in a simple way some basic difficulties. We first consider time-dependent Couette flows between rotating cylinders, assuming (because of translational symmetry along the axis and rotational symmetry around it) that the velocity $v = u_\theta$ is purely circumferential, and that $v = v(r,t)$.

A first surprising fact is the result that the flow is not determined by the convection-diffusion equation $D\zeta/Dt = \nu \nabla^2 \zeta$. This is easily seen by considering the uniformly accelerated, locally irrotational Couette flow defined mathematically by

$$(3.1) \quad v(r,t) = t/r, \quad a \leq r \leq b,$$

as an initial value problem. The fluid is initially motionless; the walls are then accelerated uniformly with accelerations $v_t(a,t) \equiv 1/a$ and $v_t(b,t) \equiv 1/b$. Since the flow is locally irrotational, with velocity potential $\phi = t\theta$, it has zero vorticity: $\zeta \equiv 0$ thus trivially satisfies the vorticity equation $D\zeta/Dt = \nu \nabla^2 \zeta$. Yet it is obvious that whirling the walls as indicated does not instantaneously (at least for small ν) carry the fluid with it!

The explanation is obvious: since θ is multiple-valued, it requires internal torque to drive the motion! (A pressure jump $\Delta p = 2\pi/\rho$ across a radial 'cut' would give at least the initial acceleration.) For us, the main corollary is the fact that we cannot simply 'integrate' the DE (1.3)--and that this difficulty applies to doubly (or multiply) connected domains generally. It is necessary to consider the shear stress as well as the pressure.

Actually, the same is true of time-dependent flow in a channel, if we allow a nonzero pressure gradient to act; see Exs. 2-3 at the end of this section. However, time-dependent 'Couette' flow differs from time-dependent 'Poiseuille' flow in that whereas the velocity held $u(y,z;t)$ is governed by the diffusion equation $u_t = \nu[u_{yy} + u_{zz}]$ in the latter, this is not true of $v = u_\theta$ in Couette flow. Instead, letting $v = u_\theta$ be the angular component of velocity, the governing DE is

$$(4.2) \quad v_t = v[v_{rr} + \frac{1}{r} v_r - v/r^2] .$$

The last term, which is absent in the case of heat conduction (and pure diffusion), is associated with the principle of conservation of moment of momentum, as we shall see.

We first compute the angular component of shear stress, $\sigma_{r\theta}$. Since rotation with constant angular velocity $\omega = v(r)/r$ has zero rate-of-strain, the angular component of the rate-of-strain is clearly

$$r(\partial\omega/\partial r) = v'(r) - v(r)/r .$$

Hence the circumferential shear stress is $\sigma_{r\theta} = \mu[v'(r) - v(r)/r]$, the resultant force $2\pi r$ times this, and the moment (or 'torque')

$$(4.3) \quad N(r) = 2\pi r \mu [rv'(r) - v(r)]$$

The net moment on the ring (of mass $2\pi\rho r dr$) of fluid between r and $r+dr$ is therefore

$$N'(r)dr = 2\pi\mu[r^2v''(r) + rv'(r) - v(r)] dr.$$

The rate of increase of the moment of momentum being $2\pi\rho r^2 v_t(r)dr$, we therefore have

$$(4.4) \quad \rho v_t = \mu[v''(r) + \frac{1}{r} v'(r) - v(r)/r^2] ,$$

as claimed in (4.2).¹⁰ This can be integrated numerically by the methods of §2.

Rectangular cavity. A favorite example with which to illustrate the basic idea underlying computations of time-dependent incompressible viscous flows is the flow in the rectangular cavity $[0,a] \times [0,b]$, induced by sliding one wall against a fluid initially at rest. The mathematical problem is to solve the DE $u_t = \nu(u_{xx} + u_{yy})$

¹⁰Cf. Batchelor [B1, §4.5].

in the rectangle specified, for given initial conditions $\underline{u}(\underline{x};0) = (u(x,y;0), v(x,y;0))$, and the boundary conditions

$$(4.5) \quad \underline{u}(0,y;t) \equiv (0,1) ,$$

and $\underline{u}(\underline{x};0)$ on the other three walls. Knowing the vorticity $\zeta(x,y;t_n)$ at time t_n , one can determine the stream function $\psi(x,y;t_n)$ by solving the Poisson DE

$$(4.6) \quad -\nabla^2 \psi = \zeta, \quad u = \partial \psi / \partial y, \quad v = -\partial \psi / \partial x ,$$

and then use the vorticity equation

$$(4.7) \quad \partial \zeta / \partial t = \nu \nabla^2 \zeta = -u \partial \zeta / \partial x - v \partial \zeta / \partial y ,$$

to determine (approximately) $\zeta(x,y;t_{n+1})$. The rest of this section will be concerned with the efficient implementation of (4.6)-(4.7).

Staggered mesh. The adoption of a 'staggered mesh' in incompressible plane flow problems greatly facilitates the consistent use of first central differences.¹¹ For convenient reference, the appropriate mesh is displayed in Figure 2; it will help to explain the notation $p_{i,j}^m$, $u_{i\pm 1/2}^m$, $v_{i,j\pm 1/2}^m$, $\psi_{i\pm 1/2,j\pm 1/2}^m$ used in the difference formulas below. For simplicity, we will assume a square mesh of side h , but analogous formulas hold for a uniform rectangular mesh of sides $\Delta x = h$ and $\Delta y = k$. Typical difference formulas in this mesh are:

$$u_{i+1/2,j} = (\phi_{i+1,j} - \phi_{i,j})/h = (\psi_{i+1/2,j+1/2} - \psi_{i+1/2,j-1/2})/h$$

$$\begin{aligned} \zeta_{i+1/2,j+1/2} &= (v_{i+1,j+1/2} - v_{i,j+1/2})/2h + (u_{i+1/2,j+1} - u_{i+1/2,j})/h \\ &= (\psi_{i+3/2,j+1/2} + \psi_{i+1/2,j+3/2} + \psi_{i-1/2,j+1/2} \\ &\quad + \psi_{i+1/2,j-1/2} - 4\psi_{i+1/2,j+1/2})/h \end{aligned}$$

¹¹This is used in the MAC codes mentioned in Chap. 3, §12; cf. Roache [C14], p. 197. Roache does not treat viscosity.

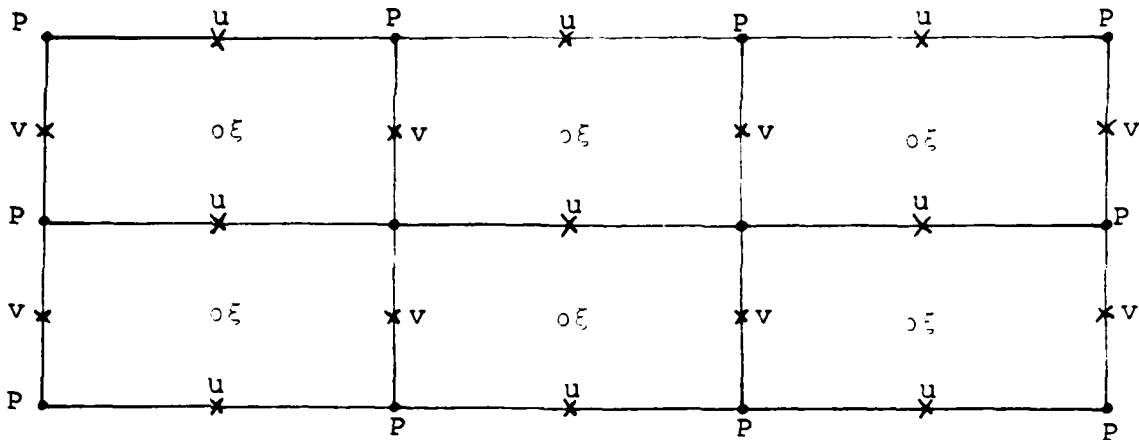


Figure 2

LOCATION of 'AVERAGE' PHYSICAL QUANTITIES in a TYPICAL MESH SQUARE:

ϕ, p, u_x, v_y are at the mesh-points (x_i, y_i) (the "nodes of the mesh").

u, u_t are at the midpoints $(x_{i+1/2}, y_j)$ of horizontal mesh segments.

v, v_t are at the midpoints $(x_i, y_{j+1/2})$ of vertical mesh segments.

ψ, ζ, u_y, v_x and their time derivatives are at the centers of mesh squares.

Solution of (4.6). To solve the Poisson DE (4.6) in a square (or rectangle) for the boundary condition $\psi = 0$ of the flow penetration (the boundary a streamline) is a "model problem" for whose solution many methods are available. The Fast Fourier Transform (FFT), implemented in a package called FISHPAK,¹² is to be recommended as exceptionally efficient. Denoting $i+1/2$ and

¹²By Swartztrauber and Sweet at the National Center for Atmospheric Research in Boulder, Colorado.

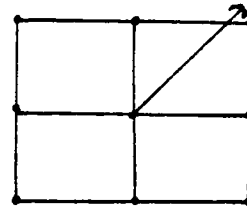
$j+1/2$ by i' and j' , the problem is to solve

$$(4.8) \quad \psi_{i',j'} = \frac{1}{4}[\psi_{i'+1,j'} + \psi_{i',j'+1} + \psi_{i'-1,j'} + \psi_{i',j'-1}] + h^2 \zeta_{i',j'}/4$$

In a unit square, the mesh-lengths $h = 1/16, 1/32, 1/48, 1/64$ are to be recommended.

Solution of (4.7). To solve the vorticity equation (4.7) is less standard; unless Lagrangian coordinates are used, it is very hard to avoid numerical diffusion of vorticity, which is, of course, spurious. In the example chosen, this is not too serious, but in calculating the evolution of a vortex sheet, it would be. For smooth flows at moderate Re ,

since there is no flow across the boundary, one can take a time-step Δt long enough so that, away from the boundary, 1-3 mesh squares are traversed



per step. Using a predictor-corrector (modified Euler) method, perhaps iterating more than once so as to approximate trapezoidal integration (Crank-Nicolson), and then correcting for physical diffusion, fairly good results can be hoped for.

5. Vorticity transport. The preceding problems illustrate the basic mechanism underlying two-dimensional incompressible viscous flows: that they are governed by the convection and diffusion of vorticity (and boundary conditions; see below). We will now examine this mechanism more closely, with special reference to its accurate and efficient numerical simulation.

To this end, we will first rewrite the difference equations at the end of §3, in a changed notation. We will index ζ and ψ by integers, and set $i' = i-1/2$, $i'' = i+1/2$, $j' = j-1/2$, and $j'' = j+1/2$ to simplify the notation. We recall the vorticity equation

$$(5.1) \quad D\zeta/Dt = \partial\zeta/\partial t + u\partial\zeta/\partial x + v\partial\zeta/\partial y = \nu\nabla^2\zeta,$$

and the fact that the stream function ψ can be determined from the DE $\zeta = -\nabla^2\psi$ and the values of ψ on the boundary, and then new values of u and v computed using the equations

$$(5.2) \quad -\nabla^2\psi = \zeta, \quad u = \partial\psi/\partial y, \quad v = -\partial\psi/\partial x.$$

For example, as a variant on the problem of §2, knowing the total amount of fluid $\psi_1(t)$ being forced through a two-dimensional channel of arbitrary cross-section as a function of time, one can set $\psi(t) \equiv 0$ on the lower wall and $\psi(t) = \psi_1(t)$ on the upper wall of the channel, and compute from these time-dependent plane Poiseuille flow. The next step consists in discretizing (5.1)-(5.2).

In the above notation, evidently

$$(5.3) \quad hu_{i,j'} = \psi_{i,j} - \psi_{i,j-1}, \quad hu_{i,j''} = \psi_{i,j+1} - \psi_{i,j},$$

with $O(h^2)$ accuracy, while

$$(5.4) \quad \begin{aligned} h^2\zeta_{i,j} &= h[u_{i,j'} - u_{i,j''} - v_{i',j} + v_{i'',j}] \\ &= 4\psi_{i,j} - \psi_{i,j} = -[\delta_{xx} + \delta_{yy}]\psi_{i,j}, \end{aligned}$$

also with $O(h^2)$ accuracy, as can be verified as assuming that $\psi \in C^4$, as is always the case in the interior of the flow.

Convection and diffusion. Equation (5.1) exhibits the Navier-Stokes equations for plane flows as representing a balance between convection and diffusion (of vorticity). A similar balance is achieved by the concentration $\sigma(\underline{x};t)$ of any chemical quantity being transported by a known velocity-field $\underline{u}(\underline{x};t)$. It is governed by the linear DE $\sigma_t + \underline{u} \cdot \nabla \sigma = \alpha \nabla^2 \sigma$, where α is the diffusivity.

Thus, in a time-independent plane velocity field $(u(x,y), v(x,y))$, one can use the following crude two-step method. At each time-step, one can first approximate the effect of pure convection by

$$(5.5) \quad \bar{\sigma}(x,y,t+\Delta t) = \sigma(x-u\Delta t, y-v\Delta t, t),$$

where the right side is approximated by bilinear interpolation:

$$(5.6) \quad \sigma(x_i+\theta h, y_j+\tilde{\theta} h) = \theta' \tilde{\theta}' \sigma_{i,j} + \theta \tilde{\theta}' \sigma_{i+1,j} \\ + \theta' \tilde{\theta} \sigma_{i,j+1} + \theta \tilde{\theta} \sigma_{i+1,j+1}.$$

The mesh square in which (5.6) is to be applied depends on the quadrant in which $(u,v)_{i,j}$ lies (as in the Box Method), and $\theta' = 1-\theta$, $\tilde{\theta}' = 1-\tilde{\theta}$. For stability, one must make $\Delta t \leq h/\max[u,v]$.

Reynolds number effects. For a given representative length scale d and velocity scale U , clearly the right side of (5.1) is dominant when $Re = Ud/\nu \ll 1$, while the left side is dominant when $Re \gg 1$. This becomes especially obvious if we multiply (5.1) by ρ , to get

$$\rho \left[\frac{\partial \zeta}{\partial t} + u \frac{\partial \zeta}{\partial x} + v \frac{\partial \zeta}{\partial y} \right] = \mu \nabla^2 \zeta.$$

As $\rho \rightarrow 0$, we get the limiting case of 'Stokes' or 'creeping' plane flow. This is evidently governed by the biharmonic equation

$$(5.7) \quad \nabla^4 \psi = \nabla^2 (\nabla^2 \psi) = -\nabla^2 \zeta = 0,$$

whose numerical solution will be discussed in §6.

Conservation law form. At the opposite extreme, setting $\mu = 0$ (i.e., in the case of an ideal fluid), we get the 'conservation law form' of the vorticity equation:

$$(5.8) \quad \partial \zeta / \partial t + \operatorname{div}(\mu \mathbf{u}) = 0 .$$

This expresses Kelvin's conservation law for circulation $\Gamma = \iint \gamma \, dx dy$, and holds in the 'plane vortex flows' discussed briefly in Chap. 1, §10. Unfortunately, there seems to be no analogous 'conservation law form' in the viscous case.¹³

In between these two extremes, one finds a dazzling variety of real flows (cf. Chap. 2, §9), and a corresponding variety of 'optimal' numerical methods. This is especially surprising for incompressible viscous flows satisfying time-independent boundary conditions. Thus ordinary wakes become periodic when $Re > 60$ or so; flow in pipes often becomes turbulent when $Re > 2000$; boundary layers are typically turbulent when $Re > 2 \times 10^5$.

It is suggestive and sometimes convenient to express this dependence by rewriting the governing DE in terms of dimensionless variables. These can be defined by setting $\mathbf{x}' = \mathbf{x}/d$, $t' = tU/d$, $\mathbf{u}' = \mathbf{u}/U$, and $p' = (p-p_0)/\rho U^2$. In physical language, this 'rescales' the problem (by choice of unit) so as to make $\rho = d = U = 1$, and to express the pressure in multiples of twice the stagnation pressure. Of course, it does not model cavitation phenomena (e.g., boiling) or gravity effects (e.g., free convection).

In terms of the new variables, the incompressibility condition still holds (we have $\nabla \cdot \mathbf{u}' = 0$), while the Navier-Stokes equations assume the dimensionless form

$$(5.9) \quad \frac{\partial u'_i}{\partial t'} + \sum_k u'_k \frac{\partial u'_i}{\partial x'_k} = - \frac{\partial p'}{\partial x'_i} + \frac{1}{Re} \nabla^2 u'_i .$$

The rest of this chapter will be devoted to describing numerical techniques that have successfully predicted observed velocity fields in some especially simple limiting cases, at moderate cost.

¹³ Formula (2.10) in Roache [C14, p. 11] is incorrect, because it omits the shear stress boundary term.

After considering experience with the simpler models discussed in Chapters 4-6, it seems not surprising that, when $Re > 10^3$ (as is commonly the case), to make accurate and reliable predictions is still extremely difficult and expensive.

6. Stokes flows. We have already stated, in Chap. 2, §11, some of the basic analytical properties of time-independent 'Stokes flows', in the limit as $Re \downarrow 0$. In this section, we will consider their numerical determination.

After eliminating gravity as usual (in homogeneous fluids of constant density) by considering $P = p + \rho G$ instead of the ordinary pressure p , the assumption that the convective acceleration $\sum u_k \frac{\partial u_i}{\partial x_k}$ is negligible in comparison with the true acceleration $\partial u_i / \partial t$ leads to the time-dependent Stokes (or 'creeping flow') approximation

$$(6.1) \quad \rho \frac{\partial u_i}{\partial t} = \mu \nabla^2 u_i - \partial P / \partial x_i .$$

Taking the curl of the preceding DE, we see that in plane flows, the vorticity $\zeta = v_x - u_y$ satisfies

$$(6.2) \quad \rho \frac{\partial \zeta}{\partial t} = \mu \nabla^2 \zeta ,$$

a pure diffusion equation. This can be semi-discretized at interior points with $O(h^2)$ accuracy by the difference approximation of §4, on the staggered mesh described there.¹⁴ However, the approximation of the boundary condition of no slip is more difficult to interpret in terms of ζ .

Roache [C14, pp. 139-41] comments at length on this difficulty, and recommends using (at least along straight walls) the following formula due to Thom:

$$(6.3) \quad \zeta_w = 2(\psi_{w+1} - \psi_w) / \Delta n^2 .$$

He derives this formula by a Taylor series expansion, and cites numerical experiments of C.E. Pearson¹⁵ to support its practical validity.

¹⁴ Using a 9-point difference approximation, $O(h^4)$ accuracy can be achieved.

¹⁵ J. Fluid Mech. 21 (1965), 611-33. For Thom's work, see Proc. Roy. Soc. A141 (1933), 651-66, and his comments in Chap. 11 of A. Thom and C.J. Apelt, "Field Computations in Engineering and Physics," van Nostrand, 1961.

Boundary conditions. Along a flat wall parallel to the x-axis, either stationary or moving with constant velocity U parallel to itself, we clearly have $u = \text{const.}$, and so

$$(6.4) \quad u_x = u_{xx} = v = v_x = v_{xx} = 0 .$$

Since $u_x + v_y = 0$ in plane flow, we also have $v_y = 0$ there. Consequently, u_y is the only nonzero entry in the 'rate of strain' matrix

$$\begin{pmatrix} u_x & u_y \\ v_x & v_y \end{pmatrix} ,$$

giving rise to a pure shear stress

$$\begin{pmatrix} 0 & u_y \\ 0 & 0 \end{pmatrix} .$$

For the same reason, $\zeta = v_x - u_y = -u_y$, and the shear stress is also

$$\begin{pmatrix} 0 & \zeta \\ 0 & 0 \end{pmatrix} .$$

This is not true in the case of a circular wall of radius a rotating with angular velocity ω about $(0,a)$, for example. Near $(0,0)$, we have $(u,v) = \omega(a-y,x)$ and so $\zeta = u_y = v_x = -2\omega$, instead of $\zeta = \omega$.

Square cavity. The preceding remark illustrates the practical complexity of solving numerically even the linear, parabolic DE (6.2) for time-dependent plane Stokes flows inside cavities and around obstacles of general shape. Therefore, we will consider only the simplest case of steady flow in a square cavity, already mentioned in §4, and treated in detail by Chow (with a computer program) in [G2, pp. 276-89]. We will, however, contrast the boundary conditions of §4 with those of constant shear stress S ,

$\zeta = S/\mu$ on the fourth wall. Thus, we will contrast the problem of solving $\nabla^4\psi = 0$ for the boundary conditions of given ψ and $\partial\psi/\partial n$, with that of solving the same DE for given ψ and $\zeta = \partial^2\psi/\partial n^2$. Both problems have analogues in the theory of the bending of flat elastic plates, about which more is known than about plane Stokes flows.

Plate bending analogy. In this theory, 'plates' with given boundary ψ and $\partial\psi/\partial n$ are called clamped plates, while the latter are said to be simply supported. Both cases have been extensively treated,¹⁶ and the numerical treatment of Stokes flows can be largely based on that for elastic plates--in which the inhomogeneous DE $\nabla^4\psi = f(x,y)$ of a loaded plate is most interesting.

Variational principle. Much as the solution of the Laplace equation $\nabla^2\phi = 0$ for given boundary values ('Dirichlet-type' boundary conditions), minimizes the Dirichlet integral

$$\iint (\phi_x^2 + \phi_y^2) dx dy ,$$

so solutions of the biharmonic DE $\nabla^4\psi = 0$ for given boundary values ψ and normal derivatives $\partial\psi/\partial n$ minimize the integral

$$(6.3) \quad \iint (\nabla^2\psi)^2 dx dy = \iint (\psi_{xx} + \psi_{yy})^2 dx dy$$

This minimum principle for biharmonic functions, discovered in 1868 by Helmholtz in the context of Stokes flows, asserts that any Stokes flow minimizes the rate of conversion of mechanical energy into heat.

¹⁶See T. Szilard, "Theory and Analysis of Plates", Prentice-Hall, 197 . His Chap. 3 (pp. 158-324) deals with numerical methods.

7. Finite element methods. The variational principles just stated have many analogues, e.g., for inhomogeneous elliptic problems and for elliptic DE's with variable coefficients. It is not surprising that such problems arise in statics, since equilibrium states typically minimize the potential energy. It is their occurrence in fluid dynamics that is truly remarkable. Thus, not only do plane Stokes flows minimize $\iint_{\Omega} \zeta^2 dx dy$, as Helmholtz showed in 1868, but three-dimensional Stokes flows minimize $\iiint |\underline{\omega}(\underline{x})|^2 dR$ under a variety of conditions [A6, Arts. 329, 344].

In both solids and fluids, variational principles characterize the solutions of elliptic boundary value problems of order $2p$ as those functions u which minimize an integral of a quadratic function of u and its partial derivatives of order p or less. The exact solution is then approximated by constructing a finite-dimensional approximating subspace of a suitably chosen function space, and then minimizing the integral of interest in this subspace.¹⁷ Since solutions of elliptic boundary value problems are typically smooth, it is much easier to construct satisfactory approximating subspaces of moderate dimension (300 or so) for elliptic than for hyperbolic problems.

The following construction describes the most commonly used procedure for constructing such 'approximating subspaces'. First, the domain Ω is subdivided into triangles ("triangulated") or rectangles (or other quadrangles), in each of which the function $\psi(x,y)$ is approximated by some elementary (usually polynomial or rational) function.

For the potential flows discussed in Chap. 4, continuous and piecewise linear (in triangles) or bilinear (in rectangles) functions ordinarily suffice. The minimization of the Dirichlet integral gives a 9-point approximation. These approximating functions are uniquely determined (through interpolation) by 'nodal values' assumed at the mesh-points, and define globally continuous piecewise linear (or bilinear) functions where Dirichlet integrals are computable by simple algebraic formulas.

¹⁷ This is called the Rayleigh-Ritz method; Rayleigh and Ritz however used small subspaces of globally defined functions.

However, for fourth-order DE's, the relevant variational principle only applies to continuously differentiable functions. Procedures for constructing such functions are said to provide 'conforming' finite elements. In the case of a rectangular cavity, in whose interior a fluid is impelled by sliding one side, very good approximating subspaces are provided by piecewise bicubic Hermite and spline approximants.

Piecewise bicubic Hermite subspace. For a given rectangular subdivision π , the subspace $h_3(\pi)$ of piecewise bicubic Hermite polynomials corresponds one-one to the specification of numerical values of u, u_x, u_y, u_{xy} at all mesh-points. Given these values, a unique 'conforming' (i.e., C^1) piecewise bicubic interpolant to them can be constructed, with four components.

$$\begin{aligned} \text{Even-even:} & \quad 1, x^2, y^2, x^2y^2 \\ \text{Even-odd:} & \quad y, x^2y, y^3, x^2y^3 \\ \text{Odd-even:} & \quad x, xy^2, x^3y, x^3y^2 \\ \text{Odd-odd:} & \quad xy^3, x^3y, xy^3, x^3y^3. \end{aligned}$$

By utilizing the indicated symmetries (with respect to an origin at the centroid of each rectangle) the coefficients of the relevant polynomial $\sum_{i,j} a_{ij} x^i y^j$ can be computed by solving 4 sets of four simultaneous linear equations, each in as many unknowns.

Bicubic spline subspace. In any rectangle Ω with sides parallel to the coordinate axes, subdivided by vertical lines $x = x_i$ ($i = 0, 1, \dots, I$) and horizontal lines $y = y_j$ ($j = 0, 1, \dots, J$) the twice differentiable functions constitute a 'spline' subspace of the space $h_3(\tau)$ of the preceding space, having only $(I+3)(J+3)$ as contrasted with $4(I+1)(J+1)$ unknowns. However, its use gives rise to many technical algebraic difficulties including that of using a well-conditioned basis of 'B-spline' functions whose 'support' consists of only 16 mesh points. Moreover the proper way to handle cubic splines in non-rectangular domains is still a mystery. See Carl de Boor's "A Practical Guide to Splines" for more information.

For these and other reasons, the most successful numerical treatments of Stokes flows have used more traditional finite elements.¹⁸

¹⁸See [G3]; [G9]; R. Glowinski and O. Pironneau, *Numer. Math.* 33 (1979), 397-424; J.C. Nedelec, *ibid.* 39 (1982), 97-112.

8. Boundary layers. We next take up the computation of velocity profiles in time-independent (laminar) boundary layers. Our account will be based on a 1978 survey article [G5] by H.B. Keller, himself a leading contributor to the subject.

The (parabolic) DE's to be integrated are, as in Chapt. 2, §10:

$$(8.1) \quad uu_x + vu_y = -P'(x) + (vu_y)_y,$$

the equations of motion ('momentum conservation'). Here $P(x) = p/\rho$, and $P(x) + \frac{1}{2}\rho U^2 = P_0$ is a constant, where $U = U(x) = \lim_{y \rightarrow \infty} u(x,y)$. We also have the incompressibility condition $u_x + v_y = 0$, and $u(x,0) = 0$.

To integrate the system (8.2)-(8.4) of first-order DE's in the (x,y)-plane, Keller's ingenious Box Scheme¹⁹ is recommended, as having been successfully applied to a wide variety of problems. Like the Crank-Nicolson scheme discussed earlier, it is an implicit scheme designed to treat parabolic problems in two independent variables with $O(h^2)$ accuracy and $O(h)$ time steps. (In boundary layer theory, distance in the direction of flow plays the role of time."

Specifically, as presented in [G6], Keller's Box Scheme is designed to integrate the following three partial DE's:²⁰

$$(8.2) \quad \partial u / \partial x + \partial v / \partial y = 0, \quad (\text{"continuity"})$$

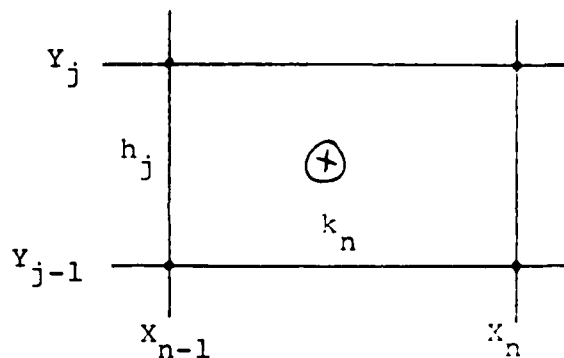
$$(8.3) \quad \tau = \nu \partial u / \partial y, \quad (\text{"shear stress"})$$

$$(8.4) \quad u \frac{\partial u}{\partial x} = \frac{\partial \tau}{\partial y} - P'(x) - \nu \frac{\partial u}{\partial y} \quad (\text{"motion"})$$

¹⁹This is not to be confused with the Box Scheme developed by H.A. Thomas in 1938, to compute the downstream progress of flood waves (a hyperbolic problem).

²⁰It is assumed that units have been chosen making $\rho = 1$; $-P'(x) = UU'(x)$, where $U = \lim_{y \rightarrow \infty} u(x,y)$ is the local velocity outside the boundary layer. $y \rightarrow \infty$

It assigns one equation to each box-shaped mesh cell, with the conventions indicated in the attached sketch. To achieve $O(h^2)$ accuracy without using a staggered mesh, the following notations are consistently adopted:



$$[w]_{j-1/2}^n \equiv \frac{1}{2}(w_j^n + w_{j-1}^n), \quad \left[\frac{\partial w}{\partial y}\right]_{j-1/2}^n \equiv \frac{1}{h_j}(w_j^n - w_{j-1}^n);$$

$$\left[\frac{\partial w}{\partial x}\right]_{j-1/2}^{n-1/2} \equiv \frac{1}{k_n}([w]_{j-1/2}^n - [w]_{j-1/2}^{n-1}).$$

(8.5)

$$\left[\frac{\partial w}{\partial y}\right]_{j-1/2}^{n-1/2} \equiv \frac{1}{2}(\left[\frac{\partial w}{\partial y}\right]_{j-1/2}^n + \left[\frac{\partial w}{\partial y}\right]_{j-1/2}^{n-1}),$$

$$[w]_{j-1/2}^{n-1/2} \equiv \frac{1}{2}([w]_{j-1/2}^n + [w]_{j-1/2}^{n-1}).$$

In this notation, Keller's Box Scheme utilizes the following difference approximations:

$$\left[\frac{\partial u}{\partial x}\right]_{j-1/2}^{n-1/2} + \left[\frac{\partial v}{\partial y}\right]_{j-1/2}^{n-1/2} = 0;$$

$$(8.6) \quad [\tau]_{j-1/2}^n = [v]_{j-1/2}^n \left[\frac{\partial u}{\partial y}\right]_{j-1/2}^n;$$

$$[u]_{j-1/2}^{n-1/2} \left[\frac{\partial u}{\partial x}\right]_{j-1/2}^{n-1/2} + [v]_{j-1/2}^{n-1/2} \left[\frac{\partial u}{\partial y}\right]_{j-1/2}^{n-1/2} = -\left[\frac{\partial p}{\partial x}\right]_{j-1/2}^{n-1/2} + \left[\frac{\partial \tau}{\partial y}\right]_{j-1/2}^{n-1/2}$$

Note Keller's treatment of the equation of continuity (8.2). Substitution into it from the notational conventions of (8.5) gives

$$(8.7) \quad \frac{1}{2\Delta x}(u_j^n + u_{j-1}^n - u_j^{n-1} - u_{j-1}^{n-1}) = \frac{1}{2\Delta y}(v_j^n - v_{j-1}^{n-1} + v_j^{n-1} - v_{j-1}^{n-1}) .$$

Thus algebraically, there are $3(J+1)$ variables and only $3J$ equations, one for each interval between mesh points. The relevant DE's may be thought of as averaged over each box.

REFERENCES for CHAP. 7

- [G1] "The Mechanical Properties of Fluids", a series of essays by eminent experts, Blackie, 1925.
- [G2] R.M. Davies (ed.), "Cavitation in Real Liquids", Elsevier, 1964.
- [G3] V. Girault and P.A. Raviart, "Finite Element Approximation of the Navier-Stokes Equations", Springer, 1979.
- [G4] W.A. Gross, "Gas Film Lubrication", Wiley, 1962.
- [G5] H.B. Keller, "Numerical Methods in Boundary Layer Theory", Annual Rev. Fluid Mech. 10 (1978), 417-33.
- [G6] R.W. MacCormack and Harvard Lomax, "Numerical solution of compressible viscous flows", Annual Rev. Fluid Mech. 11 (1979), 289-316.
- [G7] S.A. Orszag and M. Israeli, "Numerical simulation of viscous incompressible flows", Annual Rev. Fluid Mech. 6 (1974), 281-318.
- [G8] O. Pinkus and B. Sternlicht, "Theory of Hydrodynamic Lubrication", McGraw-Hill, 1961.
- [G9] R. Rautmann (ed.), "Approximate Methods for Navier-Stokes Problems", Springer Lecture Notes in Math. #771 (1980).
- [G10] Roger Temam, "Navier-Stokes Equations", North-Holland, 1977.

APPENDIX A

LAGRANGIAN DYNAMICAL SYSTEMS

Introduction. Lagrange's classic Mécanique Analytique envisaged Euler's partial differential equations for fluid dynamics in a much more general context: that of a conservative dynamical system. Denoting 'kinetic' and 'potential' energy by T and V , and assuming for simplicity a finite number of degrees of freedom, he noted that the evolution of any such system is determined by the variational equations

$$(A1) \quad \frac{d}{dt} \left(\frac{\partial L}{\partial \dot{q}_i} \right) = \frac{\partial L}{\partial q_i}, \quad \dot{q}_i = dq_i/dt.$$

Here $L(\underline{q}, \dot{\underline{q}}) = T - V$ is called the Lagrangian; the 'generalized coordinates' q_1, \dots, q_r can be arbitrary.

Eq. (A1) is the Euler-Lagrange variational equation for the condition that the action integral $\int L(\underline{q}, \dot{\underline{q}}) dt$ be stationary-- i.e., in Lagrange's notation, that $\delta \int L(\underline{q}, \dot{\underline{q}}) dt = 0$ for all infinitesimal variations $\delta \underline{q}(t)$ in 'configuration space' having the same endpoints $\underline{q}(t_0) = \underline{q}_0$ and $\underline{q}(t_1) = \underline{q}_1$. Because of this, it is often called the Principle of Least Action.¹ It was used by Liouville, Hamilton, Jacobi, and others to 'geometrize' much of mechanics, and their concepts helped to inspire the theories of relativity and quantum mechanics in the early 20th century.

The reversibility in time of Euler's equations (Chap. 1, §7) suggests that moving fluids can be treated as conservative (Lagrangian) dynamical systems having infinitely many degrees of freedom. For example, the potential flows of an ideal fluid satisfy a more complicated version of (A1), with $T = (\rho_0/2) \iiint (\nabla \phi \cdot \nabla \phi) dR$ the Dirichlet integral and $V = mg\bar{y}(t)$ where \bar{y} is the height of the center of gravity. Likewise, the theory of sound exemplifies many aspects of Lagrange's general theory of 'small

¹See C. Lanczos, "The Variational Principles of Mechanics", Univ. of Toronto Press, 1949, esp. p. 115 ff. For connections with quantum mechanics, see G.W. Mackey, "Foundations of Quantum Mechanics",

oscillations' of conservative dynamical systems (see Chapter 2, §§3-4, and Chapter 5).

Analogies between the continuum mechanics and the 'dynamics of particles and rigid bodies' having a finite number of degrees of freedom are of more than philosophical interest for numerical fluid dynamics. They also have a technical interest, because 'finite element' and other semidiscrete approximations (so-called because variations in space are discretized, but not those in time) can often be interpreted as conservative (Lagrangian) dynamical systems.

Small oscillations. In the case of dynamical systems having a finite number of degrees of freedom, the theory of small oscillations can be briefly summarized as follows. The potential energy is near its minimum value V_0 , the 'state' of stable static equilibrium. Therefore we have

$$(A2) \quad V = V_0 + \frac{1}{2} \sum a_{ij} q_i q_j ,$$

to a first approximation, the 'stiffness matrix' $A = ||a_{ij}||$ being symmetric and positive definite.

Likewise, the kinetic energy is quadratic to a first approximation in small oscillations (since $T = 0$ when $V = V_0$, $T+V$ being constant in any case). Therefore, we can write

$$(A3) \quad T = \frac{1}{2} \sum m_{ij} \dot{q}_i \dot{q}_j ,$$

where the 'inertial matrix' $M = ||m_{ij}||$ is also symmetric and positive definite.²

Evidently, $\partial L / \partial q_i = \sum a_{ij} q_j$ for all i (summation is with respect to repeated indices). Likewise, $\partial L / \partial \dot{q}_i = \sum m_{ij} \dot{q}_j$, and so $d(\partial L / \partial \dot{q}_i) / dt = \sum m_{ij} \ddot{q}_j$, in Newton's notation (whereby dots signify derivatives with respect to time). Hence the equations

²The most familiar case is that of the moments and products of inertia of a rigid body; the 'added mass' coefficients of an ideal fluid are analogous.

of motion for a conservative dynamical system undergoing 'small oscillations' are, in vector form,

$$(A4) \quad M\ddot{\underline{q}} = A\underline{q} .$$

Normal modes. By a 'normal mode' of (small) oscillation is meant one of the form $\underline{q}(t) = \underline{q}_k \begin{Bmatrix} \cos \\ \sin \end{Bmatrix} \omega_k t$. In complex form (i.e., setting $\underline{q}(t) = \text{Re } \underline{Q}(t)$), normal modes refer to solutions $\underline{Q}(t) = \underline{Q}_k e^{i\omega_k t}$. Substituting into (A4), we see that the normal modes correspond to the generalized eigenfunctions of the system

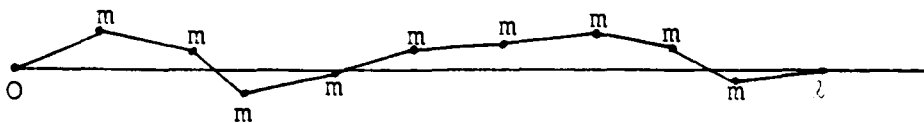
$$(A5) \quad M\underline{Q}_k + \lambda_k A\underline{Q}_k = 0 ,$$

where M and A are positive definite and symmetric. These are the stationary points of the Rayleigh quotient

$$(A6) \quad R(\underline{q}) = \underline{q}^T M \underline{q} / \underline{q}^T A \underline{q} ,$$

where $\delta R = 0$ with $\underline{q} = \underline{Q}_k \neq \underline{0}$.

Example 1. The semi-discretization of a vibrating string, first studied by John Bernoulli (in 1728), provides a classical example of a Lagrangian dynamical system. Bernoulli approximated a taut string of length ℓ , linear density ρ , and under tension τ , by $n-1$ equally spaced beads of mass $m = \rho h$, where $h = \ell/n$.



In equilibrium, the j -th particle is assumed to be at $x_j = jh$, and it is supposed free to vibrate laterally, with $y_j = y_j(t)$ and $y_0 = y_n = 0$. The kinetic energy $T = \frac{1}{2} m \sum \dot{y}_j^2$, obviously, while the potential energy of lateral displacement to distance y_j is the tension times the stretching of the string:

$$V = h\tau \sum_{j=1}^n \{1 + [(y_j - y_{j-1})/h]^2\}^{1/2}$$

In the 'small oscillation' approximation obtained by neglecting

infinitesimals of degree four, this is

$$(A7) \quad V = (\tau/2h) \sum_{j=1}^n (y_j - y_{j-1})^2$$

$$= \tau \left\{ \sum_{j=1}^{n-1} y_j^2 - \sum_{j=2}^n y_{j-1} y_j \right\} / h$$

In this example, $M = mI$ is a scalar matrix, and (A4) simplifies to

$$(A8) \quad \rho \ddot{y}_j = \tau (y_{j+1} - 2y_j + y_{j-1}) / h^2$$

This is the semidiscretization of the vibrating string equation

$$(A9) \quad y_{tt} = c^2 y_{xx}, \quad c^2 = T/\rho,$$

since the R.H.S. of (A8) is τ times the second central difference quotient.

The normal modes of vibration are given explicitly by the solutions

$$(A10) \quad y_j = \phi_{kj} = \sin \frac{kj\pi}{n} \begin{Bmatrix} \cos \\ \sin \end{Bmatrix} \omega_k t$$

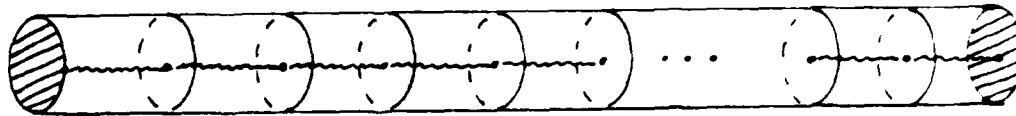
of the eigenproblem defined by

$$(A10') \quad \delta^2 y_j + K^2 y_j = 0, \quad j = 1, \dots, n-1,$$

and the boundary ('endpoint') conditions $y_0 = y_n = 0$. Note that the k -th eigenvalue is

$$(A11) \quad K^2 = 4n^2 \sin^2 \left(\frac{k\pi}{2n} \right) = \pi^2 k^2 - \frac{\pi^4 k^4}{6n^4} + \dots$$

Example 2. Sound waves can be approximated similarly, by supposing a uniform tube of length $\ell = nh$ divided into $n-1$



segments of length h , and two end segments each of length $h/2$, by partitions of mass ρh . These half-segments are included in order to impose the boundary conditions $u_x(0) = u_x(\ell) = 0$ by the symmetry relations $u_0(t) = u(-h/2, t) = -u_1(t)$ and $u_{n+1}(t) = u(\ell+h/2, t) = -u_n(t)$.

Let $x_j(t) = (j - \frac{1}{2})h + \xi_j(t)$ denote the position of the j -th partition for $j = 1, \dots, n$, and let the pressure in the j -th segment be

$$(A12) \quad p = p_0 - A(\xi_j - \xi_{j-1}) .$$

Since $(\xi_j - \xi_{j-1})/h$ is the specific volume $1/\rho$, this corresponds to setting $p = p_0 - hA/\rho$, a Chaplygin equation of state. Hence it implies that $c^2 = dp/d\rho = hA/\rho^2$. Newtons Law $F = ma$ clearly gives

$$\rho h \ddot{\xi}_j(t) = A[(\xi_j - \xi_{j-1}) - (\xi_{j+1} - \xi_j)] = A \delta_{xx}(\xi_j) .$$

Since $A = \rho c^2/h$, this in turn is equivalent after simplification to

$$(A13) \quad \ddot{\xi}_j(t) = c^2(\xi_{j+1} - 2\xi_j + \xi_{j-1})/h^2 ,$$

much as in (A9).

APPENDIX B

CONFORMAL MAPS AND POTENTIAL FLOWS*

Riemann's Mapping Theorem (originally based on physical intuition), states that all simply connected domains (omitting two points) are conformally equivalent. By considering the ∞ as an ordinary point of the "Riemann Sphere", we can also map the exterior of any connected set conformally onto the exterior of a circle.

For many regions, such mappings can be accomplished by elementary functions, sometimes through the intermediary of the upper and/or lower half-planes, $y \geq 0$ and $y \leq 0$. (Note that half of the W-domain of many plane potential flows having an axis of symmetry can be taken as the upper or lower half-plane, by taking the axis of symmetry as the real axis. For others, the complex potential domain is an infinite strip.)

Since the similarity group consists of the $cz + \gamma$ ($c = a + ib \neq 0$, $\gamma = \alpha + i\beta$), and the orientation-inverting $cz^* + \gamma$ ($c \neq 0$), any half-plane will do. Likewise, W-domains bounded by two streamlines, $\psi = 0$ and $\psi = c$, are mapped onto a half-plane by $e^{\pi W/c}$. This is a result from $e^W = e^{\phi + i\psi} = e^\phi (\cos \psi + i \sin \psi)$, which fills out a circular sector.

Moebius group. Each 'linear fractional' transformation

$$(B1) \quad z \rightarrow (\alpha z + \beta) / (\gamma z + \delta) , \quad \alpha\delta \neq \beta\gamma ,$$

defines a one-one orientation-preserving conformal transformation of the Riemann sphere onto itself. The set of all such transformations is called the Moebius group. In (B1), $\alpha, \beta, \gamma, \delta$ are complex numbers, and the Riemann sphere consists of the complex z-plane and a 'point of infinity', ∞ . This 'Riemann sphere' can be mapped conformally onto its equatorial plane by 'Ptolemaic projection'. This projection, along straight lines

* I wish to thank Lt. Cdr. D. W. Cornell at the Naval Postgraduate School for his help in editing this appendix.

emanating from the North pole, has the remarkable property of carrying circles into circles--as do all transformations of the form (B1).

In particular, every transformation

$$(B2) \quad z \rightarrow (az + b)/(cz + d), \text{ with } a, b, c, d \text{ real,}$$

and $ad > bc$ maps the $\begin{Bmatrix} \text{upper} \\ \text{lower} \end{Bmatrix}$ half-plane onto itself. Note that the real linear fractional group of all such transformations is exactly triply transitive on cyclically ordered triples of points. Also, the function $t = (1 + iz)/(1 - iz)$ maps the $\begin{Bmatrix} \text{lower} \\ \text{upper} \end{Bmatrix}$ half-plane onto the $\begin{Bmatrix} \text{exterior} \\ \text{interior} \end{Bmatrix}$ of the unit circle. Moreover the rigid rotations $t \rightarrow e^{i\alpha t}$ are the only conformal transformations that carry the $\begin{Bmatrix} \text{interior} \\ \text{exterior} \end{Bmatrix}$ of the unit circle $|t| = 1$ that leave $\begin{Bmatrix} \infty \\ 0 \end{Bmatrix}$ invariant. As another example, note that the conformal transformations

$$(B3) \quad z \rightarrow \frac{z + b}{bz + 1}, \quad b \text{ real, } |b| < 1,$$

map the unit disk and the real axis onto themselves, and leave $z = \pm 1$ invariant.

Triple transitivity. It is easy to verify algebraically that, over the real or complex field (or any other field), there is one and only one Moebius transformation (B1) that carries $0, 1, \infty$ into a specified triple of distinct points z_0, z_1, z_2 on the complex sphere. Those mapping ∞ onto itself are the similarity transformations

$$(B4) \quad z \mapsto \alpha z + \beta, \quad \alpha = a + ia' \neq 0, \quad \beta = b + ib',$$

they constitute a four-parameter group depending on the four real parameters a, a', b, b' .

Joukowski transformation.¹ Very useful (and possessing beautiful properties) is the conformal transformation defined by

¹This is the name given in aerodynamics to the transformation (B5), whose properties were known much earlier. We will assume the reader to be familiar with the real hyperbolic and the complex exponential functions; cf. G.B. Thomas, "Calculus and Analytic Geometry", Alternate Ed. Chapt. 7 of the Schaum Outlint by Murray Spiegel also contains many useful formulas.

$$(B5) \quad z + \frac{1}{2}\left(z + \frac{1}{z}\right) = f(z) .$$

This is a 2-valent function mapping the complex sphere onto itself so that all points except $z = \pm 1$ are covered twice. Indeed, $w = f(z)$ if and only if $z^2 + 1 = 2zw$, or

$$(B5') \quad z = w \pm \sqrt{w^2 - 1} .$$

Moreover $z = f(z)$ and $dw/dz = (1 - z^{-2})/2 = 0$ at these points, near which for small complex ϵ , $\frac{1}{2}[(\epsilon F1) + 1/(\epsilon F1)] = F1 F\epsilon^2 + 0(\epsilon^2)$, so that angles are doubled.

In the log-polar coordinates defined by $z = re^{i\theta} = e^{\lambda} e^{i\theta}$ ($\lambda = \ln r$), clearly

$$(B6) \quad w = \cosh \lambda \cos \theta + i \sinh \lambda \sin \theta .$$

Hence circles $\lambda = \text{const.}$ ($\lambda > 0$) and radii $\theta = \text{const.}$ are mapped onto ellipses and hyperbolas having the common foci $(\pm 1, 0)$ (i.e., $w = \pm 1$) in the complex w -plane. The circles with $\lambda < 0$ and $r < 1$ interior to the unit disk are mapped onto the same ellipses with an opposite orientation (i.e., turned 'inside out').

It is also suggestive to visualize the effect of (B5) on the complex sphere, conformally equivalent to the z -plane with ∞ under Ptolemaic projection. It doubles both colatitude ϑ and longitude ϕ , if $z = \pm 1$ are taken as the poles, and the great circle through these is mapped onto a semicircle traced twice. By combining with Moebius transformations, we see that circles through ± 1 go into circular arcs, a fact that is useful in two-dimensional airfoil theory.

Complex projective line. Partly for its own interest, we next recall a few basic facts about the "geometry" of the Riemann sphere. Considered from the algebraic standpoint of analytic geometry, the complex sphere can be thought of as a projective 'line', whose 'points' are the sets $\{\lambda \underline{z}\}$ with $\lambda \neq 0$ variable, and $\underline{z} = (z_1, z_2)^T \neq \underline{0}$. That is, they are the ratios z_2/z_1 ,

where $0/0$ is excluded as meaningless but $z_1/0 = \infty$. The action $\underline{z} \mapsto A\underline{z}$ of $A = \begin{pmatrix} a & b \\ c & d \end{pmatrix}$ on \underline{z} corresponds to the linear fractional transformation (B2).

The cross-ratio of four complex numbers (z_1, z_2, z_3, z_4) is

$$(B7) \quad \chi(z_1, z_2; z_3, z_4) = \frac{(z_1 - z_2)(z_3 - z_4)}{(z_1 - z_3)(z_2 - z_4)}$$

Under (B2), for $w_i = (az_i + b)/(cz_i + d)$ clearly

$$\begin{aligned} w_1 - w_2 &= \frac{az_1 + b}{cz_1 + d} - \frac{az_2 + b}{cz_2 + d} \\ &= \frac{(ad - bc)(z_1 - z_2)}{(cz_1 + d)(cz_2 + d)}. \end{aligned}$$

From this it is obvious that

$$(w_1 - w_2)(w_3 - w_4) = \frac{(ad - bc)^2 (z_1 - z_2)(z_3 - z_4)}{\prod_{i=1}^4 (cz_i + d)},$$

and from this and (B7), that

$$(B8) \quad \chi(w_1, w_2; w_3, w_4) = \chi(z_1, z_2; z_3, z_4)$$

In words: the cross-ratio is invariant under the Möbius group.

THEOREM A. Four points z_1, z_2, z_3, z_4 in the complex plane are concylic (i.e., they lie on a common circle) if and only if $\chi(z_1, z_2, z_3, z_4)$ is real.

We omit the proof.

COROLLARY. Any Moebius transformation carries straight lines and circles into straight lines or circles.

THEOREM B. There is one and only one Moebius transformation (B1) which carries a given triple of distinct points (z_1, z_2, z_3) into a given triple (w_1, w_2, w_3) : the Moebius group is exactly triple transitive on the Riemann sphere.

Plotting streamlines and equipotentials. The creators of the mathematical theory of two-dimensional airfoil lift (Joukowsky, Kutta, Karman-Trefftz, Mises) were well aware of the preceding facts, and used them to construct Joukowsky flows past special profiles.² With modern computers and graphics capabilities, any intelligent graduate student can do the same for general profiles.

However, to computerize the plotting of streamlines and equipotentials for the potential flow with circulation Γ around a unit circle requires a careful use of elementary complex analysis. The complex potential $W = \phi + i\psi$ is

$$(B9) \quad W = z + z^{-1} + i\gamma \ln z, \quad j = \Gamma/2\pi.$$

Hence $\phi = (r+r^{-1}) \cos \theta - \gamma \theta$, while $\psi = (r-r^{-1}) \sin \theta + \gamma \ln r$. Because $\theta = \text{Im}\{\ln z\}$ is a multiple-valued function when $\gamma \neq 0$, several complications arise.

Before discussing these complications, we note some useful formulas. First,

$$(B10) \quad \zeta = dW/dz = 1 - z^{-2} + i\gamma/z.$$

Multiplying through by z^2 , and solving the resulting quadratic equation $z^2 + i\gamma z = 1$, we find that the stagnation points z_1, z_2 are at

$$(B11) \quad z = -(i\gamma/2) \pm \sqrt{1 - \gamma^2/4}.$$

Here $1 - (\gamma^2/4) = -\Delta/4$ is $(-1/4)$ times the discriminant of (B10). Correspondingly, there are three cases, of which $|\gamma| < 2$ (two stagnation points), is of the greatest aerodynamic interest. In this case, in polar coordinates, the z_j in (B11) are at

$$(B12) \quad z_j = i \sin \theta_s = \cos \theta_s,$$

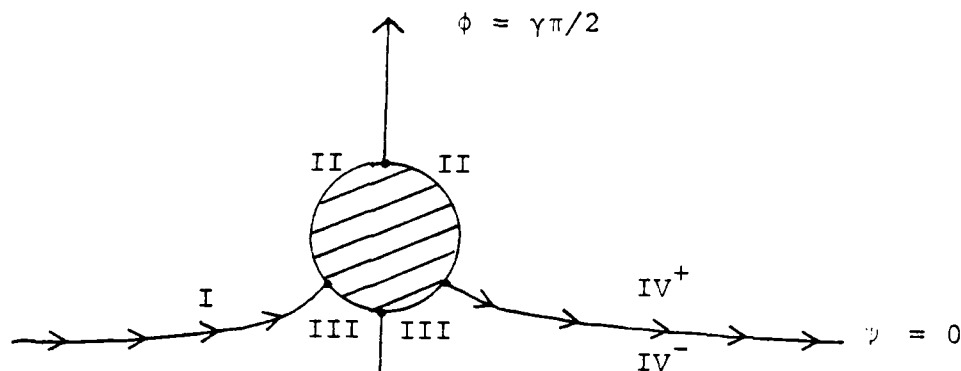
where $\theta_s = \arcsin(\gamma/2)$, $\sin \theta_s = \gamma/2$.

²For a collection of explicit conformal mappings, see H. Kober, "Dictionary of Conformal Representations", Dover, 1952.

The dividing streamline $= 0$ sketched below is easily plotted, as a function of r . We have

$$(B13) \quad y = r \sin \theta = (-\gamma \ell \ln r) / (1 - r^{-2})$$

$$x = \sqrt{r^2 - y^2}$$



Segmentation. However, for later plotting purposes, it is important to segment the dividing streamline into five pieces as shown: I) $r > 1, x < 0$, II) $r = 1, \theta_s \leq \theta \leq \pi - \theta_s$ as shown (where $\theta_s < 0, \gamma < 0$), III) $\pi - \theta_s < \pi < 2\pi + \theta_s$, IV) a mirror copy of the segment I, with the sign of x reversed.

The mesh points (ϕ_i, ψ_j) . Values of $z_{i,0} = (x(\phi_i, 0), y(\phi_i, 0))$ must be stored separately for each of the streamline segments I, II, III, IV⁺, IV⁻, as starting points for the equipotentials (level lines of ϕ) to be computed later; the spacing h of the ϕ_i is to be determined later. This is because θ jumps by 2π in going from IV⁺ to IV⁻, while ϕ jumps by the circulation $\Gamma = 2\pi\gamma$.

Symmetry. Since there is symmetry about the y -axis of streamlines and equipotentials, we might as well let $\phi = 0$ at $(0, 1)$, which thus is mapped onto the origin of the (ϕ, ψ) -plane. This amounts to adding $\Gamma/4 = \pi\gamma/2$ to ϕ and W , as defined by Eq. (B9).

The graphing problem. As is standard,³ one should impose a square mesh with side $h = \Delta\phi = \Delta\psi$ in the (ϕ, ψ) -plane, including the y -axis of symmetry as one of the equipotentials to be graphed. This brings out the vertical symmetry of horizontal potential flows with circulation around a circular cylinder, conventionally invoked to explain the Magnus effect.

Plotting streamlines. The choice of procedure best for plotting streamlines $z(\phi, \psi_j)$ depends on the graphics package (DISSPLA?) and (Tektronix?) computer available; because the appropriate principal values of θ and ϕ may differ, streamlines passing above the cylinder may want a different subroutine from those passing below the cylinder. (When $|\gamma| > 2$, one must also consider vortex lines.)

Above the cylinder, when $\psi > 0$, I recommend starting from the y -axis, where $\psi = r - r^{-1} + \Gamma \ln r$, and (cf. (B10)) integrating the DE

$$(B14) \quad dz/dW = 1/[1 + (i\gamma/z) - z^{-2}] ,$$

at intervals of (say) $h/3$ in ϕ . One can use Newton's method with (B9) as a 'corrector' to eliminate cumulative error. By symmetry, it suffices to compute and store half of each streamline above the cylinder.

Below the cylinder, one can initiate the computation of each streamline similarly. However, unless $\Gamma/4$ is an integral multiple of h , the negative y -axis will no longer be an equipotential to be plotted. (If $\Gamma/2$ is an odd integral multiple of h , the displayed equipotentials will still be symmetric about the y -axis, although the y -axis itself will not be one of the equipotentials displayed.)

Plotting equipotentials. Whatever the constant value of $\phi(0, y) = \Gamma/2$ for $y < 0$, it should be easy to compute accurately $z(\phi_i, \psi_j)$ for $\psi_j = jh$ ($j < 0$) and $\phi_i = ih$, by solving (B14)

³Cf. Chow, Kuethé and Chow; also Streeter.

as before from the initial value $\phi(0,y) = \Gamma/2$ instead of 0. Since for $\psi < 0$,

$$(B15) \quad y(\Gamma/2+t, \psi) = y(\Gamma/2-t, \psi) ,$$

and

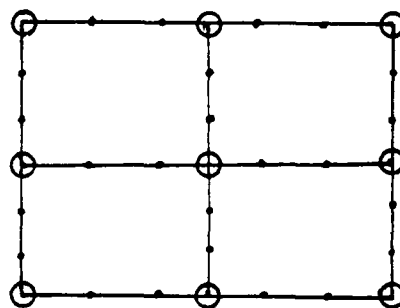
$$(B15') \quad x(\Gamma/2+t, \psi) = -y(\Gamma/2-t, \psi) ,$$

one should be able to compute a complete raster of $z_{ij} = z(\phi_i, \psi_j)$ by this process, using fourth-order real or complex Runge-Kutta (which does not depend for its accuracy on uniform mesh spacing).

Checking. I would then store two arrays of the 800 or fewer grid points z_{ij} computed in this way, one for the domain on and above the dividing streamline, and one for the domain on and below the dividing streamline. For equipotentials not going near the stagnation points $z = e^{i\theta} s$, the DE (B15) will be non-singular, and one can integrate it with respect to the real variable ψ from $\psi = 0^+$ upward to recompute the z_{ij} .

After having verified that the new z_{ij} match the old z_{ij} , after debugging if necessary, one can then tackle the part of the flow below the dividing streamline in the same way.

Storage. Depending on the plotting method used by DISSPLA or other graphics package, storage of at most 5 points per z_{ij} (dividing each mesh segment into three equal parts in the (ϕ, ψ) -plane) should give ample accuracy if combined with parametric cubic spline or other interpolation. Finally, storage of x_{ij} , y_{ij} , and their partial derivative, with respect to ϕ and ψ could be combined with cubic Hermite interpolation to generate the requisite grid with at most 4800 stored real numbers.



Representing airfoils. Actually, using complex algebra, for each γ , 3200 real numbers (the real and imaginary components

of the z_{ij} and $z'_{ij} = (dz/dW)_{i,j}$ would suffice. Given a Joukowski or other profile analytically defined by $w = w(z)$, one could then use this table of real numbers to compute the real and imaginary components of $w_{ij} = w(z_{ij})$ and (by the Chain Rule) the products

$$(dw/dW)_{ij} = w'(z_{ij})z'_{ij}$$

would suffice.

APPENDIX C
FOURIER ANALYSIS

Fourier analysis provides a unique tool for solving (pure) initial value problems involving linear partial DE's with constant coefficients. At the same time it is the best tool for analyzing the errors and stability of difference and finite element approximations to such DE's in intervals and box-shaped domains.¹

There are three main underlying ideas, each of which is extraordinarily simple. The first of these concerns the formal properties of complex exponential functions. For any real wave vector $\underline{k} = (k_1, \dots, k_m)$, the function

$$(C1) \quad e^{i\underline{k} \cdot \underline{x}} = \cos(\underline{k} \cdot \underline{x}) + i \sin(\underline{k} \cdot \underline{x})$$

is defined and has absolute value one everywhere in R^m . Moreover for each j ,

$$(C1') \quad \frac{\partial}{\partial x_j} (e^{i\underline{k} \cdot \underline{x}}) = ik_j e^{i\underline{k} \cdot \underline{x}}.$$

Therefore, if p is any polynomial and D_j signifies $\partial/\partial x_j$, then the DE

$$(C2) \quad u_t = p(D_1, \dots, D_m)u,$$

is solved for the initial data

$$(C3) \quad u(\underline{x}; 0) = e^{i\underline{k} \cdot \underline{x}}$$

by the function

$$(C3') \quad u(\underline{x}; t) = e^{\omega t} e^{i\underline{k} \cdot \underline{x}},$$

¹Cf. Appendix G, on "Courant stability conditions and amplification matrices".

where $\omega = p(iD_1, \dots, iD_m)$. Since $|e^{\omega t}| = \exp\{\text{Re}(\omega)t\}$, the rate of growth of the solution is easily computed.

Example 1. For the diffusion equation $u_t = au_{xx}$, $m = 1$ and the solution of the initial value problem for $u(x,0) = e^{ikx}$ is $u(x,t) = e^{-ak^2t} e^{ikx}$.

Only slightly more complicated is (for example), the wave equation with $m = 2$:

$$(C4) \quad u_{tt} = c^2(u_{xx} + u_{yy}) .$$

Example 2. The solution of the DE (C4) for the initial conditions

$$(C4') \quad u(x,y;0) = ae^{i(kx+k'y)}, \quad u_t(x,y;0) = a'e^{i(kx+k'y)},$$

a, a' arbitrary complex numbers, is

$$(C5) \quad u(b e^{i\omega t} + b' e^{-i\omega t}) e^{i(kx+k'y)},$$

where b and b' satisfy

$$(C5') \quad a = b + b', \quad a' = i\omega(b - b'),$$

with $\omega = c \sqrt{k^2 + k'^2}$, so that

$$(C5'') \quad b = \frac{1}{2}[a + (a'/i\omega)], \quad b' = \frac{1}{2}[a - (a'/i\omega)].$$

In the real domain the two linearly independent complex solutions

$$e^{i(kx+k'y)+i\omega t}, \quad e^{i(kx+k'y)-i\omega t}$$

(k, k' , and ω all real) generate four linearly independent real solutions:

$$\begin{Bmatrix} \cos \\ \sin \end{Bmatrix} (kx+k'y) \begin{Bmatrix} \cos \\ \sin \end{Bmatrix} \omega t .$$

The second key idea of Fourier analysis is the representability of a wide class of functions, especially square-integrable functions, as superpositions of solutions of the form just indicated. This is possible in many cases, and especially for sound waves (Chap. 2, §§2-3; Chap. 3, §9; Chap. 5), because of the Plancherel Theorem stated below.

Plancherel's Theorem. Let $u(\underline{x})$ be any (Lebesgue) square-integrable function in R^m . For each wave vector $\underline{k} \in R^m$, let

$$(C6) \quad f(\underline{k}) = \frac{1}{\pi^m} \int_{R^m} e^{-i\underline{k} \cdot \underline{x}} u(\underline{x}) dx_1 \cdots dx_m .$$

Then we have almost everywhere (i.e., except zero)

$$(C6') \quad u(\underline{x}) = \int_{R^m} f(\underline{k}) e^{i\underline{k} \cdot \underline{x}} dk_1 \cdots dk_m ,$$

Finally,

$$(C6'') \quad \int_{R^m} |u(\underline{x})|^2 dx_1 \cdots dx_m = \pi^{m/2} \int_{R^m} |f(\underline{k})|^2 dk_1 \cdots dk_m .$$

In the case of sound waves, since all $\omega(k_1, \dots, k_m)$ are real, $|e^{i\omega(\underline{k})}| = 1$ for all \underline{k} . Hence $|f(\underline{k}; t)|^2 = |f(\underline{k})|^2$ and so the L^2 -norm of $u(\underline{x}; t)$,

$$\left[\int_{R^m} |u(\underline{x}; t)|^2 dx_1 \cdots dx_m \right] = ||u(t)||^2$$

is independent of t (it is an invariant).

APPENDIX D
NAVIER-STOKES EQUATIONS

The following discussion summarizes, with a few critical remarks, the classical derivation by Stokes¹ of the Navier-Stokes equations of Chap. 2 (8.1).

Relative to Cartesian axes, we define the stress tensor as the matrix $P = ||p_{ij}||$, where p_{ij} is the i -th force-component, per unit surface area perpendicular to the j -th coordinate axis, right-handed orientation of axes being understood. Specifically, we consider the force directed from the side of positive x_j to the negative side, across the (x_{j+1}, x_{j+2}) -plane, all subscripts mod 3.

We define the rate-of-strain tensor as the matrix $||\partial u_i / \partial x_j||$. The symmetric and skew components of this are then given by

$$e_{ij} = \frac{1}{2}(\partial u_i / \partial x_j + \partial u_j / \partial x_i) \quad (D1)$$

$$r_{ij} = \frac{1}{2}(\partial u_i / \partial x_j - \partial u_j / \partial x_i) .$$

Clearly, the matrix $R = ||r_{ij}||$ has the form of Fig. 1, which represents rigid rotation with angular velocity ("spin")-vector (α, β, γ) . Thus, the physical rate of deformation is due entirely to $E = ||e_{ij}||$. For this reason, E (or $2E$ in Goldstein) is often called the rate-of-strain tensor.

$$\begin{pmatrix} 0 & \gamma & \beta \\ -\gamma & 0 & \alpha \\ -\beta & -\alpha & 0 \end{pmatrix}$$

Fig. 1

The matrices P and $||\partial u_i / \partial x_j||$ have direct interpretations as linear transformations. Clearly, relative to moving axes making

¹Trans. Camb. Phi. Soc. 8 (1845), 287- ; Papers, i, 75-

the local velocity at the origin zero, we have

$$(D2) \quad du_i = \sum (\partial u_i / \partial x_k) dx_k .$$

Similarly, if $\underline{dS} = (dS_1, dS_2, dS_3)$ is any infinitesimal element of surface area perpendicular to the vector \underline{dS} , the i -th component of force on \underline{dS} is

$$(D3) \quad dX_i = \sum P_{ik} dS_k .$$

This is less obvious, but can be proved, following Cauchy, by considering the additivity of stress on long, thin triangular prisms undergoing finite acceleration (total stress/volume bounded), whose dimensions are allowed to shrink to zero. In summary, P represents a linear transformation from vector surface area to the force across that area, while $\|\partial u_i / \partial x_k\|$ is one from relative position to relative velocity.

DEFINITION. A Newtonian fluid is one in which P depends linearly on E , in a way which is invariant under orthogonal transformation.

Explanation. By linear dependence, we mean that $P_{ij} = \sum c_{ij}^{kl} e_{kl}$, for some coefficient tensor. The interpretation of orthogonal invariance requires a more lengthy explanation.

Rules of transformation. Obviously, if $A = \|\|a_{ij}\|\|$ is any orthogonal matrix, then

$$(D4) \quad Y_i = \sum a_{ik} x_k \quad (\text{in matrix notation, } Y = AX) ,$$

is an orthogonal transformation of coordinates corresponding to new Cartesian axes. If $|A| = 1$, then orientation (right-handedness) is preserved, and A defines a rigid rotation (through a finite angle).² Hence A transforms force-components X_i , distance-components, and components of vector area dS_i according to the same rules of transformation:

²The R of Fig. 1 represents a rate of rotation (spin) in radians per second; A is dimensionless.

$$(D5) \quad Y_i = \sum a_{ik} X_k, \quad dT_i = \sum a_{ik} dS_k$$

Hence, if $||q_{ij}||$ is the stress tensor in the new (right-handed, Cartesian) coordinate system defined by any orthogonal A , we will have

$$(D5') \quad Y_i = \sum q_{ik} dT_k, \quad \text{whence} \quad AX = QA \, dS.$$

Since $A^{-1} = A^T$ for any orthogonal matrix, this yields the general rules of transformation

$$(D6) \quad A^T Q A = P, \quad Q = A P A^T$$

for the stress tensor, under all A with $|A| = 1$.

A similar argument, with $U = (du_1, du_2, du_3)$ taking the place of X , shows that if $v_i = \sum a_{ik} u_k$ denotes velocity relative to the new axes, then

$$(D7) \quad ||\partial v_i / \partial y_j|| = A ||\partial u_k / \partial x_k|| A^T.$$

Moreover, the transformation $C \rightarrow A C A^T$ leaves invariant the decomposition of C into symmetric and skew components, since

$$A(C+C^T)A^T = A C A^T + A C^T A^T = A C A^T + (A C A^T)^T.$$

Hence, E and R in (D1) transform according to

$$(D8) \quad E \rightarrow A E A^T \quad \text{and} \quad R \rightarrow A R A^T,$$

under any orientation-preserving orthogonal transformation.³

Principal axes. Formula (D8) shows that the symmetric rate-of-strain tensor E transforms like a quadratic form. Hence we can always choose A so as to make E diagonal; the associated

³For a detailed derivation of (D6)-(D8), see H. Jeffreys, "Cartesian tensors", Cambridge Univ. Press, 1931, Chs. VII and IX (cf. Goldstein, p. 95. footnote).

axes are called principal axes for E . We shall now consider the dependence of P on E relative to such principal axes. We can assume $R = 0$ (by hypothesis, R does not affect P), without losing generality.

In this case, the matrix $||\partial u_i / \partial x_j||$ is diagonal, with diagonal entries a, b, c . The flow is kinematically invariant (up to infinitesimals of higher order) under all reflections $y_i = \pm x_i$. Consider reflection in (say) the (x_1, x_3) -plane, with $Y_1 = x_1, Y_2 = -x_2, Y_3 = x_3$. The stress across the (x_2, x_3) -plane, from the side $x_1 > 0$ will be unchanged, since the flow is unchanged. Hence we conclude that $X_2 = -X_2$ if $ds = (ds_1, 0, 0)$; $p_{21} = 0$ under principal axes. But a similar argument applies to $p_{12}, p_{23}, p_{32}, p_{13}$ and p_{31} , proving

LEMMA 1. If E is diagonal, then $P = D$ is diagonal.

COROLLARY. The stress tensor $P = ||p_{ij}||$ is symmetric, under any Cartesian axes.

For, $P = ADA^T$, where D is the diagonal stress matrix for some set of principal axes. Hence $P^T = (ADA^T)^T = ADA^T = P$.

Viscosity coefficients. We now consider the incompressible case, that u_i/x_j (or, equivalent, E) has trace zero. This condition is physically independent of the choice of axes. In this case, relative to principal axes, D is a superposition of two matrices of the type of Figs. 2a-2b, which are moreover the same except for the labelling of axes.

$$\begin{pmatrix} a & 0 & 0 \\ 0 & -a & 0 \\ 0 & 0 & 0 \end{pmatrix} \qquad \begin{pmatrix} 0 & 0 & 0 \\ 0 & b & 0 \\ 0 & 0 & -b \end{pmatrix}$$

Fig. 2a

Fig. 2b

But these matrices arise from the simple shear flow having the constant rate-of-strain tensor of Fig. 3a, which is usually used to define viscosity. The associated quadratic form is kx_1x_2 ; relative to principal axes $y_1 = (x_1+x_2)/\sqrt{2}$, $y_2 = (x_2-x_1)/\sqrt{2}$, this becomes $(y_1^2 - y_2^2)/2$, with diagonal matrix D as in Fig. 3c.

$$\begin{pmatrix} 0 & k & 0 \\ 0 & 0 & 0 \\ 0 & 0 & 0 \end{pmatrix}$$

Fig. 3a

$$E = \begin{pmatrix} 0 & k/2 & 0 \\ k/2 & 0 & 0 \\ 0 & 0 & 0 \end{pmatrix}$$

Fig. 3b

$$D = \begin{pmatrix} k/2 & 0 & 0 \\ 0 & -k/2 & 0 \\ 0 & 0 & 0 \end{pmatrix}$$

Fig. 3c

In Lemma 1, considering the symmetry between D and $-D$ under permutation of axes, we see that the stress matrix $Q(D)$ must have diagonal entries $\mu'k/2, -\mu'k/2, 0$. In short, $Q = \mu'D$, for some constant μ' , which is positive since outward flow away from the (x_2, x_3) -plane exerts tension (cf. basic definition of P).

Arguing similarly for the case of Fig. 2b, and noting that μ' must be the same since the axes are merely renamed, we see that $Q = \mu'D$ in general. But this equation is preserved under (D6)-(D8). We conclude that $P = \mu'E$ in general.

But finally, in the simple shear flow of Fig. 3b, $p_{12} = \mu k$ (by definition of units of viscosity). Hence

THEOREM 1. In any incompressible Newtonian fluid, the viscous stresses must satisfy

$$(D9) \quad P = 2\mu E, \quad \text{or} \quad p_{ij} = \mu \left(\frac{\partial u_i}{\partial x_j} + \frac{\partial u_j}{\partial x_i} \right), \quad \text{(Normal Stresses not discussed)}$$

for a suitable "coefficient of (shear) viscosity" μ .

Physically, we must have $\mu > 0$ to prevent the creation of mechanical energy; this can be viewed as a special case of the Second Law of Thermodynamics.

In a compressible fluid, D is at any point the sum of a volume-conserving rate-of-strain matrix (trace zero) and a pure dilatation with rate-of-strain matrix cI , where I is the identity matrix. A reconsideration of invariance under reflections shows that this must be opposed by a stress matrix cI in any Newtonian fluid. The constant $-\lambda > 0$ is called the bulk viscosity.

Stokes gave a classic, metaphysical "proof" that $3\gamma + 2\mu = 0$, reproduced in Lamb [A6, p. 574]. We will comment on this result (true only in monatomic gases) in Appendix B.

APPENDIX E
MOLECULAR MODELS OF MATTER

These notes are based on [C2] and the following references:

- [J] J.H. Jeans, "Dynamical Theory of Gases", 4th ed., Cambridge Univ. Press, 1925.
[J'] J.H. Jeans, "Kinetic Theory of Gases", Cambridge Univ. Press, 1940.

Kinetic theory of gases. Without question, the kinetic theory of gases has been the most successful 'molecular model' of a fluid; 'Model #7' of the Table on p. 3 should therefore be thought of as referring above all to this theory. In its simplest form, the main assumptions of this model are as follows.

Small molecules, of mass m and diameter σ , move in straight lines of average length λ (the 'mean free path') between successive binary collisions, which are elastic. It can be shown that an isotropic Gaussian statistical distribution of velocities, with probability density

$$(E1) \quad \left(\frac{hm}{\pi}\right)^{3/2} e^{-hm(u^2+v^2+w^2)}$$

is time-invariant ('stable') for a wide variety of laws of binary repulsion. In (E1) h is a parameter inversely proportional to temperature. For a non-dense gas, ternary collisions can be neglected; the 'state' of any molecule is moreover assumed to be independent of its velocity.¹

From these assumptions, one can derive the equation [J, p. 116]:

$$(E2) \quad pV = NRT ,$$

for the (kinetic) pressure p in a volume V of gas containing N molecules. More generally, in a mixture of gases of masses

¹Thus such high-temperature phenomena as excitation, radiation, ionization, and dissociation are ignored in classical kinetic theory.

m_i , writing $u^2+v^2+w^2 = c^2$, one can show that the mean kinetic energy per molecule of a given species, $\frac{1}{2}m_i c_i^2$, is the same for all species. From this it follows that the number N_0 of molecules per cc. at a given pressure and temperature is the same for all gases (Avogadro's Law).²

At $T = 0^\circ\text{C} = 273^\circ\text{K}$ and $p \approx 1 \text{ Kg/cm}^2$ (standard atmospheric pressure), $N \approx 2.7 \times 10^{19}$ [J, p. 8]. Likewise, one can show that

$$(E3) \quad \frac{3}{2}RT = \frac{1}{2}m\bar{c}^2, \quad \bar{c}^2 = u^2+v^2+w^2,$$

so that $\bar{c} \approx 500$ meters/sec in air at 0°C . (Here and above the numerical value of R depends on the units of temperature, as does the mechanical equivalent of heat,

$$(E4) \quad J = 4.184 \times 10^7 \text{ dyne cm/gm. cal.})$$

Central force laws. 'Central force' laws $F = f(r)$ depending only on the distance r between nearby molecules imply some remarkably simple formulas. Thus they imply that the viscosity $\mu = \frac{1}{3}\lambda\bar{c}\rho$ [J, p. 277]. The remarkable fact that gas viscosity depends only on the temperature, regardless of the pressure, is a corollary. Less successful is the prediction that the material (self)-diffusivity D has the same value as $\nu = \mu/\rho$, the kinematic viscosity [J, p. 320]. They also imply that the thermal conductivity $K = \mu C_V$.

Empirically, the ratio $K/\mu C_V$ is called the Prandtl number of a gas. In [J', p. 189], one finds the values $Pr = 2.4-2.5$ for He and A, 1.9 for O_2 , N_2 and air, and 1.58 for CO_2 . Landau and Lifschitz [B6, p. 203] give the value 0.733 for air, as well as $Pr = 0.044$ for mercury, 16.6 for "alcohol" ($\text{C}_6\text{H}_5\text{CH}_2$?) and 7250 for glycerine. They also claim that Pr is "just a constant of the material" (sic!).

Monatomic gases. The preceding assumptions are clearly most plausible for monatomic gases such as He, A, Kr, etc. The same

²Inferred from chemical (combustion?) experiments. For historical remarks about the kinetic theory of gases, see [J, §9 and §60].

is true of the consequence of an 'elastic sphere' model (bouncing billiard balls), which would imply $\mu \propto \sqrt{T}$. Actually, the formula $\mu = \mu_0 (T/273)^n$ is fitted to empirical data on gas viscosity; the n giving the best fit ranges from about 0.68 to 1. Stokes' prediction that the shear viscosity μ and the bulk viscosity μ' are related by the equation $3\mu' + 2\mu = 0$, also in agreement with the central force model, does seem to hold for monatomic gases.

Specific heats. Specific heats tend to be less variable. Theory predicts that

$$(E5) \quad C_p - C_v = R/mJ ,$$

and that (in monatomic gases) C_v just measures the total kinetic energy of translation (the total kinetic energy for monatomic gases).

The adiabatic constant $C_p/C_v = \gamma = 1 + \frac{2}{3+n}$, where n is the number of 'internal' degrees of freedom of motion (rotation and vibration), is also successfully predicted by kinetic theory. In monatomic gases, $n = 0$ and so $\gamma \approx 5/3$ for He, Ar, Kr, and Hg (mercury vapor). In diatomic gases, $n = 2$ and so $\gamma \approx 1.4$ in H_2 , N_2 , O_2 , and air [J, p. 190]. (In Cl_2 , $\gamma \approx 1.33$ however, while in polyatomic gases, γ is even less.)

Molecular slip. There is in fact some 'molecular slip' in rarefied gases, associated with a tendency to nearly specular reflection. See [J', p. 192],³ where 'accommodation coefficient' is discussed. When $\lambda \gg d$,

$$Q = \pi a^2 \rho \bar{u} = 2a^3 (p_1 - p_2) / cL$$

³The summary in Goldstein [A5, pp. 676-80] sounds more negative. Some of the \$50 billion spent in the 1960's by NASA went to rarefied gas dynamics. See the volumes on Rarefied Gas Dynamics (Academic Press, 1961 and 1969), edited by L. Talbot and by L. Trilling and H.Y. Wachman, respectively. The lead article by J.P. Hartnett in the first emphasizes the need for maintaining "scrupulously clean surfaces" in measuring thermal accommodation coefficients, while that by M.N. Kogan in the second gives a comprehensive and up-to-date historical review of the subject.

is proportional to the pressure gradient times the cube of the pipe radius, not a^4 as in Poiseuille flow. To derive the accommodation coefficient, quantum theory is needed, and quantum theory is beyond the scope of this book.

Mass-spring models. Von Neumann's initial 'mass-spring' model for plane shock waves in air had much more in common with molecular models of crystalline solids than it did with Maxwell's kinetic theory of gases. However, the same is true of many other difference approximations used in numerical fluid dynamics. Therefore, we will conclude this Appendix with a few remarks (mostly bibliographical) about the mass-spring models for crystals, noting that Leon Brillouin's booklet [C2] contains a wealth of supplementary ideas.⁴

Elastic 'solids'. One notable class of molecular models was proposed by Poisson and Cauchy,⁵ to provide a basis for the 'rational mechanics' of elastic solids.⁶ According to this model, solids are composed of periodic arrays of atoms connected by springs (perfect crystals). Using analytical arguments, Cauchy was led by this model to develop a 'uniconstant' theory of elasticity, in which the Poisson ratio (lateral contraction)/(axial elongation) was a predictable 0.25, much as μ/μ' must be 0.67 in a perfect monatomic gas.

⁴ See also L. Brillouin and M. Parodi, "Propagation des Ondes dans les Milieux Périodiques", Masson-Dunod, 1956.

⁵ Curiously, after proposing a continuum model in 1822-23, Cauchy later abandoned it in favor of the 1829 molecular model of Poisson, and extended it to crystals. See the Historical Introduction to A.E.H. Love's "Theory of Elasticity".

⁶ We use this phrase in the sense of Poisson. Poisson conceived of 'mécanique rationnelle' as an inclusive, self-contained subject. Thus he writes in the Preface of his Traité de Mécanique, Paris, 1811; "My choice of proofs is neither exclusively synthetic nor (exclusively) analytic. I have sought clarity and simplicity above all, always preferring demonstrations that shed the most light on the truths that one wishes (sic!) to prove, ... often combining geometric considerations and algebraic formulas in treating the same question".

Periodic mass-spring models helped Kelvin to understand and predict piezoelectric effects. They also led Max Born to a realistic model for the specific heat of halide crystals; the Preface of his "Dynamik der Kristallgitter" (Teubner, 1914) begins with an admirable summary of the capabilities and limitations of mass-spring models of solid crystals.

Much more recently, Léon Brillouin [C2] used analogous models (and the 'electromechanical analogy') to provide qualitative explanations for various features of the spectra of crystals, and for designing 'pass-band' filters in transmission lines (for both telephonic communication and electrical power). In his books, Brillouin takes as his first example the Newton-Lagrange-von Neumann model for sound waves, which we will discuss again as a computational scheme in Chapter 5. Brillouin considers the effect of vibrating the end bead of a semi-infinite periodic array sinusoidally (harmonically), so that $x_0(t) = A \sin \omega t$. This excites sinusoidal oscillations in the other beads, having the same frequency and amplitude, but different phases up to a certain cutoff frequency ω_{\max} . Below this frequency, we will have

$$(E6) \quad x_j(t) = A \sin \omega (c_h t - jh - \alpha) .$$

In this range, the molecular spacing h produces some dispersion: $c_h(\omega)$ depends on h , as well as a phase-lag $\alpha = \alpha(\omega)$. Such a dispersion is perceptible experimentally for highly ultrasonic frequencies. Above the cutoff frequency (i.e., for $\omega > \omega_{\max}$), the transmitted oscillations die out exponentially: the 'solid' is 'opaque' to them.

In spite of their many notable successes from the standpoint of Natural Philosophy (see Chapter 1, §2), mass-spring models of solids as periodic structures have serious limitations from the standpoint of exact science. Thus Cauchy's 'uniconstant' theory of elasticity was finally rejected in favor of a 'rariconstant' theory of elasticity. Poisson ratios actually range from 0.25

to 0.5 or more. And the (1954) edition of Born and Huang's "Crystal Physics" contains not a trace of the molecular models that were the central theme of Born's 1912 "Theorie der Kristallgitter".

APPENDIX F

'COURANT' STABILITY CONDITIONS AND AMPLIFICATION MATRICES¹

For some special 'model problems', associated with linear, constant-coefficient DE's in box-shaped domains, errors and orders of accuracy of approximate semi-discretizations and "full" discretizations of initial value problems can be estimated reliably by expanding in obvious eigenfunctions.

A basis of eigenfunctions for the linear difference operator $\delta_{xx} u$ is provided by the functions $\sin j\pi x$ ($j = 1, \dots, n-1$). A little manipulation of trigonometric identities gives:

$$\begin{aligned} \sin j\pi(x+h) - 2 \sin j\pi x + \sin j\pi(x-h) &= \\ (F1) \quad (2 \cos j\pi h - 2) \sin j\pi x &= \lambda_j \sin j\pi x, \end{aligned}$$

where $\lambda_j = 4 \sin^2(j\pi h/2)$. Hence, in two dimensions, with a square mesh:

$$(F2) \quad \nabla_h^2 \phi_{j,j}, = (j^2 + j'^2) \pi^2 h^2 + O(h^4),$$

where $\phi_{j,j}(x,y) = \sin j\pi x \sin j'\pi y$.

From these formulas, we can easily estimate the errors and accuracy of the semi-discretized heat and wave equations.

Semi-discretizations. The 'method of lines' (MOL) replaces DE's such as $u_t = \alpha u_{xx}$ and $u_{tt} = c^2 \nabla^2 u$ by their semi-discretizations:

$$(F3a) \quad u_t = \alpha u_{xx},$$

$$(F3b) \quad u_t = \alpha (u_{xx} + u_{yy}),$$

$$(F3c) \quad u_{tt} = c^2 u_{xx}, \text{ and}$$

¹Cf. Chapter 3, §3.

$$(F3d) \quad u_{tt} = c^2 (u_{xx} + u_{yy}) .$$

For the stated boundary conditions, and the DE (F3a), the semi-discretization

$$(F4) \quad u_t = \alpha \delta_{xx} u / h^2$$

and the boundary conditions $u(0) = u(1) = 0$, give a quite good semi-discretization. If

$$u(x,0) = \sum_{j=1}^{n-1} c_j \sin j\pi x ,$$

formulas (F1) show that the (exact) solution of the semi-discretized DE

$$(F5) \quad u(x,t) = \sum c_j e^{-\lambda_j t} \sin j\pi x ,$$

where $\lambda_j = 4 \sin^2(j\pi h/2) / h^2$. This is because the coefficient $c_j(t) = c_j e^{-\lambda_j t}$ is the solution of $c_j'(t) = -\lambda_j c_j$, whereas the exact solution of the DE is

$$(F6) \quad \sum c_j e^{-j^2 \pi^2 x t} .$$

Error Analysis: $u_t = \alpha u_{xx}$. The basic principles underlying the error analysis of the DE's (F3b)-(F3d) are illustrated quite well by the 'heat equation' (F3a). To fix ideas, we will therefore analyze this case first in some detail.

We first observe that, by the Riesz-Fischer theorem, any continuous initial temperature distribution $u(x,0) = f(x)$ can be approximated arbitrarily closely in the 'mean square' or l_2 -norm for sufficiently large n , by a truncated sine series

$$(F7) \quad \sum_{j=1}^n b_j \sin j\pi x, \quad b_j = 2 \int_0^1 f(x) \sin j\pi x dx .$$

If $f \in C_0^2[0,1]$ --i.e., if f has two continuous derivatives and $f(0) = f(1) = 0$,--the error is $O(1/n^2)$ and the approximation is close in the uniform norm $\max |f(x) - S_n(x)|$.

We next recall that the evolution in time of a temperature distribution under the action of the heat equation is a 'contraction semigroup' under both the ℓ_2 -norm and the uniform norm. This means that if $u(x,t)$ and $v(x,t)$ are any two (even 'weak!') solutions of $u_t = \alpha u_{xx}$, then we have the inequality

$$(F8) \quad |||u(x,t') - v(x,t')||| < |||u(x,t) - v(x,t)|||$$

if $t' > t$, regardless of whether $|||\cdot|||$ is the ℓ_2 -norm or the uniform norm. (Exceptionally, if $u \equiv v$, equality can hold in (F8).)

References. Rigorous proofs of the preceding results are fairly straightforward, but rather lengthy. Good expositions of (F7) are in Courant-John "Calculus" and Widder's "Advanced Calculus". More precise results referring to trigonometric interpolation (as contrasted with 'approximation' by least squares) were proved by Dunham Jackson, whose book can also be recommended to analysts. As regards (F8), this is obvious from (F5) in the ℓ_2 -norm. The uniform norm result is treated in Protter and Weinberger. Contraction in the ℓ_1 -norm is also provable, from a consideration of the Green's function.

Because the "evolution equation" for heat conduction is a contraction semigroup in the Hilbert space we can use the triangle inequality to prove that $L_2[0,1] \cong \ell_2(N)$, the semi-discretization error in this space is bounded by the sum of the initial interpolation error $|||u_0(x) - u_h(x)|||$ and the error in the rate of dissipation stemming from the spatial difference approximation $\nabla_h^2 u = (\delta_{xx} u)/h^2$ to $\nabla^2 u$. This is easily verified to be

$$(F9) \quad \left[\sum (|c_j| \cdot |e^{-\mu_j t} - e^{-\lambda_j t}|)^2 \right]^{1/2},$$

where $\mu_j = j^2 \pi^2$ and by (F1), since $\nabla_h^2 u = (\delta_{xx} u)/h^2$,

$$(F9') \quad \lambda_j = [2 - 2 \cos j\pi h] / h^2 .$$

Expanding in Taylor series:

$$\lambda_j - \mu_j = (j^4 \pi^4 h^2 / 12) - (j^6 \pi^6 h^4 / 360) + \dots ;$$

more importantly, $\lambda_j > \mu_j$. Therefore

$$|e^{-\mu_j t} - e^{-\lambda_j t}| = e^{-\mu_j t} [1 - e^{-(\lambda_j - \mu_j)t}]$$

is positive; moreover it is small for small jt because the second factor is small, and small for large jt because the first factor is small.

Full discretizations. All semi-discretizations of $u_t = \alpha u_{xx}$ are dissipative. More precisely, they correspond to a (large) strictly stable² system of (linear, constant-coefficient) system of ordinary DE's in the $u_j(t)$. However, full discretizations with too large a Courant number $r = \alpha \Delta t / \Delta x^2$ can be explosively unstable. More precisely, if $r > 1/2$ is held fixed as $h = 1/n$ tends to zero, then the 'approximate' solutions computed (even in 'exact arithmetic') by the explicit method of CFL do not tend to any limit for fixed $t > 0$, but oscillate increasing. Stated another way, the CFL algorithm does not successfully 'arithmetize Analysis' for $r > 1/2$.

To explain this, we note that the explicit method proposed in [17] amounts to integrating the semi-discretization

$$(F10) \quad u_t = (\alpha/h^2) \delta_{xx} u = \alpha \nabla_h^2 u$$

by the Euler-Cauchy polygon method. Rewriting (F10) in vector notation as

$$(F11) \quad \underline{u}'(t) = A[\underline{u}], \quad A = \alpha \delta_{xx} / h^2 ,$$

²See Birkhoff-Rota, "Ordinary Differential Equations", 3rd edition, Chaps. 3 and 6.

or in component notation as $u_j' = \sum a_{jk} u_k$, this amounts to iterating

$$(F12) \quad \underline{u}(t+\Delta t) = \underline{u}(t) + \Delta t A[\underline{u}] = (I+\Delta t A)\underline{u} .$$

The expression $(I+\Delta t A)$ is called the amplification matrix of the CFL scheme.

If we try to approximate $u(x,t)$ by the CFL scheme with fixed r , we get $(I+\Delta t A)^{1/\Delta t}$. For $r > 1/2$, the norm of this matrix, which is the $1/\Delta t = \alpha/r\Delta x^2 = \alpha/n^2 r$ power of $(I+\Delta t A)$, tends to infinity as $\Delta t \rightarrow 0$. To show this we note that for $h = 1/n$, the most unstable eigenfunction $\sin j\pi x$ of (F11) and (F12) is $u_0(x) = \phi_{n-1}(x) = \sin(n-1)\pi x$; at the mesh points $x = x_j = j/n$, we have $\sin(n-1)\pi j/n = (-1)^j \sin \pi j/n$. We omit proving that (F11) becomes unstable when r slightly exceeds $1/2$.

Crank-Nicolson. In contrast to (F12), the trapezoidal method for integrating (F10) gives the Crank-Nicolson recursion formula

$$\underline{u}(t+\Delta t) = \underline{u}(t) + \Delta t [A\underline{u}(t) + A\underline{u}(t+\Delta t)]/2 .$$

Simplifying algebraically, we get

$$(F13) \quad \underline{u}(t+\Delta t) = \frac{2I-A}{2I+A} \underline{u} .$$

The matrix

$$(2I-A)/(2I+A) = I - A + A^2/2 - A^3/4 + \dots$$

in (F13) is thus the amplification matrix of the Crank-Nicolson method. Since the eigenvalues of A are all positive, the eigenvalues of the amplification matrix are all in the interval $(0,1)$, and hence the Crank-Nicolson algorithm is stable for all choices of r .³

³For further details and extensions, see R.S. Varga, "Matrix Iterative Analysis", Chap. 8.

APPENDIX G

TWO-DIMENSIONAL AIRFOIL THEORY

In §11 of Chapter 1, we explained the basic idea of two-dimensional airfoil theory: that lift is due to the circulation $\Gamma = \int \underline{u} \cdot d\underline{x}$ around an airfoil. We also derived the basic formula $L = \rho \Gamma U$ for the predicted lift (the predicted drag is zero). In this Appendix we will derive this formula more rigorously, using Cauchy's theory of complex integration. We will also derive a formula for the moment M . Our starting point will be the following basic existence theorem, whose truth we will assume without proof.

THEOREM 1. There exists a unique potential flow with given circulation Γ around an airfoil moving (through an ideal fluid) with given speed U at a given 'angle of attack' α . Moreover, if the airfoil (wing) has a sharp 'trailing edge', precisely one of these has everywhere finite velocity.

The relevant formulas are by far the simplest in the case of the flow around a circle with center at the origin, which we can imagine as a plane section of a circular cylinder. The most general such flow is a superposition of a uniform flow field, a dipole velocity field in the opposite direction, and a pure vortex at the origin. The resulting complex potential $W = \phi + i\psi$ is then of the form of Chap. 1, (11.6):

$$(G1) \quad W = U[e^{-i\alpha}z + e^{i\alpha}/z + i\gamma \ln z] ;$$

since $\ln z = \ln|z| + i\theta$, its circulation $\Gamma = 2\pi\gamma$. Hence the complex velocity vector (the conjugate of $W'(z)$) is given at $z = e^{i\beta}$ by:

$$(G2) \quad W'(t) = ie^{-i\beta}[\gamma - 2 \sin(\alpha - \beta)] .$$

If $|\gamma| < 2$, there are two 'stagnation points' $W'(z) = 0$, and they occur where $\beta = \pm \arcsin(\gamma/2)$. Again normalizing to the

case $U = 1$, we find by integrating the Bernoulli equation that the net pressure thrust is perpendicular to the flow direction $e^{i\alpha}$ (a 'lift' L), and is equal to

$$(G3) \quad \rho \oint 2\gamma \sin^2(\alpha - \beta) d\beta = 2\pi\rho\gamma = \rho\Gamma U$$

(since $U = 1$).

We now show that the same formula holds generally. In order to prove this, we first use contour integration to prove:

THEOREM 2 (Blasius).¹ let a fixed airfoil profile C be in a locally irrotational flow of an incompressible, non-viscous fluid, with complex potential W . Then the drag D , lift L , and moment M about the origin acting on C are expressed (in complex notation) by the formulas

$$(G4) \quad D - iL = \frac{1}{2} i\rho \oint_C \left(\frac{dW}{dz}\right)^2 dz$$

$$(G5) \quad M = -\frac{1}{2} \rho \operatorname{Re}\left\{\oint_C z \left(\frac{dW}{dz}\right)^2 dz\right\},$$

provided gravity is neglected.

Proof. The pressure on C is, at any point, $\frac{1}{2}\rho(p_0 - |\xi|^2)$ by Bernoulli's Theorem. Since the resultant of a constant pressure is zero, we can suppose $p_0 = 0$. The thrust on an infinitesimal element dz of C can thus be taken as

$$\begin{aligned} -\frac{1}{2}\rho u^2 \cdot idz &= -\frac{1}{2}i\rho(dW/dz)(dW/dz)^*dz \\ &= -\frac{1}{2}i\rho(dW/dz)^*dW. \end{aligned}$$

But along C , $dV = 0$ and $dW = dU = dW^*$. Hence the complex conjugate $D - iL$ of the thrust satisfies

$$D - iL = \frac{1}{2}i\rho \oint (dW/dz)dW = \frac{1}{2}i\rho \oint (dW/dz)^2 dz.$$

¹H. Blasius, Zeits. f. Math. Phys. 58 (1910), - .

The counterclockwise moment about 0 of the vector $idz = -dy + idx$ acting on the point $z = x + iy$, is $ydy + xdx = \text{Re}\{z dz^*\}$. Hence the moment of the pressure on C is

$$-\frac{1}{2} \rho \oint \text{Re}\{u^2 z dz^*\} = -\frac{1}{2} \rho \text{Re}\{\oint (dW/dz) z dW^*\}.$$

Since $dW^* = dW$ on C , this implies (G5).

The formulas of Blasius involve single-valued, analytic complex integrands. Therefore, by Cauchy's Integral Theorem, their value is the same for all contours going once around C . This fact is very convenient.

Thus, if we expand W at infinity, as

$$(G6) \quad W = z + \frac{i\Gamma}{2\pi} \ln z + c_0 + c_1/z + c_2/z^2 + \dots,$$

we obtain by a simple calculation

$$(G6') \quad (dW/dz)^2 = 1 + i\Gamma/\pi z - (\Gamma^2/4\pi^2 + 2c_1)/z^2 + \dots$$

Hence, integrating term-by-term the Laurent expansion obtained by substituting from (6.6') into (6.4), we obtain

$$(G7) \quad D = iL = \frac{1}{2} i \rho (i\Gamma/\pi) \oint dz/z = -i \rho \Gamma,$$

as usual in the calculus of residues. This gives the celebrated Kutta-Joukowski Theorem.²

THEOREM 2. Under the hypothesis of Theorem 1 the drag D is zero, and the lift L is $\rho F U$.

(In (G6) we have assumed $v_\infty = 1$; since the formula $L = \rho F v_\infty$ is dimensionally homogeneous, it suffices to discuss this case, using inertial similitude.)

COROLLARY. (Two-dimensional d'Alembert Paradox). An Euler flow exerts no lift or drag on an object.

²W. Kutta, Ill. aeronaut. Mitt. (1902); Sitzb. bayr. Akad. Wiss. (1910); N. Joukowski, Zeit. Flugtech. Motorluftschiffahrt, vol. 1 (1910), p. 281 and vol. 3 (1912), p. 81.

AD-A135 900

NNMERICAL FLUID DYNAMICS(U) HARVARD UNIV CAMBRIDGE MA
G BIRKHOFF 1983 N00014-75-C-0596

4/4

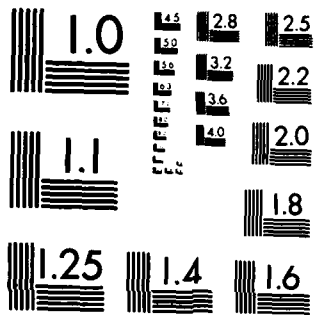
UNCLASSIFIED

F/G 20/4

NL



END
FILMED
1984
DTIC



MICROCOPY RESOLUTION TEST CHART
NATIONAL BUREAU OF STANDARDS-1963-A

Substituting from (G6') into (G4), we obtain a simple expression due to von Mises,³

$$(G8) \quad M = -\frac{1}{2} \rho \operatorname{Re}\{-\frac{\Gamma^2}{4\pi^2} + 2c_1\} 2\pi i = -2\pi \rho \operatorname{Im}\{c_1\} .$$

Again, putting this in dimensionally homogeneous form, we get

THEOREM 4. Under the hypotheses of Theorem 1, the moment M is $2\pi\rho$ times the velocity times the normal component $\operatorname{Im}\{c_1\} = b_1$ of the "bicirculation vector" b_1 .

The "bicirculation vector" of a flow without circulation is independent of the choice of origin, and is simply the dipole moment of the flow at infinity. Thus, in the case of the ellipse

$$x = (1+a^2) \cos \sigma , \quad y = (1-a^2) \sin \sigma ,$$

we have for horizontal flow

$$W = t + 1/t = z + (1-a^2)/z + \dots ,$$

since $t = z - a^2/t = z - a^2/z - \dots$. This has horizontal dipole moment $1 - a^2$. Similarly, for vertical flow

$$W = -i(t-t^{-1}) = iz - ia^2/z - i/z = i[z - (1+z^2)/z + \dots] .$$

This has vertical dipole moment $-(1 + a^2)$.

It follows that the force moment is zero for flow parallel to the horizontal and vertical "principal axes". For oblique flow, with $\zeta_\infty = \cos \alpha - i \sin \alpha$, the dipole moment is obtained by superposition, as

$$((1 - a^2) \cos \alpha, \quad -(1 + a^2) \sin \alpha) .$$

³R. von Mises, Zeit. Flugtech. Motorluftschiffahrt, 1917, pp. 157-163, and 1920, pp. 67-73 and 87-89. See also his Theory of Flight, p. 183.

The component of this perpendicular to the velocity vector $(\cos \alpha, \sin \alpha)$ is $2a^2 \cos \alpha \sin \alpha = a^2 \sin 2\alpha$. Hence the counter-clockwise "broadside moment" M is $-2\pi\rho a^2 \sin 2\alpha$, by (G8).

A similar result holds for potential flows in general, with respect to suitable "principal axes" for translation.

END

FILMED

1-84

DTIC